

**THE USE OF VARIOUS  
TRANSFORMS IN THE  
SOLUTION OF BOUNDARY  
VALUE PROBLEMS IN LINEAR  
ELASTICITY**

by

**ABDELNASER SHAMSI**

A thesis submitted to  
the Faculty of Science, University of Glasgow,  
for the degree of Doctor of Philosophy

February 20, 1998

ProQuest Number: 13834234

All rights reserved

INFORMATION TO ALL USERS

The quality of this reproduction is dependent upon the quality of the copy submitted.

In the unlikely event that the author did not send a complete manuscript and there are missing pages, these will be noted. Also, if material had to be removed, a note will indicate the deletion.



ProQuest 13834234

Published by ProQuest LLC (2019). Copyright of the Dissertation is held by the Author.

All rights reserved.

This work is protected against unauthorized copying under Title 17, United States Code  
Microform Edition © ProQuest LLC.

ProQuest LLC.  
789 East Eisenhower Parkway  
P.O. Box 1346  
Ann Arbor, MI 48106 – 1346



*Thens 11038 (copy 2)*

# Contents

<b>Contents</b>	<b>i</b>
<b>Abstract</b>	<b>iii</b>
<b>Preface</b>	<b>iv</b>
<b>1 Introduction</b>	<b>1</b>
1.1 Historical Background . . . . .	1
1.2 Introduction . . . . .	2
1.2.1 Gum Rubber . . . . .	4
1.2.2 Polyethylene . . . . .	5
<b>2 Basic Equations</b>	<b>8</b>
2.1 Introduction . . . . .	8
2.2 Constitutive Theory of Elasticity . . . . .	9
2.2.1 Incompressible Materials . . . . .	12
2.2.2 Equilibrium Equations . . . . .	13
<b>3 Bessel Functions</b>	<b>15</b>
3.1 Introduction . . . . .	15
3.2 Bessel Functions . . . . .	15
3.3 Modified Bessel Functions . . . . .	17
3.4 Orthogonality of Bessel Functions . . . . .	19
3.5 Fourier-Bessel Series . . . . .	20
3.6 Weber-Orr Transforms . . . . .	21



<b>4</b>	<b>Response of an Incompressible Elastic Annulus to a Periodic Axial Driving Force</b>	<b>23</b>
4.1	Introduction . . . . .	23
4.2	Governing Equations . . . . .	23
4.3	Boundary Conditions . . . . .	25
4.3.1	Non-dimensional Problem . . . . .	26
4.4	Transformed Equations . . . . .	27
4.4.1	Solution Procedure . . . . .	29
4.5	Fourier-series Representation . . . . .	31
4.5.1	Static Problem . . . . .	36
4.6	Numerical Solution . . . . .	36
4.7	Conclusions for the Static Problem . . . . .	37
4.7.1	Accumulated Static Shear Stress . . . . .	39
4.7.2	Static Shear Stress . . . . .	39
4.7.3	Static surface deformation . . . . .	39
4.8	Dynamic Deformation . . . . .	40
4.8.1	Dynamic Accumulated Shear Stress . . . . .	45
4.8.2	Dynamic Shear Stress . . . . .	45
4.8.3	Dynamic surface deformation . . . . .	45
<b>5</b>	<b>Response of a Compressible Elastic Annulus to a Periodic Axial Driving Force</b>	<b>62</b>
5.1	Introduction . . . . .	62
5.2	Compressible Viscoelasticity Theory . . . . .	62
5.3	Displacement Equations . . . . .	63
5.4	Boundary Conditions . . . . .	64
5.4.1	Non-dimensional Problem . . . . .	65
5.5	Transformed Equations . . . . .	66
5.6	General Solution . . . . .	67
5.7	Fourier Series Representation . . . . .	68
5.7.1	Function $h_0(z)$ . . . . .	71
5.7.2	Surface Deformation $h(r, 1)$ . . . . .	72
5.7.3	Static Problem . . . . .	73

5.7.4	Boundary Conditions . . . . .	74
5.8	Numerical Details . . . . .	74
5.9	Conclusions . . . . .	75
5.9.1	Accumulated static shear stress . . . . .	76
5.9.2	Static shear stress . . . . .	76
5.9.3	Static surface deformation . . . . .	79
5.10	Dynamic Deformation . . . . .	85
5.10.1	Dynamic Accumulated Shear Stress . . . . .	86
5.10.2	Dynamic shear stress . . . . .	86
5.10.3	Dynamic surface deformation . . . . .	103
<b>6</b>	<b>Axially Loaded Column of an Incompressible Elastic Material</b>	<b>116</b>
6.1	Introduction . . . . .	116
6.2	Linear Deformation of a Slab . . . . .	116
6.2.1	Boundary Conditions . . . . .	117
6.2.2	Non-dimensional Problem . . . . .	118
6.3	Solution Procedure . . . . .	118
6.3.1	Transformed Equations . . . . .	118
6.4	General Solution . . . . .	119
6.5	Fourier-Bessel Series Representation . . . . .	120
6.5.1	Evaluation of Applied Force . . . . .	122
6.5.2	Evaluation of Functions $h_0(r)$ . . . . .	123
6.5.3	Evaluation of $u(1, z)$ . . . . .	123
6.6	Boundary Conditions . . . . .	123
6.7	Results and Conclusion . . . . .	124
<b>7</b>	<b>Axially Loaded Column of Compressible Elastic Material</b>	<b>127</b>
7.1	Introduction . . . . .	127
7.2	Linear Deformation of a Slab . . . . .	127
7.2.1	Boundary Conditions . . . . .	128
7.2.2	Non-dimensional Problem . . . . .	129
7.3	Solution Procedure . . . . .	129
7.3.1	Transformed Equations . . . . .	129

7.3.2	General Solution . . . . .	130
7.4	Fourier-Bessel Series Representation . . . . .	131
7.4.1	Evaluation of the applied force . . . . .	132
7.4.2	Evaluation of Functions $h_0(r)$ . . . . .	133
7.4.3	Evaluation of $u(1, z)$ . . . . .	133
7.5	Boundary Conditions . . . . .	134
7.6	Results and Conclusion . . . . .	135
<b>A</b>	<b>Results for Chapters 4 and 5</b>	<b>139</b>
<b>B</b>	<b>Results for Chapters 6 and 7</b>	<b>144</b>
<b>C</b>	<b>Fortran program for chapter 4</b>	<b>147</b>
<b>D</b>	<b>Fortran program for chapter 5</b>	<b>164</b>
<b>E</b>	<b>Auxiluray Fortran program for chapter 4 and 5</b>	<b>181</b>
<b>F</b>	<b>Fortran program for chapter 6</b>	<b>185</b>
<b>G</b>	<b>Fortran program for chapter 7</b>	<b>197</b>
<b>H</b>	<b>Fortran Code to Isolate Zero's of Bessel and Cylinder Functions</b>	<b>210</b>
H.1	Zero of Bessel function $J_1$ . . . . .	210
H.2	Zero of cylinder function $C_{11}$ . . . . .	213
<b>I</b>	<b>Fortran Code to Evaluate Bessel Functions</b>	<b>218</b>
I.1	Bessel function $J_0(x)$ . . . . .	218
I.2	Bessel function $J_1(x)$ . . . . .	220
I.3	Bessel function $Y_0(x)$ . . . . .	221
I.4	Bessel function $Y_1(x)$ . . . . .	224
I.5	Modified Bessel function $I_0(x)$ . . . . .	226
I.6	Modified Bessel function $I_1(x)$ . . . . .	228
	<b>Bibliography</b>	<b>231</b>

To my mother's spirit, my father,  
my wife Amira and my children,  
Khadija and Abdelkader

## Abstract

This thesis uses combinations of Fourier, Hankel and Weber-Orr transforms to solve boundary value problems in linear elasticity for compressible and incompressible isotropic elastic materials occupying two different geometries. The basic equation of elasticity are developed using the theory of successive approximations as originally described by Green and Adkins [16].

The first problem studies the deformation of an elastic annulus formed by punching a circular hole axially through the centre of a circular disk of uniform thickness. A rigid shaft is passed through this hole and bonded to the annulus. Deformation is induced by applying static and dynamic forces to the shaft. General solutions to this problem are obtained using Weber-Orr transforms in the radial variable and Fourier transforms in the axial variable. The exact problem is thereby reduced to a pair of integral equations which are then solved by representing the two unknown functions using a suitable spectral expansion. The coefficients of these expansions are obtained by solving a system of linear equations. In fact, the solution of the static problem has been approximated by Adkins & Gent [11]. Very good agreement is obtained with their approximate model for a thick annulus but the agreement deteriorates as the annulus becomes thinner principally due to the increasing presence of boundary layer effect.

The second problem investigates the deformation of a right circular column under axial load. The plane ends of the column are covered by rigid plates that are bonded to it while its curved surface is stress-free. Moghe and Neff's [27] construct two mathematically different but physically equivalent series solutions to this problem. The first solution is based on the roots of the Bessel function  $J_0(x)$  while the second uses the roots of the Bessel function  $J_1(x)$ . Unfortunately both "equivalent" solutions predict different shapes for the radial displacement of the curved free surface. The discrepancy is most striking where the curved surface joins the rigid plates. This problem is converted into a pair of integral equations using Fourier transforms in the axial variable and Hankel transforms in the radial variable. Our analysis predicts a curved surface that most resembles that derived by Moghe and Neff using the zeros of  $J_0(x)$ .

## Preface

This thesis is submitted to the Mathematics Department in the University of Glasgow in accordance with the requirements of the degree of Doctor of Philosophy.

I would like to take this opportunity to express my best wishes and sincere gratitude to my supervisor, Dr. K.A. Lindsay, for his advice, guidance, helpful comments and encouragement throughout my research time in the Mathematics Department. I am very grateful to him for all his help .

I would also like to extend my best wishes and thanks to the Head of Department, Professor D. R. Fearn, and to many other members of staff and research students at the Mathematics Department for their support and kindness to me during my stay at Glasgow.

I also wish to thank the Syrian Government, and especially Aleppo University, for affording me the opportunity to study for a higher degree, for the award of a scholarship and for their financial support throughout my time of study.

Finally, I offer my best wishes and grateful thanks to my family in Syria. Special thanks is due to my wife and children for their patience with me and their continued support.

# Chapter 1

## Introduction

### 1.1 Historical Background

The notion of “elasticity” was conceived in the seventeenth century by Robert Hooke (1678) who observed that extension of an elastic strand and the force required to induce this extension were in direct proportion provided the extension was “small”. In more than one dimension, this empirical law generalises naturally to the idea that for small deformations, induced stress is proportional to strain. This is commonly known as Hooke’s Law [1]. In the early nineteenth century, the Theory of Elasticity became a separate branch of Science when L. Navier (1821) [2] became the first scientist to investigate the general equation of equilibrium and motion of elastic solids. The work of A. Cauchy (1822) and S. Poisson (1829) (see [2]) followed shortly afterwards.

A body is considered to be purely elastic if it has infinite memory for a “reference shape” in which it naturally resides in the absence of externally applied forces and to which it will naturally return if deformed and released. On the other hand, if no such memory exists then the body is considered to exhibit fluid properties. Of course, in practice real materials have some measure of both properties and are said to be Viscoelastic. For purely elastic bodies, the forces generated within the body (stress) are connected to the gradients of the displacement of particles of the body from their natural position (strain) whereas in fluids it is the time derivative of these gradients (rate of strain) that is important. In a viscoelastic material both effects are present. The Theory of Elasticity describes the connection between the stresses and strains acting in a purely elastic body and is subdivided into linear theory (typically “small” deformations) and non-linear theory. This

thesis will be concerned only with the linear theory of elasticity.

The theory of viscoelasticity has been investigated by many scientists, but Boltzman (1874) is thought to be the first to formulate the three dimensional theory for an isotropic medium while Volterra (1909) investigated anisotropic solids [3]. An introduction to the theory of linear viscoelasticity is described by Christensen [7] and Wilhelm Flugge [8]. In recent years, there has been significant progress on stress distribution problems in viscoelastic materials (see Lee [4] and Radok [5] and the references therein). Graffi and Hayes [6] have investigated wave propagation in linear viscoelastic materials.

## 1.2 Introduction

In chapter two, the basic equations of linear elasticity are developed for compressible and incompressible (isotropic) states using the theory of successive approximations. Full details of this theory are described by Green and Adkins [16]. In the final section of this chapter, equilibrium equations in cylindrical coordinates are stated and it is these that are used in subsequent chapters.

In chapter three, Bessel functions and modified Bessel functions, finite Weber-Orr transforms and their inversions are presented. The latter are generalisations of Hankel transforms and rely on properties of Weber-Orr functions. The original integral theorem for these functions was discovered by Weber [17] and Orr [9] and [18]. Watson [19] and Titchmarsh [20] give a proof of Weber's integral representation. Weber-Orr transforms are used to solve the boundary value problems arising in chapters four and five. Full details for these transformations are found in [9]. Fourier-Bessel series (see Tolstov [10]) are described in the final section of chapter three and used in chapters six and seven.

In chapters four and five, viscoelastic behaviour is investigated for static and dynamic states and for incompressible and compressible problems. This work investigates small axial deformations of an annulus of elastic material. The annulus is formed from a uniform disk of thickness  $d$  and radius  $b$  by removing an axial cylindrical hole of radius  $a$  ( $a < b$ ) from the centre of the disk. Axial deformation is induced by the application of an axial force to a rigid shaft that passes through this hole and is bonded to the material of the annulus. Annuli composed of incompressible and compressible isotropic elastic materials are considered separately. The presence of circles of "infinite" but integrable stress that



arise where the rod first joins the annulus, suggest that the solutions for compressible and incompressible materials may exhibit significantly different physical features in addition to the obvious mathematical differences arising from the fact that the underlying equations for compressible and incompressible materials are fundamentally different.

Let cylindrical polar coordinates  $(r, \theta, z)$  be chosen so that the annulus occupies the region

$$a \leq r \leq b, \quad -\pi \leq \theta \leq \pi, \quad 0 \leq z \leq d.$$

Suppose that the outer boundary  $r = b$  is fixed and that, in the usual notation of tensor calculus, deformation  $\mathbf{v} = v^i \mathbf{g}_i$  is induced in the annulus by applying a periodic axial force to the rigid rod. In effect, the configuration closely resembles a shock absorber. This research primarily explores the relationship between the geometry of the annulus and its frequency response and it is novel in the respect that it uses Weber-Orr transforms [9] and also develops an exact mathematical solution to the linear elastic problem in which all natural boundary conditions are satisfied. The dynamic problem is completely new but the static deformation problem has been discussed by Adkins & Gent [11] who obtain the approximate relations

$$F = \frac{2\pi\mu dH}{\log \beta + Qa^2/d^2}, \quad Q = \frac{3}{8} \left[ \frac{(\beta^2 - 1)^2 - 4\beta^2(\log \beta)^2}{\beta^2 - 1} \right], \quad (1.2.1)$$

between  $F$ , the applied axial force, and  $H$ , the induced axial deformation. where  $\mu$  is the usual elastic shear modulus and  $\beta = b/a$  (ratio of the outer to inner radius of the annulus). Their results are based on bending and shear stress theories which fail to recognise that the top and bottom plane faces of the annulus are stress-free boundaries. The parameter  $Q$  appearing in (1.2.1) was introduced by Adkins & Gent to describe the effects of bending stress on axial deformation. When  $Q = 0$ , shear stress effects only are included in formula (1.2.1). Hence this research provides an opportunity to compare exact predictions of linear elasticity with  $H_{ss}$ , the axial displacement predicted on the basis of shear stress only (the case  $Q = 0$ ) and  $H_{sb}$ , the axial displacement predicted on the basis of shear and bending stresses. Formula (1.2.1) yields the relations

$$H_{ss} = \frac{F \log \beta}{2\pi\mu d}, \quad H_{sb} = \frac{F(\log \beta + a^2 Q/d^2)}{2\pi\mu d}. \quad (1.2.2)$$

It is easily verified that  $Q > 0$  when  $\beta > 1$  so that  $H_{sb} > H_{ss}$ ; that is, bending effects increase axial displacement for a given axial force. Subsequent analysis confirms that (1.2.1) is remarkably accurate over a large variety of annuli, being almost always within 10% of the theoretical answer and very often within 1% accuracy.

Static results are conveniently derived as limits of a slowly varying periodic axial force of constant magnitude. In order to prevent unbridled motion at resonant frequencies, viscous damping effects are included in this discussion. Thus, the stress tensor has form

$$t^{ij} = -pg^{ij} + \mu(v^i|{}^j + v^j|{}^i) + \eta \frac{\partial}{\partial t} (v^i|{}^j + v^j|{}^i) , \quad (1.2.3)$$

where  $\eta$  is shear viscosity. Unfortunately, realistic shear moduli and shear viscosities are frequency-dependent constitutive functions and are commonly modelled by the formulae

$$\mu(\omega) = \int_0^\infty \frac{g(\tau)\omega^2\tau^2 d\tau}{1 + \omega^2\tau^2} , \quad \eta(\omega) = \int_0^\infty \frac{g(\tau)\tau d\tau}{1 + \omega^2\tau^2} , \quad (1.2.4)$$

where  $g(\tau)$  is a relaxation function. Treloar [12] discusses these relations in more detail. In this particular application, frequency  $\omega$  of the applied forcing term enters the analysis through two non-dimensional parameters

$$\xi = \frac{\eta\omega}{\mu} , \quad \sigma = \frac{\rho\omega^2 d^2}{\mu} , \quad (1.2.5)$$

where  $\rho$  is material density. Rather than explore the effects of particular functions  $g(\tau)$  in formulae (1.2.4), here qualitative aspects of the axial vibration problem, particularly with reference to free surface shape and dependence of resonant response on the geometry of the annulus, are investigated. Frequency-dependent expressions for  $\xi$  and  $\sigma$  in gum rubber and polyethylene are illustrated in figures 1.1-1.4 respectively.

### 1.2.1 Gum Rubber

For pure gum rubber, Treloar [12] provides experimental data for  $\omega\eta(\omega)$  and  $\mu(\omega)$  over a frequency range 20-200Hz at 50°C. In fact,  $\mu$  ( $\approx 3.5\text{N/m}^2$ ) is effectively independent of frequency so that the graph of  $\sigma$  is quadratic in  $\omega$ . Figures 1.1 and 1.2 have extrapolated this information beyond Treloar's frequency domain.

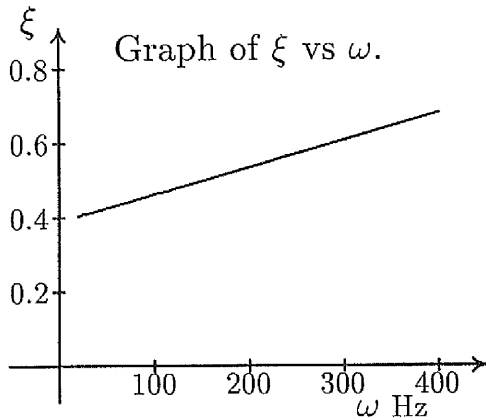


Figure 1.1:  $\xi(\omega)$  for gum rubber.

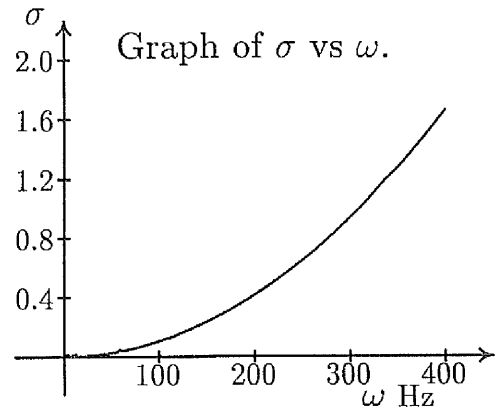


Figure 1.2:  $\sigma(\omega)$  for gum rubber.

### 1.2.2 Polyethylene

Kolsky & Hillier [13] provide experimental data for low density polyethylene at  $10^\circ\text{C}$ . Its mechanical properties are well modelled up to 20KHz by complex elastic modulus  $\mu + i\omega\eta = k(i\omega)^n$ , where  $k$  is a positive constant and  $n \approx 0.1$ . Thus  $\xi = \pi n/2 \approx 0.16$  and this is independent of  $\omega$ . On the other hand,  $\mu(\omega)$  rapidly increases at low frequencies but quickly flattens out to 5 or 6 times its low frequency value. Figures 1.3 & 1.4 illustrate the behaviour of  $\xi$  and  $\sigma$  for polyethylene.

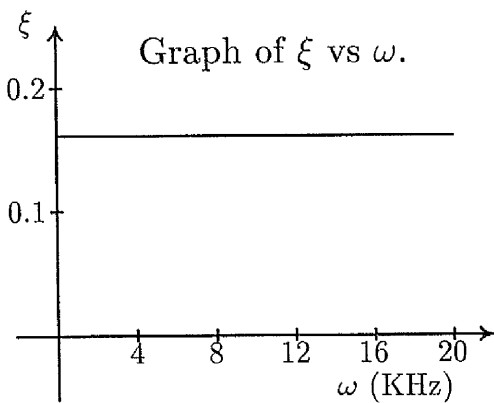


Figure 1.3:  $\xi(\omega)$  for polyethylene.

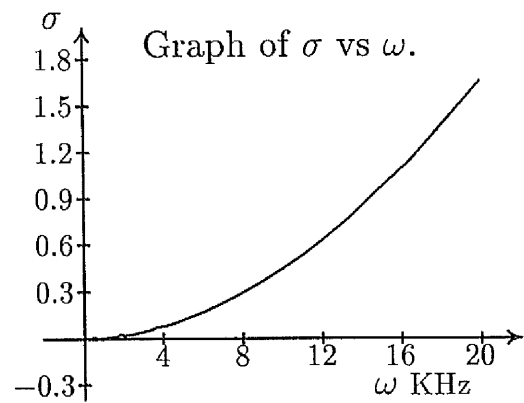


Figure 1.4:  $\sigma(\omega)$  for polyethylene.

Despite dramatic change in  $\mu$  at low frequencies, both curves for  $\sigma$  are qualitatively similar. It can be seen that values of  $\sigma$  over a large frequency range are dominated by  $\omega^2$

unless  $\mu$  follows a similar power law. This is unlikely for real materials. Hence  $\xi(\omega)$  is approximately constant or is a mildly increasing function of  $\omega$  while  $\sigma(\omega)$  is probably well described by a quadratic function of  $\omega$ .

Finally, our mathematical analysis relies heavily on properties of finite Weber-Orr transforms which are numerically inverted to determine solutions. This family of transforms are uncommon, as can be seen by the fact that they are not specifically described in Erdélyi *et al* [14]. The most detailed account of their properties is provided by Olesiak [15].

The appearance of resonance for dynamic problems in chapters four and five can be briefly evaluated by the following:

The kinetic energy (KE) of an annulus of uniform thickness  $d$ , outer radius  $b$  and containing a hole of radius  $a$  is given by

$$KE = \int_V \rho v_i^2 dV ,$$

where  $dV = 2\pi r d(dr)$  and  $v_i = \dot{x}(\beta - r)/(\beta - 1)$  are, respectively, volume and velocity of an infinitesimal element of the annulus ( $r, r+dr$ ). Then

$$KE = \int_1^\beta 2\pi r d \frac{(\beta - r)^2}{(\beta - 1)^2} \dot{x}^2 \rho dr = \frac{\pi d \dot{x}^2 \rho}{(\beta - 1)^2} \int_1^\beta r(\beta - r)^2 dr = \frac{(\beta + 3)M \dot{x}^2}{12(\beta + 1)} ,$$

where  $M = \rho\pi(\beta^2 - 1)d$ . The elastic potential energy (PE) is approximated by

$$PE = -kx^2/2 ,$$

where  $k = F/H$ , in which  $F$  is defined in (1.2.1), by using Lagrange formula

$$\frac{d}{dt} \left( \frac{\partial L}{\partial \dot{x}} \right) - \frac{\partial L}{\partial x} = 0 ,$$

where  $L = KE + PE$ . Hence

$$\ddot{x} + \omega^2 x = 0 ,$$

where

$$\omega^2 = \frac{12\mu}{\rho(\beta - 1)(\beta + 3)[Q/\nu^2 + \log \beta]} .$$

Values of  $\omega$  are given in Table (1.1) for various values of parameters  $\beta$  and  $\nu = d/a$  with  $\rho = \mu = 1$ .

Projected natural frequency $f_\omega$ .												
$\beta$	$\nu = \frac{1}{4}$	$\nu = \frac{1}{2}$	$\nu = \frac{3}{4}$	$\nu = 1$	$\nu = 2$	$\nu = 3$	$\nu = 4$	$\nu = 5$	$\nu = 6$	$\nu = 7$	$\nu = 8$	$\nu = 9$
1.5	2.577	3.250	3.444	3.521	3.599	3.615	3.620	3.622	3.624	3.625	3.625	3.625
2.0	0.850	1.334	1.561	1.673	1.808	1.837	1.847	1.852	1.855	1.856	1.857	1.858
3.0	0.246	0.449	0.596	0.696	0.864	0.911	0.929	0.938	0.943	0.946	0.948	0.949
4.0	0.116	0.222	0.311	0.381	0.531	0.585	0.608	0.620	0.626	0.630	0.633	0.635
5.0	0.068	0.132	0.190	0.239	0.363	0.417	0.442	0.456	0.463	0.468	0.472	0.474
6.0	0.045	0.088	0.128	0.164	0.264	0.314	0.340	0.355	0.363	0.369	0.373	0.375
7.0	0.032	0.063	0.092	0.119	0.200	0.246	0.272	0.287	0.296	0.302	0.306	0.309
8.0	0.024	0.047	0.069	0.090	0.157	0.198	0.223	0.238	0.247	0.253	0.258	0.261
9.0	0.019	0.037	0.054	0.071	0.126	0.163	0.186	0.201	0.210	0.217	0.221	0.225
10.0	0.015	0.029	0.044	0.057	0.104	0.136	0.158	0.172	0.182	0.188	0.193	0.196

Table 1.1: Table of values of frequency for selected values of  $\nu$  and  $\beta$ .

# Chapter 2

## Basic Equations

### 2.1 Introduction

Basic equations of elasticity and various aspects of notation are introduced in this chapter. Let  $x_i$  denote current coordinates at time  $t$  of a material point  $P$  which originally had coordinates  $X_A$  at time  $t_0$ . Then motion in a continuum is characterised by the equation

$$x_i = x_i(X_A, t) , \quad (2.1.1)$$

where  $x_i(X_A, t)$  are continuously differentiable functions of  $\mathbf{X}$  and  $t$  such that their Jacobian is never zero. Under these circumstances,  $x_i = x_i(X_A, t)$  is an invertible mapping with inverse  $X_A = X_A(x_i, t)$ . Consider a deformation in which points  $X_A$  and  $X_A + dX_A$  are deformed into  $x_i$  and  $x_i + dx_i$  respectively. Let the distance between  $x_i$  and  $x_i + dx_i$  be  $ds$  and between  $X_A$  and  $X_A + dX_A$  be  $dS$ . Then

$$ds^2 = dx_i dx_i = \frac{\partial x_i}{\partial X_A} \frac{\partial x_i}{\partial X_B} dX_A dX_B = C_{AB} dX_A dX_B , \quad (2.1.2)$$

or alternatively,

$$dS^2 = dX_A dX_A = \frac{\partial X_A}{\partial x_i} \frac{\partial X_A}{\partial x_j} dx_i dx_j = B_{ij} dx_i dx_j . \quad (2.1.3)$$

Hence

$$ds^2 - dS^2 = \begin{cases} (C_{AB} - \delta_{AB}) dX_A dX_B = 2L_{AB} dX_A dX_B , \\ (\delta_{ij} - B_{ij}) dx_i dx_j = 2E_{ij} dx_i dx_j , \end{cases} \quad (2.1.4)$$

where  $L_{AB}$  and  $E_{ij}$  are known as the *Lagrangian* and *Eulerian* finite strain tensors, respectively. Suppose now that

$$x_i = \delta_{iA} X_A + u_i, \quad \text{or equivalently} \quad X_A = (x_k - u_k) \delta_{kA}. \quad (2.1.5)$$

Then

$$\frac{\partial x_i}{\partial X_A} = \delta_{iA} + \frac{\partial u_i}{\partial X_A}, \quad \frac{\partial X_A}{\partial x_i} = \delta_{iA} - \frac{\partial u_k}{\partial x_i} \delta_{kA}. \quad (2.1.6)$$

Then  $L_{AB}$  and  $E_{ij}$  become

$$\begin{aligned} L_{AB} &= \frac{1}{2} \left( \frac{\partial u_A}{\partial X_B} + \frac{\partial u_B}{\partial X_A} + \frac{\partial u_i}{\partial X_A} \frac{\partial u_i}{\partial X_B} \right), \\ E_{ij} &= \frac{1}{2} \left( \frac{\partial u_i}{\partial x_j} + \frac{\partial u_j}{\partial x_i} - \frac{\partial u_k}{\partial x_i} \frac{\partial u_k}{\partial x_j} \right). \end{aligned} \quad (2.1.7)$$

Whenever the continuum is a rigid body,  $L_{AB} = E_{ij} = 0$ . When displacement  $u$  is small, there is no distinction between  $L_{AB}$  and  $E_{ij}$  calculated to first order in  $u$  (the linear theory of elasticity). General theory of elasticity is developed first and the linear theory of elasticity is then extracted from it.

## 2.2 Constitutive Theory of Elasticity

General constitutive theory of an isotropic solid is now presented. Elastic displacements are expanded in a power series in a “small” non-dimensional parameter  $\varepsilon$  and constitutive equations for linear theory of elasticity for an isotropic solid are extracted from general constitutive theory. In this work, it is more convenient to use nominal stress tensor  $\mathbf{S}$ , which is related to the more familiar Cauchy-Green stress tensor  $\sigma$  by

$$\mathbf{S} = J \mathbf{F}^{-1} \sigma, \quad (2.2.8)$$

where  $J = \det \mathbf{F}$  and  $\mathbf{F} = [x_{i,A}]$  is the usual deformation gradient tensor. Suppose that the material has specific strain energy function  $\hat{W}$ , which is assumed to be a function of deformation gradient tensor  $\mathbf{F}$  only. Since  $\hat{W}$  is invariant under all superposed rigid body motion, then all occurrences of  $\mathbf{F}$  in  $\hat{W}$  must be replaced by  $\mathbf{C} = \mathbf{F}^T \mathbf{F} = [x_{i,A} x_{i,B}]$ , where  $\mathbf{C}$  is the Cauchy-Green strain tensor. Furthermore, if the material is also isotropic then it follows that

$$\hat{W} = \hat{W}(\mathbf{C}) = \hat{W}(I_1, I_2, I_3), \quad (2.2.9)$$

where  $I_1$ ,  $I_2$  and  $I_3$  are the invariants of  $\mathbf{C}$  defined by

$$I_1 = \text{Tr } \mathbf{C} , \quad I_2 = \frac{1}{2} [(\text{Tr } \mathbf{C})^2 - \text{Tr } \mathbf{C}^2] , \quad I_3 = \det \mathbf{C} . \quad (2.2.10)$$

Using an energy argument or an entropy inequality, it can be shown that Cauchy-Green stress tensor  $\sigma$  and nominal stress tensor  $\mathbf{S}$  are related to energy function  $\hat{W}$  through the expressions

$$\sigma = J^{-1} \mathbf{F} \left( \frac{\partial \hat{W}}{\partial \mathbf{C}} + \frac{\partial \hat{W}}{\partial \mathbf{C}^T} \right) \mathbf{F}^T , \quad \mathbf{S} = \left( \frac{\partial \hat{W}}{\partial \mathbf{C}} + \frac{\partial \hat{W}}{\partial \mathbf{C}^T} \right) \mathbf{F}^T . \quad (2.2.11)$$

In view of (2.2.9) and (2.2.10),  $\mathbf{S}$  can be rewritten in the form

$$\mathbf{S} = \sum_{k=1}^3 \frac{\partial \hat{W}}{\partial I_k} \left( \frac{\partial I_k}{\partial \mathbf{C}} + \frac{\partial I_k}{\partial \mathbf{C}^T} \right) \mathbf{F}^T . \quad (2.2.12)$$

It can be shown from definitions (2.2.10) that

$$\frac{\partial I_1}{\partial \mathbf{C}} + \frac{\partial I_1}{\partial \mathbf{C}^T} = 2\mathbf{I} , \quad \frac{\partial I_2}{\partial \mathbf{C}} + \frac{\partial I_2}{\partial \mathbf{C}^T} = 2I_1\mathbf{I} - 2\mathbf{C} , \quad \frac{\partial I_3}{\partial \mathbf{C}} + \frac{\partial I_3}{\partial \mathbf{C}^T} = I_3\mathbf{C}^{-1} . \quad (2.2.13)$$

When results (2.2.13) are substituted into expression (2.2.12) for stress, the result is

$$\mathbf{S} = 2 \left[ \frac{\partial \hat{W}}{\partial I_1} \mathbf{I} + (I_1\mathbf{I} - \mathbf{C}) \frac{\partial \hat{W}}{\partial I_2} + I_3\mathbf{C}^{-1} \frac{\partial \hat{W}}{\partial I_3} \right] \mathbf{F}^T . \quad (2.2.14)$$

In particular, stress in an unstrained body ( $\mathbf{F} = \mathbf{I}$ ,  $\mathbf{C} = \mathbf{I}$ ) is

$$\mathbf{S}_0 = 2 \left( \frac{\partial \hat{W}}{\partial I_1} + 2 \frac{\partial \hat{W}}{\partial I_2} + \frac{\partial \hat{W}}{\partial I_3} \right) \bigg|_E \mathbf{I} , \quad (2.2.15)$$

where the notation  $|_E$  denotes evaluation of a function in an unstrained (or equilibrium) state; that is, when

$$I_1 = I_2 = 3, \quad I_3 = 1 . \quad (2.2.16)$$

In all future work, the unstrained body will be assumed to be stress-free, so that  $\hat{W}$  inherently satisfies the property

$$\left( \frac{\partial \hat{W}}{\partial I_1} + 2 \frac{\partial \hat{W}}{\partial I_2} + \frac{\partial \hat{W}}{\partial I_3} \right) \bigg|_E = 0 . \quad (2.2.17)$$



In linear theory, no distinction exists between engineering stress (stress measured per unit area of the unstrained body) and Cauchy stress (stress measured per unit area of the deformed body). In the following analysis, reference coordinates are chosen from the geometry of the undeformed state. The deformation gradient tensor is then expressed by

$$\mathbf{F} = \mathbf{I} + \varepsilon \mathbf{H} + \dots, \quad (2.2.18)$$

where  $\mathbf{I}$  is the identity and  $\mathbf{H}$  is the first order displacement gradient tensor. The corresponding expression for  $\mathbf{C}$ , correct to first order in  $\varepsilon$  is

$$\mathbf{C} = \mathbf{I} + \varepsilon(\mathbf{H} + \mathbf{H}^T). \quad (2.2.19)$$

Green and Adkins [16] introduced three new independent invariants  $J_1$ ,  $J_2$  and  $J_3$  that are connected to  $I_1$ ,  $I_2$  and  $I_3$  by the relationship:

$$\begin{aligned} J_1 &= I_1 - 3 = 2\varepsilon \text{Tr} \mathbf{H} + O(\varepsilon^2), \\ J_2 &= I_2 - 2I_1 + 3 = O(\varepsilon^2), \\ J_3 &= I_3 - I_2 + I_1 - 1 = O(\varepsilon^3). \end{aligned} \quad (2.2.20)$$

In view of (2.2.20), the isotropic strain energy function  $\hat{W}$  is now re-expressed in terms of  $W$

$$W(J_1, J_2, J_3) = \hat{W}(I_1, I_2, I_3), \quad (2.2.21)$$

so that

$$\left. \frac{\partial W}{\partial J_1} \right|_E = \frac{\partial \hat{W}}{\partial I_1} + 2 \frac{\partial \hat{W}}{\partial I_2} + \frac{\partial \hat{W}}{\partial I_3} \Big|_E, \quad (2.2.22)$$

where  $|_E$  also denotes the configuration in which  $J_1 = J_2 = J_3 = 0$ . In terms of derivatives of  $W$  with respect to  $J_1$ ,  $J_2$  and  $J_3$ , formulae (2.2.14) for the nominal stress tensor  $\mathbf{S}$  becomes

$$\mathbf{S} = 2W_1 \mathbf{F}^T + 2W_2 [I_1 \mathbf{F}^T - 2\mathbf{F}^T - \mathbf{F}\mathbf{C}^T] + 2W_3 [\mathbf{F}^T - I_1 \mathbf{F}^T + \mathbf{F}\mathbf{C}^T + I_3 \mathbf{F}^{-1}], \quad (2.2.23)$$

where

$$W_k = \left. \frac{\partial W}{\partial J_k} \right|_E, \quad k = 1, \dots, 3. \quad (2.2.24)$$

Stress tensor (2.2.23) is now expanded as far as first order in  $\varepsilon$  in two steps:

- (i) Replace  $\mathbf{F}$ ,  $\mathbf{C}$  and  $J_1$  in (2.2.23) by their expressions in terms of  $\mathbf{I}$  and  $\mathbf{H}$  and expand as far as first order in  $\varepsilon$ .
- (ii) Replace the exact partial derivatives of  $W$  with suitable power series expansions in  $\varepsilon$ . In fact,

$$\frac{\partial W}{\partial J_k} = W_k|_E + W_{k1}|_E J_1 + O(\varepsilon^2) . \quad (2.2.25)$$

The algebraic details are tedious and it can be shown that the final first order expansion of the nominal stress tensor is

$$\mathbf{S} = \varepsilon[\lambda(\text{Tr } \mathbf{H})\mathbf{I} + \mu(\mathbf{H} + \mathbf{H}^T)] , \quad (2.2.26)$$

where the Lamé constants  $\lambda$  and  $\mu$  are defined in terms of the derivatives of  $W$  by the relationship

$$\lambda = 4 \left( \frac{\partial W}{\partial J_2} + \frac{\partial^2 W}{\partial J_1^2} \right) , \quad \mu = -2 \frac{\partial W}{\partial J_2} . \quad (2.2.27)$$

From (2.2.26), the nominal stress tensor can be expressed in component forms

$$\begin{aligned} t_{ij} &= \lambda H_{k,k} \delta_{ij} + \mu (H_{i,j} + H_{j,i}) , & (\text{Cartesian Tensor}) , \\ t^{ij} &= \lambda H^r|_r g^{ij} + \mu (H^i|{}^j + H^j|{}^i) , & (\text{General Tensor}) , \end{aligned} \quad (2.2.28)$$

where a subscripted comma denotes partial differentiation and  $|$  denotes covariant differentiation with respect to metric  $g_{ij}$  in these expressions.

### 2.2.1 Incompressible Materials

Constitutive formulae for a linearly elastic *incompressible* isotropic solid can be extracted from expressions (2.2.28) by recognising that, in this event,  $I_3 = 1$ , so that  $W$  no longer contains  $I_3$ . Furthermore,

$$\text{Tr } \mathbf{H} \rightarrow 0 , \quad \lambda = 4 \left| \frac{\partial W}{\partial I_2} + \frac{\partial^2 W}{\partial I_1^2} \right| \rightarrow \infty ,$$

in such a way that

$$4\lambda \text{Tr}(\mathbf{H}) \rightarrow -p , \quad (2.2.29)$$

where  $p$  is an arbitrary function of position and time — it acts like a pressure subject to the laws of Fluid Mechanics. Hence, the first order nominal stress tensor for an incompressible isotropic material is

$$\mathbf{S} = \varepsilon[ -p\mathbf{I} + \mu(\mathbf{H} + \mathbf{H}^T)] , \quad (2.2.30)$$

or in component form

$$t^{ij} = -pg^{ij} + \mu(H^i|{}^j + H^j|{}^i) . \quad (2.2.31)$$

It is common practice to re-express Lamé coefficients  $\lambda$  and  $\mu$  in terms of more familiar elastic moduli such as Young's modulus  $E$ , Poisson's ratio  $\nu_0$  and bulk modulus  $K$ . In fact,

$$\begin{aligned} E &= \frac{\mu(3\lambda + 2\mu)}{\lambda + \mu} && \text{Young's modulus ,} \\ \nu_0 &= \frac{\lambda}{2(\lambda + \mu)} && \text{Poisson's ratio ,} \\ K &= \lambda + \frac{2}{3}\mu && \text{Bulk modulus .} \end{aligned} \quad (2.2.32)$$

Furthermore,

$$\lambda = \frac{E\nu_0}{(1 + \nu_0)(1 - 2\nu_0)} , \quad \mu = \frac{E}{2(1 + \nu_0)} , \quad K = \frac{E}{3(1 - 2\nu_0)} . \quad (2.2.33)$$

If it is assumed that real materials deform in the direction of an applied force then  $E$ ,  $K$  and  $\mu$  are all positive. Hence Poisson's ratio  $\nu_0 \in (-1, 1/2)$  from which it follows that there may be a negative value for  $\lambda$ , the first Lamé constant.

### 2.2.2 Equilibrium Equations

The equilibrium equations are in component form

$$t^{ij}|_i + \rho f^j = \rho a^j , \quad (2.2.34)$$

where  $\rho$  is density and  $f^j$  and  $a^j$  are components of external body force and material acceleration and  $t^{ij}|_i$  is the divergence of the stress tensor. Specifically

$$t^{ij}|_i = \frac{\partial t^{ij}}{\partial x^i} + \Gamma_{im}^i t^{mj} + \Gamma_{im}^j t^{im} , \quad (2.2.35)$$

where  $\Gamma_{jk}^i$  are the *Christoffel Symbols* of the second kind and are derived from derivatives of metric tensor  $g^{ij}$ . For example, in the case of cylindrical polar coordinates, non-zero Christoffel Symbols are given by

$$\Gamma_{22}^1 = -r \ , \quad \Gamma_{21}^2 = \Gamma_{12}^2 = \frac{1}{r} \ . \quad (2.2.36)$$

In the absence of external body forces, equilibrium equations in cylindrical polar coordinates  $(r, \theta, z)$  take the form

$$\begin{aligned} \frac{\partial t^{11}}{\partial r} + \frac{\partial t^{21}}{\partial \theta} + \frac{\partial t^{13}}{\partial z} + \frac{t^{11}}{r} - r t^{22} &= \rho a^1 \ , \\ \frac{\partial t^{12}}{\partial r} + \frac{\partial t^{22}}{\partial \theta} + \frac{\partial t^{32}}{\partial z} + 3 \frac{t^{12}}{r} &= \rho a^2 \ , \\ \frac{\partial t^{13}}{\partial r} + \frac{\partial t^{23}}{\partial \theta} + \frac{\partial t^{33}}{\partial z} + \frac{t^{13}}{r} &= \rho a^3 \ . \end{aligned} \quad (2.2.37)$$

# Chapter 3

## Bessel Functions

### 3.1 Introduction

Main properties of Bessel Functions are now recorded and are used to develop less well-known properties of Weber-Orr functions which form the basis of the Weber-Orr transform that is used extensively in this thesis.

### 3.2 Bessel Functions

Using the substitution  $x = \lambda r$ , the differential equation

$$r^2 \frac{d^2 u}{dr^2} + r \frac{du}{dr} + (\lambda^2 r^2 - \nu^2)u = 0 , \quad (3.2.1)$$

may be simplified to canonical form

$$x^2 \frac{d^2 u}{dx^2} + x \frac{du}{dx} + (x^2 - \nu^2)u = 0 . \quad (3.2.2)$$

This is called *Bessel's equation* of order  $\nu$ . Using a power series solution, it can be shown that the Bessel equation has a solution  $J_\nu(x)$  defined by expanding the infinite series

$$J_\nu(x) = \sum_{k=0}^{\infty} \frac{(-1)^k x^{\nu+2k}}{2^{\nu+2k} k! \Gamma(\nu + k + 1)} , \quad (3.2.3)$$

This is called the Bessel function of the first kind of order  $\nu$ . By symmetry,  $J_{-\nu}(x)$  is also a solution of (3.2.2) and this can be shown to be functionally independent of  $J_\nu(x)$  provided  $\nu$  is not an integer. In this case, equation (3.2.2) has general solution

$$u = AJ_\nu(x) + BJ_{-\nu}(x) . \quad (3.2.4)$$

However, if  $\nu = n$  is an integer then  $J_{-n}(x) = (-1)^n J_n(x)$  so that  $J_\nu(x)$  and  $J_{-\nu}(x)$  are now dependent functions. Thus, expression (3.2.4) is no longer a general solution of the Bessel equation and it is now necessary to find another function  $Y_n(x)$  that is functionally independent of  $J_n(x)$ . Resolution of this dilemma centres on properties of function  $Y_\nu(x)$  defined for general  $\nu$  by

$$Y_\nu(x) = \frac{\cos \nu\pi J_\nu(x) - J_{-\nu}(x)}{\sin \nu\pi} . \quad (3.2.5)$$

By construction,  $Y_\nu(x)$  is a solution of Bessel equation (3.2.2) and is commonly called the Weber-Bessel function of the second kind of order  $\nu$ . Self evidently, if  $\nu$  is not an integer, then  $J_\nu(x)$  and  $Y_\nu(x)$  are independent functions. However, if L'Hôpital's rule is used to interpret the definition of  $Y_\nu(x)$  when  $\nu$  is an integer, then

$$Y_n(x) = \lim_{\nu \rightarrow n} Y_\nu(x) = \frac{1}{\pi} \left[ \frac{\partial J_\nu(x)}{\partial \nu} - (-1)^n \frac{\partial J_{-\nu}(x)}{\partial \nu} \right]_{\nu=n} , \quad (3.2.6)$$

is a solution of Bessel's equation that is functionally independent of  $J_n(x)$ . If  $W$  is the Wronskian of  $J_\nu(x)$  and  $Y_\nu(x)$ , then

$$W = \begin{vmatrix} J_\nu(x) & Y_\nu(x) \\ J'_\nu(x) & Y'_\nu(x) \end{vmatrix} = J_\nu(x)Y'_\nu(x) - Y_\nu(x)J'_\nu(x) . \quad (3.2.7)$$

Since  $J_\nu(x)$  and  $Y_\nu(x)$  satisfy Bessel's equations (3.2.2),

$$\begin{aligned} x^2 J''_\nu(x) + x J'_\nu(x) + (x^2 - \nu^2) J_\nu(x) &= 0 , \\ x^2 Y''_\nu(x) + x Y'_\nu(x) + (x^2 - \nu^2) Y_\nu(x) &= 0 . \end{aligned} \quad (3.2.8)$$

By multiplying the first of these equation by  $Y_\nu(x)$  and the second by  $J_\nu(x)$  and subtracting them, it follows that

$$\frac{d}{dx} [x (J_\nu(x)Y'_\nu(x) - Y_\nu(x)J'_\nu(x))] = 0 , \quad (3.2.9)$$

with integrated form:

$$J_\nu(x)Y'_\nu(x) - Y_\nu(x)J'_\nu(x) = \frac{A}{x} , \quad (3.2.10)$$

in which  $A$  is a constant independent of  $x$  but potentially dependent on  $\nu$ . In view of the definition of  $Y_\nu(x)$ , relation (3.2.10) yields

$$J_{-\nu}(x)J'_\nu(x) - J_\nu(x)J'_{-\nu}(x) = \frac{C \sin \nu\pi}{x} . \quad (3.2.11)$$

Furthermore, the left hand side of equation (3.2.11) can be rewritten using expression (3.2.3) for  $J_\nu(x)$  leading to

$$J_{-\nu}(x)J'_\nu(x) - J_\nu(x)J'_{-\nu}(x) = \sum_{k=0}^{\infty} \sum_{l=0}^{\infty} \frac{\lambda(k-l+\nu)(-1)^{k+l}}{k! l! \Gamma(1+k+\nu)\Gamma(1+l-\nu)} \left(\frac{x}{2}\right)^{2k+2l-1}, \quad (3.2.12)$$

from which it follows (by considering  $l = k = 0$ ) that  $C = 2/\pi$ . Hence

$$J_\nu(x)Y'_\nu(x) - J'_\nu(x)Y_\nu(x) = \frac{2}{\pi x}. \quad (3.2.13)$$

It is now clear that the general solution of the Bessel equation (3.2.1) is

$$u = AJ_\nu(\lambda r) + BY_\nu(\lambda r), \quad (3.2.14)$$

for all real values of  $\nu$  provided  $Y_\nu(x)$  is suitably interpreted when  $\nu$  is an integer. Figure (3.1) illustrates the general shape of  $J_0(x)$  and  $Y_0(x)$  for finite  $x$ , while figure (3.2) similarly illustrates the behaviour of  $J_1(x)$  and  $Y_1(x)$ .

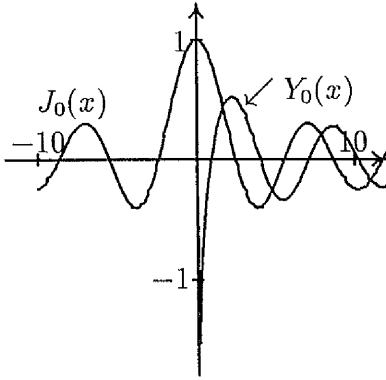


Figure 3.1: Graph of  $J_0(x)$  and  $Y_0(x)$  versus  $x$ .

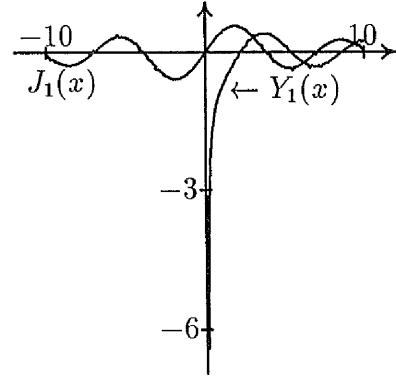


Figure 3.2: Graph of  $J_1(x)$  and  $Y_1(x)$  versus  $x$ .

### 3.3 Modified Bessel Functions

When  $x$  is replaced by  $ix$ , equation (3.2.2) becomes

$$x^2 \frac{d^2 u}{dx^2} + x \frac{du}{dx} - (x^2 + \nu^2)u = 0, \quad (3.3.15)$$

which is known as the Modified Bessel equation of order  $\nu$ . The general solution of (3.3.15) can be deduced from  $J_\nu(x)$  and  $Y_\nu(x)$  by replacing  $x$  with  $ix$ . Since the resulting

functions have complex values, it is more convenient to introduce  $I_\nu(x)$ , which is commonly called the Modified Bessel function of the first kind of order  $\nu$  using the definition

$$I_\nu(x) = e^{-\nu\pi i/2} J_\nu(ix) = \sum_{k=0}^{\infty} \frac{(x)^{\nu+2k}}{2^{\nu+2k} k! \Gamma(\nu + k + 1)} . \quad (3.3.16)$$

The Modified Bessel function of the third kind (often called the Modified Hankel function) is defined in terms of  $I_\nu(x)$  by

$$K_\nu(x) = \frac{\pi}{2} \frac{I_{-\nu}(x) - I_\nu(x)}{\sin \nu\pi} . \quad (3.3.17)$$

The general solution of equation (3.3.15) is therefore

$$u = AI_\nu(x) + BK_\nu(x) . \quad (3.3.18)$$

As with Bessel functions, this general solution is valid for all  $\nu$  provided  $K_\nu(x)$  is interpreted (using L'Hôpital's rule) as the limit given by

$$K_n(x) = \lim_{\nu \rightarrow n} K_\nu(x) = \frac{(-1)^n}{2} \left[ \frac{\partial I_{-\nu}(x)}{\partial \nu} - \frac{\partial I_\nu(x)}{\partial \nu} \right]_{\nu=n} , \quad (3.3.19)$$

when  $\nu = n$ , an integer. In view of the definition of  $Y_\nu(x)$  in (3.2.5) and the connection between  $I_\nu(x)$  and  $J_\nu(x)$  in (3.3.16), it follows from (3.3.17) that  $K_\nu(x)$  can be re-expressed in the form

$$K_\nu(x) = \frac{i\pi}{2} e^{\nu\pi i/2} [J_\nu(ix) + iY_\nu(ix)] . \quad (3.3.20)$$

Repetition of the Wronskian argument for  $I_\nu(x)$  and  $K_\nu(x)$  reveals that both functions are independent and satisfy the relationship

$$I_\nu(x)K'_\nu(x) - I'_\nu(x)K_\nu(x) = -\frac{1}{x} . \quad (3.3.21)$$

Figure (3.3) illustrates the general shape of  $I_0(x)$  and  $K_0(x)$  for finite  $x$  while figure (3.4) serves the same rôle for  $I_1(x)$  and  $K_1(x)$ .

Finally, it is convenient to record here that  $J_\nu(\lambda r)$  and  $Y_\nu(\lambda r)$  satisfy the relationships

$$\begin{aligned} \frac{d}{dr}[r^\nu J_\nu(\lambda r)] &= \lambda r^\nu J_{\nu-1}(\lambda r) , & \frac{d}{dr}[r^{-\nu} J_\nu(\lambda r)] &= -\lambda r^{-\nu} J_{\nu+1}(\lambda r) , \\ \frac{d}{dr}[r^\nu Y_\nu(\lambda r)] &= \lambda r^\nu Y_{\nu-1}(\lambda r) , & \frac{d}{dr}[r^{-\nu} Y_\nu(\lambda r)] &= -\lambda r^{-\nu} Y_{\nu+1}(\lambda r) , \end{aligned} \quad (3.3.22)$$



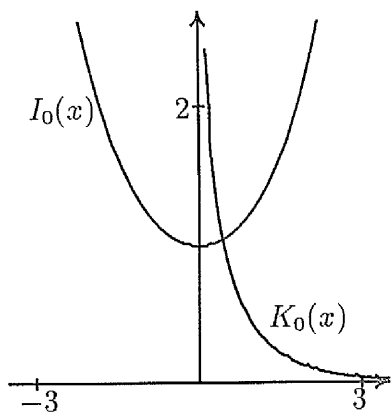


Figure 3.3: Graph of  $I_0(x)$  and  $K_0(x)$  versus  $x$ .

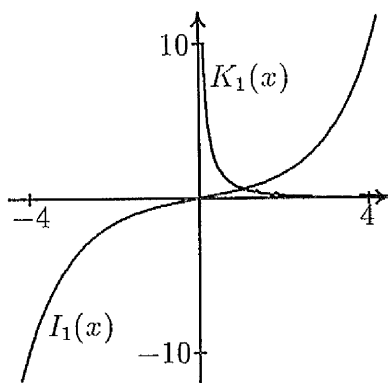


Figure 3.4: Graph of  $I_1(x)$  and  $K_1(x)$  versus  $x$ .

while the functions  $I_\nu(\lambda r)$  and  $K_\nu(\lambda r)$  satisfy

$$\begin{aligned} \frac{d}{dr}[r^\nu I_\nu(\lambda r)] &= \lambda r^\nu I_{\nu-1}(\lambda r), & \frac{d}{dr}[r^{-\nu} I_\nu(\lambda r)] &= \lambda r^{-\nu} I_{\nu+1}(\lambda r), \\ \frac{d}{dr}[r^\nu K_\nu(\lambda r)] &= -\lambda r^\nu K_{\nu-1}(\lambda r), & \frac{d}{dr}[r^{-\nu} K_\nu(\lambda r)] &= -\lambda r^{-\nu} K_{\nu+1}(\lambda r), \end{aligned} \quad (3.3.23)$$

for all real values of  $\nu$ .

### 3.4 Orthogonality of Bessel Functions

Let  $\xi$  and  $\mu$  be two different, non-zero real numbers and let  $u = J_\nu(\xi r)$  and  $w = J_\nu(\mu r)$ . Then  $u$  and  $w$  satisfy the Bessel equations

$$r^2 u'' + r u' + (\xi^2 r^2 - \nu^2) u = 0, \quad r^2 w'' + r w' + (\mu^2 r^2 - \nu^2) w = 0. \quad (3.4.24)$$

Multiplying the first equation by  $w$ , the second equation by  $u$  and subtracting yields the identity

$$(\xi^2 - \mu^2) \int_0^a r u w dr = [r(u'w - uw')]_{r=0}^{r=a}. \quad (3.4.25)$$

Some important results in the theory of orthogonal expansions in terms of Bessel functions are now described. Several of them are used widely in this thesis.

- (a) Suppose that  $\lambda = \xi$  and  $\lambda = \mu$  are different zeros of  $J_\nu(\lambda a)$ ; that is,  $J_\nu(\xi a) = J_\nu(\mu a) = 0$ . Then the left hand side of (3.4.25) vanishes. Hence  $J_\nu(\xi r)$  and  $J_\nu(\mu r)$

are orthogonal over the interval  $[0, a]$  in the sense that

$$\int_0^a r J_\nu(\xi r) J_\nu(\mu r) dr = 0 .$$

- (b) Suppose that  $\lambda = \xi$  and  $\lambda = \mu$  are different zeros of  $J'_\nu(\lambda a)$ ; that is,  $J'_\nu(\xi a) = J'_\nu(\eta a) = 0$ . Then the left hand side of (3.4.25) vanishes, indicating that  $J_\nu(\xi r)$  and  $J_\nu(\mu r)$  are orthogonal over the interval  $[0, a]$  in the sense that

$$\int_0^a r J_\nu(\xi r) J_\nu(\mu r) dr = 0 .$$

This is a similar result to the previous item — the difference lies in the choice of a set of zeros.

- (c) Suppose that  $\lambda = \xi$  and  $\lambda = \mu$  are different zeros of  $J_{\nu+1}(\lambda a)$ ; that is,  $J_{\nu+1}(\xi a) = J_{\nu+1}(\mu a) = 0$ . Result (3.3.22) enables  $J_{\nu+1}(\lambda r)$  to be re-expressed in the form

$$J_{\nu+1}(\lambda r) = \frac{\nu}{\lambda r} J_\nu(\lambda r) - J'_\nu(\lambda r) , \quad (3.4.26)$$

(and the left hand side of (3.4.25) vanishes) This result gives rise to yet another family of zeros for which the members of the family  $J_\nu(\lambda r)$  are all mutually orthogonal over  $[0, a]$ .

On the other hand, when  $\lambda = \xi = \mu$  the equation (3.4.25) can be reworked so that

$$\int_0^a r J_\nu^2(\lambda r) dr = a \lim_{\mu \rightarrow \lambda} \frac{\mu J_\nu(\lambda a) J'_\nu(\mu a) - \lambda J_\nu(\mu a) J'_\nu(\lambda a)}{\lambda^2 - \mu^2} . \quad (3.4.27)$$

L'Hopital's rule is now used to evaluate this limit and leads to the result that

$$\int_0^a r J_\nu^2(\lambda r) dr = \frac{a^2}{2} \left[ J_\nu'^2(\lambda a) + \left( 1 - \frac{\nu^2}{a^2 \lambda^2} \right) J_\nu^2(\lambda a) \right] . \quad (3.4.28)$$

This integral arises in calculating coefficients of the Fourier-Bessel series.

## 3.5 Fourier-Bessel Series

Let  $f$  be a function defined on  $[0, a]$ . Then  $f$  is said to have a Fourier-Bessel series representation over  $[0, a]$  if

$$f(r) \sim \sum_{k=1}^{\infty} f_k J_\nu(\lambda_k r) , \quad (3.5.29)$$

where  $\lambda_k$  are the roots of  $J_\nu(\lambda a) = 0$  or the roots of  $J'_\nu(\lambda a) = 0$ . If  $f$  is a real piecewise continuous function of bounded variation in  $(0, a)$  such that

$$\int_0^a \sqrt{r} |f(r)| dr ,$$

it can be proved that series (3.5.29) converges to  $f(r)$  if  $f$  is continuous at  $r$ , otherwise the series converges to

$$\frac{1}{2}[f(r+) + f(r-)] , \quad (3.5.30)$$

the “average value” of  $f(r)$  at point  $r$ . Coefficients  $f_n$  are determined by first multiplying the series (3.5.29) by  $rJ_\nu(\lambda_n r)$  and then integrating the result over  $[0, a]$ . Orthogonality of Bessel functions eliminates all terms except one so that

$$\int_0^a r f(r) J_\nu(\lambda r) dr = f_n \int_0^a r J_\nu^2(\lambda r) dr . \quad (3.5.31)$$

Evaluation of the right hand side of (3.5.31) depends on the choice of  $\lambda_n$  but follows from equation (3.4.28)

(a) If  $\lambda_1, \lambda_2, \dots$  are the roots of  $J_\nu(\lambda a) = 0$  then

$$f_n = \frac{2}{a^2 J_{\nu+1}^2(\lambda_n a)} \int_0^a x f(x) J_\nu(\lambda_n x) dx . \quad (3.5.32)$$

(b) If  $\lambda_1, \lambda_2, \dots$  are the roots of  $J'_\nu(\lambda a) = 0$  then

$$f_n = \frac{2\nu^2}{a^2 (a^2 \lambda_n^2 - \nu^2) J_\nu^2(\lambda_n a)} \int_0^a x f(x) J_\nu(\lambda_n x) dx . \quad (3.5.33)$$

## 3.6 Weber-Orr Transforms

General forms of finite Weber-Orr transforms are derived from finite Hankel transforms originally defined by Sneddon [22]. Olesiak [15] provides detailed discussion of the properties of infinite Weber-Orr transforms together with some applications in the theory of elasticity. The general form of the finite Hankel transform of  $f(x)$  is

$$\bar{f}(\lambda) = \int_a^b x f(x) K(\lambda, x) dx \quad 0 \leq a < b . \quad (3.6.34)$$

If  $a > 0$  then (3.6.34) is of Weber-Orr type with kernel function

$$K(\lambda, r) = C_{\mu, \nu}(\lambda r, \lambda a) = J_\mu(\lambda r) Y_\nu(\lambda a) - Y_\mu(\lambda r) J_\nu(\lambda a) , \quad (3.6.35)$$

in which  $\mu$  and  $\nu$  are positive integers and  $J_\mu(x)$ ,  $Y_\mu(x)$  are respectively the Bessel function of the first and second kinds, both of order  $\mu$ . General properties of  $C_{\mu\nu}$  can easily be established from those of Bessel functions. In particular,

$$\begin{aligned} C_{\mu\nu}(\lambda r, \lambda a) &= -C_{\nu\mu}(\lambda r, \lambda a), \quad C_{\mu\mu}(x\lambda, x\lambda) \equiv 0, \quad C_{(1+\mu)\mu}(\lambda r, \lambda r) = \frac{2}{\pi\lambda r}, \\ \frac{d}{dr}(r^{-\mu}C_{\mu\nu}(\lambda r, \lambda a)) &= -\lambda r^{-\mu}C_{(1+\mu)\nu}(\lambda r, \lambda a), \\ \frac{d}{dr}(r^\mu C_{\mu\nu}(\lambda r, \lambda a)) &= \lambda r^\mu C_{(\mu-1)\nu}(\lambda r, \lambda a). \end{aligned} \quad (3.6.36)$$

The inverse transform can be represented by the series

$$f(r) = f_0 + \sum_{n=1}^{\infty} f_n C_{\mu\nu}(\lambda r, \lambda a), \quad (3.6.37)$$

where  $\lambda_n$  are chosen to be the positive roots of equation  $C_{\mu\nu}(\lambda b, \lambda a) = 0$  and coefficients  $f_0, f_1 \dots$  can be evaluated by first multiplying the series (3.6.37) by  $rC_{\mu\nu}(\lambda_n r, \lambda_n a)$  and then integrating the result over  $[a, b]$ . The functions  $C_{\mu\nu}(\lambda_n r, \lambda_n a)$  can be proved to be mutually orthogonal by a repetition of the argument that was used for  $J_\nu(\lambda r)$  and  $Y_\nu(\lambda r)$ .

It can be shown that

$$\begin{aligned} f_0 &= \frac{2}{b^2 - a^2} \int_a^b r f(r) dr, \\ f_n &= \frac{\pi^2 \lambda^2}{2} \frac{J_\mu^2(\lambda b)}{J_\mu^2(\lambda a) - J_\mu^2(\lambda b)} \int_a^b r f(r) C_{\mu\nu}(\lambda r, \lambda a) dr. \end{aligned} \quad (3.6.38)$$

## Chapter 4

# Response of an Incompressible Elastic Annulus to a Periodic Axial Driving Force

### 4.1 Introduction

This chapter investigates small axial deformations of an incompressible isotropic elastic material formed into the shape of an annulus of uniform thickness  $d$ , outer radius  $b$  and containing an axial cylindrical hole of radius  $a$  ( $a < b$ ). A rigid shaft passes through this hole and is bonded to the material of the annulus. Let cylindrical polar coordinates  $(r, \theta, z)$  be chosen so that the annulus occupies the region

$$a \leq r \leq b, \quad -\pi \leq \theta \leq \pi, \quad 0 \leq z \leq d.$$

Suppose that outer boundary  $r = b$  is fixed and that, in the usual notation of tensor calculus, displacement  $\mathbf{v} = v^i \mathbf{g}_i$  is induced in the annulus by the application of periodic axial forces to the rigid rod. In effect, the configuration closely resembles a shock absorber.

### 4.2 Governing Equations

Suppose that the undeformed annulus is parameterised by coordinates  $\theta^i$  with covariant metric tensor  $g_{ij}$  and base vectors  $\mathbf{g}_i$  and that the deformation is described by the

representation

$$\mathbf{x} = \mathbf{X} + \varepsilon \mathbf{v} + \varepsilon^2 \mathbf{w} + \dots, \quad (4.2.1)$$

where  $\varepsilon$  is a “small” parameter. Constitutive theory of incompressible isotropic solids, taking account of viscous effects, leads to the linear stress tensor

$$t^{ij} = -pg^{ij} + \mu (v^i|{}^j + v^j|{}^i) + \eta \frac{\partial}{\partial t} (v^i|{}^j + v^j|{}^i), \quad (4.2.2)$$

where  $p$  is an arbitrary function of position and time and the notation  $|$  denotes covariant differentiation with respect to metric  $g_{ij}$ . Details are available in Green and Adkins [16] whose notation has been used here. Moreover, the incompressibility condition constrains  $\mathbf{v}$  to satisfy  $\text{div } \mathbf{v} = v^i|_i = 0$ . In the absence of external body forces, the balance of linear momentum requires that

$$\rho \frac{\partial^2 x^j}{\partial t^2} = t^{ij}|_i. \quad (4.2.3)$$

Suppose that a periodic force, modelled by  $F(t) = F e^{if_\omega t}$ , is applied to the rigid shaft and induces time-dependent displacement  $\mathbf{v}(\mathbf{x}, t) = \mathbf{v}(\mathbf{x}) e^{if_\omega t}$  and pressure  $p(\mathbf{x}, t) = p(\mathbf{x}) e^{if_\omega t}$ . In these circumstances, the stress tensor (4.2.2) is represented by  $t^{ij}(\mathbf{x}, t) = t^{ij}(\mathbf{x}) e^{if_\omega t}$  where

$$t^{ij}(\mathbf{x}) = -pg^{ij} + (\mu + if_\omega \eta)(v^i|{}^j + v^j|{}^i). \quad (4.2.4)$$

Displacement  $\mathbf{v}(\mathbf{x})$  is solenoidal and the momentum equation corresponding to (4.2.3) is

$$-\rho f_\omega^2 v^j = t^{ij}|_i. \quad (4.2.5)$$

The axial nature of the proposed deformation suggests that  $\mathbf{v}(\mathbf{x})$  has component form

$$\mathbf{v} = u(r, z) \mathbf{g}_1 + h(r, z) \mathbf{g}_3, \quad (4.2.6)$$

and on this basis, non-zero components of the stress tensor are

$$\begin{aligned} t^{11} &= -p + 2\mu(1 + i\xi) \frac{\partial u}{\partial r}, & t^{22} &= -\frac{p}{r^2} + 2\mu(1 + i\xi) \frac{u}{r^3}, \\ t^{33} &= -p + 2\mu(1 + i\xi) \frac{\partial h}{\partial z}, & t^{13} = t^{31} &= \mu(1 + i\xi) \left( \frac{\partial u}{\partial z} + \frac{\partial h}{\partial r} \right). \end{aligned} \quad (4.2.7)$$

Since the material is incompressible then  $u(r, z)$  and  $h(r, z)$  satisfy

$$\text{div } \mathbf{v} = \frac{\partial u}{\partial r} + \frac{u}{r} + \frac{\partial h}{\partial z} = 0. \quad (4.2.8)$$

When constitutive relations (4.2.7) are substituted into momentum equations (4.2.5), it is easily verified that the second of these equations is satisfied provided  $p = p(r, z)$ . The remaining equations yield

$$\begin{aligned} -\rho f_{\omega}^2 u &= -\frac{\partial p}{\partial r} + \mu(1 + i\xi) \left( 2\frac{\partial^2 u}{\partial r^2} + \frac{\partial^2 u}{\partial z^2} + \frac{\partial^2 h}{\partial r \partial z} + \frac{2}{r} \frac{\partial u}{\partial r} - 2\frac{u}{r^2} \right), \\ -\rho f_{\omega}^2 h &= -\frac{\partial p}{\partial z} + \mu(1 + i\xi) \left( 2\frac{\partial^2 h}{\partial z^2} + \frac{\partial^2 h}{\partial r^2} + \frac{\partial^2 u}{\partial r \partial z} + \frac{1}{r} \frac{\partial u}{\partial z} + \frac{1}{r} \frac{\partial h}{\partial r} \right). \end{aligned} \quad (4.2.9)$$

### 4.3 Boundary Conditions

Equations (4.2.9) must be supplemented by suitable boundary conditions which ensure that

- (a) boundaries  $z = 0$  and  $z = d$  are stress free;
- (b) the outer boundary of the annulus is held fixed;
- (c) every point on the inner boundary of the annulus is similarly displaced by an amount  $H e^{i(f_{\omega} t + \phi)}$  where  $H$  and  $\phi$  are constants to be determined;
- (d) the shear stress over the outer and inner cylindrical surfaces of the body both integrate to the applied driving force  $F e^{i f_{\omega} t}$ .

These conditions are now treated in sequence. On  $z = d$ , the unit outward normal is  $\mathbf{g}_3$  and the related stress vector is  $\mathbf{t} = n_i t^{ij} \mathbf{g}_j = t^{3j} \mathbf{g}_j = t^{31} \mathbf{g}_1 + t^{33} \mathbf{g}_3$ . Since  $z = d$  is required to be stress-free, then  $t^{31} = t^{33} = 0$  on  $z = d$ . A similar argument yields the same result for  $z = 0$ . In view of expressions (4.2.7), horizontal boundaries  $z = 0$  and  $z = d$  are stress-free provided that

$$-p + 2\mu(1 + i\xi) \frac{\partial h}{\partial z} = 0, \quad \frac{\partial u}{\partial z} + \frac{\partial h}{\partial r} = 0, \quad \text{on } z = 0, d, \quad (4.3.10)$$

where factor  $e^{i f_{\omega} t}$  has been cancelled. On  $r = b$ , the outer boundary, both radial and axial displacements are zero whereas on  $r = a$ , the inner boundary, the radial displacement is zero but the rod itself moves in sympathy with the forcing term but with a constant phase shift. Hence on the cylindrical boundaries

$$\left. \begin{array}{l} u = 0 \\ h = 0 \end{array} \right\} \text{ on } r = b, \quad \left. \begin{array}{l} u = 0 \\ h = H e^{i\phi} \end{array} \right\} \text{ on } r = a, \quad (4.3.11)$$

where factor  $e^{if\omega t}$  has again been cancelled. The boundary  $r = a$  has outward unit normal  $-\mathbf{g}_1$  and so the stress vector on the inner boundary is  $\mathbf{t} = -t^{11}\mathbf{g}_1 - t^{13}\mathbf{g}_3$ . Accumulated shear stress on cylindrical boundaries must balance the applied force and hence

$$F e^{if\omega t} \mathbf{g}_3 = - \left( \iint t^{13} dA \right) \mathbf{g}_3 = -2\pi\mu(1+i\xi)R \left( \int_0^d \left( \frac{\partial h}{\partial a} + \frac{\partial u}{\partial z} \right) dz \right) e^{if\omega t} \mathbf{g}_3 , \quad (4.3.12)$$

where  $R = a$  and  $R = b$  denote respectively inner and outer boundaries. In conclusion, applied force  $F$  enters the boundary value problem subject to conditions:

$$F = -2\pi\mu(1+i\xi)a \int_0^d \frac{\partial h(a, z)}{\partial r} dz , \quad F = -2\pi\mu(1+i\xi)b \int_0^d \frac{\partial h(b, z)}{\partial r} dz . \quad (4.3.13)$$

### 4.3.1 Non-dimensional Problem

Before analysing the boundary value problem just posed, it is good mathematical practice to non-dimensionalise all preceding equations and boundary conditions. Let non-dimensional coordinates  $r^*$ ,  $z^*$ , non-dimensional displacements  $u^*$ ,  $h^*$ , non-dimensional pressure  $p^*$  and non-dimensional parameters be introduced by the definitions

$$\begin{aligned} r^* &= \frac{r}{a}, & z^* &= \frac{z}{d}, & u^* &= \frac{u}{d}, & h^* &= \frac{h}{d}, \\ p^* &= \frac{p}{\mu}, & \nu &= \frac{d}{a}, & \xi &= \frac{f\omega\eta}{\mu}, & \sigma &= \frac{\rho f\omega^2 d^2}{\mu}. \end{aligned} \quad (4.3.14)$$

Algebraic details of this operation are suppressed but after some analysis in which the incompressibility condition is used to further simplify the momentum equations, it can be shown that momentum equations (4.2.9) and incompressibility condition (4.2.5) reduce ultimately to

$$\begin{aligned} -\nu \frac{\partial p}{\partial r} + (1+i\xi) \frac{\partial^2 u}{\partial z^2} - \nu(1+i\xi) \frac{\partial^2 h}{\partial r \partial z} &= -\sigma u, \\ -\frac{\partial p}{\partial z} + (1+i\xi) \frac{\partial^2 h}{\partial z^2} + (1+i\xi)\nu^2 \left( \frac{\partial^2 h}{\partial r^2} + \frac{1}{r} \frac{\partial h}{\partial r} \right) &= -\sigma h, \\ \frac{\partial h}{\partial z} + \nu \left( \frac{\partial u}{\partial r} + \frac{u}{r} \right) &= 0, \end{aligned} \quad (4.3.15)$$

where the superscript star notation has been dropped although all quantities appearing in (4.3.15) are non-dimensional. Similarly, boundary conditions (4.3.10), (4.3.11) and



(4.3.13) have non-dimensional form

$$\begin{aligned}
& -p + 2(1 + i\xi)\frac{\partial h}{\partial z} = 0, \quad \frac{\partial u}{\partial z} + \nu\frac{\partial h}{\partial r} = 0, \quad \text{on } z = 0, 1 \\
& u = 0, \quad h = He^{i\phi}, \quad \frac{F}{2\pi\mu d^2} = -(1 + i\xi) \int_0^1 \frac{\partial h(1, z)}{\partial r} dz, \quad \text{on } r = 1 \\
& u = 0, \quad h = 0, \quad \frac{F}{2\pi\mu d^2} = -(1 + i\xi)\beta \int_0^1 \frac{\partial h(\beta, z)}{\partial r} dz, \quad \text{on } r = \beta,
\end{aligned} \tag{4.3.16}$$

where  $\beta = b/a$  and  $H$  and  $\phi$  are constants to be determined. Equations (4.3.15) and (4.3.16) constitute the final form of the boundary value problem.

## 4.4 Transformed Equations

Solutions to (4.3.15) and (4.3.16) are obtained using finite Weber-Orr transforms, which were introduced in Chapter two.

Equations (4.3.15) can be transformed naturally in two ways

- Take the  $C_{00}$  transform of  $p$  and  $h$  and the  $C_{10}$  transform of  $u$ . In this case, unknown functions introduced by the integration process relate to normal stress on cylindrical surfaces  $\mathcal{S}_1 = \{(r, z) : r = 1, z \in [0, 1]\}$  and  $\mathcal{S}_2 = \{(r, z) : r = \beta, z \in [0, 1]\}$ .
- Take the  $C_{01}$  transform of  $p$  and  $h$  and the  $C_{11}$  transform of  $u$ . In this case, unknown functions introduced by the integration process relate to shear stress on cylindrical surfaces  $\mathcal{S}_1$  and  $\mathcal{S}_2$ .

In this work, the second approach is preferred since some of the boundary requirements listed in (4.3.16) already involve shear stress on  $\mathcal{S}_1$  and  $\mathcal{S}_2$ . Let finite Weber-Orr transforms  $\bar{u}(z, \lambda)$ ,  $\bar{h}(z, \lambda)$  and  $\bar{p}(z, \lambda)$  be defined by the integrals

$$\begin{aligned}
\bar{u}(z, \lambda) &= \int_1^\beta ru(r, z)C_{11}(\lambda r, \lambda) dr, \\
\bar{h}(z, \lambda) &= \int_1^\beta rh(r, z)C_{01}(\lambda r, \lambda) dr, \\
\bar{p}(z, \lambda) &= \int_1^\beta rp(r, z)C_{01}(\lambda r, \lambda) dr,
\end{aligned} \tag{4.4.17}$$

where parameter  $\lambda$  is chosen to be a root of  $C_{11}(\beta\lambda, \lambda) = 0$ . Finally, note that  $u(r, z)$  and  $h(r, z)$  can be recovered from their respective finite Weber-Orr transforms using the

formulae

$$\begin{aligned}
u(r, z) &= \frac{\pi^2}{2} \sum_{n=1}^{\infty} \frac{\lambda_n^2 J_1^2(\lambda_n \beta) \bar{u}(\lambda_n, z)}{J_1^2(\lambda_n) - J_1^2(\lambda_n \beta)} C_{11}(\lambda_n r, \lambda_n) , \\
h(r, z) &= h_0(z) + \frac{\pi^2}{2} \sum_{n=1}^{\infty} \frac{\lambda_n^2 J_1^2(\lambda_n \beta) \bar{h}(\lambda_n, z)}{J_1^2(\lambda_n) - J_1^2(\lambda_n \beta)} C_{01}(\lambda_n r, \lambda_n) ,
\end{aligned} \tag{4.4.18}$$

where  $\lambda_n, n = 1, 2, \dots$  are the positive roots of  $C_{11}(\lambda \beta, \lambda) = 0$  so that

$$h_0(z) = \frac{2}{\beta^2 - 1} \int_1^\beta r h(r, z) dr . \tag{4.4.19}$$

Now multiply the third of field equations (4.3.15) (the incompressibility condition) by  $r$  and integrate with respect to  $r$  over  $[1, \beta]$  to obtain:

$$\frac{d}{dz} \left( \int_1^\beta r h(r, z) dr \right) = \int_1^\beta r \frac{\partial h}{\partial z} dr = - \int_1^\beta \left( u + r \frac{\partial u}{\partial r} \right) dr = - [ru(r, z)]_1^\beta = 0 . \tag{4.4.20}$$

Hence, it is now clear from (4.4.19) that  $h_0 = C$ , an unknown constant. Of course, functions  $\bar{u}, \bar{h}$  appearing in (4.4.18) are just Weber-Orr transforms of  $u$  and  $h$  respectively. These are determined by first transforming the original field equations (4.3.15) and boundary conditions (4.3.16) and then integrating the resulting system of ordinary differential equations. The first of the field equations (4.3.15) is multiplied by  $rC_{11}(\lambda r, \lambda)$ , the other two are multiplied by  $rC_{01}(\lambda r, \lambda)$  and the resulting three equations are now integrated with respect to  $r$  over the interval  $[1, \beta]$ . The technical details are straightforward and use only the properties of the Weber-Orr functions outlined in (3.6.36) (see appendix A for further details of the transformation). In conclusion,  $\bar{u}(z, \lambda)$ ,  $\bar{h}(z, \lambda)$  and  $\bar{p}(z, \lambda)$  satisfy the ordinary differential equations

$$\begin{aligned}
(1 + i\xi) \frac{d^2 \bar{u}}{dz^2} + \omega \bar{p} + (1 + i\xi) \omega \frac{d\bar{h}}{dz} &= -\sigma \bar{u} , \\
(1 + i\xi) \left( \frac{d^2 \bar{h}}{dz^2} - \omega^2 \bar{h} \right) - \frac{d\bar{p}}{dz} + \frac{2\nu^3}{\pi\omega} (1 + i\xi) g(z) &= -\sigma \bar{h} , \\
\frac{d\bar{h}}{dz} + \omega \bar{u} &= 0 ,
\end{aligned} \tag{4.4.21}$$

in which

$$\begin{aligned}
g(z) &= g_1(z) - \frac{J_1(\lambda)}{J_1(\lambda\beta)} g_\beta(z) , \quad \omega = \nu \lambda , \\
g_1(z) &= \frac{\partial h(1, z)}{\partial r} , \quad g_\beta(z) = \frac{\partial h(\beta, z)}{\partial r} .
\end{aligned} \tag{4.4.22}$$

These equations form a fourth order system of ordinary differential equations. The original boundary conditions (4.3.16) on  $z = 0$  and  $z = 1$  are now suitably transformed to obtain the four boundary conditions

$$\left. \begin{aligned} \frac{d\bar{u}}{dz} - \omega\bar{h} &= 0, \\ -\bar{p} + 2(1+i\xi)\frac{d\bar{h}}{dz} &= 0, \end{aligned} \right\} \quad \text{on } z = 0, 1. \quad (4.4.23)$$

It is clear from definitions of the  $\lambda$ 's that solution (4.4.18) for  $u(r, z)$  automatically ensures that  $u(1, z) = u(\beta, z) = 0$  and hence unknown functions  $g_1(z)$ ,  $g_2(z)$  and values for  $H$ ,  $\phi$  and  $C$  must be chosen to satisfy the remainder of the boundary conditions (4.3.16); that is,

$$\begin{aligned} h &= 0, & \frac{F}{2\pi\mu d^2} &= -\beta(1+i\xi) \int_0^1 g_\beta(t) dt & \text{on } r = \beta, \\ h &= He^{i\phi}, & \frac{F}{2\pi\mu d^2} &= -(1+i\xi) \int_0^1 g_1(t) dt & \text{on } r = 1. \end{aligned} \quad (4.4.24)$$

#### 4.4.1 Solution Procedure

Solution procedure begins by recognising that  $\bar{u}$  and  $\bar{h}$  can easily be eliminated from equations (4.4.21) so that  $\bar{p}$  satisfies

$$\frac{d^2\bar{p}}{dz^2} - \omega^2\bar{p} = \frac{2\nu^3}{\pi\omega}(1+i\xi)\frac{dg}{dz}. \quad (4.4.25)$$

It is a relatively straightforward matter to confirm that

$$\bar{p} = A \cosh \omega z + B \sinh \omega z + \frac{2\nu^3}{\pi\omega}(1+i\xi) \int_0^z g(t) \cosh \omega(z-t) dt, \quad (4.4.26)$$

where  $A$  and  $B$  are constants to be determined by boundary conditions (4.4.23). In view of the solution for  $\bar{p}$ , it now follows from equations (4.4.21) that  $\bar{h}$  satisfies the second order ordinary differential equation

$$\frac{d^2\bar{h}}{dz^2} - \Omega^2\bar{h} = \frac{\omega}{1+i\xi} (A \sinh \omega z + B \cosh \omega z) + \frac{2\nu^3}{\pi} \int_0^z g(t) \sinh \omega(z-t) dt, \quad (4.4.27)$$

where

$$\Omega^2 = \omega^2 - \frac{\sigma}{1+i\xi}. \quad (4.4.28)$$

As with the equation for  $\bar{p}$ , it is easily verified that (4.4.27) has general solution

$$\begin{aligned} \bar{h} &= C \sinh \Omega z + D \cosh \Omega z + \frac{\omega}{\sigma} (A \sinh \omega z + B \cosh \omega z) \\ &\quad + \frac{2\nu^3}{\pi\sigma}(1+i\xi) \int_0^z g(t) \left[ \sinh \omega(z-t) - \frac{\omega}{\Omega} \sinh \Omega(z-t) \right] dt, \end{aligned} \quad (4.4.29)$$

where  $C$  and  $D$  are two further constants of integration. Once  $\bar{h}$  is known,  $\bar{u}$  is obtained directly from (4.4.21) and has the form

$$\begin{aligned}\bar{u} = & -\frac{\Omega}{\omega} [C \cosh \Omega z + D \sinh \Omega z] - \frac{\omega}{\sigma} [A \cosh \omega z + B \sinh \omega z] \\ & - \frac{2\nu^3}{\pi\sigma} (1 + i\xi) \int_0^z g(t) [\cosh \omega(z-t) - \cosh \Omega(z-t)] dt .\end{aligned}\quad (4.4.30)$$

Let three new functions,  $G_1(z)$ ,  $G_\beta(z)$  are  $G(z)$ , be introduced by the definitions

$$G_1(z) = \int_0^z g_1(t) dt , \quad G_\beta(z) = \int_0^z g_\beta(t) dt , \quad G(z) = \int_0^z g(t) dt . \quad (4.4.31)$$

These manoeuvres facilitate the solution procedure for two reasons

- They provide a natural mechanism for the introduction of the externally supplied driving force  $F$ . Indeed, the boundary conditions (4.4.24) are conveniently rewritten in the form

$$\frac{F}{2\pi\mu d^2} = -(1 + i\xi)G_1(1) , \quad \frac{F}{2\pi\mu d^2} = -\beta(1 + i\xi)G_\beta(1) . \quad (4.4.32)$$

- If the shear stress is singular on  $r = 1$  at  $z = 0, 1$ ; that is  $g_1(z)$  has integrable singularities at these points (as is likely to be the case), then any numerical procedure which aims to find  $g_1(z)$  directly is doomed to failure. On the other hand,  $G_1(z)$  is a well behaved function which is zero by construction at  $z = 0$  and is finite at  $z = 1$ . A similar remark applies to  $G_\beta(z)$ .

It is a straightforward matter to replace occurrences of  $g(t)$  in expressions (4.4.26), (4.4.29) and (4.4.30) with  $G(t)$ , obtaining new forms in the process

$$\begin{aligned}\bar{p} = & A \cosh \omega z + B \sinh \omega z + \frac{2\nu^3}{\pi\omega} (1 + i\xi) G(z) \\ & + \frac{2\nu^3}{\pi} (1 + i\xi) \int_0^z G(t) \sinh \omega(z-t) dt , \\ \bar{h} = & C \sinh \Omega z + D \cosh \Omega z + \frac{\omega}{\sigma} (A \sinh \omega z + B \cosh \omega z) \\ & + \frac{2\nu^3}{\pi\sigma} (1 + i\xi) \omega \int_0^z G(t) [\cosh \omega(z-t) - \cosh \Omega(z-t)] dt , \\ \bar{u} = & -\frac{\Omega}{\omega} [C \cosh \Omega z + D \sinh \Omega z] - \frac{\omega}{\sigma} [A \cosh \omega z + B \sinh \omega z] \\ & - \frac{2\nu^3}{\pi\sigma} (1 + i\xi) \int_0^z G(t) [\omega \sinh \omega(z-t) - \Omega \sinh \Omega(z-t)] dt .\end{aligned}\quad (4.4.33)$$

Coefficients  $A$ ,  $B$ ,  $C$  and  $D$  are determined from boundary conditions (4.5.52). Let parameters  $\alpha$  and  $\varphi$  be defined by the ratios

$$\alpha = \frac{2\omega^2}{\omega^2 + \Omega^2}, \quad \varphi = \frac{2\Omega\omega}{\omega^2 + \Omega^2}. \quad (4.4.34)$$

It can be quickly established that the most general form for expressions (4.4.33) satisfying the two boundary conditions (4.4.23) at  $z = 0$  is:

$$\begin{aligned} \bar{p} &= -\frac{\sigma}{\omega}(C\varphi \cosh \omega z + \frac{D}{\alpha} \sinh \omega z) + \frac{2\nu^3}{\pi\omega}(1 + i\xi)G(z) \\ &\quad + \frac{2\nu^3}{\pi}(1 + i\xi) \int_0^z G(t) \sinh \omega(z - t) dt, \\ \bar{h} &= C(\sinh \Omega z - \varphi \sinh \omega z) + D(\cosh \Omega z - \frac{\cosh \omega z}{\alpha}) \\ &\quad + \frac{2\nu^3}{\pi\sigma}(1 + i\xi)\omega \int_0^z G(t) [\cosh \omega(z - t) - \cosh \Omega(z - t)] dt, \\ \bar{u} &= C\varphi(\cosh \omega z - \frac{\cosh \Omega z}{\alpha}) + \frac{D}{\alpha}(\sinh \omega z - \varphi \sinh \Omega z) \\ &\quad - \frac{2\nu^3}{\pi\sigma}(1 + i\xi) \int_0^z G(t) [\omega \sinh \omega(z - t) - \Omega \sinh \Omega(z - t)] dt. \end{aligned} \quad (4.4.35)$$

Parameters  $C$  and  $D$  are now determined by applying boundary conditions (4.4.23) at  $z = 1$ . In fact, these parameters are solutions of the simultaneous equations

$$\begin{aligned} C(\alpha\varphi \sinh \omega - \sinh \Omega) + D(\cosh \omega - \cosh \Omega) &= \\ \frac{2\nu^3}{\pi\sigma}\omega(1 + i\xi) \int_0^1 G(t) [\alpha \cosh \omega(1 - t) - \cosh \Omega(1 - t)] dt, \\ C\varphi(\cosh \Omega - \cosh \omega) + D(\varphi \sinh \Omega - \frac{\sinh \omega}{\alpha}) &= \frac{\nu^2\varphi}{\pi\omega\Omega}G(1) \\ -\frac{2\nu^3}{\pi\sigma}\omega(1 + i\xi) \int_0^1 G(t) [\sinh \omega(1 - t) - \varphi \sinh \Omega(1 - t)] dt. \end{aligned}$$

## 4.5 Fourier-series Representation

Derivation of final expressions for  $\bar{p}$ ,  $\bar{h}$  and  $\bar{u}$  is algebraically complicated. Unlike a conventional transform technique, expressions (4.4.33) for transformed pressure  $\bar{p}$ , transformed displacements  $\bar{u}$  and  $\bar{h}$  are still unknown in that they contain integrals involving the unknown function  $G(t)$ . In order to handle these integrals,  $G(t)$  is represented by a complex valued Fourier series in a real variable  $z \in [0, 1]$ . Two options present themselves

- (a) Extend  $G_1(t)$ ,  $G_\beta(t)$  into  $[-1, 0]$  as odd functions (giving two sine series). These series converge to zero at  $z = 1$  and so this approach is satisfactory provided that  $G_1(1) = G_\beta(1) = 0$  or, alternatively, that their values are not required in subsequent analysis. It is self evident from (4.4.24) that values for  $G_1(1)$  and  $G_\beta(1)$  will be required and that these values are not zero. Hence it makes no sense mathematically to represent  $G_1$  and  $G_\beta$  by a half-range sine series and an attempt to do so is likely to experience serious numerical difficulties arising from the non-uniform convergence of these series in the vicinity of  $z = 1$  (i.e. the Gibb's phenomenon).
- (b) Extend  $G_1(t)$  and  $G_\beta(t)$  into  $[-1, 0]$  as an even function (giving a cosine series). In this case both  $G_1$  and  $G_\beta$  can be evaluated at  $z = 0$  and  $z = 1$  by direct substitution into their Fourier series.

In view of these comments,  $G_1$  and  $G_\beta$  are now represented by the half range cosine series

$$G_1(z) = \sum_{r=0}^{\infty} G_r^{(1)} \cos(r\pi z), \quad G_\beta(z) = \sum_{r=0}^{\infty} G_r^{(\beta)} \cos(r\pi z), \quad (4.5.36)$$

where

$$G_1(0) = \sum_{r=0}^{\infty} G_r^{(1)} = 0, \quad G_\beta(0) = \sum_{r=0}^{\infty} G_r^{(\beta)} = 0. \quad (4.5.37)$$

Occurrences of  $G$  in  $\bar{p}$ ,  $\bar{u}$  and  $\bar{h}$  are now replaced by the infinite series

$$G(z) = \sum_{r=1}^{\infty} G_r \cos(r\pi z), \quad G_r = G_r^{(1)} - \frac{J_1(\lambda)}{J_1(\lambda\beta)} G_r^{(\beta)} = G_r^{(1)} - f(\lambda) G_r^{(\beta)}, \quad (4.5.38)$$

where  $f(\lambda)$  is defined to be the ratio

$$f(\lambda) = \frac{J_1(\lambda)}{J_1(\lambda\beta)}. \quad (4.5.39)$$

For future convenience, let  $\chi_n$ ,  $Q(\lambda)$ ,  $\psi(\lambda)$  and  $\phi(\lambda)$  be defined by

$$\begin{aligned} \chi_n &= \frac{n^2 \pi^2 (\Omega^2 + 2\omega^2 + n^2 \pi^2)}{(\omega^2 + n^2 \pi^2)(\Omega^2 + n^2 \pi^2)}, \\ Q(\lambda) &= 2 \cosh \omega \cosh \Omega - 2 - \left( \alpha \varphi + \frac{1}{\alpha \varphi} \right) \sinh \omega \sinh \Omega, \\ \psi(\lambda) &= \frac{\sigma}{\omega^2 \Omega Q(\lambda)} [\alpha \varphi \sinh \omega (\cosh \Omega - 1) - \sinh \Omega (\cosh \omega - 1)], \\ \phi(\lambda) &= \frac{\sigma}{\omega^2 \Omega Q(\lambda)} [\alpha \varphi \sinh \omega (\cosh \Omega + 1) - \sinh \Omega (\cosh \omega + 1)]. \end{aligned} \quad (4.5.40)$$

For reasons that will shortly become clear, all even coefficients in the Fourier series of  $G_1(z)$  and  $G_\beta(z)$  are identically zero except in  $G_0^{(1)}$  and  $G_0^{(\beta)}$ , where values are determined to ensure that  $G_1(0) = G_\beta(0) = 0$ . In order to obtain this symmetry, the following analysis treats even and odd coefficients separately. It can be shown that

$$\begin{aligned} \bar{h}(\lambda, z) = & \frac{\nu^3 \omega}{\pi \sigma} \sum_{n=1}^{\infty} (G_{2n} \chi_{2n} R(z) + G_{2n-1} \chi_{2n-1} S(z)) \\ & - 2\nu^3 \omega \sum_{k=1}^{\infty} \frac{k G_k \sin(k\pi z)}{(\omega^2 + k^2 \pi^2)(\Omega^2 + k^2 \pi^2)}, \end{aligned} \quad (4.5.41)$$

where  $R(z)$  and  $S(z)$  are given by

$$\begin{aligned} R(z) &= \psi(\lambda) \left[ \frac{\sinh \Omega(\frac{1}{2} - z)}{\sinh(\Omega/2)} - \frac{1}{\alpha} \frac{\sinh \omega(\frac{1}{2} - z)}{\sinh(\omega/2)} \right], \\ S(z) &= \phi(\lambda) \left[ \frac{\cosh \Omega(\frac{1}{2} - z)}{\cosh(\Omega/2)} - \frac{1}{\alpha} \frac{\cosh \omega(\frac{1}{2} - z)}{\cosh(\omega/2)} \right]. \end{aligned} \quad (4.5.42)$$

Similar lengthy expressions can be derived for  $\bar{p}$  and  $\bar{u}$  but since this work is aimed at a description of surface deformation induced by a periodic axial force, then an additional complication introduced by these solutions contributes nothing to the task in hand. In particular, they have no rôle to play in the determination of the Fourier components of  $G$ . Once these are known, pressure and radial displacement may be calculated as required. Hence  $\bar{h}(\lambda, 1)$ , the transform of surface deformation, is expressed in terms of Fourier coefficients by the formula

$$\bar{h}(\lambda, 1) = \frac{\nu^3}{2\pi\omega(1+i\xi)} \sum_{n=1}^{\infty} (G_{2n-1} \phi(\lambda_n) \chi_{2n-1} - G_{2n} \psi(\lambda_n) \chi_{2n}), \quad (4.5.43)$$

and the resulting surface deformation is calculated from (4.4.18) by

$$h(r, 1) = C + \frac{\pi^2}{2} \sum_{n=1}^{\infty} \frac{\lambda_n^2 \bar{h}(\lambda_n, 1)}{f^2(\lambda_n) - 1} C_{01}(\lambda_n r, \lambda_n), \quad (4.5.44)$$

having recognised that  $h_0(z) = C$ , a constant. It remains now to calculate Fourier coefficients for  $G_1(z)$  and  $G_\beta(z)$ . The key to success lies in the observation that if  $R(z)$  and  $S(z)$  are replaced by their half-range sine series in  $[-1, 1]$ , the resulting series will be the half-range sine series of  $\bar{h}(\lambda, z)$ . Of course,  $\bar{h}(\lambda, 1)$  cannot be computed from this series but the representation is exact for  $z \in (0, 1)$ . This is the reason for separate treatment of  $\bar{h}(\lambda, 1)$ . Straightforward calculus reveals that  $R(z)$  and  $S(z)$  have half-range Fourier sine

series

$$\begin{aligned} R(z) &= \frac{2\sigma\psi(\lambda)}{\omega^2\pi(1+i\xi)} \sum_{k=1}^{\infty} \chi_{2k} \frac{\sin 2k\pi z}{2k}, \\ S(z) &= \frac{2\sigma\phi(\lambda)}{\omega^2\pi(1+i\xi)} \sum_{k=1}^{\infty} \chi_{2k-1} \frac{\sin (2k-1)\pi z}{(2k-1)}. \end{aligned} \quad (4.5.45)$$

Hence  $\bar{h}(\lambda, z)$  has half-range Fourier series representation

$$\bar{h}(\lambda, z) = \sum_{k=1}^{\infty} h_k(\lambda) \frac{\sin k\pi z}{k}, \quad (4.5.46)$$

where the coefficients  $h_k(\lambda)$  are given by

$$h_k(\lambda) = \begin{cases} \frac{2\psi(\lambda)\nu^3\chi_k}{\pi^2\omega(1+i\xi)} \sum_{j=1}^{\infty} G_{2j}\chi_{2j} - \frac{2\nu^3\omega k^2 G_k}{(\omega^2 + k^2\pi^2)(\Omega^2 + k^2\pi^2)} & k \text{ even}, \\ \frac{2\phi(\lambda)\nu^3\chi_k}{\pi^2\omega(1+i\xi)} \sum_{j=1}^{\infty} G_{2j-1}\chi_{2j-1} - \frac{2\nu^3\omega k^2 G_k}{(\omega^2 + k^2\pi^2)(\Omega^2 + k^2\pi^2)} & k \text{ odd}. \end{cases} \quad (4.5.47)$$

In particular, coefficients  $h_{2k-1}(\lambda)$  depend only on *odd* Fourier coefficients of  $G_1(z)$ ,  $G_\beta(z)$  whereas coefficients  $h_{2k}(\lambda)$  depend only on *even* Fourier coefficients of  $G_1(z)$  and  $G_\beta(z)$ . It follows from (4.4.18) that the full solution for  $h(r, z)$  is

$$h(r, z) = C + \frac{\pi^2}{2} \sum_{k=1}^{\infty} \left( \sum_{n=1}^{\infty} \frac{\lambda_n^2 C_{01}(\lambda_n r, \lambda_n)}{f^2(\lambda_n) - 1} h_k(\lambda_n) \right) \frac{\sin k\pi z}{k}, \quad z \in (0, 1). \quad (4.5.48)$$

Choice of  $\lambda_n$ ,  $n \geq 1$ , guarantees that  $u = 0$  on curved surfaces  $r = 1, \beta$ ,  $0 < z < 1$ . It follows immediately from (4.4.18) and from properties of Weber-Orr kernels that

$$\begin{aligned} h(1, z) = H &= C - \pi \sum_{k=1}^{\infty} \left( \sum_{n=1}^{\infty} \frac{\lambda_n}{f^2(\lambda_n) - 1} h_k(\lambda_n) \right) \frac{\sin k\pi z}{k}, \\ h(\beta, z) = 0 &= C - \frac{\pi}{\beta} \sum_{k=1}^{\infty} \left( \sum_{n=1}^{\infty} \frac{\lambda_n f(\lambda_n)}{f^2(\lambda_n) - 1} h_k(\lambda_n) \right) \frac{\sin k\pi z}{k}, \end{aligned} \quad (4.5.49)$$

where  $H$  is an unknown complex constant to be determined. Both these equations are regarded as identities to be satisfied for all  $z \in (0, 1)$ . In effect, the Fourier coefficients of each sum are interpreted as coefficients of their half-range Fourier sine series for some appropriate constant. Since

$$\sum_{k=1}^{\infty} \frac{2A}{\pi} [1 - (-1)^k] \frac{\sin k\pi z}{k} = \begin{cases} A & z \in (0, 1) \\ 0 & z = 0 \\ -A & z \in (-1, 0), \end{cases}$$



it follows instantly from (4.5.49) that

$$\begin{aligned}\pi \sum_{n=1}^{\infty} \frac{\lambda_n}{f^2(\lambda_n) - 1} h_k(\lambda_n) &= \frac{2(C - H)}{\pi} [1 - (-1)^k], \\ \pi \sum_{n=1}^{\infty} \frac{\lambda_n f(\lambda_n)}{f^2(\lambda_n) - 1} h_k(\lambda_n) &= \frac{2\beta C}{\pi} [1 - (-1)^k].\end{aligned}\quad (4.5.50)$$

Equations (4.5.50) are supplemented by the pair of equations (4.4.32) which introduce the driving force into the problem. Note that

$$G_1(1) = \sum_{k=0}^{\infty} G_k(-1)^k = G_0 + \sum_{k=1}^{\infty} G_k(-1)^k = -\sum_{k=1}^{\infty} G_k^{(1)} [1 - (-1)^k] = -2 \sum_{k=1}^{\infty} G_{2k-1}^{(1)}, \quad (4.5.51)$$

with a similar expression for  $G_\beta(1)$ . Hence equations (4.4.32) become

$$\frac{F}{2\pi\mu d^2} = 2(1 + i\xi) \sum_{k=1}^{\infty} G_{2k-1}^{(1)}, \quad \frac{F}{2\pi\mu d^2} = 2\beta(1 + i\xi) \sum_{k=1}^{\infty} G_{2k-1}^{(\beta)}. \quad (4.5.52)$$

As stated already, even Fourier coefficients of  $G_1(z)$  and  $G_\beta(z)$  appear only in coefficients  $h_{2k}(\lambda)$  which in turn appear in a system of homogeneous linear equations. Hence this problem has a solution in which all even Fourier coefficients of  $G_1(z)$  and  $G_\beta(z)$  are zero except possibly  $G_0^{(1)}$  and  $G_0^{(\beta)}$ , whose values are chosen to ensure that  $G_1(0) = G_\beta(0) = 0$ . Hence

$$\begin{aligned}G_1(z) &= G_0^{(1)} + \sum_{k=1}^{\infty} G_{2k-1}^{(1)} \cos(2k-1)\pi z, \\ G_\beta(z) &= G_0^{(\beta)} + \sum_{k=1}^{\infty} G_{2k-1}^{(\beta)} \cos(2k-1)\pi z.\end{aligned}\quad (4.5.53)$$

In view of this important result, expression (4.5.44) for the surface deformation is now modified to

$$h(r, 1) = C + \frac{\pi\nu^2}{4(1 + i\xi)} \sum_{k=1}^{\infty} \sum_{n=1}^{\infty} \frac{\lambda_n [G_{2k-1}^{(1)} - f(\lambda_n) G_{2k-1}^{(\beta)}]}{f^2(\lambda_n) - 1} \phi(\lambda_n) \chi_{2k-1} C_{01}(\lambda_n r, \lambda_n). \quad (4.5.54)$$

Equations (4.5.50) which determine unknown Fourier coefficients of  $G_1(z)$ ,  $G_\beta(z)$  and values of  $C$  and  $H$  become

$$\begin{aligned}\sum_{j=1}^{\infty} \sum_{n=1}^{\infty} \frac{[G_{2j-1}^{(1)} - f(\lambda_n) G_{2j-1}^{(\beta)}]}{f^2(\lambda_n) - 1} C_{2k-1, 2j-1}(\lambda_n) &= \frac{2(C - H)}{\pi\nu^2}, \\ \sum_{j=1}^{\infty} \sum_{n=1}^{\infty} \frac{f(\lambda_n) [G_{2j-1}^{(1)} - f(\lambda_n) G_{2j-1}^{(\beta)}]}{f^2(\lambda_n) - 1} C_{2k-1, 2j-1}(\lambda_n) &= \frac{2\beta C}{\pi\nu^2},\end{aligned}\quad (4.5.55)$$

where

$$C_{2k-1,2j-1}(\lambda) = \phi(\lambda)\chi_{2k-1}\chi_{2j-1} - \frac{\omega^2(2k-1)^2\pi^2\delta_{k,j}}{[\omega^2 + (2k-1)^2\pi^2][\Omega^2 + (2k-1)^2\pi^2]}. \quad (4.5.56)$$

Solution of equations (4.5.55) is facilitated by solving an equivalent pair of equations formed by the sum and difference of equations (4.5.55). The equivalent system is

$$\begin{aligned} \sum_{j=1}^{\infty} \sum_{n=1}^{\infty} \left( \frac{G_{2j-1}^{(1)} - f(\lambda_n)G_{2j-1}^{(\beta)}}{f(\lambda_n) - 1} \right) C_{2k-1,2j-1}(\lambda_n) &= \frac{2}{\pi\nu^2}[(\beta+1)C - H], \\ \sum_{j=1}^{\infty} \sum_{n=1}^{\infty} \left( \frac{G_{2j-1}^{(1)} - f(\lambda_n)G_{2j-1}^{(\beta)}}{f(\lambda_n) + 1} \right) C_{2k-1,2j-1}(\lambda_n) &= \frac{2}{\pi\nu^2}[(\beta-1)C + H]. \end{aligned} \quad (4.5.57)$$

#### 4.5.1 Static Problem

Solution to the static problem can be obtained from (4.5.57) as  $\sigma \rightarrow 0$ , or equivalently, as  $\Omega \rightarrow \omega$ . It is a matter of algebra to show that

$$\phi(\lambda) = \frac{4\sigma\omega}{(\omega^2 + \Omega^2)^2} \frac{1}{\tanh(\omega/2) - \alpha\beta \tanh(\Omega/2)}, \quad (4.5.58)$$

and, using L'Hopital's rule, it can be established easily that

$$\lim_{\sigma \rightarrow 0} \phi(\lambda) = -\frac{2}{\omega} \left( \frac{\cosh \omega + 1}{\sinh \omega - \omega} \right). \quad (4.5.59)$$

In conclusion, the static equivalent of expression (4.5.56) is

$$C_{2k-1,2j-1} = -\frac{2}{\omega} \left( \frac{\cosh \omega + 1}{\sinh \omega - \omega} \right) \chi_{2k-1}\chi_{2j-1} - \frac{\omega^2(2k-1)^2\pi^2\delta_{k,j}}{[\omega^2 + (2k-1)^2\pi^2]^2}, \quad (4.5.60)$$

where  $\chi_k$  has the simplified form

$$\chi_k(\lambda) = \frac{k^2\pi^2(3\omega^2 + k^2\pi^2)}{(\omega^2 + k^2\pi^2)^2}. \quad (4.5.61)$$

## 4.6 Numerical Solution

Previous analysis makes it clear that the Fourier coefficients of unknown functions  $G_1(t)$  and  $G_\beta(t)$  are obtained by the solution of a system of linear equations. Of course, in practice, both  $G_1(t)$  and  $G_\beta(t)$  are given half-range cosine series of finite length, say

$N + 1$  terms, so that

$$\begin{aligned} G_1(t) &= G_0^{(1)} + \sum_{k=1}^N G_{2k-1}^{(1)} \cos(2k-1)\pi z, \\ G_\beta(t) &= G_0^{(\beta)} + \sum_{k=1}^N G_{2k-1}^{(\beta)} \cos(2k-1)\pi z. \end{aligned} \tag{4.6.62}$$

Bearing in mind that  $G_0^{(1)}$  and  $G_0^{(\beta)}$  are determined by conditions  $G_1(0) = G_\beta(0) = 0$ , as described in (4.5.37), equations (4.5.57) may now be regarded as a set of  $2N$  simultaneous equations relating  $2N + 2$  complex variables  $G_1^{(1)}, \dots, G_{2N-1}^{(1)}, G_1^{(\beta)}, \dots, G_{2N-1}^{(\beta)}, C$  and  $H$ . The system is completed by two further complex simultaneous equations arising from boundary conditions (4.5.52). These equations are now solved by an SVD method although they are well- conditioned for any sensible choice of physical parameters.

## 4.7 Conclusions for the Static Problem

Tables (4.1) display values of  $H_{ss}$  (axial displacement based on shear stress only) and  $H_{sb}$  (axial displacement based on shear and bending stress) as a percentage of  $H_{lt}$ , the axial displacement predicted by the Linear Theory of Elasticity for a fixed applied load. Results are displayed for parameter values  $\beta = b/a = 1.5, 2, 3, 4, 5, 6, 7, 8, 9$ ,  $\nu = d/a = 0.25, 0.5, 0.75, 1, 2, 3, 4, 5, 6, 7, 8, 9$ , the parameter  $\xi = \sigma = 0$  since  $f_\omega = 0$ , and  $F = 1/\ln \beta$ . These results range over sheet-like geometries (large  $\beta$  and small  $\nu$ ) to collar-like geometries (small  $\beta$  and large  $\nu$ ). There is an impressive agreement between the displacement predicted by the bending and shear model of Adkins & Gent [11] (as described in the introduction) and the exact linear displacement. Clearly, for most practical engineering applications, the methodology of Adkins & Gent embodies all the physical characteristics of the linear solution. Indeed the error is at most 5% over a wide range of annular geometries. The results are consistent with intuitive thinking in the respect that collar-like geometries are largely controlled by shear stress but as the geometry becomes more sheet-like, bending stresses soon dominate. In the most extreme sheet-like geometry investigated, ( $\beta \geq 6.0$  and  $\nu = 0.25$ ), the table suggests that shear stress accounts for at most 1% of the action, whereas in the most collar-like geometry investigated ( $\beta = 1.5$  and  $\nu = 4.0$ ), shear stress accounts for around 97% of the action. Of course, primitive shear stress theories cannot satisfy zero stress boundary conditions

	Linear Elastic Displacement			Shear & Bending Stress Displacement (Gent and Adkins)			Shear & Bending Stress %			Shear Stress Only %		
$\nu$	$\beta = 1.5$	$\beta = 2$	$\beta = 3$	$\beta = 1.5$	$\beta = 2$	$\beta = 3$	$\beta = 1.5$	$\beta = 2$	$\beta = 3$	$\beta = 1.5$	$\beta = 2$	$\beta = 3$
0.25	1.986	4.663	14.67	1.981	4.788	15.03	100	103	102	50	21	7
0.50	1.308	1.957	4.407	1.245	1.947	4.507	95	99	102	76	51	23
0.75	1.180	1.470	2.540	1.109	1.421	2.559	94	97	101	85	68	39
1.00	1.129	1.301	1.896	1.061	1.237	1.877	94	95	99	89	77	53
2.00	1.061	1.127	1.286	1.015	1.059	1.219	96	94	95	94	89	78
3.00	1.040	1.081	1.169	1.007	1.026	1.097	97	95	94	96	92	86
4.00	1.030	1.060	1.121	1.004	1.015	1.055	97	96	94	97	94	89
5.00	1.024	1.047	1.095	1.002	1.009	1.035	98	96	95	98	95	91
6.00	1.020	1.039	1.078	1.002	1.007	1.024	98	97	95	98	96	93
7.00	1.017	1.033	1.066	1.001	1.005	1.018	98	97	95	98	97	94
8.00	1.015	1.029	1.057	1.001	1.004	1.014	99	98	96	99	97	95
9.00	1.013	1.026	1.051	1.001	1.003	1.011	99	98	96	99	97	95

	Linear Elastic Displacement			Shear & Bending Stress Displacement (Gent and Adkins)			Shear & Bending Stress %			Shear Stress Only %		
$\nu$	$\beta = 4$	$\beta = 5$	$\beta = 6$	$\beta = 4$	$\beta = 5$	$\beta = 6$	$\beta = 4$	$\beta = 5$	$\beta = 6$	$\beta = 4$	$\beta = 5$	$\beta = 6$
0.25	29.88	49.52	73.11	30.43	50.24	73.97	102	101	101	3	2	1
0.50	8.162	13.03	18.89	8.358	13.31	19.24	102	102	102	12	8	5
0.75	4.189	6.336	8.925	4.270	6.471	9.108	102	102	102	24	16	11
1.00	2.815	4.012	5.460	2.840	4.077	5.561	101	102	102	36	25	18
2.00	1.510	1.803	2.157	1.460	1.769	2.140	97	98	99	66	55	46
3.00	1.272	1.402	1.558	1.204	1.342	1.507	95	96	97	79	71	64
4.00	1.186	1.261	1.349	1.115	1.192	1.285	94	95	95	84	79	74
5.00	1.143	1.194	1.252	1.074	1.123	1.182	94	94	94	88	84	80
6.00	1.116	1.155	1.197	1.051	1.085	1.127	94	94	94	90	87	84
7.00	1.098	1.130	1.163	1.038	1.063	1.093	94	94	94	91	88	86
8.00	1.085	1.112	1.139	1.029	1.048	1.071	95	94	94	92	90	88
9.00	1.075	1.098	1.122	1.023	1.038	1.056	95	95	94	93	91	89

	Linear Elastic Displacement			Shear & Bending Stress Displacement (Gent and Adkins)			Shear & Bending Stress %			Shear Stress Only %		
$\nu$	$\beta = 7$	$\beta = 8$	$\beta = 9$	$\beta = 7$	$\beta = 8$	$\beta = 9$	$\beta = 7$	$\beta = 8$	$\beta = 9$	$\beta = 7$	$\beta = 8$	$\beta = 9$
0.25	100.3	131.0	164.8	101.3	132.1	166.0	101	101	101	1	1	1
0.50	25.67	33.29	41.74	26.08	33.77	42.27	102	101	101	4	3	2
0.75	11.92	15.30	19.04	12.15	15.56	19.34	102	102	102	8	7	5
1.00	7.138	9.030	11.13	7.270	9.193	11.32	102	102	102	14	11	9
2.00	2.570	3.036	3.554	2.568	3.048	3.579	100	100	101	39	33	28
3.00	1.739	1.944	2.172	1.697	1.910	2.146	98	98	99	58	51	46
4.00	1.450	1.565	1.692	1.392	1.512	1.645	96	97	97	69	64	59
5.00	1.317	1.390	1.471	1.251	1.328	1.413	95	95	96	76	72	68
6.00	1.244	1.295	1.351	1.174	1.228	1.287	94	95	95	80	77	74
7.00	1.198	1.237	1.279	1.128	1.167	1.211	94	94	95	83	81	78
8.00	1.168	1.198	1.231	1.098	1.128	1.161	94	94	94	86	83	81
9.00	1.146	1.171	1.197	1.077	1.101	1.127	94	94	94	87	85	84

Table 4.1: Core axial displacement as a percentage of that predicted by the linear theory of elasticity, for applied force  $F = 1/\ln \beta$ .

on the flat boundaries of the annulus. In qualitative terms, there is a region close to exterior boundaries  $z = 0$ ,  $z = d$  in which the primitive shear stress solution mutates into a solution which satisfies stress-free boundary conditions. For collar-like geometries, this region is relatively small but becomes more significant as the geometry becomes progressively sheet-like.

The following three subsections display accumulated shear stresses  $G_1(z)$  and  $G_\beta(z)$ , related shear stress  $g_1(z)$  and  $g_\beta(z)$  and finally, surface deformation  $h(r, 1)$  for a selection of  $\nu$  values in  $[0.25, 9]$ . Each graph contains six curves, one for each of  $\beta = 1.5, 2, 3, 4, 5, 9$ .

### 4.7.1 Accumulated Static Shear Stress

Behaviour of inner accumulated shear stress  $G_1(z)$  and outer accumulated shear stress are illustrated in Figures 4.1 and 4.2 respectively.

### 4.7.2 Static Shear Stress

Recall that shear stress on inner and outer boundaries is just the gradient of accumulated shear stress on these boundaries. Figures 4.3 and 4.4 display  $g_1(z)$  and  $g_\beta(z)$ , shear stresses on inner and outer boundaries respectively. Each graph corresponds to the gradient of the respective accumulated shear stress  $G_1(z)$  and  $G_\beta(z)$  appearing in figures 4.1 and 4.2.

### 4.7.3 Static surface deformation

The approximate shape of the deformed surface is consistent with intuitive thinking although the precise nature of its approach to outer and inner circular boundaries is perhaps less clear. Figures 4.5 and 4.6 depict static surface deformation  $h(r, 1)$  from inner boundary  $r = 1$  to outer boundary  $r = \beta$  where  $\beta$  (ratio of outer radius to inner) takes values between 1.5 and 9.0 for each different thickness ratio  $\nu$ .

Tables 4.2 records the displacement  $h(r, 1)$  for selected  $r$  values in  $[1, \beta]$  and various aspect ratios  $\nu$ . These results indicate that surface displacement  $h(r, 1)$  is always a monotonically decreasing function of  $r$ . Furthermore,  $H = h(1, 1)$ , the induced displacement of the rod, is an increasing function of  $\beta$  and a decreasing function of  $\nu$ . Increasing  $\beta$  or decreasing  $\nu$

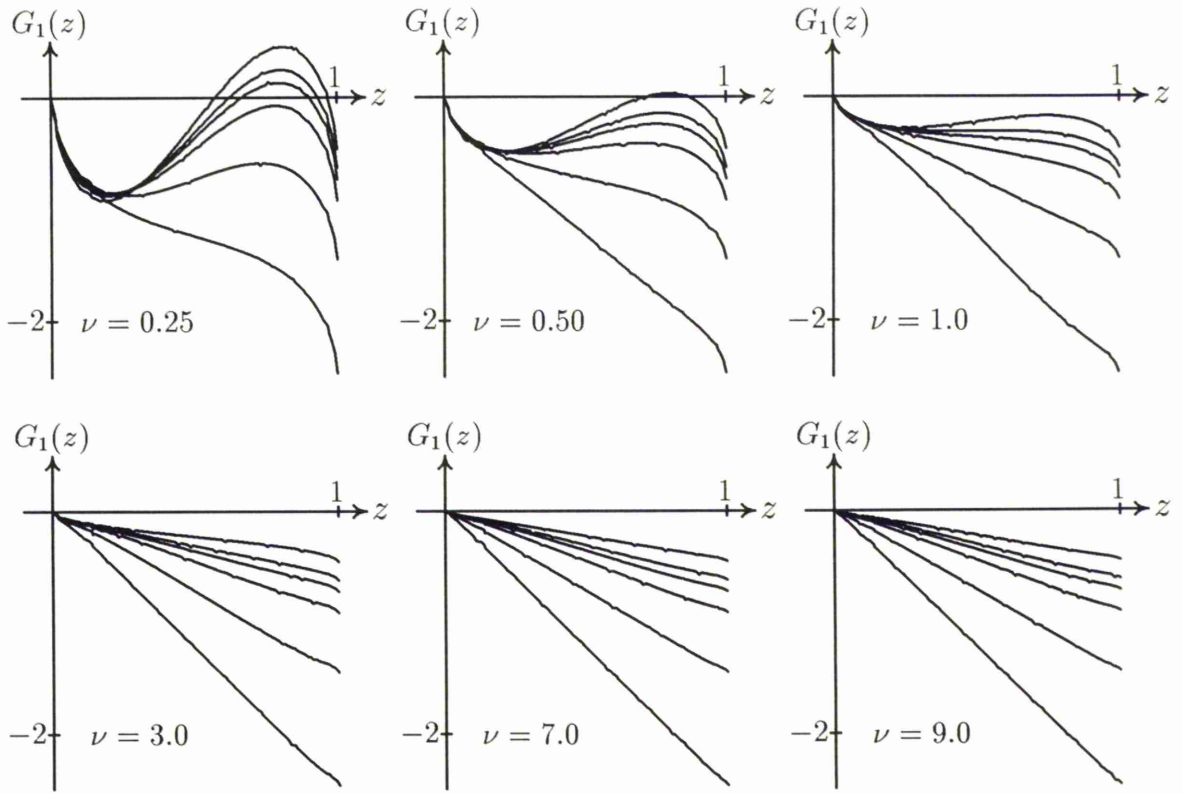


Figure 4.1: Graphs of  $G_1(z)$  when  $\nu = 0.25, 0.5, 1.0, 3.0, 7.0, 9.0$  for a static applied axial force. As the annulus moves from a sheet-like geometry (small  $\nu$  and large  $\beta$ ) to a collar-like geometry (large  $\nu$  and small  $\beta$ ), graphs of accumulated shear stress migrate progressively from a volatile nature to approximately straight lines. Transition between sheet-like and collar-like geometries can be considered to occur along a line  $\nu = \nu(\beta)$ , defined by the criterion that accumulated shear stress just becomes a monotonic function of  $z$ . In particular, accumulated shear stress across a membrane can oppose the applied axial force (see  $\nu = 0.25$  and  $\beta \geq 5.0$ ) over large areas of contact.

are equivalent to increasing the sheet-like characteristics of an annulus. Hence, sheet-like annuli deform more than collar-like annuli for a given applied force. These findings are all consistent with intuitive thinking.

## 4.8 Dynamic Deformation

Until now, all results are based on an applied axial force that is fixed in time. The remainder of this chapter, however, assumes that the applied force is now oscillatory. In principle, it is possible to produce the entire spectral response of any annulus over a range of frequencies. However, the process is numerically very intensive and so the results are

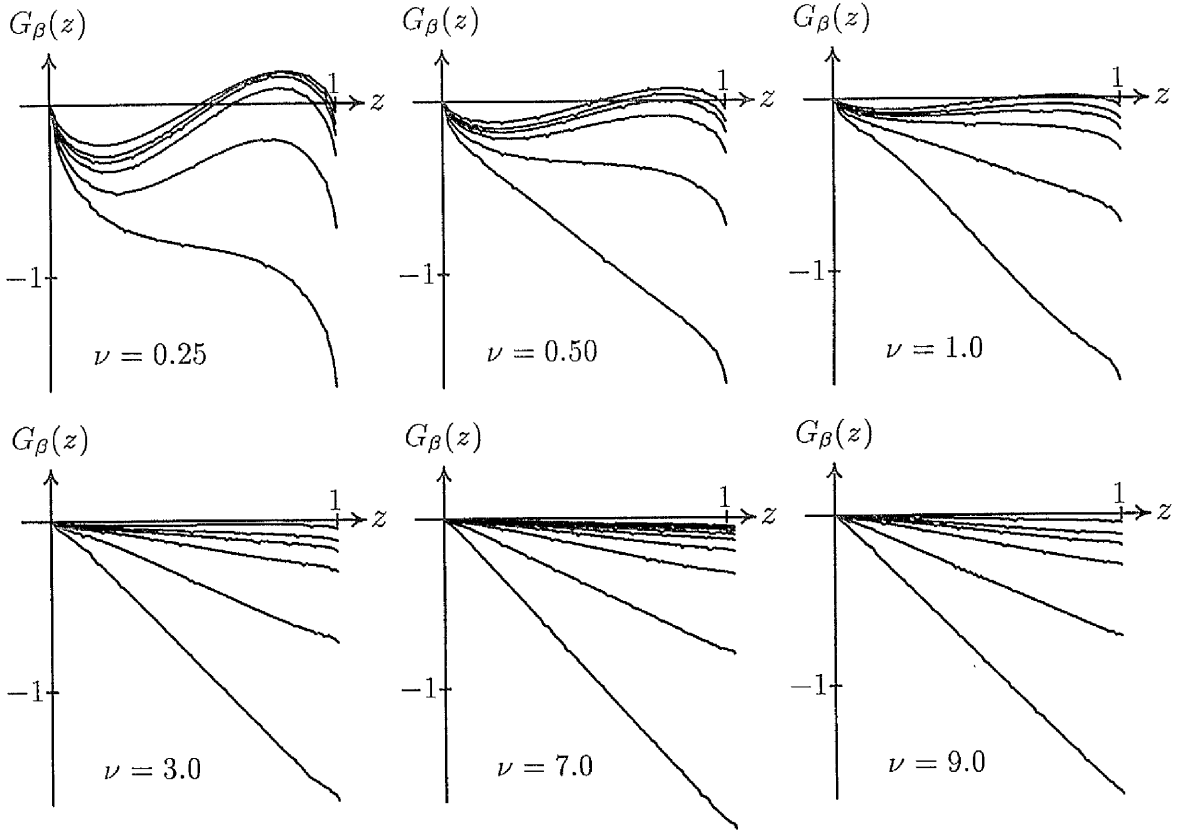


Figure 4.2: Graphs of  $G_\beta(z)$  when  $\nu = 0.25, 0.5, 1.0, 3.0, 7.0, 9.0$  for a static applied axial force. Accumulated shear stress on the outer boundary is qualitatively similar to that on the inner boundary, except that its variability as a function of  $\nu$  and  $\beta$  is noticeably less pronounced.

presented for restricted frequencies  $f_\omega = 0.5, 1.0, 2.0$ , and  $5.0$ , the value of parameters  $\sigma$  and  $\xi$ , which appears in (4.3.14) are taken to be the quantities  $d^2\rho/\mu = 1$  and  $\eta/\mu = 1$ , and for the same range of values of parameters  $\beta$  and  $\nu$  that were used in the static problem.

Figures 4.7—4.15 illustrate accumulated shear stresses  $G_1(z)$  and  $G_\beta(z)$ , shear stresses  $g_1(z)$  and  $g_\beta(z)$  and dynamic surface deformation  $h(r, 1)$  for selected frequencies  $f$ . In fact, all graphs display the amplitude of these functions since their Fourier coefficients in the dynamic problem are complex valued.

Comment on the graphs is divided into cases  $\nu \leq 1.0$  and  $\nu \geq 3.0$ . As has been previously mentioned, small values of  $\nu$  are representative of sheet-like annuli, whereas large values of  $\nu$  are more typical of collar-like annuli. When  $\nu \leq 1.0$ , behavior of  $G_1(z)$  and  $G_\beta(z)$  changes dramatically around frequency  $f_\omega = 1$ . For frequencies greater than  $2.0$ , it

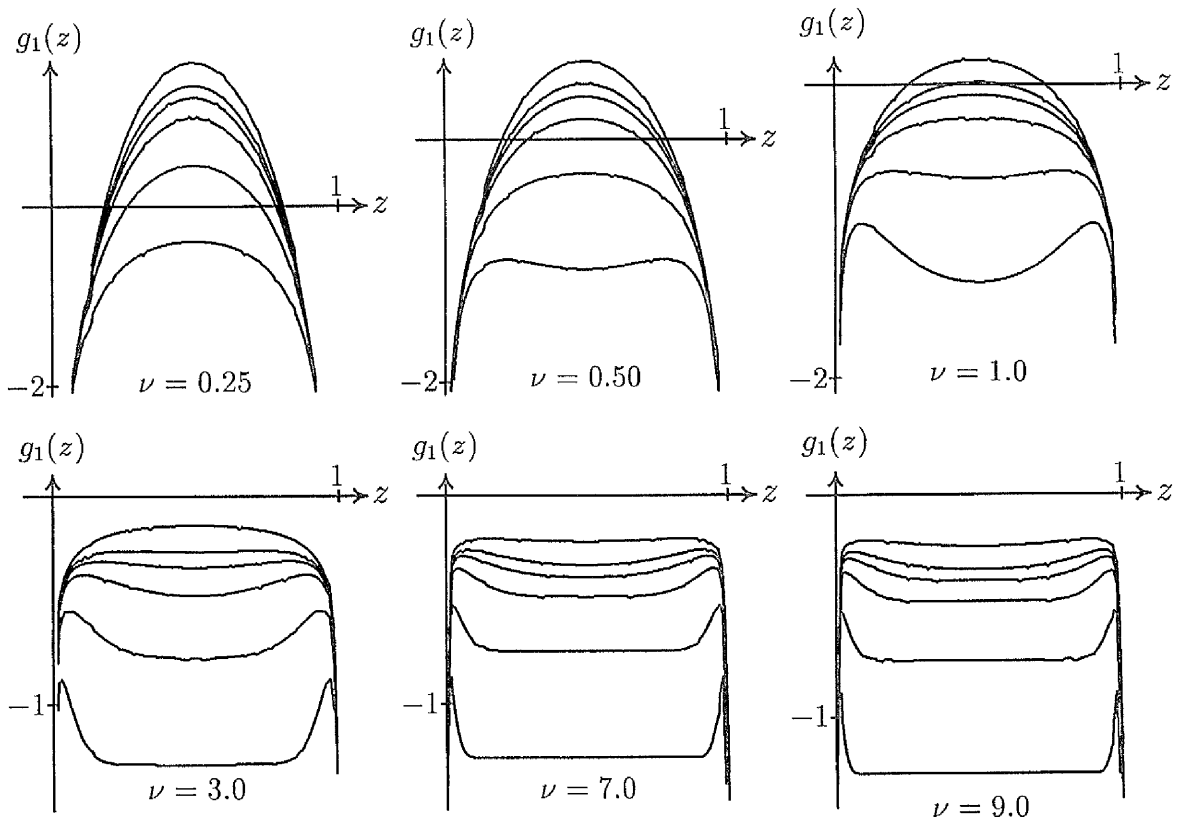


Figure 4.3: Graphs of  $g_1(z)$  when  $\nu = 0.25, 0.5, 1.0, 3.0, 7.0, 9.0$  for a static applied axial force. As the annulus moves from a sheet-like geometry (small  $\nu$  and large  $\beta$ ) to a collar-like geometry (large  $\nu$  and small  $\beta$ ), the shear stress moves from a rapidly varying function of  $z$  to one which is largely constant across the interior of the annulus. Boundary layer effects are particularly pronounced when the geometry is collar-like. Furthermore, for sheet-like annuli, interior shear stress changes algebraic sign and acts in a counter-intuitive way by opposing action of the externally applied force over a significant area of the surface of contact with the rod.

would appear that accumulated shear stresses all increase monotonically and all enjoy the same approximate shape irrespective of the value of  $\beta$ . For frequencies less than 1.0, accumulated shear stress is often monotonic but not exclusively so. Moreover, there are stress boundary layers that are particularly pronounced when  $\beta$  is small. The influence of boundaries is more closely illustrated in Figures (4.9) which display the structure of shear stress across the surface of contact with the rod. In almost all circumstances, there is clear evidence for stress boundary layers with low, almost constant, stress in the interior of the material. This is particularly noticeable when  $\beta$  is large; that is, the annulus is sheet-like.



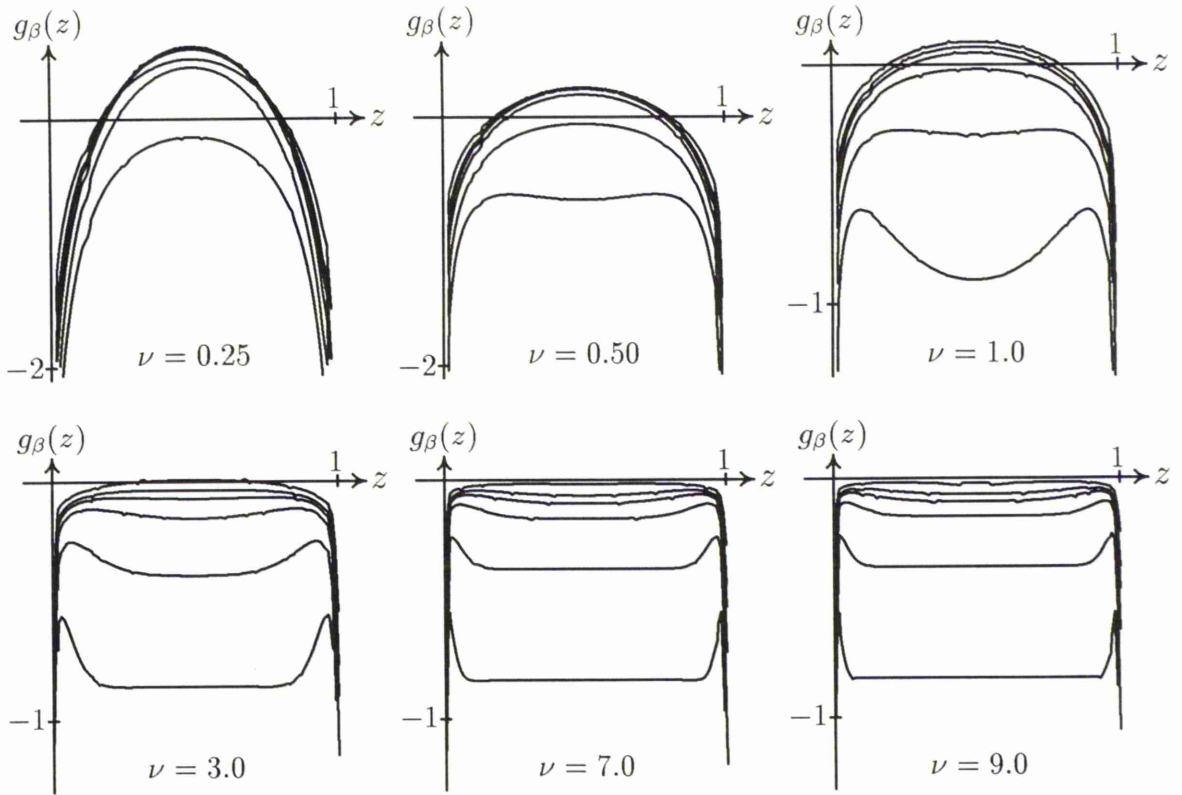


Figure 4.4: Graphs of  $g_\beta(z)$  when  $\nu = 0.25, 0.5, 1.0, 3.0, 7.0, 9.0$  for a static applied axial force. As expected, shear stress on the outer boundary is qualitatively similar to that on the inner boundary except that most of its features are less pronounced.

The rogue curves sprinkled across some of the diagrams are thought to be due to the presence of resonance. This view is supported by a rough calculation of the natural frequencies of oscillation of the elastic annulus (see page 6 and 7 of the introduction). To summarise briefly

- (a) The effect of resonance manifests itself through the appearance of rogue stress distribution curves. Resonant frequency is a decreasing function of  $\beta$  and an increasing function of  $\nu$ . Calculations are consistent with the crude estimate of resonant frequency based on elementary mechanical arguments.
- (b) Stress distribution on the oscillating rod is typically U-shaped, indicating the presence of stress boundary layers on the upper and lower boundaries of the slab. Often the stress profile is quite flat in the central region and would appear to be almost independent of  $\beta$ ,  $\nu$  and  $f_\omega$  except when near resonance.

r	$\beta = 1.5 \quad f_w = 0$				
	$\nu = 0.25$	$\nu = 0.5$	$\nu = 1$	$\nu = 3$	$\nu = 9$
1.000	1.9860	1.3085	1.1292	1.0399	1.0132
1.017	1.7729	1.0835	0.9090	0.8327	0.8004
1.033	1.7155	1.0367	0.8684	0.7959	0.7705
1.067	1.6126	0.9599	0.8020	0.7353	0.7138
1.100	1.5031	0.8896	0.7427	0.6810	0.6616
1.133	1.3827	0.8212	0.6866	0.6296	0.6120
1.167	1.2530	0.7536	0.6325	0.5801	0.5641
1.200	1.1174	0.6866	0.5799	0.5321	0.5176
1.233	0.9794	0.6205	0.5287	0.4855	0.4724
1.267	0.8425	0.5557	0.4789	0.4400	0.4284
1.300	0.7100	0.4927	0.4303	0.3958	0.3855
1.333	0.5850	0.4318	0.3829	0.3526	0.3438
1.367	0.4705	0.3732	0.3366	0.3104	0.3030
1.400	0.3687	0.3168	0.2909	0.2688	0.2629
1.433	0.2804	0.2616	0.2449	0.2270	0.2227
1.467	0.2015	0.2036	0.1955	0.1822	0.1809
1.483	0.1586	0.1691	0.1658	0.1555	0.1593
1.500	0.0000	0.0000	0.0000	0.0000	0.0000

r	$\beta = 4.0 \quad f_w = 0$				
	$\nu = 0.25$	$\nu = 0.5$	$\nu = 1$	$\nu = 3$	$\nu = 9$
1.000	29.882	8.1620	2.8145	1.1862	1.0746
1.100	29.760	7.9369	2.5314	0.8900	0.7935
1.200	29.284	7.7777	2.4419	0.8292	0.7385
1.400	27.693	7.3288	2.2680	0.7350	0.6531
1.600	25.483	6.7331	2.0744	0.6572	0.5830
1.800	22.870	6.0417	1.8633	0.5890	0.5220
2.000	20.020	5.2948	1.6424	0.5276	0.4676
2.200	17.064	4.5249	1.4190	0.4715	0.4183
2.400	14.113	3.7590	1.1993	0.4200	0.3733
2.600	11.261	3.0201	0.9886	0.3721	0.3318
2.800	8.5903	2.3282	0.7916	0.3276	0.2934
3.000	6.1715	1.7011	0.6124	0.2861	0.2576
3.200	4.0697	1.1547	0.4549	0.2473	0.2240
3.400	2.3432	0.7034	0.3224	0.2105	0.1922
3.600	1.0451	0.3604	0.2175	0.1750	0.1611
3.800	0.2247	0.1373	0.1387	0.1380	0.1287
3.900	0.0075	0.0692	0.1035	0.1161	0.1095
4.000	0.0000	0.0000	0.0000	0.0000	0.0000

r	$\beta = 6.0 \quad f_w = 0$				
	$\nu = 0.25$	$\nu = 0.5$	$\nu = 1$	$\nu = 3$	$\nu = 9$
1.000	73.110	18.892	5.4603	1.5576	1.1218
1.167	72.892	18.665	5.1631	1.2239	0.8026
1.333	71.626	18.312	5.0253	1.1437	0.7371
1.667	67.446	17.211	4.6910	1.0192	0.6392
2.000	61.773	15.747	4.2792	0.9120	0.5624
2.333	55.187	14.062	3.8193	0.8125	0.4979
2.667	48.104	12.258	3.3347	0.7181	0.4419
3.000	40.840	10.412	2.8437	0.6282	0.3922
3.333	33.652	8.5886	2.3614	0.5433	0.3477
3.667	26.756	6.8406	1.9005	0.4637	0.3072
4.000	20.336	5.2148	1.4719	0.3902	0.2701
4.333	14.554	3.7481	1.0854	0.3233	0.2359
4.667	9.5544	2.4797	0.7497	0.2636	0.2041
5.000	5.4678	1.4407	0.4726	0.2112	0.1742
5.333	2.4130	0.6608	0.2615	0.1655	0.1454
5.667	0.4991	0.1671	0.1218	0.1233	0.1154
5.833	0.0021	0.0346	0.0754	0.0997	0.0977
6.000	0.0000	0.0000	0.0000	0.0000	0.0000

r	$\beta = 9.0 \quad f_w = 0$				
	$\nu = 0.25$	$\nu = 0.5$	$\nu = 1$	$\nu = 3$	$\nu = 9$
1.000	164.84	41.736	11.127	2.1715	1.1971
1.267	164.15	41.430	10.807	1.8037	0.8391
1.533	161.04	40.615	10.558	1.7043	0.7614
2.067	151.09	38.065	9.8590	1.5400	0.6502
2.600	137.91	34.724	8.9767	1.3838	0.5664
3.133	122.85	30.922	7.9878	1.2284	0.4975
3.667	106.83	26.882	6.9459	1.0744	0.4384
4.200	90.510	22.776	5.8914	0.9243	0.3863
4.733	74.453	18.737	4.8572	0.7804	0.3396
5.267	59.112	14.880	3.8711	0.6449	0.2974
5.800	44.876	11.301	2.9567	0.5199	0.2590
6.333	32.091	8.0869	2.1351	0.4073	0.2238
6.867	21.063	5.3133	1.4251	0.3088	0.1915
7.400	12.070	3.0496	0.8439	0.2260	0.1615
7.933	5.3628	1.3586	0.4069	0.1598	0.1330
8.467	1.1756	0.2985	0.1286	0.1081	0.1040
8.733	0.0949	0.0221	0.0511	0.0836	0.0870
9.000	0.0000	0.0000	0.0000	0.0000	0.0000

Table 4.2: Tables of incompressible surface deformation for static problem for  $\beta = 1.5, 4, 6$  and  $9$  and for different values of  $\nu$ .

(c) Negative internal stress; that is, stress that opposes the prevailing driving force is possible but does not occur often.

### 4.8.1 Dynamic Accumulated Shear Stress

Figures 4.7 and 4.8 illustrate general behaviour of accumulated shear stress over the cylindrical surface of contact for selected values of  $\nu$ ,  $\beta$  and frequency  $f_\omega$ .

### 4.8.2 Dynamic Shear Stress

Figures 4.9 and 4.10 illustrate shear stress distribution across inner and outer cylindrical contact surfaces.

### 4.8.3 Dynamic surface deformation

Figures 4.11 - 4.15 illustrate the behaviour of dynamic surface deformation  $h(r, 1)$  for frequencies  $f_\omega = 0.5, 1.0, 2.0$  and  $5.0$ , and for selected values of  $\beta$  and  $\nu$ . The graphs divide into two cases,  $\beta = 1.5$  and  $\beta \geq 2.0$ , irrespective of the value of  $\nu$  (non-dimensional thickness of annulus). When  $\beta = 1.5$ , it is clear that  $h(r, 1)$  decreases monotonically with  $r$  — thick and thin annuli seem to behave in a qualitatively similar manner.

However, when  $\beta \geq 2.0$ , thin and thick materials behave differently. For thin layers, the graphs exhibit resonance effects on different occasions and demonstrate that resonant frequency is a decreasing function of  $\beta$  when  $\nu$  is fixed and is an increasing function of  $\nu$  when  $\beta$  is fixed. This is entirely consistent with the expression for base resonant frequency based on a crude mechanical argument given in the introduction, namely

$$f_\omega^2 = \frac{12\mu}{\rho(\beta - 1)(\beta + 3)[\log \beta + Q/\nu^2]}, \quad Q = \frac{3(\beta^2 - 1)^2 - 4\beta^2(\log \beta)^2}{8(\beta^2 - 1)}.$$

For  $f_\omega \leq 1.0$ , the figures suggest that the free surface of the annulus can be expected to have a "corrugated" appearance which disappears as frequency is increased beyond 2.0. For annuli with relatively small holes, say  $\beta \geq 6.0$ , it would appear that at frequencies higher than the natural frequency, the material in the vicinity of the hole responds to the oscillatory force in a way which is dependent on radial displacement up to  $r = 2.5$  but thereafter the remaining material seems to deform as a solid body whose surface displacement is small and almost constant. Figures 4.12 - 4.15 show more clearly the behaviour of  $h(r, 1)$ . To summarise briefly,

- (a) For annuli of a given aspect ratio  $\nu$ , resonance effects become increasingly evident as  $\beta$  is increased. For small  $\beta$  (collar-like annuli), surface deformation decreases monotonically to zero as  $r \rightarrow \beta$ . As  $\beta$  is increased, surface deformation is no longer monotonic and, in particular, maximum surface deformation may not occur at the inner hole. For large  $\beta$  (sheet-like annuli), surface deformation has a corrugated character.
- (b) As aspect ratio  $\nu$  is increased for fixed  $\beta$  and frequency, surface deformation moves from a corrugated character to a monotonic character due to the fact that resonant frequency is an increasing function of  $\nu$ .
- (c) Surface deformation  $h(r, 1)$  is not necessarily a monotonic function of  $r$  at all frequencies. It would appear that material near the oscillating rod can undergo large oscillations while material more distant from the rod tends to behave like a rigid body, moving in unison with a small and effectively constant axial displacement.

Table 4.3 illustrates relative magnitude of maximum surface displacement for dynamic and static deformations.

$\nu$	$\beta$	Dynamic deformation		Static deformation
		$f_\omega$	$h(1,1)$	$h(1,1)$
1.00	4.00	0.5	4.5750	2.8145
0.25	1.50	1.0	1.8814	1.9860
0.75	2.00	2.0	0.7110	1.4699
0.75	1.50	5.0	0.2338	1.1805

Table 4.3: This table describes amplification of surface displacement generated through the presence of resonance effects for a selection of annuli and frequencies.

Tables 4.4 - 4.7 display maximum surface deformation  $|h(r, 1)|$  versus radial distance  $r \in [1.0, \beta]$  for fixed aspect ratios  $\nu$  and for frequencies  $f_\omega = 0.5, 1.0, 2.0$  and  $5.0$  respectively.

r	$\beta = 1.5 \quad f_\omega = 0.5$				
	$\nu = 0.25$	$\nu = 0.5$	$\nu = 1$	$\nu = 3$	$\nu = 9$
1.000	2.1210	1.1988	1.0149	0.9305	0.9062
1.017	1.9129	0.9935	0.8170	0.7451	0.7159
1.033	1.8550	0.9510	0.7805	0.7122	0.6892
1.067	1.7497	0.8811	0.7210	0.6579	0.6385
1.100	1.6341	0.8169	0.6678	0.6094	0.5918
1.133	1.5038	0.7543	0.6173	0.5634	0.5474
1.167	1.3613	0.6921	0.5686	0.5191	0.5045
1.200	1.2105	0.6303	0.5214	0.4761	0.4630
1.233	1.0560	0.5693	0.4753	0.4344	0.4225
1.267	0.9023	0.5094	0.4304	0.3937	0.3832
1.300	0.7536	0.4512	0.3867	0.3541	0.3448
1.333	0.6140	0.3950	0.3441	0.3155	0.3075
1.367	0.4872	0.3410	0.3024	0.2777	0.2710
1.400	0.3761	0.2893	0.2613	0.2405	0.2351
1.433	0.2818	0.2388	0.2200	0.2031	0.1992
1.467	0.2000	0.1860	0.1757	0.1630	0.1618
1.483	0.1562	0.1545	0.1490	0.1391	0.1425
1.500	0.0000	0.0000	0.0000	0.0000	0.0000

r	$\beta = 4.0 \quad f_\omega = 0.5$				
	$\nu = 0.25$	$\nu = 0.5$	$\nu = 1$	$\nu = 3$	$\nu = 9$
1.000	0.5259	0.7253	4.5750	1.1607	0.9628
1.100	0.5277	0.7648	4.2782	0.8886	0.6356
1.200	0.5172	0.7841	4.1678	0.8305	0.6617
1.400	0.4413	0.8133	3.9332	0.7399	0.5852
1.600	0.3070	0.8253	3.6402	0.6639	0.5224
1.800	0.1542	0.8115	3.2954	0.5958	0.4678
2.000	0.0342	0.7653	2.9148	0.5331	0.4190
2.200	0.0359	0.6860	2.5148	0.4749	0.3749
2.400	0.0924	0.5789	2.1106	0.4206	0.3345
2.600	0.1714	0.4545	1.7168	0.3698	0.2973
2.800	0.2357	0.3259	1.3462	0.3226	0.2629
3.000	0.2459	0.2068	1.0108	0.2787	0.2308
3.200	0.1958	0.1092	0.7210	0.2381	0.2007
3.400	0.1145	0.0421	0.4855	0.2004	0.1721
3.600	0.0485	0.0156	0.3103	0.1646	0.1443
3.800	0.0246	0.0141	0.1928	0.1281	0.1153
3.900	0.0165	0.0091	0.1462	0.1067	0.0981
4.000	0.0000	0.0000	0.0000	0.0000	0.0000

r	$\beta = 6.0 \quad f_\omega = 0.5$				
	$\nu = 0.25$	$\nu = 0.5$	$\nu = 1$	$\nu = 3$	$\nu = 9$
1.000	0.3667	1.0797	1.3014	1.4953	1.0079
1.167	0.3359	0.9928	1.3348	1.1833	0.7212
1.333	0.2864	0.9217	1.3598	1.1090	0.6625
1.667	0.1518	0.6916	1.3829	0.9928	0.5747
2.000	0.0494	0.4302	1.3647	0.8913	0.5058
2.333	0.0913	0.2293	1.3023	0.7956	0.4479
2.667	0.0995	0.1189	1.1978	0.7038	0.3975
3.000	0.0962	0.0259	1.0575	0.6156	0.3529
3.333	0.0550	0.1382	0.8919	0.5316	0.3128
3.667	0.0315	0.3111	0.7136	0.4526	0.2763
4.000	0.0528	0.4476	0.5361	0.3796	0.2429
4.333	0.0508	0.5002	0.3724	0.3132	0.2121
4.667	0.0700	0.4548	0.2338	0.2541	0.1835
5.000	0.0626	0.3351	0.1287	0.2026	0.1566
5.333	0.0565	0.1908	0.0617	0.1581	0.1306
5.667	0.0399	0.0771	0.0308	0.1176	0.1038
5.833	0.0214	0.0441	0.0247	0.0951	0.0879
6.000	0.0000	0.0000	0.0000	0.0000	0.0000

r	$\beta = 9.0 \quad f_\omega = 0.5$				
	$\nu = 0.25$	$\nu = 0.5$	$\nu = 1$	$\nu = 3$	$\nu = 9$
1.000	0.3035	0.6264	0.6541	2.6260	1.0832
1.267	0.2514	0.5505	0.5560	2.2547	0.7601
1.533	0.1648	0.4636	0.5195	2.1527	0.6903
2.066	0.0503	0.2669	0.4517	1.9767	0.5902
2.600	0.0824	0.1278	0.3977	1.7971	0.5146
3.133	0.0592	0.0462	0.3324	1.6081	0.4523
3.667	0.0107	0.1528	0.2350	1.4131	0.3986
4.200	0.0458	0.2110	0.1147	1.2171	0.3513
4.733	0.0427	0.1692	0.0858	1.0249	0.3088
5.267	0.0237	0.0863	0.1941	0.8413	0.2703
5.800	0.0336	0.0457	0.2796	0.6704	0.2352
6.333	0.0417	0.0589	0.3131	0.5164	0.2031
6.867	0.0297	0.1311	0.2915	0.3826	0.1737
7.400	0.0263	0.1709	0.2271	0.2719	0.1464
7.933	0.0468	0.1353	0.1428	0.1860	0.1206
8.466	0.0339	0.0587	0.0669	0.1223	0.0943
8.733	0.0176	0.0278	0.0403	0.0933	0.0789
9.000	0.0000	0.0000	0.0000	0.0000	0.0000

Table 4.4: Tables of incompressible amplitude of surface deformation for frequency  $f_\omega = 0.5$  when  $\beta = 1.5, 4.0, 6.0, 9.0$  and for a selection of aspect ratios  $\nu$ .

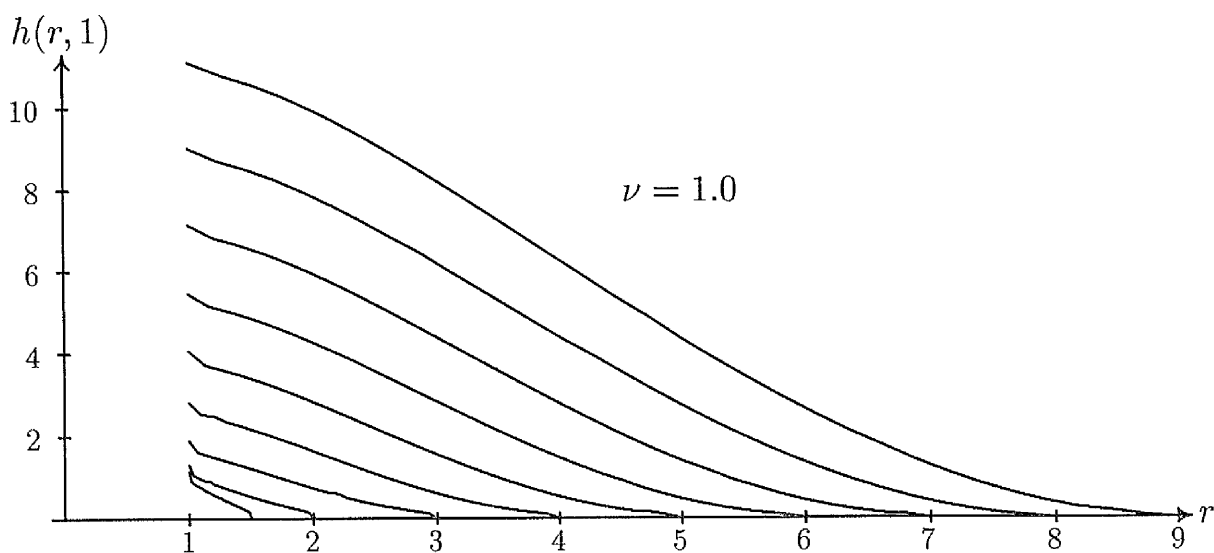
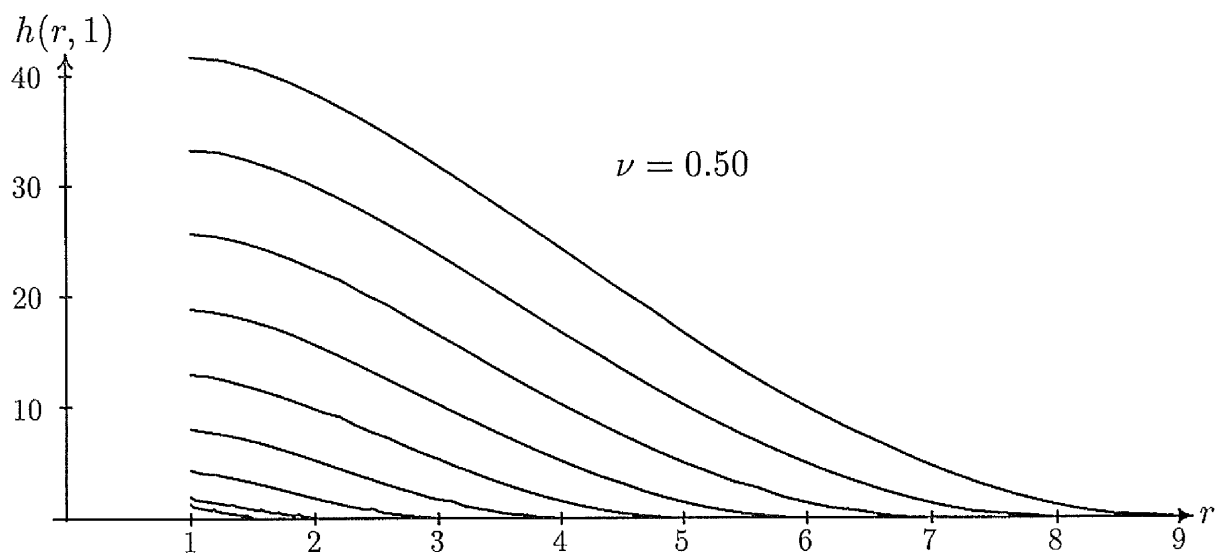
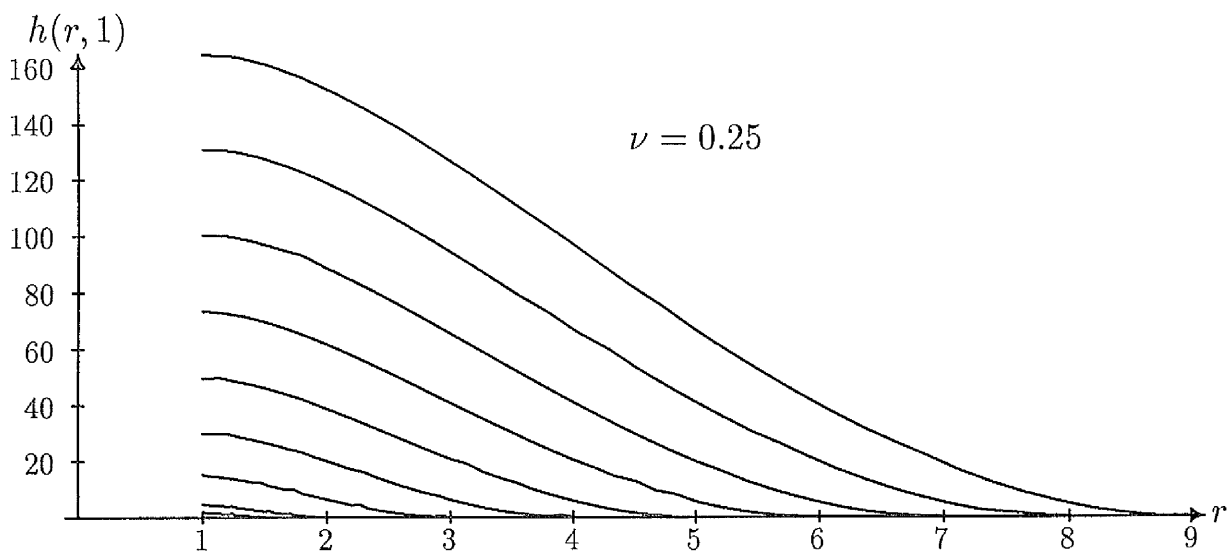


Figure 4.5: Graphs of  $h(r, 1)$  when  $\nu = 0.25, 0.5, 1.0$  for static deformation.

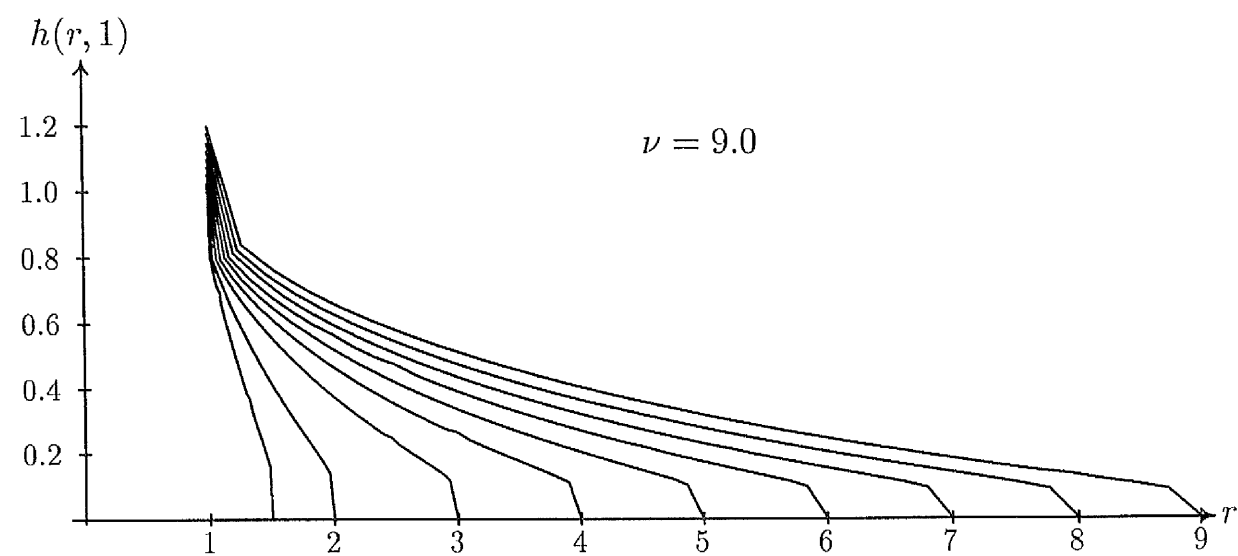
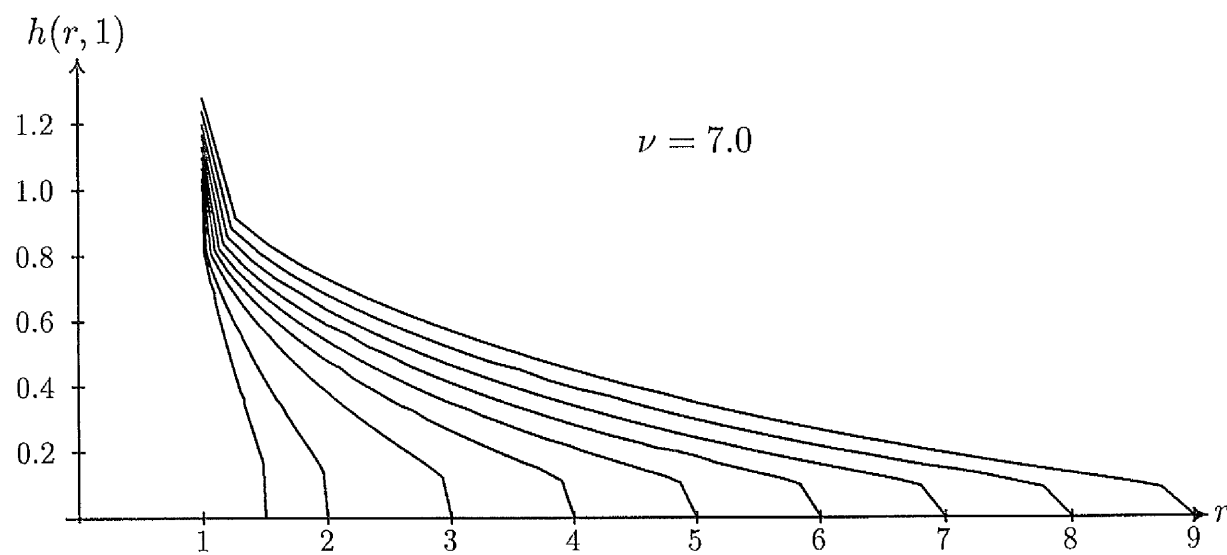
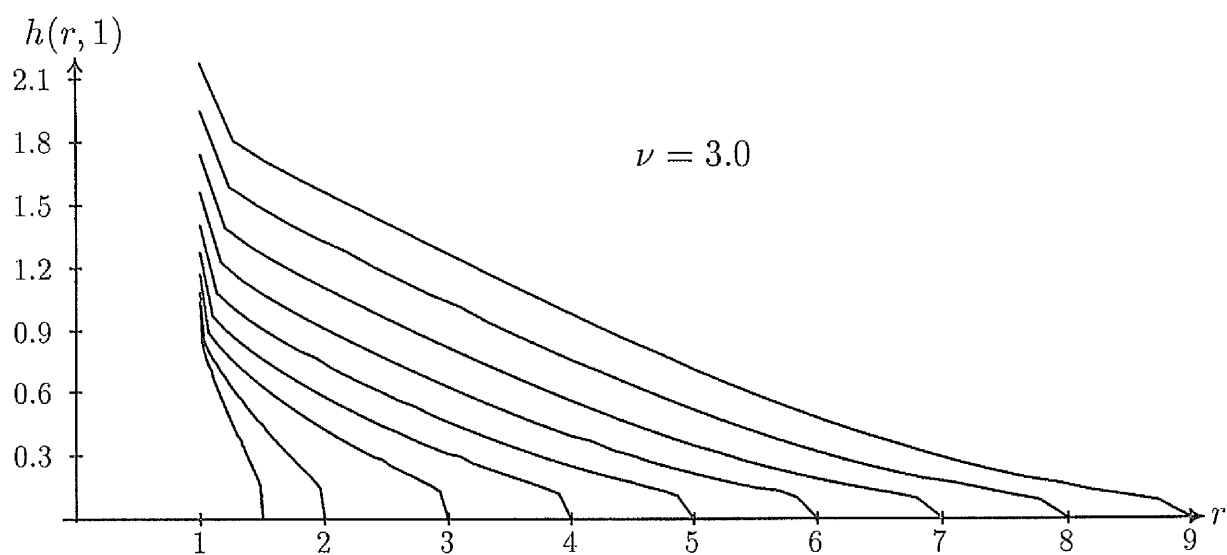


Figure 4.6: Graphs of  $h(r, 1)$  when  $\nu = 3.0, 7.0, 9.0$  for static deformation.

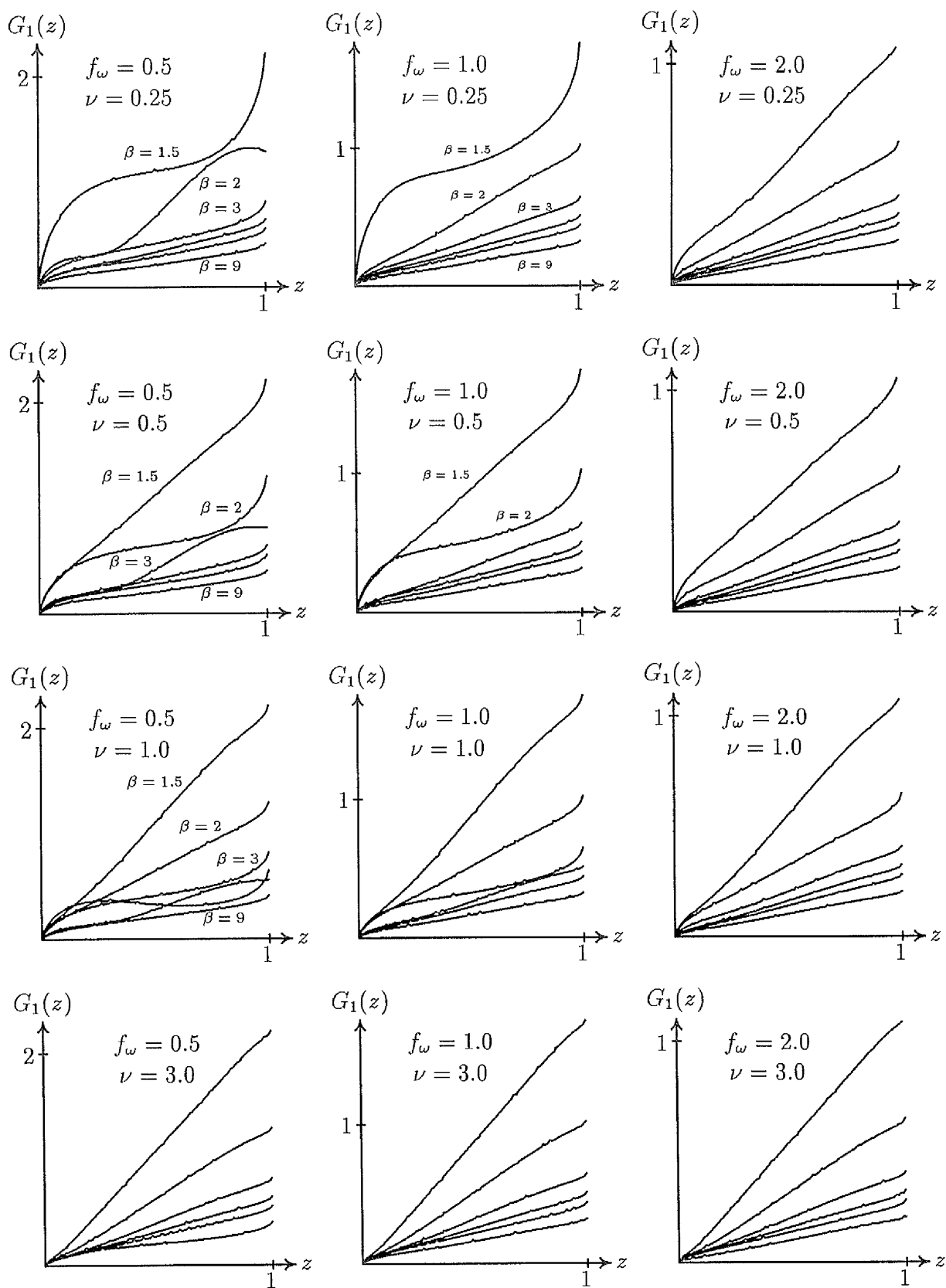


Figure 4.7: Graphs of accumulated shear stress  $G_1(z)$  when  $\nu = 0.25, 0.5, 1.0, 3.0$  and for frequencies  $f_\omega = 0.5, 1, 2$ .



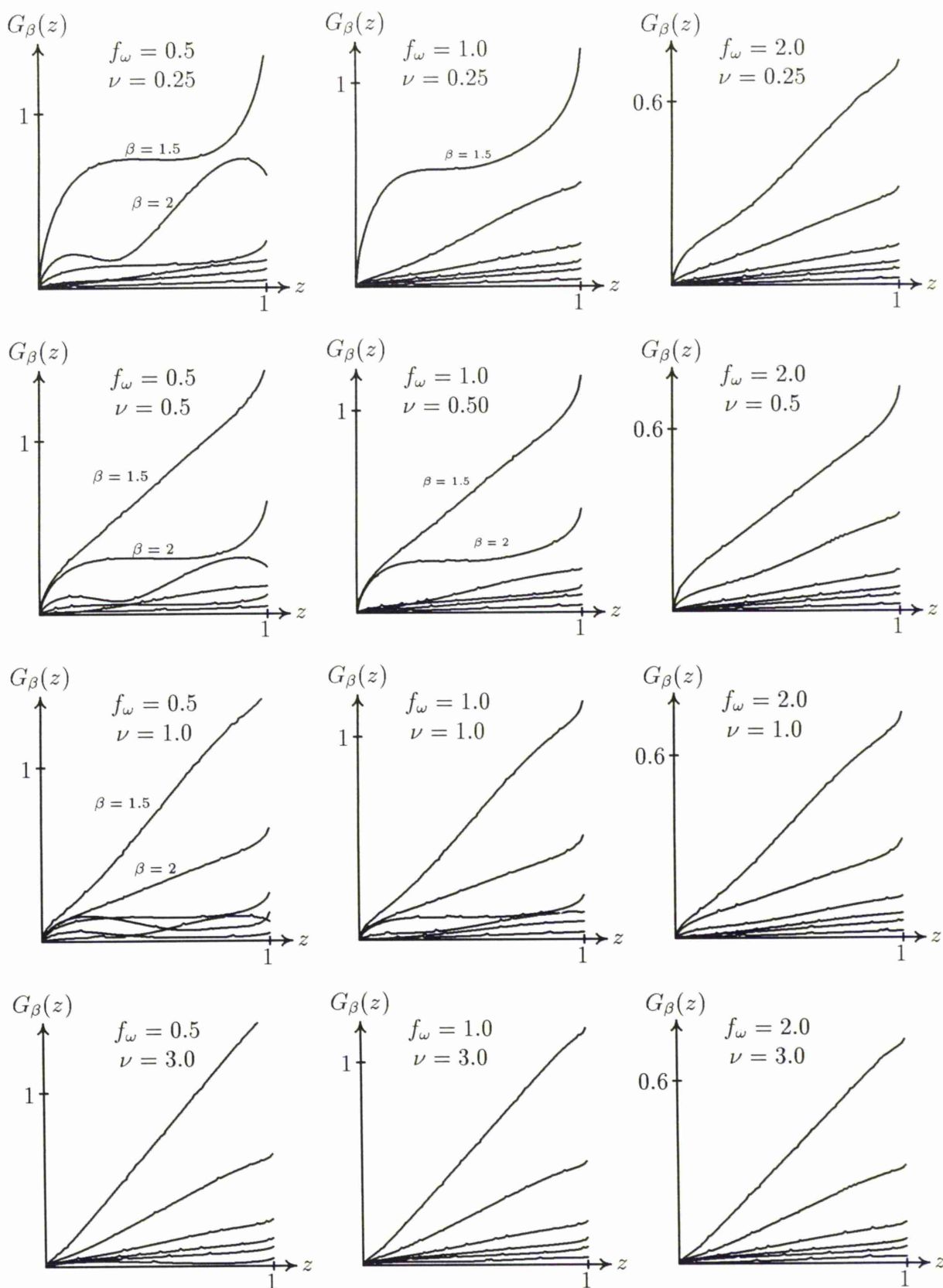


Figure 4.8: Graphs of accumulated shear stress  $G_\beta(z)$  when  $\nu = 0.25, 0.5, 1.0, 3.0$  and for frequencies  $f_\omega = 0.5, 1, 2$ .

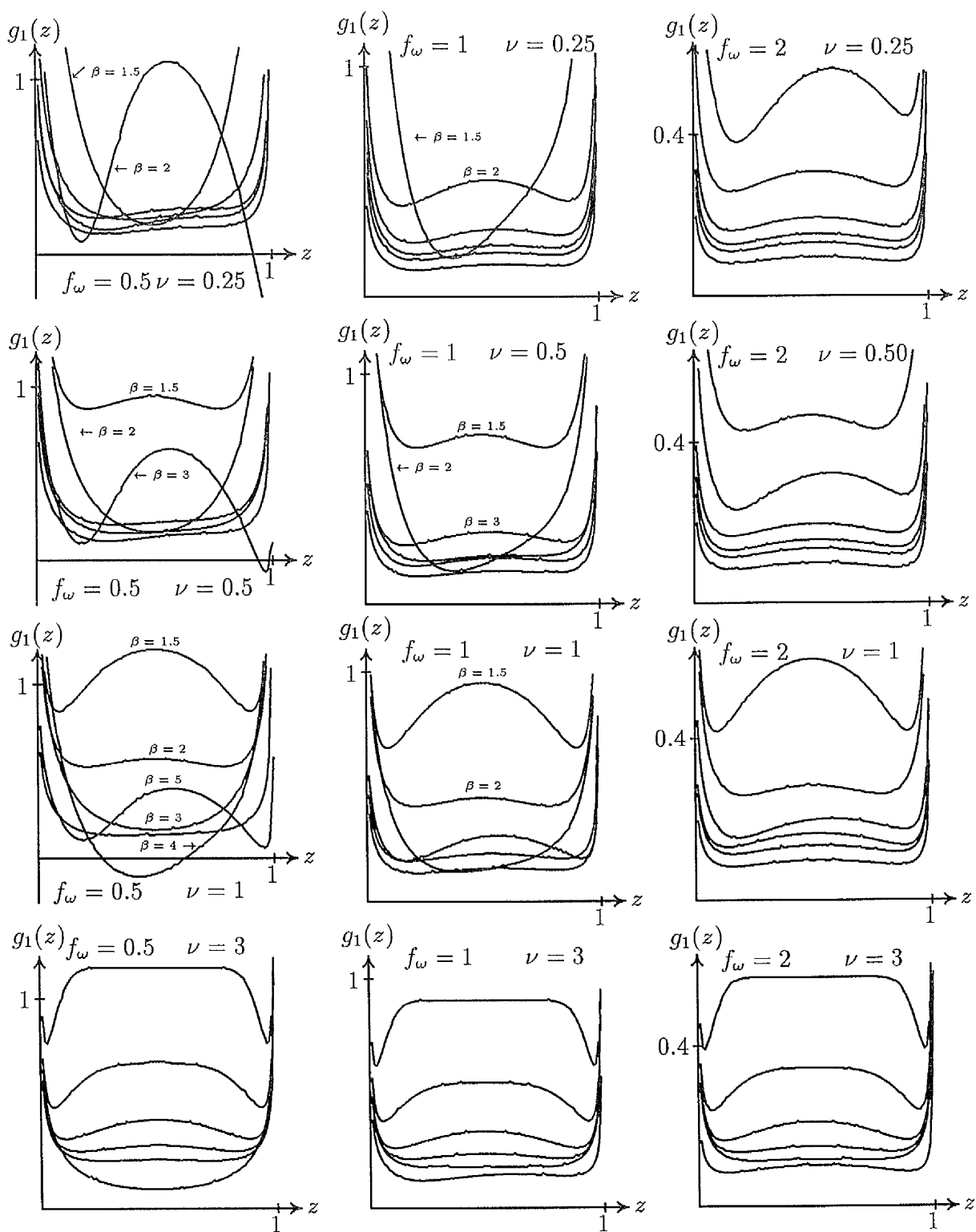


Figure 4.9: Graphs of shear stress  $g_1(z)$  when  $\nu = 0.25, 0.5, 1.0, 3.0$  and for frequencies  $f_\omega = 0.5, 1, 2$ . Component pictures correspond to their counterparts in accumulated shear stress  $G_1(z)$  illustrated in Figure 4.7.

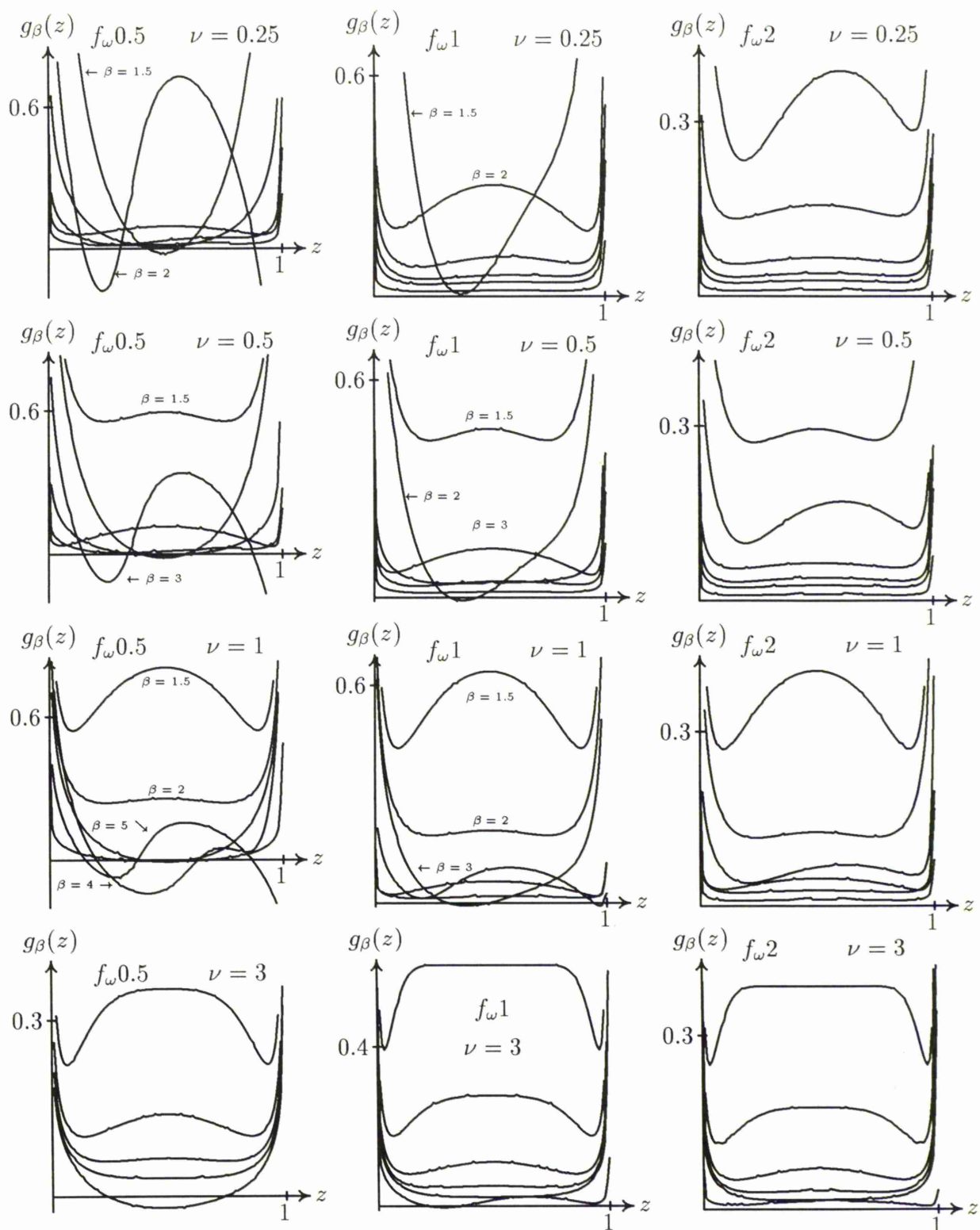


Figure 4.10: Graphs of shear stress  $g_\beta(z)$  when  $\nu = 0.25, 0.5, 1.0, 3.0$  and for frequencies  $f_\omega 0.5, 1, 2$ . Component pictures correspond to their counterparts in accumulated shear stress  $G_\beta(z)$  illustrated in figure 4.8.

r	$\beta = 1.5 \quad f_\omega = 1.0$				
	$\nu = 0.25$	$\nu = 0.5$	$\nu = 1$	$\nu = 3$	$\nu = 9$
1.000	1.8814	0.9817	0.8082	0.7361	0.7165
1.017	1.6965	0.8144	0.6506	0.5895	0.5660
1.033	1.6503	0.7801	0.6216	0.5634	0.5449
1.067	1.5648	0.7235	0.5744	0.5205	0.5048
1.100	1.4667	0.6712	0.5321	0.4821	0.4679
1.133	1.3524	0.6199	0.4919	0.4457	0.4328
1.167	1.2245	0.5687	0.4531	0.4107	0.3989
1.200	1.0872	0.5177	0.4154	0.3767	0.3660
1.233	0.9455	0.4671	0.3786	0.3437	0.3341
1.267	0.8043	0.4175	0.3428	0.3115	0.3029
1.300	0.6684	0.3692	0.3079	0.2801	0.2726
1.333	0.5421	0.3227	0.2739	0.2496	0.2431
1.367	0.4293	0.2782	0.2407	0.2197	0.2143
1.400	0.3328	0.2357	0.2080	0.1903	0.1859
1.433	0.2533	0.1945	0.1751	0.1607	0.1575
1.467	0.1861	0.1516	0.1399	0.1289	0.1279
1.483	0.1504	0.1261	0.1187	0.1100	0.1126
1.500	0.0000	0.0000	0.0000	0.0000	0.0000

r	$\beta = 4.0 \quad f_\omega = 1.0$				
	$\nu = 0.25$	$\nu = 0.5$	$\nu = 1$	$\nu = 3$	$\nu = 9$
1.000	0.2196	0.3868	1.1353	0.9447	0.7631
1.100	0.1851	0.3238	1.0350	0.7244	0.5635
1.200	0.1578	0.3001	1.0203	0.6778	0.5245
1.400	0.0879	0.2445	0.9834	0.6050	0.4640
1.600	0.0271	0.1890	0.9262	0.5435	0.4142
1.800	0.0289	0.1399	0.8500	0.4881	0.3710
2.000	0.0571	0.0947	0.7589	0.4369	0.3323
2.200	0.0675	0.0556	0.6581	0.3891	0.2973
2.400	0.0591	0.0528	0.5528	0.3444	0.2653
2.600	0.0434	0.0879	0.4485	0.3026	0.2358
2.800	0.0361	0.1211	0.3504	0.2636	0.2084
3.000	0.0436	0.1377	0.2631	0.2274	0.1830
3.200	0.0579	0.1337	0.1903	0.1940	0.1591
3.400	0.0638	0.1116	0.1341	0.1631	0.1364
3.600	0.0532	0.0786	0.0946	0.1339	0.1144
3.800	0.0304	0.0447	0.0682	0.1043	0.0914
3.900	0.0181	0.0301	0.0571	0.0870	0.0778
4.000	0.0000	0.0000	0.0000	0.0000	0.0000

r	$\beta = 6.0 \quad f_\omega = 1.0$				
	$\nu = 0.25$	$\nu = 0.5$	$\nu = 1$	$\nu = 3$	$\nu = 9$
1.000	0.1540	0.2793	0.4179	1.2938	0.8022
1.167	0.1161	0.2308	0.3504	1.0334	0.5742
1.333	0.0769	0.2034	0.3345	0.9724	0.5277
1.667	0.0055	0.1358	0.2997	0.8764	0.4580
2.000	0.0309	0.0687	0.2607	0.7906	0.4033
2.333	0.0330	0.0116	0.2180	0.7079	0.3572
2.667	0.0213	0.0339	0.1708	0.6270	0.3171
3.000	0.0219	0.0538	0.1197	0.5483	0.2815
3.333	0.0254	0.0551	0.0677	0.4726	0.2494
3.667	0.0235	0.0508	0.0195	0.4011	0.2203
4.000	0.0238	0.0489	0.0207	0.3348	0.1936
4.333	0.0250	0.0476	0.0477	0.2747	0.1690
4.667	0.0214	0.0484	0.0602	0.2215	0.1462
5.000	0.0230	0.0501	0.0589	0.1755	0.1247
5.333	0.0297	0.0439	0.0468	0.1364	0.1041
5.667	0.0228	0.0267	0.0290	0.1015	0.0827
5.833	0.0133	0.0165	0.0195	0.0823	0.0701
6.000	0.0000	0.0000	0.0000	0.0000	0.0000

r	$\beta = 9.0 \quad f_\omega = 1.0$				
	$\nu = 0.25$	$\nu = 0.5$	$\nu = 1$	$\nu = 3$	$\nu = 9$
1.000	0.1191	0.2235	0.4094	1.5647	0.8713
1.267	0.0711	0.1703	0.3394	1.3385	0.6123
1.533	0.0248	0.1271	0.3098	1.2949	0.5567
2.067	0.0215	0.0430	0.2327	1.2156	0.4769
2.600	0.0128	0.0145	0.1497	1.1243	0.4163
3.133	0.0129	0.0392	0.0768	1.0194	0.3663
3.667	0.0132	0.0381	0.0237	0.9042	0.3230
4.200	0.0126	0.0254	0.0175	0.7833	0.2846
4.733	0.0130	0.0211	0.0457	0.6611	0.2501
5.267	0.0127	0.0278	0.0730	0.5422	0.2188
5.800	0.0130	0.0293	0.0929	0.4310	0.1903
6.333	0.0128	0.0237	0.0982	0.3313	0.1642
6.867	0.0128	0.0231	0.0872	0.2463	0.1403
7.400	0.0132	0.0304	0.0654	0.1783	0.1182
7.933	0.0118	0.0327	0.0420	0.1280	0.0973
8.467	0.0157	0.0214	0.0228	0.0924	0.0762
8.733	0.0104	0.0124	0.0149	0.0763	0.0638
9.000	0.0000	0.0000	0.0000	0.0000	0.0000

Table 4.5: Tables of incompressible amplitude of surface deformation for frequency  $f_\omega = 1.0$  when  $\beta = 1.5, 4.0, 6.0, 9.0$  and for a selection of aspect ratios  $\nu$ .

r	$\beta = 1.5 \quad f_\omega = 2.0$				
	$\nu = 0.25$	$\nu = 0.5$	$\nu = 1$	$\nu = 3$	$\nu = 9$
1.000	0.5562	0.6286	0.5144	0.4659	0.4532
1.017	0.4874	0.5215	0.4141	0.3730	0.3580
1.033	0.4743	0.4998	0.3957	0.3566	0.3446
1.067	0.4502	0.4639	0.3657	0.3294	0.3193
1.100	0.4225	0.4307	0.3388	0.3051	0.2959
1.133	0.3902	0.3978	0.3133	0.2821	0.2737
1.167	0.3539	0.3650	0.2886	0.2599	0.2523
1.200	0.3152	0.3321	0.2645	0.2384	0.2315
1.233	0.2755	0.2995	0.2411	0.2175	0.2113
1.267	0.2365	0.2675	0.2183	0.1971	0.1916
1.300	0.1996	0.2364	0.1960	0.1773	0.1724
1.333	0.1658	0.2065	0.1743	0.1579	0.1537
1.367	0.1359	0.1779	0.1531	0.1390	0.1355
1.400	0.1099	0.1507	0.1323	0.1204	0.1176
1.433	0.0873	0.1244	0.1114	0.1017	0.0996
1.467	0.0665	0.0972	0.0890	0.0816	0.0809
1.483	0.0551	0.0810	0.0756	0.0696	0.0712
1.500	0.0000	0.0000	0.0000	0.0000	0.0000

r	$\beta = 4.0 \quad f_\omega = 2.0$				
	$\nu = 0.25$	$\nu = 0.5$	$\nu = 1$	$\nu = 3$	$\nu = 9$
1.000	0.0806	0.1574	0.2716	0.6049	0.4838
1.100	0.0569	0.1228	0.2268	0.4642	0.3572
1.200	0.0420	0.1097	0.2174	0.4347	0.3326
1.400	0.0157	0.0809	0.2001	0.3885	0.2942
1.600	0.0132	0.0531	0.1807	0.3494	0.2627
1.800	0.0187	0.0321	0.1592	0.3140	0.2353
2.000	0.0188	0.0237	0.1363	0.2811	0.2108
2.200	0.0170	0.0266	0.1130	0.2504	0.1886
2.400	0.0166	0.0327	0.0906	0.2215	0.1683
2.600	0.0171	0.0383	0.0708	0.1944	0.1495
2.800	0.0171	0.0422	0.0551	0.1692	0.1322
3.000	0.0163	0.0434	0.0442	0.1459	0.1160
3.200	0.0163	0.0414	0.0373	0.1244	0.1009
3.400	0.0183	0.0362	0.0320	0.1045	0.0865
3.600	0.0190	0.0282	0.0259	0.0858	0.0725
3.800	0.0139	0.0181	0.0180	0.0669	0.0580
3.900	0.0090	0.0124	0.0134	0.0559	0.0493
4.000	0.0000	0.0000	0.0000	0.0000	0.0000

r	$\beta = 6.0 \quad f_\omega = 2.0$				
	$\nu = 0.25$	$\nu = 0.5$	$\nu = 1$	$\nu = 3$	$\nu = 9$
1.000	0.0579	0.1109	0.2079	0.6901	0.5103
1.167	0.0326	0.0776	0.1552	0.5441	0.3654
1.333	0.0148	0.0605	0.1383	0.5127	0.3359
1.667	0.0078	0.0278	0.1050	0.4634	0.2917
2.000	0.0101	0.0099	0.0741	0.4191	0.2570
2.333	0.0083	0.0156	0.0488	0.3759	0.2277
2.667	0.0087	0.0200	0.0312	0.3333	0.2021
3.000	0.0087	0.0201	0.0246	0.2916	0.1794
3.333	0.0087	0.0184	0.0290	0.2514	0.1590
3.667	0.0087	0.0170	0.0373	0.2135	0.1404
4.000	0.0087	0.0164	0.0440	0.1785	0.1234
4.333	0.0087	0.0168	0.0468	0.1470	0.1077
4.667	0.0088	0.0184	0.0449	0.1193	0.0931
5.000	0.0083	0.0200	0.0385	0.0956	0.0794
5.333	0.0090	0.0187	0.0292	0.0754	0.0663
5.667	0.0093	0.0128	0.0184	0.0573	0.0527
5.833	0.0064	0.0083	0.0129	0.0473	0.0446
6.000	0.0000	0.0000	0.0000	0.0000	0.0000

r	$\beta = 9.0 \quad f_\omega = 2.0$				
	$\nu = 0.25$	$\nu = 0.5$	$\nu = 1$	$\nu = 3$	$\nu = 9$
1.000	0.0448	0.0856	0.1564	0.3655	0.5569
1.267	0.0160	0.0506	0.1073	0.2861	0.3919
1.533	0.0010	0.0292	0.0875	0.2704	0.3566
2.067	0.0055	0.0033	0.0504	0.2462	0.3060
2.600	0.0046	0.0112	0.0220	0.2227	0.2674
3.133	0.0047	0.0108	0.0098	0.1981	0.2355
3.667	0.0047	0.0091	0.0167	0.1722	0.2077
4.200	0.0047	0.0094	0.0214	0.1459	0.1830
4.733	0.0047	0.0096	0.0216	0.1201	0.1608
5.267	0.0047	0.0095	0.0198	0.0959	0.1406
5.800	0.0047	0.0095	0.0186	0.0744	0.1222
6.333	0.0047	0.0096	0.0192	0.0564	0.1054
6.867	0.0047	0.0092	0.0208	0.0426	0.0899
7.400	0.0047	0.0091	0.0213	0.0324	0.0757
7.933	0.0046	0.0106	0.0186	0.0246	0.0624
8.467	0.0052	0.0092	0.0122	0.0178	0.0489
8.733	0.0045	0.0060	0.0081	0.0143	0.0410
9.000	0.0000	0.0000	0.0000	0.0000	0.0000

Table 4.6: Tables of incompressible amplitude of surface deformation for frequency  $f_\omega = 2.0$  when  $\beta = 1.5, 4.0, 6.0, 9.0$  and for a selection of aspect ratios  $\nu$ .

r	$\beta = 1.5 \quad f_\omega = 5.0$				
	$\nu = 0.25$	$\nu = 0.5$	$\nu = 1$	$\nu = 3$	$\nu = 9$
1.000	0.0969	0.2310	0.2245	0.2043	0.1987
1.017	0.0816	0.1903	0.1807	0.1636	0.1570
1.033	0.0779	0.1823	0.1727	0.1564	0.1511
1.067	0.0714	0.1690	0.1596	0.1445	0.1400
1.100	0.0652	0.1567	0.1479	0.1338	0.1297
1.133	0.0590	0.1448	0.1367	0.1237	0.1200
1.167	0.0532	0.1329	0.1259	0.1140	0.1106
1.200	0.0478	0.1210	0.1154	0.1046	0.1015
1.233	0.0431	0.1094	0.1052	0.0954	0.0926
1.267	0.0390	0.0981	0.0952	0.0864	0.0840
1.300	0.0355	0.0871	0.0855	0.0777	0.0756
1.333	0.0323	0.0765	0.0760	0.0693	0.0674
1.367	0.0289	0.0663	0.0668	0.0610	0.0594
1.400	0.0249	0.0565	0.0577	0.0528	0.0515
1.433	0.0201	0.0468	0.0486	0.0446	0.0436
1.467	0.0143	0.0367	0.0388	0.0358	0.0354
1.483	0.0110	0.0306	0.0330	0.0305	0.0312
1.500	0.0000	0.0000	0.0000	0.0000	0.0000

r	$\beta = 4.0 \quad f_\omega = 5.0$				
	$\nu = 0.25$	$\nu = 0.5$	$\nu = 1$	$\nu = 3$	$\nu = 9$
1.000	0.0207	0.0403	0.0750	0.2318	0.2122
1.100	0.0112	0.0268	0.0544	0.1766	0.1567
1.200	0.0066	0.0214	0.0483	0.1651	0.1459
1.400	0.0037	0.0128	0.0383	0.1473	0.1290
1.600	0.0044	0.0081	0.0300	0.1322	0.1152
1.800	0.0043	0.0076	0.0235	0.1187	0.1032
2.000	0.0042	0.0085	0.0188	0.1062	0.0925
2.200	0.0043	0.0089	0.0163	0.0945	0.0827
2.400	0.0043	0.0089	0.0156	0.0837	0.0738
2.600	0.0043	0.0086	0.0161	0.0735	0.0656
2.800	0.0043	0.0085	0.0168	0.0642	0.0580
3.000	0.0043	0.0086	0.0170	0.0555	0.0509
3.200	0.0042	0.0090	0.0164	0.0475	0.0442
3.400	0.0042	0.0091	0.0147	0.0401	0.0379
3.600	0.0044	0.0083	0.0119	0.0330	0.0318
3.800	0.0041	0.0060	0.0081	0.0258	0.0254
3.900	0.0030	0.0041	0.0059	0.0216	0.0216
4.000	0.0000	0.0000	0.0000	0.0000	0.0000

r	$\beta = 6.0 \quad f_\omega = 5.0$				
	$\nu = 0.25$	$\nu = 0.5$	$\nu = 1$	$\nu = 3$	$\nu = 9$
1.000	0.0149	0.0289	0.0547	0.1511	0.2226
1.167	0.0052	0.0158	0.0355	0.1125	0.1594
1.333	0.0018	0.0099	0.0288	0.1039	0.1465
1.667	0.0023	0.0037	0.0182	0.0909	0.1272
2.000	0.0021	0.0043	0.0110	0.0802	0.1121
2.333	0.0022	0.0047	0.0078	0.0705	0.0993
2.667	0.0022	0.0045	0.0078	0.0615	0.0881
3.000	0.0022	0.0044	0.0086	0.0532	0.0782
3.333	0.0022	0.0044	0.0090	0.0457	0.0693
3.667	0.0022	0.0044	0.0092	0.0389	0.0612
4.000	0.0022	0.0044	0.0093	0.0330	0.0538
4.333	0.0022	0.0044	0.0094	0.0278	0.0469
4.667	0.0022	0.0043	0.0095	0.0234	0.0406
5.000	0.0022	0.0044	0.0091	0.0194	0.0346
5.333	0.0021	0.0047	0.0080	0.0156	0.0289
5.667	0.0023	0.0039	0.0056	0.0117	0.0229
5.833	0.0019	0.0028	0.0039	0.0095	0.0194
6.000	0.0000	0.0000	0.0000	0.0000	0.0000

r	$\beta = 9.0 \quad f_\omega = 5.0$				
	$\nu = 0.25$	$\nu = 0.5$	$\nu = 1$	$\nu = 3$	$\nu = 9$
1.000	0.0116	0.0224	0.0422	0.1002	0.2310
1.267	0.0018	0.0088	0.0232	0.0661	0.1620
1.533	0.0012	0.0033	0.0159	0.0571	0.1473
2.067	0.0012	0.0024	0.0062	0.0442	0.1261
2.600	0.0012	0.0025	0.0038	0.0346	0.1101
3.133	0.0012	0.0024	0.0049	0.0270	0.0968
3.667	0.0012	0.0024	0.0052	0.0209	0.0854
4.200	0.0012	0.0024	0.0050	0.0164	0.0752
4.733	0.0012	0.0024	0.0049	0.0136	0.0660
5.267	0.0012	0.0024	0.0048	0.0123	0.0577
5.800	0.0012	0.0024	0.0048	0.0120	0.0502
6.333	0.0012	0.0024	0.0048	0.0120	0.0433
6.867	0.0012	0.0024	0.0048	0.0116	0.0370
7.400	0.0012	0.0024	0.0051	0.0105	0.0312
7.933	0.0012	0.0024	0.0050	0.0086	0.0257
8.467	0.0012	0.0025	0.0039	0.0059	0.0201
8.733	0.0012	0.0020	0.0027	0.0042	0.0169
9.000	0.0000	0.0000	0.0000	0.0000	0.0000

Table 4.7: Tables of incompressible amplitude of surface deformation for frequency  $f_\omega = 5.0$  when  $\beta = 1.5, 4.0, 6.0, 9.0$  and for a selection of aspect ratios  $\nu$ .

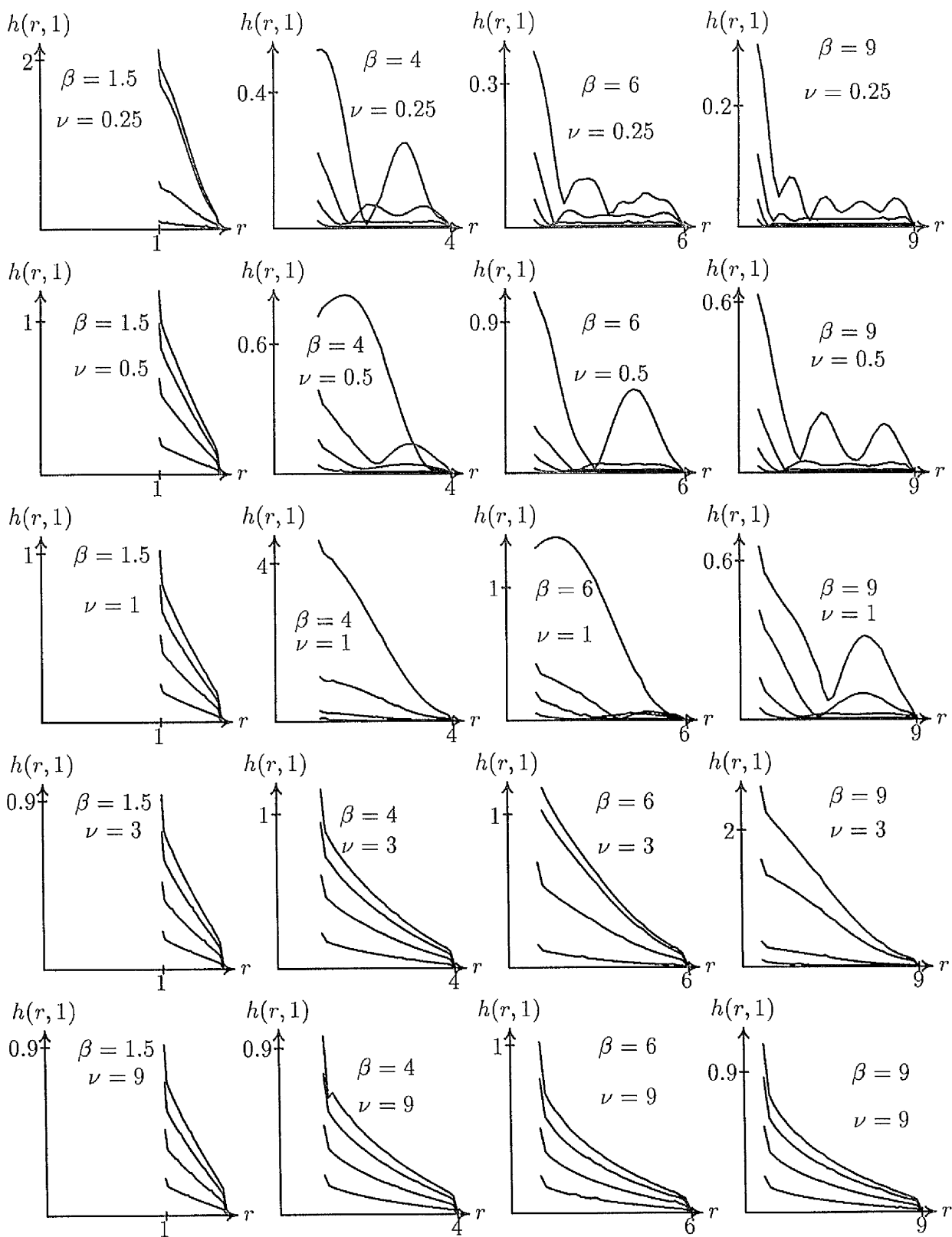


Figure 4.11: Graphs of the amplitude of dynamic surface deformation when  $\nu = 0.25, 0.5, 1.0, 3.0, 7.0, 9.0$  and for frequencies  $f_\omega = 0.5, 1, 2$  and  $5.0$ .

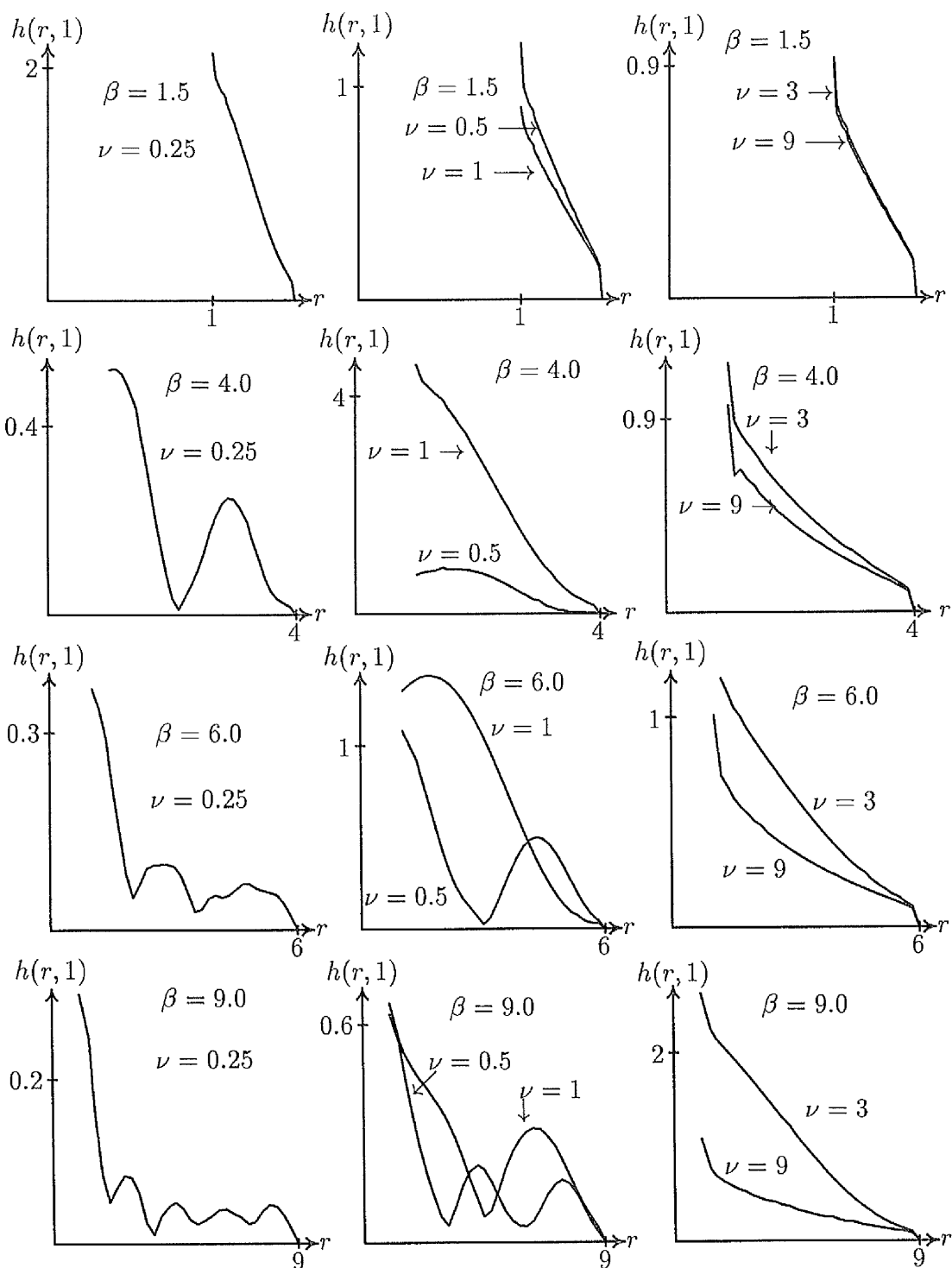


Figure 4.12: Graphs of the amplitude of dynamic surface deformation for frequency  $f_\omega = 0.5$  and for a selection of values of  $\nu$  and  $\beta$ .



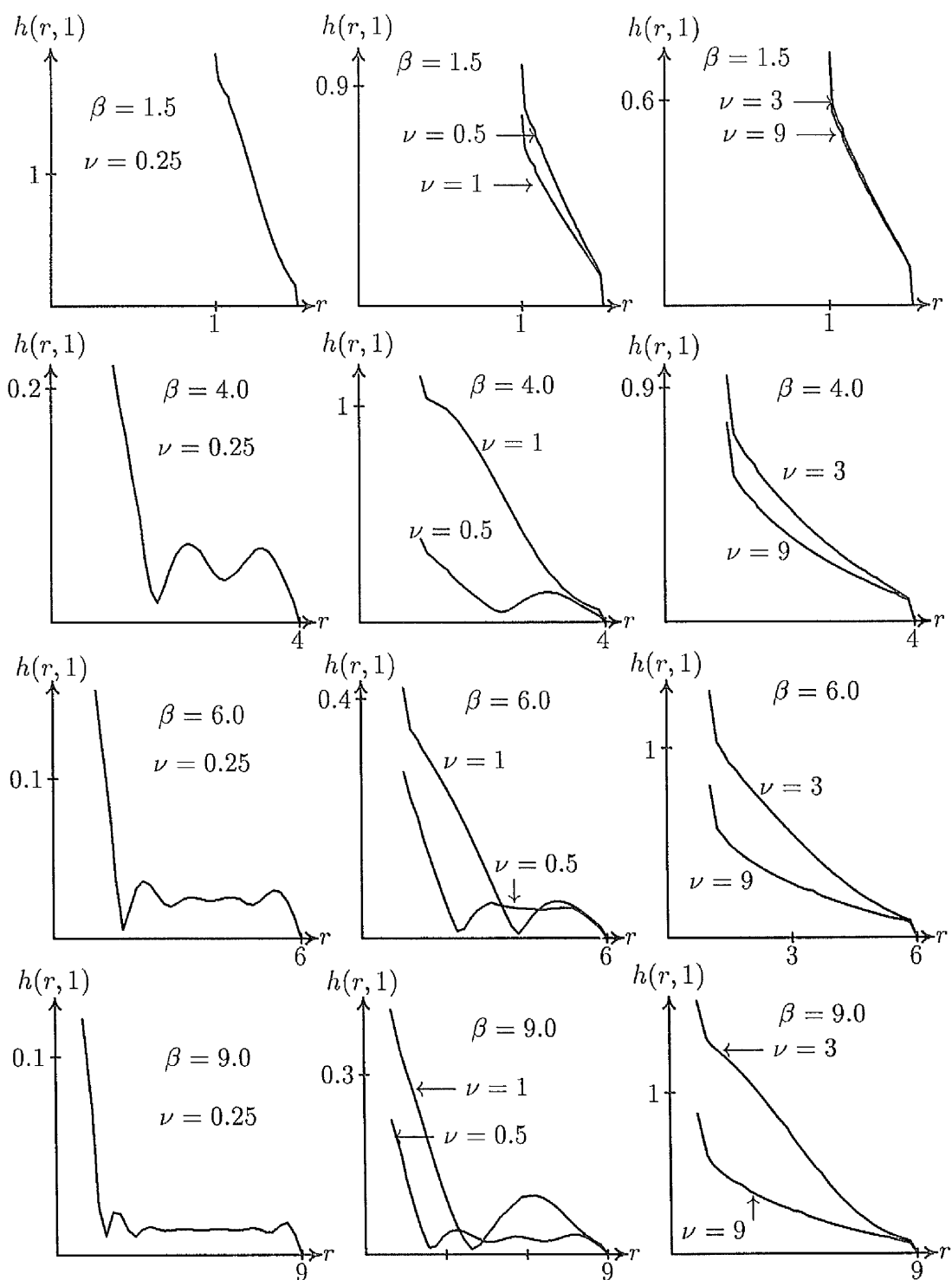


Figure 4.13: Graphs of the amplitude of dynamic surface deformation for frequency  $f_\omega = 1.0$  and for a selection of values of  $\nu$  and  $\beta$ .

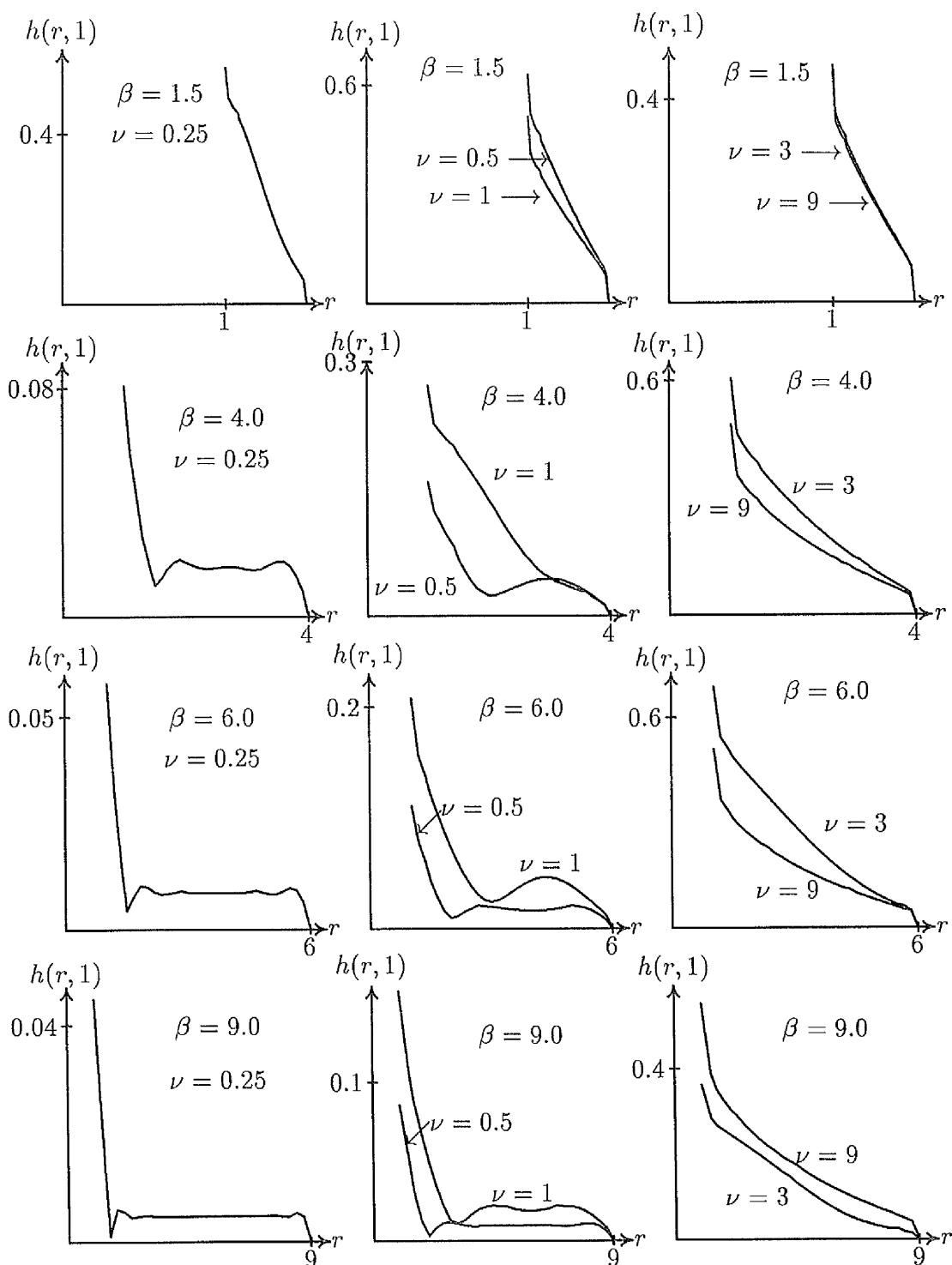


Figure 4.14: Graphs of the amplitude of dynamic surface deformation for frequency  $f_\omega = 2.0$  and for a selection of values of  $\nu$  and  $\beta$ .

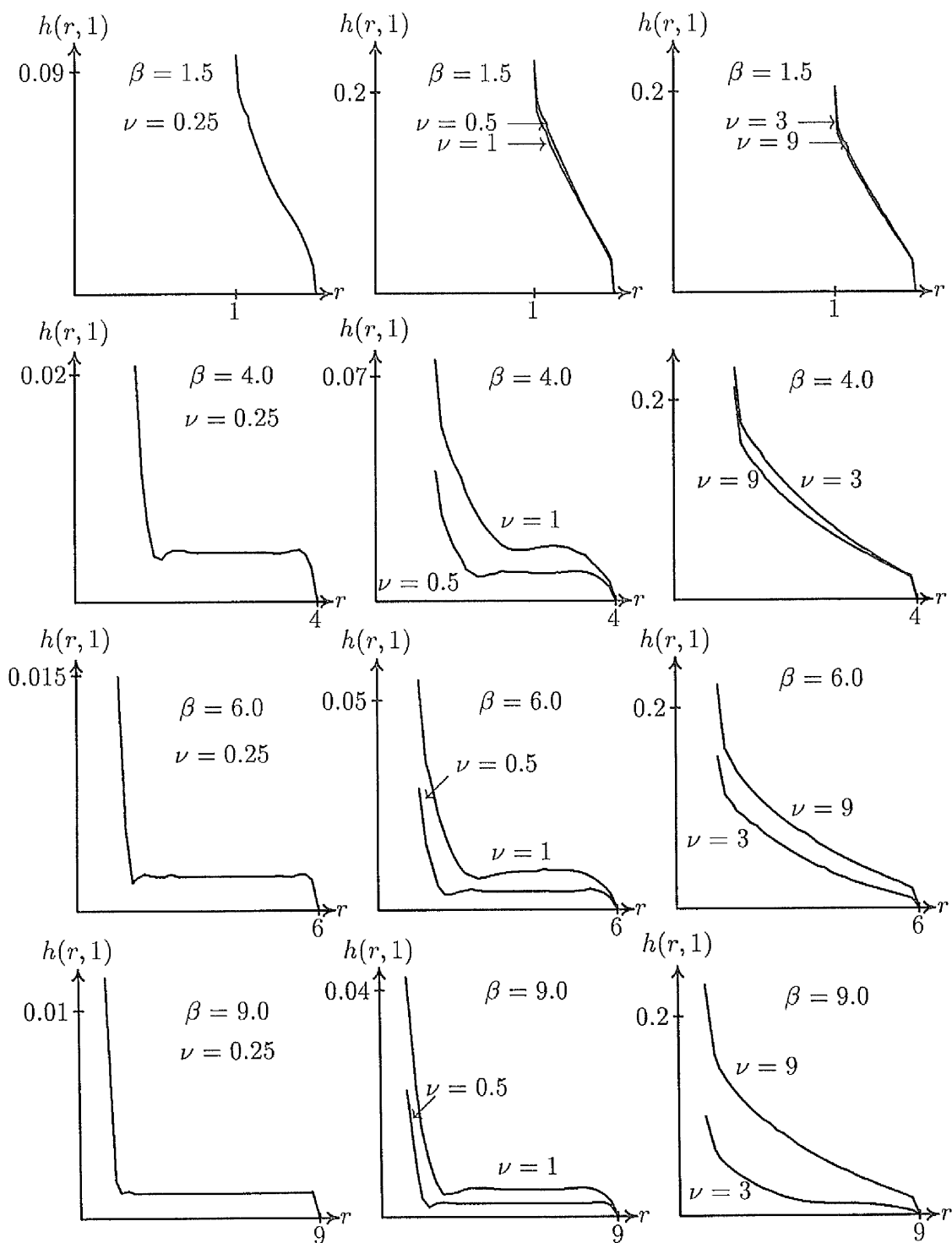


Figure 4.15: Graphs of the amplitude of dynamic surface deformation for frequency  $f_{\omega}=5.0$  and for a selection of values of  $\nu$  and  $\beta$ .

## Chapter 5

# Response of a Compressible Elastic Annulus to a Periodic Axial Driving Force

### 5.1 Introduction

This chapter examines axial deformation of a compressible isotropic elastic annulus of uniform thickness  $d$  and with outer radius  $b$  and inner radius  $a$ ; that is, one which is forced to move by bonding the fabric of the annulus to an axial shaft which neatly passes through the cylindrical hole at its centre. In terms of cylindrical polar coordinates,  $(r, \theta, z)$ , the annulus occupies the region

$$a \leq r \leq b, \quad -\pi \leq \theta \leq \pi, \quad 0 \leq z \leq d.$$

### 5.2 Compressible Viscoelasticity Theory

The linear viscoelastic stress tensor for a compressible isotropic solid is obtained from the general theory of Chapter one by appending the time derivative of the strain tensor to the compressible stress tensor to get

$$t^{ij} = \lambda v^r|_r g^{ij} + \mu(v^i|{}^j + v^j|{}^i) + \eta \frac{\partial}{\partial t}(v^i|{}^j + v^j|{}^i), \quad (5.2.1)$$

where  $\eta$  is viscosity and all other notations have their usual meanings. In the absence of external body forces, the balance of linear momentum requires that

$$\rho \frac{\partial^2 x^j}{\partial t^2} = t^{ij}|_i, \quad (5.2.2)$$

where  $\rho$  is material density. Suppose that a periodic force  $F(t) = F e^{if\omega t}$  is applied to the rigid shaft and induces the time dependent displacement  $\mathbf{v}(\mathbf{x}, t) = \mathbf{v}(\mathbf{x}) e^{if\omega t}$ . Under these circumstances, the stress tensor  $t^{ij}$  described in expression (5.2.1) has format  $t^{ij}(\mathbf{x}, t) = t^{ij}(\mathbf{x}) e^{if\omega t}$  and the momentum equations become

$$-\rho f_\omega^2 v^j = t^{ij}|_i, \quad t^{ij} = \lambda v^r|_r g^{ij} + (i\eta f_\omega + \mu)(v^i|_j + v^j|_i). \quad (5.2.3)$$

### 5.3 Displacement Equations

The axial nature of the proposed deformation suggests that  $\mathbf{v}(\mathbf{x})$  has component form

$$\mathbf{v} = w(r, z)\mathbf{g}_1 + h(r, z)\mathbf{g}_3, \quad (5.3.4)$$

with corresponding first order displacement gradient tensor

$$v^i|_j = \begin{bmatrix} \frac{\partial w}{\partial r} & 0 & \frac{\partial w}{\partial z} \\ 0 & \frac{w}{r} & 0 \\ \frac{\partial h}{\partial r} & 0 & \frac{\partial h}{\partial z} \end{bmatrix}. \quad (5.3.5)$$

When (5.3.5) is substituted into first order stress tensor (5.2.3), non-zero components of the first order stress tensor are seen to be

$$\begin{aligned} t^{11} &= \lambda \left( \frac{w}{r} + \frac{\partial h}{\partial z} \right) + (\lambda + 2\mu + 2i\eta f_\omega) \frac{\partial w}{\partial r}, \\ t^{22} &= \frac{\lambda}{r^2} \left( \frac{\partial w}{\partial r} + \frac{\partial h}{\partial z} \right) + (\lambda + 2\mu + 2i\eta f_\omega) \frac{2w}{r^3}, \\ t^{33} &= \lambda \left( \frac{w}{r} + \frac{\partial w}{\partial r} \right) + (\lambda + 2\mu + 2i\eta f_\omega) \frac{\partial h}{\partial z}, \\ t^{13} &= t^{31} = (i\eta f_\omega + \mu) \left( \frac{\partial h}{\partial r} + \frac{\partial w}{\partial z} \right). \end{aligned} \quad (5.3.6)$$

It is easily verified that the azimuthal linear momentum equation in (5.2.3) is identically satisfied (everything is zero in the absence of  $\theta$  dependence) while the remaining

momentum equations yield

$$\begin{aligned}\frac{\partial t^{11}}{\partial r} + \frac{\partial t^{13}}{\partial z} + \frac{t^{11}}{r} - r t^{22} &= -\rho f_{\omega} w, \\ \frac{\partial t^{13}}{\partial r} + \frac{\partial t^{33}}{\partial z} + \frac{t^{13}}{r} &= -\rho f_{\omega} h.\end{aligned}\tag{5.3.7}$$

When the components of stress tensor (5.3.6) are substituted into momentum equations (5.3.7), it can be shown that displacements  $h$  and  $w$  satisfy partial differential equations

$$\begin{aligned}-\rho f_{\omega}^2 w &= (\lambda + 2\mu + 2i f_{\omega} \eta) \left( \frac{\partial^2 w}{\partial r^2} + \frac{1}{r} \frac{\partial w}{\partial r} - \frac{w}{r^2} \right) + (i f_{\omega} \eta + \mu) \frac{\partial^2 w}{\partial z^2} \\ &\quad + (\lambda + \mu + i f_{\omega} \eta) \frac{\partial^2 h}{\partial r \partial z}, \\ -\rho f_{\omega}^2 h &= (i f_{\omega} \eta + \mu) \left( \frac{\partial^2 h}{\partial r^2} + \frac{1}{r} \frac{\partial h}{\partial r} \right) + (\lambda + 2\mu + 2i f_{\omega} \eta) \frac{\partial^2 h}{\partial z^2} \\ &\quad + (\lambda + \mu + i f_{\omega} \eta) \left( \frac{\partial^2 w}{\partial r \partial z} + \frac{1}{r} \frac{\partial w}{\partial z} \right).\end{aligned}\tag{5.3.8}$$

## 5.4 Boundary Conditions

Momentum equations (5.3.8) must be solved with suitable boundary conditions which ensure that boundaries  $z = 0$  and  $z = d$  are stress-free, that there is no deformation on the outer cylindrical boundary and that every point on the inner cylindrical boundary of the annulus is similarly displaced by an amount  $H e^{i(f_{\omega} t + \phi)}$ , where  $H$  and  $\phi$  are constants to be determined. The driving force is integrated into the mathematical equations by the requirement that the integral of shear stress over the inner cylindrical boundary of the annulus is applied driving force  $F e^{i\omega t}$ . Stress-free conditions on  $z = 0$  and  $z = d$  require

$$\left. \begin{aligned}t^{33} &= \lambda \left( \frac{\partial w}{\partial r} + \frac{w}{r} \right) + (\lambda + 2\mu + i f_{\omega} \eta) \frac{\partial h}{\partial z} = 0 \\ t^{31} &= \frac{\partial h}{\partial r} + \frac{\partial w}{\partial z} = 0\end{aligned} \right\} \begin{array}{l} z = 0, d \\ a < r < b \end{array}.\tag{5.4.9}$$

On the outer cylindrical boundary of the region, radial and axial displacements are both zero, whereas on the inner cylindrical boundary, radial displacement is zero but axial displacement is uniform (but unknown) for all  $z$ . Hence the displacement boundary conditions are

$$\left. \begin{aligned}w &= 0 \\ h &= 0\end{aligned} \right\} \text{ on } r = b, \quad \left. \begin{aligned}w &= 0 \\ h &= H e^{i\phi}\end{aligned} \right\} \text{ on } r = a.\tag{5.4.10}$$

Boundary  $r = a$  has outward unit normal  $-\mathbf{g}_1$  and so the stress vector on the inner boundary is  $\mathbf{t} = -t^{11}\mathbf{g}_1 - t^{13}\mathbf{g}_3$ . Balancing the accumulated shear stress on the inner boundary with applied force yields

$$\begin{aligned}
 F e^{if\omega t} \mathbf{g}_3 &= -\left(\int \int t^{13} dA\right) \mathbf{g}_3 \\
 &= -2\pi\mu(1+i\xi)a \left(\int_0^d \left(\frac{\partial w(a,z)}{\partial z} + \frac{\partial h(a,z)}{\partial r}\right) dz\right) e^{if\omega t} \mathbf{g}_3 \\
 &= -2\pi\mu(1+i\xi)a \left([w(a,z)]_0^d + \int_0^d \frac{\partial h(a,z)}{\partial r} dz\right) e^{if\omega t} \mathbf{g}_3 \\
 &= -2\pi\mu(1+i\xi)a \left(\int_0^d \frac{\partial h(a,z)}{\partial r} dz\right) e^{if\omega t} \mathbf{g}_3 .
 \end{aligned}$$

A similar analysis can be applied to the outer boundary. In conclusion, applied force  $F$  enters the boundary value problem through the conditions

$$F = -2\pi\mu(1+i\xi)a \int_0^d \frac{\partial h(a,z)}{\partial r} dz, \quad F = -2\pi\mu(1+i\xi)b \int_0^d \frac{\partial h(b,z)}{\partial r} dz. \quad (5.4.11)$$

### 5.4.1 Non-dimensional Problem

In order to expedite the solution procedure, it is convenient to rescale the coordinates  $r$  by  $a$  and  $z$  by  $d$  and to introduce non-dimensional  $u(r, z)$  and  $h(r, z)$  and non-dimensional parameters by the definitions

$$\begin{aligned}
 r^* &= \frac{r}{a}, & z^* &= \frac{z}{d}, & u^* &= \frac{w}{d}, & h^* &= \frac{h}{d}, \\
 \nu &= \frac{d}{a}, & \xi &= \frac{f\omega\eta}{\mu}, & \gamma &= -\frac{\lambda+2\mu}{2\mu}, & \sigma &= \frac{\rho f\omega^2 d^2}{\mu}.
 \end{aligned} \quad (5.4.12)$$

When (5.4.12) are substituted into momentum equations (5.3.8), boundary conditions (5.4.9) and (5.4.10) and finally into applied force (5.4.11), the resulting problem reduces to the solution of partial differential equations

$$\begin{aligned}
 \sigma u &= (1+i\xi) \frac{\partial}{\partial z} \left[ \nu \frac{\partial h}{\partial r} - \frac{\partial u}{\partial z} \right] + 2\nu(\gamma-i\xi) \frac{\partial}{\partial r} \left[ \frac{\partial h}{\partial z} + \nu \left( \frac{\partial u}{\partial r} + \frac{u}{r} \right) \right], \\
 \sigma h &= 2(\gamma-i\xi) \frac{\partial}{\partial z} \left[ \frac{\partial h}{\partial z} + \nu \left( \frac{\partial u}{\partial r} + \frac{u}{r} \right) \right] - \nu(1+i\xi) \frac{1}{r} \frac{\partial}{\partial r} \left[ r \left( \nu \frac{\partial h}{\partial r} - \frac{\partial u}{\partial z} \right) \right].
 \end{aligned} \quad (5.4.13)$$

Similarly, boundary conditions (5.4.9) and (5.4.10) and applied force (5.4.11) become

$$\begin{aligned} \nu(1 + \gamma)\left(\frac{\partial u}{\partial r} + \frac{u}{r}\right) + (\gamma - i\xi)\frac{\partial h}{\partial z} &= 0 \quad \frac{\partial u}{\partial z} + \nu\frac{\partial h}{\partial r} = 0, \quad \text{on} \quad \begin{matrix} z = 0, 1 \\ 1 < r < \beta \end{matrix} \\ u = 0, \quad h = He^{i\phi}, \quad \frac{F}{2\pi\mu d^2} &= -(1 + i\xi) \int_0^1 \frac{\partial h(1, z)}{\partial r} dz, \quad \text{on} \quad r = 1 \\ u = 0, \quad h = 0, \quad \frac{F}{2\pi\mu d^2} &= -(1 + i\xi)\beta \int_0^1 \frac{\partial h(\beta, z)}{\partial r} dz, \quad \text{on} \quad r = \beta \end{aligned} \quad (5.4.14)$$

in which the \* notation has been dropped and  $\beta = b/a$ . Equations (5.4.13) and (5.4.14) constitute the final form of the boundary value problem.

## 5.5 Transformed Equations

The general solution to equations (5.4.13) with boundary conditions (5.4.14) can be obtained using finite Weber-Orr transforms introduced in Chapter two. Let finite Weber-Orr transforms  $\bar{u}(z, \lambda)$  and  $\bar{h}(z, \lambda)$  be defined by integrals

$$\bar{u}(z, \lambda) = \int_1^\beta ru(r, z)C_{11}(\lambda r, \lambda)dr, \quad \bar{h}(z, \lambda) = \int_1^\beta rh(r, z)C_{01}(\lambda r, \lambda)dr. \quad (5.5.15)$$

Functions  $u(r, z)$  and  $h(r, z)$  can be recovered from  $\bar{u}(z, \lambda)$  and  $\bar{h}(z, \lambda)$  using the inversion formulae (see chapter two)

$$\begin{aligned} u(r, z) &= \frac{\pi^2}{2} \sum_{n=1}^{\infty} \frac{\lambda_n^2 J_1^2(\lambda_n \beta) \bar{u}(\lambda_n, z)}{J_1^2(\lambda_n) - J_1^2(\lambda_n \beta)} C_{11}(\lambda_n r, \lambda_n), \\ h(r, z) &= h_0(z) + \frac{\pi^2}{2} \sum_{n=1}^{\infty} \frac{\lambda_n^2 J_1^2(\lambda_n \beta) \bar{h}(\lambda_n, z)}{J_1^2(\lambda_n) - J_1^2(\lambda_n \beta)} C_{01}(\lambda_n r, \lambda_n), \end{aligned} \quad (5.5.16)$$

where  $\lambda_n$ ,  $n = 1, 2, \dots$  are the positive roots of  $C_{11}(\beta\lambda, \lambda) = 0$ . It is clear from properties of the  $\lambda$ 's that the solution (5.5.16) for  $u(r, z)$  automatically ensures that  $u(1, z) = u(\beta, z) = 0$ . The function  $h_0(z)$  appearing in  $h(r, z)$  is given by

$$h_0(z) = \frac{2}{\beta^2 - 1} \int_1^\beta rh(r, z)dr. \quad (5.5.17)$$

The first and second field equations (5.4.13) are multiplied by  $rC_{11}(\lambda r, \lambda)$  and  $rC_{01}(\lambda r, \lambda)$  respectively and both are now integrated with respect to  $r$  over  $[1, \beta]$ . For more details about the transformed equations, see appendix A. The result is that  $\bar{u}(z, \lambda)$  and  $\bar{h}(z, \lambda)$



satisfy ordinary differential equations

$$2\lambda^2\nu^2(\gamma - i\xi)\bar{u} + \lambda\nu(1 + 2\gamma - i\xi)\frac{d\bar{h}}{dz} + (1 + i\xi)\frac{d^2\bar{u}}{dz^2} = -\sigma\bar{u}, \quad (5.5.18)$$

$$\lambda^2\nu^2(1 + i\xi)\bar{h} + \lambda\nu(1 + 2\gamma - i\xi)\frac{d\bar{u}}{dz} + 2(\gamma - i\xi)\frac{d^2\bar{h}}{dz^2} = \sigma\bar{h} + \frac{2\nu^2(1 + i\xi)}{\pi\lambda}g(z),$$

where  $g_1(z)$  and  $g_\beta(z)$  are respectively the shear stress distributions on the inner and outer cylindrical boundaries  $r = 1$  and  $r = \beta$ . Furthermore,

$$g(z) = g_1(z) - g_\beta(z)\frac{J_1(\lambda)}{J_1(\lambda\beta)}, \quad g_1(z) = \frac{\partial h(1, z)}{\partial r}, \quad g_\beta(z) = \frac{\partial h(\beta, z)}{\partial r}. \quad (5.5.19)$$

Original boundary conditions (5.4.14) on  $z = 0$  and  $z = 1$  are now suitably transformed to obtain

$$\left. \begin{aligned} \lambda\nu(1 + \gamma)\bar{u} + (\gamma - i\xi)\frac{d\bar{h}}{dz} &= 0 \\ \frac{d\bar{u}}{dz} - \lambda\nu\bar{h} &= 0 \end{aligned} \right\} \quad \text{on } z = 0, 1, \quad (5.5.20)$$

and the remainder of the boundary conditions become

$$\begin{aligned} u = 0, \quad h = 0, \quad \frac{F}{2\pi d^2} &= -\mu(1 + i\xi)\beta \int_0^1 g_\beta(t) dt & \text{on } r = \beta, \\ u = 0, \quad h = H, \quad \frac{F}{2\pi d^2} &= -\mu(1 + i\xi) \int_0^1 g_1(t) dt & \text{on } r = 1. \end{aligned} \quad (5.5.21)$$

## 5.6 General Solution

Field equations (5.5.18) constitute a fourth order system of ordinary differential equations to be solved with boundary conditions (5.5.20). Let  $G_1(z)$ ,  $G_\beta(z)$  and  $G(z)$  be defined by the definitions

$$G_1(z) = \int_0^z g_1(t) dt, \quad G_\beta(z) = \int_0^z g_\beta(t) dt, \quad G(z) = \int_0^z g(t) dt. \quad (5.6.22)$$

Using algebraic manipulation (see appendix A for more details about the general solution), it can be shown that the most general expressions for  $\bar{u}$  and  $\bar{h}$  satisfying the boundary

conditions (5.5.20) at  $z = 0$  and  $z = 1$  are

$$\begin{aligned}\bar{u} &= -\frac{\omega(1+i\xi)}{\sigma} \left[ A(\cosh \omega z - \alpha_1 \cosh \Omega z) + B(\sinh \omega z - \frac{1}{\alpha_2} \sinh \Omega z) \right] \\ &\quad + \frac{2\nu^3(1+i\xi)}{\pi\sigma} \int_0^z G(t) [\omega \sinh \omega(z-t) - \Omega \sinh \Omega(z-t)] dt, \\ \bar{h} &= \frac{\lambda\nu(1+i\xi)}{\sigma} \left[ A(\sinh \omega z - \alpha_2 \sinh \Omega z) + B(\cosh \omega z - \frac{1}{\alpha_1} \cosh \Omega z) \right] \\ &\quad - \frac{2\nu^2(1+i\xi)}{\pi\sigma\lambda} \int_0^z G(t) [\nu^2\lambda^2 \cosh \omega(z-t) - \Omega^2 \cosh \Omega(z-t)] dt,\end{aligned}\tag{5.6.23}$$

where

$$\omega^2 = \lambda^2\nu^2 - \frac{\sigma}{1+i\xi}, \quad \Omega^2 = \lambda^2\nu^2 + \frac{\sigma}{2(\gamma-i\xi)}.\tag{5.6.24}$$

Constants  $A$  and  $B$  appearing in (5.6.23) are arbitrary and are determined from (5.5.20) at  $z = 1$ . After calculation, it can be shown that  $A$  and  $B$  are solutions of simultaneous equations

$$\begin{aligned}A[\cosh \Omega - \cosh \omega] + B[\frac{1}{\alpha} \sinh \Omega - \sinh \omega] &= -\frac{\nu(\lambda^2\nu^2 - \omega^2)}{\pi\omega\lambda^2} G(1) \\ &\quad - \frac{2\nu^3}{\pi\alpha_1} \int_0^1 G(t) [\alpha_1 \sinh \omega(1-t) - \frac{\Omega}{\omega} \sinh \Omega(1-t)] dt, \\ A[\alpha \sinh \Omega - \sinh \omega] + B[\cosh \Omega - \cosh \omega] &= \\ &\quad \frac{2\Omega\nu^3}{\omega\pi} \int_0^1 G(t) [\alpha_2 \cosh \Omega(1-t) - \frac{\omega}{\Omega} \cosh \omega(1-t)] dt,\end{aligned}\tag{5.6.25}$$

where

$$\alpha_1 = \frac{2\lambda^2\nu^2}{\omega^2 + \lambda^2\nu^2}, \quad \alpha_2 = \frac{2\omega\Omega}{\omega^2 + \lambda^2\nu^2}, \quad \alpha = \alpha_1\alpha_2.\tag{5.6.26}$$

Expressions (5.6.23) for transformed displacements  $\bar{h}$  and  $\bar{u}$  are still unknown in terms of accumulated shear stress  $G(z)$ . In view of definitions (5.6.22) for  $G_1(z)$  and  $G_\beta(z)$ , the applied force can be re-expressed in the form

$$\frac{F}{2\pi d^2} = -\mu(1+i\xi)\beta G_\beta(t), \quad \frac{F}{2\pi d^2} = -\mu(1+i\xi)G_1(t).\tag{5.6.27}$$

## 5.7 Fourier Series Representation

Since solutions (5.6.23) involve unknown function  $G(t)$ , it is now convenient to represent  $G(t)$  by a complex-valued Fourier series in real variable  $t \in [0, 1]$ . If  $G_1$  and  $G_\beta$  are

described as half-range cosine series, both  $G_1(z)$  and  $G_\beta(z)$  can be evaluated at  $z = 0$  and  $z = 1$  by direct substitution into their Fourier series. Thus

$$G_1(t) = \sum_{r=0}^{\infty} G_r^{(1)} \cos(r\pi t), \quad G_\beta(t) = \sum_{r=0}^{\infty} G_r^{(\beta)} \cos(r\pi t), \quad (5.7.28)$$

where

$$G_1(0) = \sum_{r=0}^{\infty} G_r^{(1)} = 0, \quad G_\beta(0) = \sum_{r=0}^{\infty} G_r^{(\beta)} = 0. \quad (5.7.29)$$

Occurrences of  $G$  in  $\bar{u}$  and  $\bar{h}$  are now replaced by the infinite series

$$G(z) = \sum_{r=1}^{\infty} G_r \cos(r\pi z), \quad G_r = G_r^{(1)} - \frac{J_1(\lambda)}{J_1(\lambda\beta)} G_r^{(\beta)} = G_r^{(1)} - f(\lambda) G_r^{(\beta)}, \quad (5.7.30)$$

where  $f(\lambda)$  denotes the ratio

$$f(\lambda) = \frac{J_1(\lambda)}{J_1(\lambda\beta)}. \quad (5.7.31)$$

Solution procedure now requires  $G(t)$  to be replaced by its Fourier series wherever it occurs. After some further analysis, expressions for  $\bar{u}(\lambda, z)$  and  $\bar{h}(\lambda, z)$  are

$$\begin{aligned} \bar{h}(\lambda, z) &= \frac{\nu^2(1+i\xi)}{\pi\omega\lambda\sigma Q} \sum_{n=1}^{\infty} [R(z) + (-1)^n S(z)] \chi_n G_n \\ &\quad + \frac{2\nu^2(1+i\xi)}{\lambda} \sum_{k=1}^{\infty} k K_k \sin(k\pi z) G_k, \\ \bar{u}(\lambda, z) &= \frac{\nu(1+i\xi)}{\pi\lambda^2\sigma Q} \sum_{n=1}^{\infty} [L(z) + (-1)^n K(z)] \chi_n G_n \\ &\quad + \frac{2\nu^3(1+i\xi)}{\pi\sigma} \sum_{k=0}^{\infty} \beta_k \cos(k\pi z) G_k, \end{aligned} \quad (5.7.32)$$

where

$$\begin{aligned} Q(\omega, \Omega) &= -2 + 2 \cosh \omega \cosh \Omega - \left(\alpha + \frac{1}{\alpha}\right) \sinh \omega \sinh \Omega, \\ \chi_n(\omega, \Omega) &= \frac{\Omega^2(\lambda^2\nu^2 + \omega^2)}{\Omega^2 + n^2\pi^2} - \frac{2\lambda^2\nu^2\omega^2}{\omega^2 + n^2\pi^2} + \lambda^2\nu^2 - \omega^2, \\ K_k(\omega, \Omega) &= \frac{\Omega^2}{\Omega^2 + k^2\pi^2} - \frac{\lambda^2\nu^2}{\omega^2 + k^2\pi^2}, \\ \beta_k(\omega, \Omega) &= \frac{\Omega^2}{\Omega^2 + k^2\pi^2} - \frac{\omega^2}{\omega^2 + k^2\pi^2}, \end{aligned} \quad (5.7.33)$$

$$\begin{aligned}
R(z) &= (\alpha \sinh \Omega \cosh \omega - \sinh \omega \cosh \Omega) \left[ \cosh \omega z - \frac{1}{\alpha_1} \cosh \Omega z \right] \\
&\quad - \sinh \omega z (1 - \cosh \Omega \cosh \omega + \alpha \sinh \omega \sinh \Omega) \\
&\quad - \alpha_2 \sinh \Omega z \left( 1 - \cosh \omega \cosh \Omega + \frac{1}{\alpha} \sinh \omega \sinh \Omega \right), \\
S(z) &= (\cosh \Omega - \cosh \omega) (\sinh \omega z - \alpha_2 \sinh \Omega z) \\
&\quad - (\alpha \sinh \Omega - \sinh \omega) \left[ \cosh \omega z - \frac{1}{\alpha_1} \cosh \Omega z \right], \\
L(z) &= (\alpha \sinh \Omega \cosh \omega - \sinh \omega \cosh \Omega) \left[ -\sinh \omega z + \frac{1}{\alpha_2} \sinh \Omega z \right] \\
&\quad + \cosh \omega z (1 - \cosh \Omega \cosh \omega + \alpha \sinh \omega \sinh \Omega) \\
&\quad + \alpha_1 \cosh \Omega z (1 - \cosh \omega \cosh \Omega + \frac{1}{\alpha} \sinh \omega \sinh \Omega), \\
K(z) &= (\cosh \Omega - \cosh \omega) (\alpha_1 \cosh \Omega z - \cosh \omega z) \\
&\quad - (\alpha \sinh \Omega - \sinh \omega) \left[ -\sinh \omega z + \frac{1}{\alpha_2} \sinh \Omega z \right].
\end{aligned} \tag{5.7.34}$$

When functions  $R(z)$ ,  $S(z)$ ,  $K(z)$  and  $L(z)$  are replaced by their half range series in  $[-1, 1]$ , the resulting series for  $\bar{h}(z, \lambda)$  and  $\bar{u}(z, \lambda)$  are

$$\bar{h}(z, \lambda) = \sum_{k=1}^{\infty} \bar{h}_k(\lambda) \sin(k\pi z), \quad \bar{u}(z, \lambda) = \sum_{k=0}^{\infty} \bar{u}_k(\lambda) \cos(k\pi z), \tag{5.7.35}$$

in which the coefficient of  $\bar{h}$  and  $\bar{u}$  are

$$\begin{aligned}
\bar{h}_k(\lambda) &= \frac{2(1+i\xi)}{\omega \lambda^3 \sigma} \begin{cases} k \lambda^2 \nu^2 \omega K_k G_k + k \phi_k \Phi(\omega, \Omega) \sum_{n=1}^{\infty} \chi_{2n} G_{2n} & k \text{ even} \\ k \lambda^2 \nu^2 \omega K_k G_k + k \phi_k \Psi(\omega, \Omega) \sum_{n=1}^{\infty} \chi_{2n-1} G_{2n-1} & k \text{ odd} \end{cases} \\
\bar{u}_k(\lambda) &= \frac{2\nu(1+i\xi)}{\pi \omega \lambda^2 \sigma} \begin{cases} \lambda^2 \nu^2 \omega \beta_k G_k + \gamma_k \Phi(\omega, \Omega) \sum_{n=1}^{\infty} \chi_{2n} G_{2n} & k \text{ even} \\ \lambda^2 \nu^2 \omega \beta_k G_k + \gamma_k \Psi(\omega, \Omega) \sum_{n=1}^{\infty} \chi_{2n-1} G_{2n-1} & k \text{ odd} \end{cases} \\
\bar{u}_0(\lambda) &= -\frac{\nu(1+\gamma)}{\omega \pi \lambda^2 \Omega^2 (\gamma - i\xi)} \Phi(\omega, \Omega) \sum_{n=1}^{\infty} \chi_{2n} G_{2n}.
\end{aligned} \tag{5.7.36}$$

Coefficients  $\gamma_k(\omega, \Omega)$ ,  $\phi_k(\omega, \Omega)$ ,  $\Phi_k(\omega, \Omega)$  and  $\Psi_k(\omega, \Omega)$  denote the expressions

$$\begin{aligned}\gamma_k(\omega, \Omega) &= \frac{\omega^2 + \lambda^2 \nu^2}{\Omega^2 + k^2 \pi^2} - \frac{2\omega^2}{\omega^2 + k^2 \pi^2} , \\ \phi_k(\omega, \Omega) &= \frac{\omega^2 + \lambda^2 \nu^2}{\Omega^2 + k^2 \pi^2} - \frac{2\lambda^2 \nu^2}{\omega^2 + k^2 \pi^2} , \\ \Phi(\omega, \Omega) &= \frac{\alpha \tanh(\omega/2) \tanh(\Omega/2)}{\alpha \tanh(\Omega/2) - \tanh(\omega/2)} , \\ \Psi(\omega, \Omega) &= \frac{\alpha}{\alpha \tanh(\omega/2) - \tanh(\Omega/2)} .\end{aligned}\tag{5.7.37}$$

### 5.7.1 Function $h_0(z)$

Function  $h_0(z)$  appearing in series (5.5.16) is determined by first multiplying the second equation in (5.4.13) by  $r$  and then integrating with respect to  $r$  over  $[1, \beta]$ . The result of these calculations is second order differential equation

$$\frac{d^2}{dz^2} \left( \int_1^\beta r h(r, z) dr \right) - \varphi^2 \int_1^\beta r h(r, z) dr = \frac{\nu^2(1 + i\xi)}{2(\gamma - i\xi)} [\beta g_\beta(z) - g_1(z)] ,\tag{5.7.38}$$

in which

$$\varphi^2 = \frac{\sigma}{2(\gamma - i\xi)} .$$

Equation (5.7.38) has general solution

$$\begin{aligned}\int_1^\beta r h(r, z) dr &= A^* \cosh \varphi z + B^* \sinh \varphi z \\ &+ \frac{\nu^2(1 + i\xi)}{2\varphi(\gamma - i\xi)} \int_0^z (\beta g_\beta(z) - g_1(z)) \sinh \varphi(z - t) dt .\end{aligned}\tag{5.7.39}$$

Constants  $A^*$  and  $B^*$  are determined by first multiplying the second equation of boundary conditions (5.4.14) by  $r$  and then integrating with respect to  $r$  over  $[1, \beta]$  to obtain

$$\frac{d}{dz} \int_1^\beta r h(r, z) dr = 0 , \quad z = 0, 1 .\tag{5.7.40}$$

This result applied at  $z = 0$  leads trivially to the conclusion that  $B^* = 0$ . Calculation of  $A^*$  is more involved. When  $G(t)$  is replaced by its definition (5.6.22) in terms of  $G_1(t)$  and  $G_\beta(t)$ , it can be shown from (5.7.40) at  $z = 1$  that

$$\begin{aligned}\int_1^\beta r h(r, z) dr &= \frac{\nu^2(1 + i\xi)}{2(\gamma - i\xi)} \left[ \int_0^z [\beta G_\beta(t) - G_1(t)] \cosh \varphi(z - t) dt \right. \\ &\quad \left. - \frac{\cosh \varphi z}{\sinh \varphi} \int_0^1 [\beta G_\beta(t) - G_1(t)] \sinh \varphi(1 - t) dt \right] .\end{aligned}\tag{5.7.41}$$

When  $G_\beta(z)$ ,  $G_1(z)$  are replaced by their infinite series expansions, solution  $h_0(z)$ , (5.7.41) becomes

$$h_0(z) = \frac{\nu^2(1+i\xi)}{(\beta^2-1)(\gamma-i)\sinh\varphi} \sum_{n=0}^{\infty} \frac{F_n \Delta(z)}{\varphi^2 + n^2\pi^2}, \quad (5.7.42)$$

with

$$\Delta(z) = \varphi((-1)^n \cosh \varphi z - \cosh \varphi(1-z)) + n\pi \sinh \varphi \sin n\pi z, \quad (5.7.43)$$

and when  $\cosh \varphi z$  and  $\sinh \varphi z$  are replaced by their half range sine series in  $[-1, 1]$ ,  $h_0(z)$  is finally expressed in the form

$$h_0(z) = \frac{2}{\beta^2-1} \int_1^\beta r h(r, z) dr = \frac{\nu^2(1+i\xi)}{(\beta^2-1)(\gamma-i\xi)} \sum_{k=1}^{\infty} \frac{k\pi \sin k\pi z}{k^2\pi^2 + \varphi^2} \Lambda(\varphi), \quad (5.7.44)$$

in which

$$\Lambda(\varphi) = F_k + \frac{2\varphi}{\sinh \varphi} \sum_{n=0}^{\infty} \frac{F_n}{n^2\pi^2 + \varphi^2} [1 - (-1)^k \cosh \varphi][(-1)^n + (-1)^k], \quad (5.7.45)$$

where  $F_k$  denotes  $\beta G_k^{(\beta)} - G_k^{(1)}$ . In conclusion, full solutions for  $h(r, z)$  and  $u(r, z)$  are

$$\begin{aligned} h(r, z) &= h_0(z) + \frac{\pi^2}{2} \sum_{k=1}^{\infty} \left( \sum_{n=1}^{\infty} \frac{\lambda_n^2 C_{01}(\lambda_n r, \lambda_n)}{f^2(\lambda_n) - 1} \bar{h}_k(\lambda_n) \right) \sin(k\pi z) \\ u(r, z) &= \frac{\pi^2}{2} \sum_{k=0}^{\infty} \left( \sum_{n=1}^{\infty} \frac{\lambda_n^2 C_{11}(\lambda_n r, \lambda_n)}{f^2(\lambda_n) - 1} \bar{u}_k(\lambda_n) \right) \cos(k\pi z), \end{aligned} \quad z \in (0, 1) \quad (5.7.46)$$

where the functions  $h_0(z)$ ,  $\bar{h}_k(\lambda_n r, \lambda)$  and  $\bar{u}_k(\lambda_n r, \lambda)$  are given in (5.7.44) and (5.7.36) respectively.

### 5.7.2 Surface Deformation $h(r, 1)$

Surface deformation,  $h(r, 1)$ , is given by

$$h(r, 1) = h_0(1) + \frac{\pi^2}{2} \sum_{n=1}^{\infty} \frac{\lambda_n^2 \bar{h}(\lambda_n, 1)}{f^2(\lambda_n) - 1} C_{01}(\lambda_n r, \lambda_n), \quad (5.7.47)$$

in which  $h_0(1)$  and  $\bar{h}_k(\lambda_n, 1)$  are to be computed separately because they cannot be calculated from general solutions of  $h_0(z)$  and  $\bar{h}(\lambda, z)$  respectively. In fact,  $h_0(1)$  and  $\bar{h}_k(\lambda_n, 1)$

are determined from (5.7.42) and (5.7.32) respectively by substitution  $z$  by 1, to get

$$\begin{aligned} h_0(1) &= \frac{\nu^2(1+i\xi)}{(\beta^2-1)(\gamma-i)\sinh\varphi} \sum_{n=1}^{\infty} \frac{F_n}{\varphi^2 + n^2\pi^2} [(-1)^n \cosh\varphi - 1] , \\ \bar{h}(\lambda, 1) &= \frac{-1}{2\omega\pi\lambda^3Q} \sum_{n=1}^{\infty} (-1)^n P_n \chi_n G_n , \end{aligned} \quad (5.7.48)$$

where

$$P_n = \alpha \sinh \Omega \cosh \omega - \cosh \Omega \sinh \omega - (-1)^n (\alpha \sinh \Omega - \sinh \omega) . \quad (5.7.49)$$

### 5.7.3 Static Problem

The static solution can be obtained from (5.7.36) by taking limits as  $\sigma \rightarrow 0$ , or equivalently, by eliminating  $\sigma$  and taking limits as  $\Omega \rightarrow \omega$ . Using L'Hôpital's rule, it can be shown that

$$\lim_{\sigma \rightarrow 0} h_k = \begin{cases} \hat{K}_k G_k + \frac{8k\nu}{\lambda^2\gamma(2\gamma+1)} \frac{\hat{\chi}_k}{k^2\pi^2} \frac{1 - \cosh \omega_0}{\omega_0 + \sinh \omega_0} \sum_{n=1}^{\infty} \hat{\chi}_{2n} G_{2n} & k \text{ even} \\ \hat{K}_k G_k + \frac{8k\nu}{\lambda^2\gamma(2\gamma+1)} \frac{\hat{\chi}_k}{k^2\pi^2} \frac{1 + \cosh \omega_0}{\omega_0 - \sinh \omega_0} \sum_{n=1}^{\infty} \hat{\chi}_{2n-1} G_{2n-1} & k \text{ odd,} \end{cases} \quad (5.7.50)$$

where  $\hat{\chi}_n$ ,  $\hat{K}_n$  and  $\omega_0$  denote expressions:

$$\hat{\chi}_n = \frac{n^2\pi^2[\gamma n^2\pi^2 + \omega_0^2(1+3\gamma)]}{(\omega_0^2 + n^2\pi^2)^2}, \quad \hat{K}_k = \frac{\nu^2 k}{\lambda\gamma} \frac{k^2\pi^2 - 2\gamma\omega_0^2}{(\omega_0^2 + n^2\pi^2)^2}, \quad \omega_0 = \lambda\nu . \quad (5.7.51)$$

See appendix A for more details about the limit of  $h_k$ .

#### Special case $\gamma \rightarrow -\infty$

As  $\gamma \rightarrow -\infty$ , the result for compressible materials approaches that for incompressible materials. When  $\gamma \rightarrow -\infty$ , the result (5.7.50) is the same as that for static incompressible materials (4.5.60).

### 5.7.4 Boundary Conditions

Constant  $H$ , appearing in boundary conditions  $h(1, z) = 0$  and  $h(\beta, z) = H$ , is obtained from (5.7.46) and properties of Weber-Orr kernels. It can be shown that

$$\begin{aligned} h(1, z) = H &= h_0(z) - \pi \sum_{k=1}^{\infty} \left( \sum_{n=1}^{\infty} \frac{\lambda_n}{f^2(\lambda_n) - 1} \bar{h}_k(\lambda_n) \right) \sin(k\pi z), \\ h(\beta, z) = 0 &= h_0(z) - \frac{\pi}{\beta} \sum_{k=1}^{\infty} \left( \sum_{n=1}^{\infty} \frac{\lambda_n f(\lambda_n)}{f^2(\lambda_n) - 1} \bar{h}_k(\lambda_n) \right) \sin(k\pi z). \end{aligned} \quad (5.7.52)$$

Most of the remarks made in the previous chapter are also true here. After some algebraic manipulation it follows from (5.7.52) that

$$4H = \frac{h_{2k-1}^*}{\beta - 1} + \sum_{n=1}^{\infty} \frac{h_n^{**}}{f(\lambda_n) - 1}, \quad -4H = \frac{h_{2k-1}^*}{\beta + 1} + \sum_{n=1}^{\infty} \frac{h_n^{**}}{f(\lambda_n) + 1}, \quad (5.7.53)$$

where

$$\begin{aligned} h_k^* &= \frac{\nu^2(1 + i\xi)}{\gamma - i\xi} \frac{k^2 \pi^2}{k^2 \pi^2 + \varphi^2} [F_k - C], \\ h_n^{**} &= -\varrho_{2k-1} G_{2k-1} + \eta_{2k-1} \delta(\lambda_n) \sum_{j=1}^{\infty} \eta_{2j-1} G_{2j-1}, \\ F_k &= \beta G_k^{(\beta)} - G_k^{(1)}, \\ G_k &= G_k^{(1)} - f(\lambda_n) G_k^{(\beta)}, \\ \varrho_k &= \frac{2}{\sigma} (1 + i\xi) k^2 \pi^2 K_k, \\ \eta_k &= \frac{1 + i\xi}{\sigma} \chi_k, \\ \delta(\lambda_n) &= \frac{2\sigma}{\nu^2 \lambda_n^2 \omega (1 + i\xi)} \Psi(\lambda_n), \end{aligned} \quad (5.7.54)$$

where  $C$  is a new unknown constant to be determined.

## 5.8 Numerical Details

Equations (5.7.53) represent a system of linear equations for unknown Fourier coefficients of accumulated shear stresses  $G_1(z)$  and  $G_\beta(z)$  and for unknown constants  $H$  and  $C$ . In



fact, for numerical purposes,  $G_1(z)$  and  $G_\beta(z)$  are represented by their finite half-range cosine series, so that:

$$\begin{aligned} G_1(z) &= \sum_{k=1}^{2N} G_k^{(1)} \cos k\pi z \\ G_\beta(z) &= \sum_{k=1}^{2N} G_k^{(\beta)} \cos k\pi z. \end{aligned} \tag{5.8.55}$$

Coefficients  $G_0^{(1)}$  and  $G_0^{(\beta)}$  are determined by conditions  $G_1(0) = G_\beta(0) = 0$  and now the system of linear equations (5.7.53) is reduced to one of  $2N$  equations containing  $2N + 2$  complex unknowns  $G_1^{(1)}, \dots, G_{2N-1}^{(1)}, G_1^{(\beta)}, \dots, G_{2N-1}^{(\beta)}, C$  and  $H$ . Since even coefficients of  $G$  are zero, two further conditions come from applied force (5.6.27).

Finally, the system of linear equations are solved by Singular Value Decomposition (SVD) method.

## 5.9 Conclusions

Shear stress, accumulated shear stress and surface deformation are examined (static and dynamic) for general values of  $\beta$ ,  $\nu$  and  $\gamma$ , and the applied force  $F = 1/\ln \beta$ . In fact,  $\gamma$  is expressed in terms of Lamé parameters  $\lambda$  and  $\mu$  by the formula

$$\gamma = -\frac{\lambda + 2\mu}{2\mu}$$

or equivalently in term of Poisson's ratio  $\nu_0 \in (-1, 1/2)$  by the formula:

$$\gamma = \frac{\nu_0 - 1}{1 - 2\nu_0}.$$

It is easily established that  $\gamma \in (-\infty, -2/3)$ .

Blatz & Ko [25] introduce the strain energy density function

$$\begin{aligned} U_{BK} &= \frac{\mu_0}{2} \left[ f(J_1 - 3) + (1 - f)(J_2 - 3) \right. \\ &\quad \left. - \frac{1}{1 + \gamma} \left\{ f \left( J_3^{2(1+\gamma)} - 1 \right) + (1 - f) \left( J_3^{-2(1+\gamma)} - 1 \right) \right\} \right], \end{aligned} \tag{5.9.56}$$

where  $\mu_0$  is the ground state shear modulus of the material and  $f \in [0, 1]$  is a material constant. In experimental work,  $f$  takes small values and  $\gamma \simeq -1.5$  ( $\nu_0 \simeq 0.25$ ) for a

highly compressible polyurethane foam rubber. According to Blatz & Ko [25],  $f \simeq 1$  and  $\gamma \simeq -6.75$  ( $\nu_0 \simeq 0.46$ ) for solid rubber. Hence calculations are performed for  $\gamma = -1.1$ ,  $\gamma = -1.5$ ,  $\gamma = -3.0$  and  $\gamma = -6.75$  to reflect transition from highly compressible elastic material to one which is slightly compressible.

### 5.9.1 Accumulated static shear stress

Figures (5.1) and (5.2) display graphs of the inner accumulated shear stress and the outer accumulated shear stress,  $G_1(z)$  and  $G_\beta(z)$  respectively, for four different values of  $\gamma$  and with fixed values for  $\beta$  and  $\nu$  for a static applied force. The shape of the accumulated shear stress on the inner and outer boundaries are qualitatively similar although it is clear that the outer boundary exhibits more variability than the inner boundary.

For fixed  $\beta$  and  $\nu$ , the variability of the accumulated shear stress is increased as the material becomes “more compressible” (i.e. as  $\gamma$  decreases). For fixed values of  $\beta$  and  $\gamma$ , the variability of the accumulated shear stress increases as  $\nu$  decreases; that is, a thin annulus ( $\nu = 0.25$ ) is more responsive than a thick annulus ( $\nu = 4.0$ ). Finally, for fixed values of  $\nu$  and  $\gamma$ , the variability of the accumulated shear stress increases as the annulus migrates from a collar-like geometry ( $\beta = 1.5$ ) to a sheet-like geometry ( $\beta = 9.0$ ). Of course, the variability in the accumulated shear force just reflects the behaviour of the shear stress itself. This feature is discussed in the next section.

In conclusion, when  $\nu$  starts increasing the inner and outer accumulated shear stresses progressively migrate from a volatile nature to approximately a straight line, and when the absolute value  $\gamma$  starts increasing, the graphs of  $G_1(z)$  and  $G_\beta(z)$  seem to be similar to the graphs for an incompressible material.

Of course, the compressible material will always behave differently from an incompressible material when  $|\gamma|$  is small but it is a different matter when  $\gamma$  tends to  $-\infty$ . This is described above in the special case,  $\gamma \rightarrow -\infty$ .

### 5.9.2 Static shear stress

The behaviour of the inner and outer shear stresses,  $g_1(z)$  and  $g_\beta(z)$ , for a static applied force are plotted in figures (5.3) and (5.4) respectively.

For a sheet-like geometry, ( $\nu \leq 1$  and  $\beta \geq 3$ ), the shear stress changes sign at some

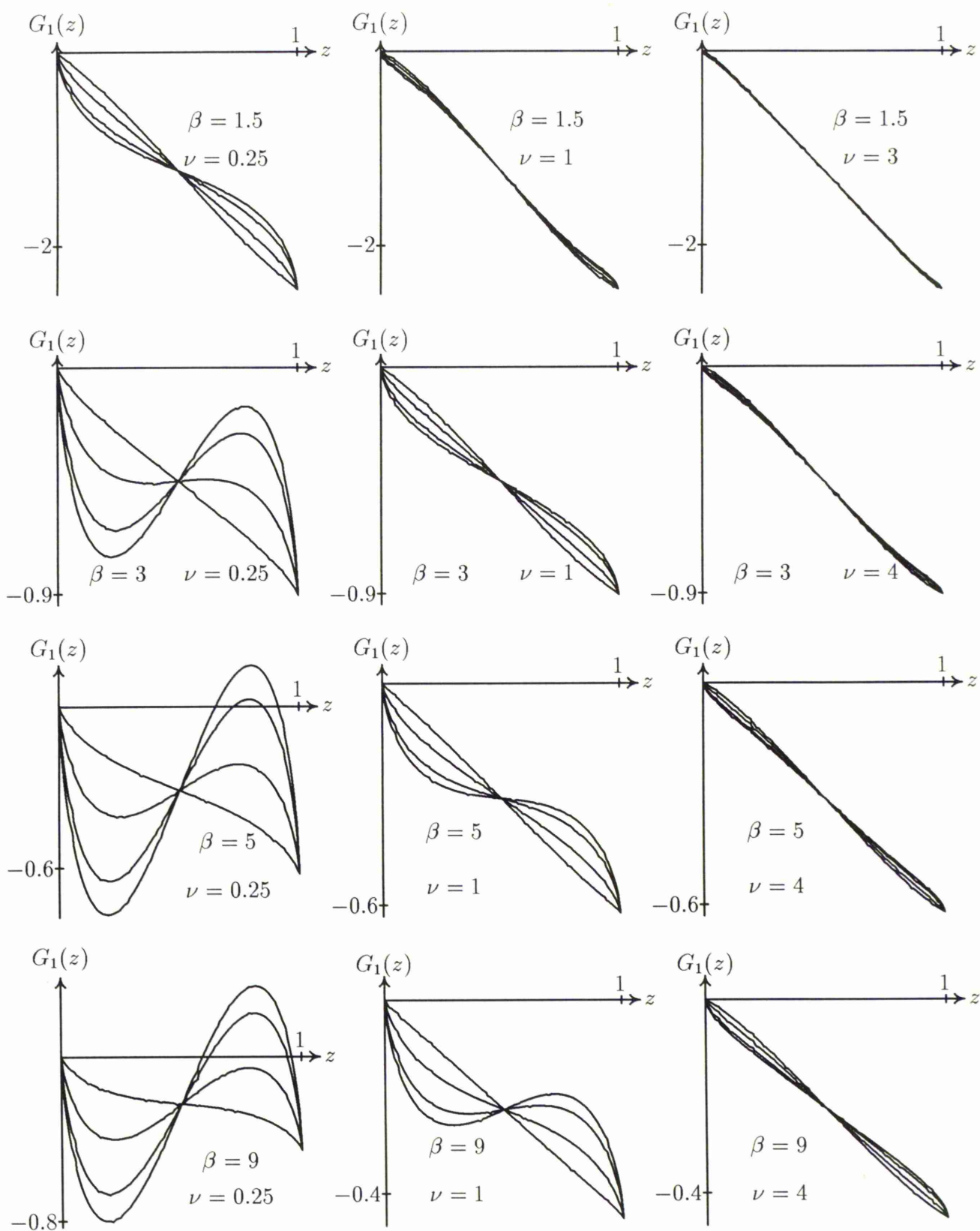


Figure 5.1: Graph of the accumulated shear stress  $G_1(z)$  for selected values of  $\nu$  and  $\beta$  when  $\gamma = -1.1, -1.5, -3.0$  and  $-6.75$ , for a static applied axial force.

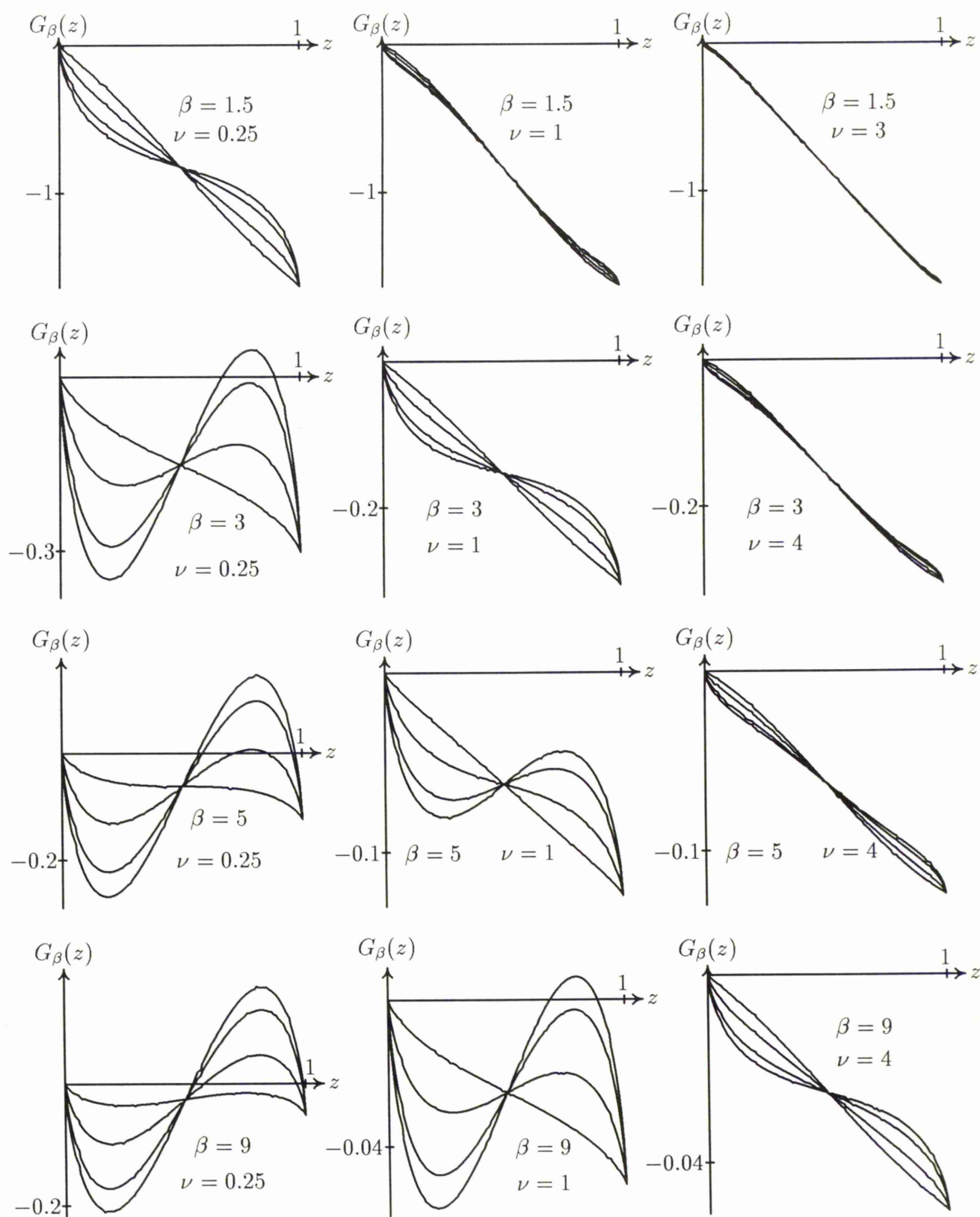


Figure 5.2: Graph of accumulated shear stress  $G_\beta(z)$  for selected values of  $\nu$  and  $\beta$  when  $\gamma = -1.1, -1.5, -3.0$  and  $-6.75$ , for a static applied axial force.

interior points if the material has sufficiently low compressibility; that is,  $\gamma$  takes a large enough negative value. Under these circumstances, the stress in the interior region of the sheet is acting in a direction that is opposite to the overall stress distribution induced by the axial force. As the annulus becomes more collar-like with increasing  $\nu$ , this effect disappears. The effect is present for ( $\nu = 1$  and  $\beta = 9$ ) but has entirely disappeared by time  $\nu = 4$ .

The graphs showing stress indicate the existence of stress boundary layers on the upper and lower boundaries of the annulus for all combinations of  $\nu$  and  $\beta$ . Significance of these boundary layers is enhanced for highly compressible materials. Indeed for such materials, the stress force in the interior of the annulus is often almost constant in contrast to that which occurs for less compressible materials. Boundary layer effects are enhanced for a collar-like annulus (bigger  $\nu$ ) but these seem less dependent on the value of  $\beta$  although increasing  $\beta$  does appear to reduce dominance of the boundary layers.

In conclusion, the kind of material, either a highly compressible material ( $\gamma = -1.5$ ), or a slightly compressible material ( $\gamma = -6.75$ ), is important when the material is thin and  $\beta$  is small. However, when  $\beta$  starts increasing the effect of  $\gamma$  is less important. When the material is thick the effect of  $\gamma$  appears for large  $\beta$ ; for example, ( $\beta = 9, \nu = 4$ ), whereas for  $\beta = 1.5$  the shear stress is almost flat for any kind of material and the shape starts changing when  $\beta$  lies between 3 and 9.

### 5.9.3 Static surface deformation

Figure (5.5) depicts the static surface deformation  $h(r,1)$  for selected values of  $\beta$ ,  $\nu$  as mentioned above.

It is clear that  $h(r,1)$  is always a monotonically decreasing function of  $r$ , for all combinations of  $\nu$ ,  $\beta$  and  $\gamma$ , the maximum deformation occurring at the hole. For fixed  $\beta$  and  $\gamma$ , the maximum deformation is a decreasing function of  $\nu$ ; that is, as the sheet thickens, it becomes more resistant to axial deformation. On the other hand, for fixed  $\nu$  and  $\gamma$ , the maximum deformation is an increasing function of  $\beta$ . In other words, a sheet like annulus deforms more than a collar-like annulus for a given applied force. For fixed  $\beta$  and  $\nu$ , the maximum deformation is an increasing function of  $\gamma$ ; that is, deformation is an increasing function of compressibility. Highly compressible materials deform further

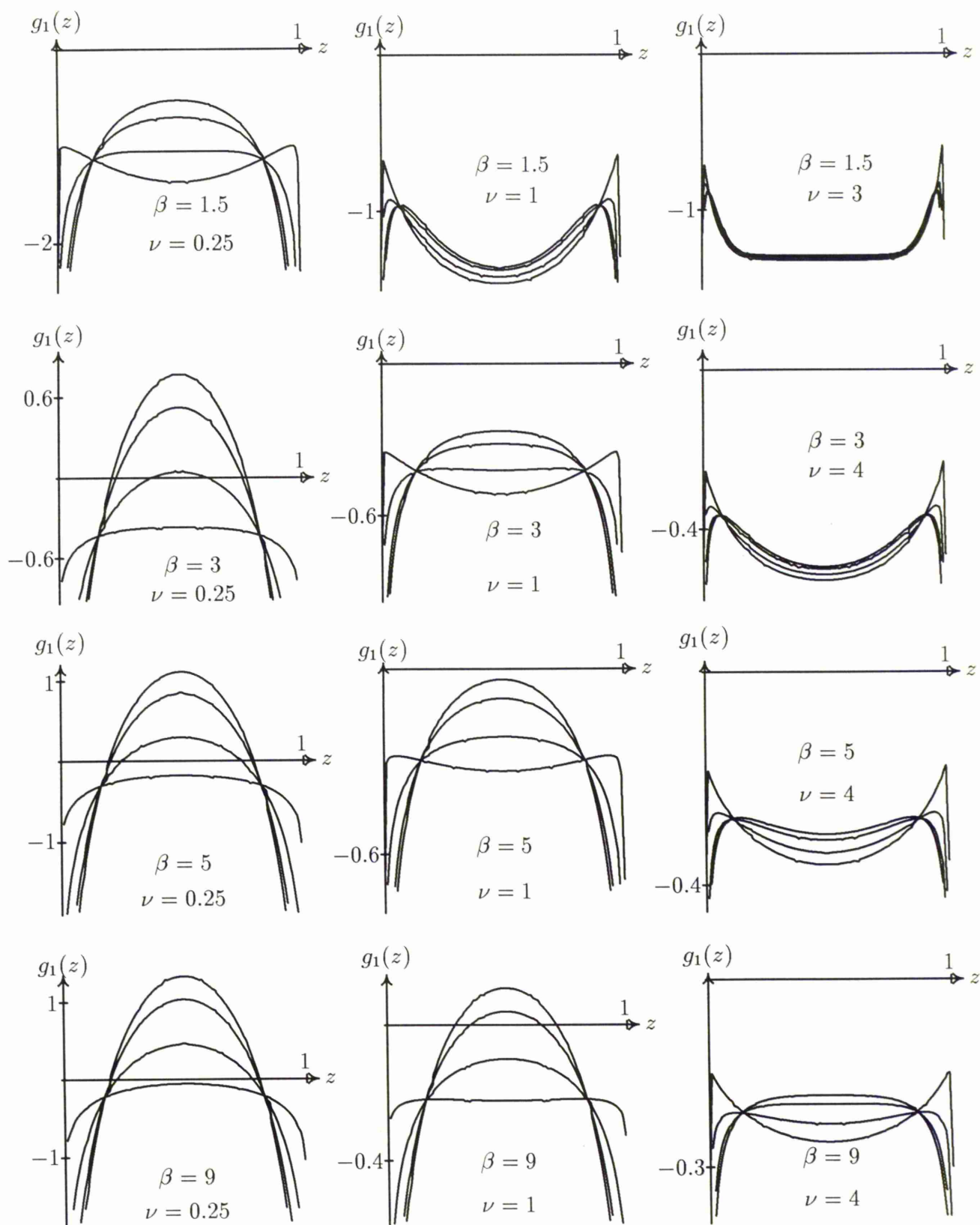


Figure 5.3: Graph of the shear stress  $g_1(z)$  for selected values of  $\nu$  and  $\beta$  and for the value of  $\gamma = -1.1, -1.5, -3.0$ , and  $-6.75$ , for a static applied axial force.

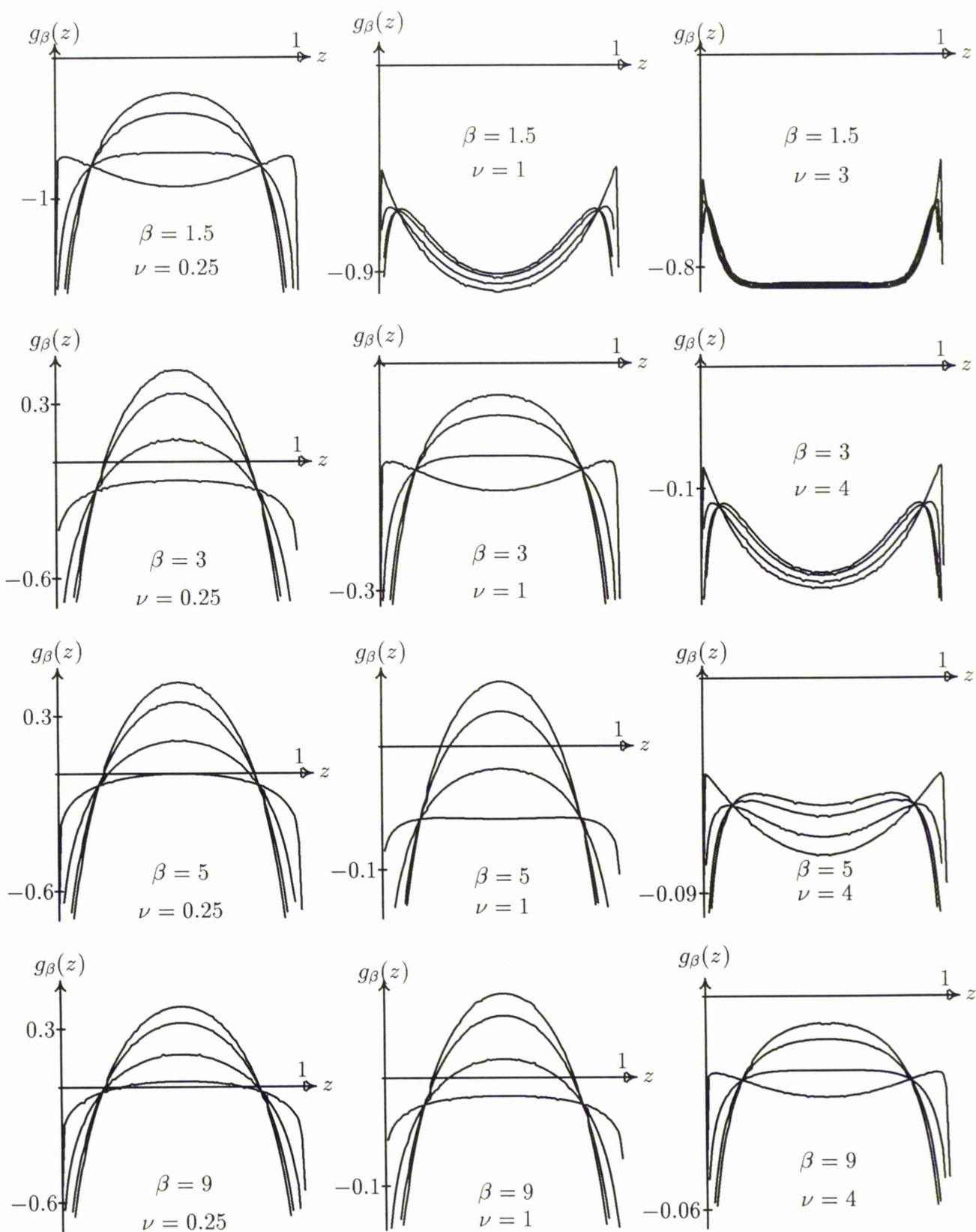


Figure 5.4: Graph of the shear stress  $g_\beta(z)$  for selected values of  $\nu$  and  $\beta$  and for the value of  $\gamma = -1.1, -1.5, -3.0$ , and  $-6.75$ , for a static applied axial force.

than less compressible materials.

Tables (5.1) - (5.4) display the value of static surface deformation  $h(r, 1)$  for selected  $r$  values in  $[1, \beta]$  and for various values of  $\nu$  and  $\gamma$ . Table indicates that  $H = h(r, 1)$  is very sensitive to change in  $\beta$  while the material is thin, but when  $\nu \geq 3$ , the value of  $H$  is less sensitive to  $\beta$  and  $\gamma$ .



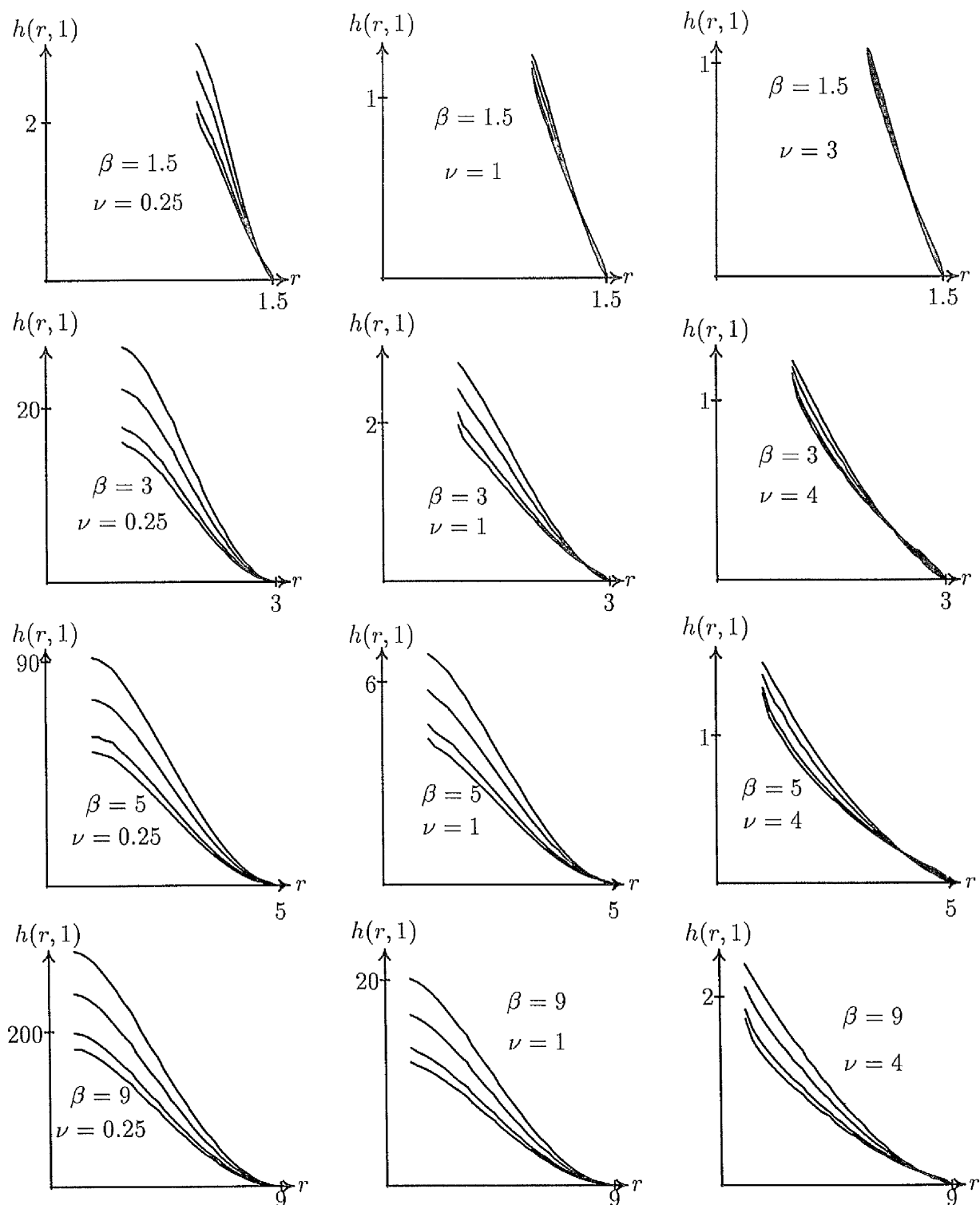


Figure 5.5: Static surface deformation  $h(r, 1)$  for selected values of  $\nu$  and  $\beta$  and for  $\gamma = -1.1, -1.5, -3.0$ , and  $-6.75$ .

r	$\beta = 1.5$			$\gamma = -1.1$		
	$\nu = 1/4$	$\nu = 1$	$\nu = 3$	$\nu = 4$	$\nu = 7$	$\nu = 9$
1.00	2.970	1.232	1.067	1.049	1.027	1.021
1.05	2.766	1.116	0.966	0.950	0.930	0.924
1.10	2.480	0.980	0.848	0.834	0.817	0.812
1.15	2.139	0.839	0.725	0.713	0.699	0.694
1.20	1.765	0.697	0.603	0.593	0.581	0.577
1.25	1.381	0.560	0.483	0.476	0.466	0.463
1.30	1.009	0.427	0.369	0.363	0.356	0.353
1.35	0.669	0.301	0.260	0.256	0.251	0.249
1.40	0.376	0.185	0.159	0.157	0.154	0.153
1.45	0.149	0.081	0.070	0.069	0.068	0.068
1.50	0.000	0.000	0.000	0.000	0.000	0.000

r	$\beta = 1.5$			$\gamma = -1.5$		
	$\nu = 1/4$	$\nu = 1$	$\nu = 3$	$\nu = 4$	$\nu = 7$	$\nu = 9$
1.00	2.605	1.197	1.058	1.043	1.024	1.019
1.05	2.377	1.053	0.930	0.917	0.900	0.895
1.10	2.130	0.923	0.815	0.803	0.789	0.784
1.15	1.842	0.793	0.700	0.690	0.678	0.674
1.20	1.528	0.665	0.587	0.579	0.569	0.565
1.25	1.207	0.541	0.478	0.471	0.463	0.460
1.30	0.895	0.422	0.373	0.367	0.361	0.359
1.35	0.609	0.309	0.272	0.269	0.264	0.262
1.40	0.363	0.202	0.178	0.176	0.173	0.172
1.45	0.168	0.103	0.090	0.090	0.088	0.088
1.50	0.000	0.000	0.000	0.000	0.000	0.000

r	$\beta = 1.5$			$\gamma = -3.0$		
	$\nu = 1/4$	$\nu = 1$	$\nu = 3$	$\nu = 4$	$\nu = 7$	$\nu = 9$
1.00	2.248	1.159	1.043	1.036	1.020	1.014
1.05	1.999	0.988	0.875	0.882	0.868	0.850
1.10	1.792	0.865	0.766	0.772	0.760	0.744
1.15	1.555	0.747	0.663	0.666	0.656	0.644
1.20	1.299	0.632	0.564	0.564	0.556	0.548
1.25	1.036	0.522	0.468	0.466	0.459	0.455
1.30	0.782	0.416	0.377	0.371	0.366	0.367
1.35	0.549	0.315	0.289	0.281	0.277	0.281
1.40	0.348	0.218	0.205	0.194	0.192	0.200
1.45	0.184	0.124	0.122	0.111	0.110	0.119
1.50	0.000	0.000	0.000	0.000	0.000	0.000

r	$\beta = 1.5$			$\gamma = -6.75$		
	$\nu = 1/4$	$\nu = 1$	$\nu = 3$	$\nu = 4$	$\nu = 7$	$\nu = 9$
1.00	2.093	1.142	1.048	1.032	1.018	1.016
1.05	1.837	0.959	0.892	0.865	0.853	0.864
1.10	1.648	0.839	0.781	0.757	0.748	0.756
1.15	1.433	0.726	0.674	0.656	0.647	0.653
1.20	1.201	0.618	0.571	0.558	0.550	0.553
1.25	0.963	0.513	0.471	0.463	0.457	0.457
1.30	0.733	0.413	0.375	0.373	0.368	0.364
1.35	0.522	0.317	0.284	0.286	0.282	0.276
1.40	0.336	0.224	0.196	0.203	0.200	0.191
1.45	0.190	0.133	0.112	0.121	0.119	0.109
1.50	0.000	0.000	0.000	0.000	0.000	0.000

Table 5.1: Values of compressible static surface deformation  $h(r,1)$  for  $\beta = 1.5$  and for selected values of  $\nu$  and  $\gamma$ .

r	$\beta = 3.0$			$\gamma = -1.1$		
	$\nu = 1/4$	$\nu = 1$	$\nu = 3$	$\nu = 4$	$\nu = 7$	$\nu = 9$
1.00	26.90	2.776	1.311	1.216	1.113	1.086
1.20	25.67	2.515	1.141	1.057	0.967	0.944
1.40	23.01	2.193	0.964	0.892	0.815	0.795
1.60	19.51	1.843	0.796	0.736	0.673	0.656
1.80	15.63	1.484	0.642	0.593	0.541	0.528
2.00	11.70	1.136	0.500	0.462	0.422	0.412
2.20	8.013	0.812	0.372	0.343	0.313	0.306
2.40	4.811	0.527	0.256	0.237	0.216	0.211
2.60	2.295	0.291	0.154	0.142	0.129	0.126
2.80	0.643	0.113	0.066	0.061	0.056	0.054
3.00	0.000	0.000	0.000	0.000	0.000	0.000

r	$\beta = 3.0$			$\gamma = -1.5$		
	$\nu = 1/4$	$\nu = 1$	$\nu = 3$	$\nu = 4$	$\nu = 7$	$\nu = 9$
1.00	22.12	2.449	1.261	1.183	1.097	1.074
1.20	21.04	2.160	1.058	0.992	0.919	0.900
1.40	18.86	1.881	0.891	0.834	0.772	0.756
1.60	16.00	1.584	0.740	0.691	0.640	0.626
1.80	12.82	1.283	0.602	0.562	0.520	0.509
2.00	9.603	0.990	0.476	0.444	0.411	0.402
2.20	6.588	0.719	0.362	0.338	0.312	0.306
2.40	3.968	0.480	0.258	0.241	0.223	0.218
2.60	1.910	0.281	0.166	0.155	0.143	0.140
2.80	0.559	0.128	0.083	0.077	0.072	0.070
3.00	0.000	0.000	0.000	0.000	0.000	0.000

r	$\beta = 3.0$			$\gamma = -3.0$		
	$\nu = 1/4$	$\nu = 1$	$\nu = 3$	$\nu = 4$	$\nu = 7$	$\nu = 9$
1.00	17.70	2.130	1.209	1.148	1.080	1.061
1.20	16.78	1.817	0.975	0.925	0.869	0.854
1.40	15.05	1.582	0.819	0.777	0.729	0.716
1.60	12.77	1.336	0.683	0.647	0.607	0.596
1.80	10.23	1.089	0.561	0.531	0.498	0.489
2.00	7.672	0.849	0.451	0.426	0.400	0.393
2.20	5.270	0.627	0.351	0.332	0.311	0.305
2.40	3.183	0.431	0.260	0.245	0.230	0.226
2.60	1.546	0.268	0.176	0.167	0.156	0.153
2.80	0.475	0.140	0.099	0.094	0.088	0.086
3.00	0.000	0.000	0.000	0.000	0.000	0.000

r	$\beta = 3.0$			$\gamma = -6.25$		
	$\nu = 1/4$	$\nu = 1$	$\nu = 3$	$\nu = 4$	$\nu = 7$	$\nu = 9$
1.00	15.90	1.992	1.185	1.133	1.072	1.055
1.20	15.04	1.672	0.938	0.895	0.847	0.833
1.40	13.49	1.455	0.789	0.752	0.710	0.699
1.60	11.45	1.231	0.659	0.628	0.593	0.583
1.80	9.178	1.006	0.544	0.518	0.489	0.481
2.00	6.881	0.789	0.440	0.419	0.395	0.388
2.20	4.728	0.587	0.346	0.329	0.310	0.305
2.40	2.859	0.410	0.260	0.247	0.233	0.229
2.60	1.394	0.262	0.181	0.172	0.162	0.159
2.80	0.438	0.145	0.106	0.101	0.095	0.094
3.00	0.000	0.000	0.000	0.000	0.000	0.000

Table 5.2: Values of compressible static surface deformation  $h(r,1)$  for  $\beta = 3.0$  and for selected values of  $\nu$  and  $\gamma$ .

r	$\beta = 5.0$					
	$\nu = 1/4$	$\nu = 1$	$\nu = 3$	$\nu = 4$	$\nu = 7$	$\nu = 9$
1.00	91.44	6.817	1.782	1.498	1.232	1.172
1.40	87.05	6.299	1.524	1.263	1.029	0.978
1.80	77.32	5.522	1.272	1.042	0.841	0.798
2.20	64.91	4.613	1.039	0.845	0.677	0.642
2.60	51.45	3.661	0.826	0.671	0.535	0.507
3.00	38.13	2.733	0.631	0.515	0.411	0.389
3.40	25.84	1.881	0.457	0.376	0.301	0.285
3.80	15.31	1.149	0.304	0.254	0.205	0.194
4.20	7.151	0.572	0.175	0.150	0.122	0.115
4.60	1.896	0.183	0.073	0.063	0.052	0.049
5.00	0.000	0.000	0.000	0.000	0.000	0.000

r	$\beta = 5.0$					
	$\nu = 1/4$	$\nu = 1$	$\nu = 3$	$\nu = 4$	$\nu = 7$	$\nu = 9$
1.00	74.86	5.739	1.643	1.413	1.197	1.146
1.40	71.20	5.228	1.351	1.143	0.958	0.917
1.80	63.25	4.582	1.124	0.939	0.780	0.746
2.20	53.10	3.830	0.921	0.765	0.631	0.602
2.60	42.09	3.045	0.737	0.612	0.503	0.480
3.00	31.20	2.280	0.570	0.476	0.392	0.374
3.40	21.15	1.579	0.421	0.356	0.294	0.280
3.80	12.54	0.976	0.290	0.249	0.208	0.198
4.20	5.865	0.501	0.179	0.157	0.132	0.126
4.60	1.572	0.179	0.086	0.077	0.065	0.062
5.00	0.000	0.000	0.000	0.000	0.000	0.000

r	$\beta = 5.0$					
	$\nu = 1/4$	$\nu = 1$	$\nu = 3$	$\nu = 4$	$\nu = 7$	$\nu = 9$
1.00	59.75	4.725	1.505	1.326	1.159	1.119
1.40	56.78	4.227	1.182	1.024	0.886	0.855
1.80	50.45	3.705	0.981	0.840	0.720	0.694
2.20	42.35	3.099	0.807	0.687	0.586	0.564
2.60	33.58	2.468	0.651	0.555	0.472	0.454
3.00	24.88	1.855	0.511	0.438	0.373	0.359
3.40	16.86	1.293	0.385	0.335	0.286	0.275
3.80	9.995	0.810	0.275	0.243	0.210	0.201
4.20	4.680	0.430	0.180	0.163	0.141	0.136
4.60	1.267	0.173	0.099	0.091	0.079	0.076
5.00	0.000	0.000	0.000	0.000	0.000	0.000

r	$\beta = 5.0$					
	$\nu = 1/4$	$\nu = 1$	$\nu = 3$	$\nu = 4$	$\nu = 7$	$\nu = 9$
1.00	53.63	4.302	1.444	1.288	1.142	1.107
1.40	50.95	3.812	1.110	0.973	0.855	0.828
1.80	45.28	3.342	0.920	0.797	0.695	0.672
2.20	38.01	2.797	0.759	0.654	0.566	0.548
2.60	30.13	2.229	0.615	0.530	0.458	0.443
3.00	22.33	1.678	0.485	0.422	0.365	0.352
3.40	15.13	1.173	0.369	0.326	0.283	0.273
3.80	8.962	0.740	0.268	0.241	0.211	0.203
4.20	4.195	0.399	0.181	0.165	0.145	0.140
4.60	1.140	0.170	0.105	0.096	0.085	0.082
5.00	0.000	0.000	0.000	0.000	0.000	0.000

Table 5.3: Values of compressible static surface deformation  $h(r,1)$  for  $\beta = 5.0$  and for selected values of  $\nu$  and  $\gamma$ .

r	$\beta = 9.0$					
	$\nu = 1/4$	$\nu = 1$	$\nu = 3$	$\nu = 4$	$\nu = 7$	$\nu = 9$
1.00	303.8	20.09	3.267	2.342	1.528	1.365
1.80	287.6	18.77	2.842	1.975	1.226	1.083
2.60	253.4	16.45	2.409	1.643	0.983	0.859
3.40	211.2	13.68	1.977	1.337	0.784	0.680
4.20	166.5	10.78	1.557	1.052	0.614	0.531
5.00	122.7	7.965	1.163	0.790	0.466	0.403
5.80	82.79	5.396	0.809	0.557	0.336	0.293
6.60	48.81	3.209	0.506	0.358	0.225	0.198
7.40	22.64	1.519	0.265	0.195	0.130	0.116
8.20	5.907	0.423	0.095	0.075	0.054	0.049
9.00	0.000	0.000	0.000	0.000	0.000	0.000

r	$\beta = 9.0$					
	$\nu = 1/4$	$\nu = 1$	$\nu = 3$	$\nu = 4$	$\nu = 7$	$\nu = 9$
1.00	248.5	16.58	2.852	2.099	1.438	1.305
1.80	235.2	15.40	2.406	1.702	1.100	0.986
2.60	207.2	13.50	2.036	1.412	0.879	0.780
3.40	172.7	11.23	1.672	1.151	0.703	0.620
4.20	136.1	8.850	1.321	0.910	0.555	0.488
5.00	100.4	6.543	0.993	0.690	0.426	0.376
5.80	67.71	4.439	0.698	0.493	0.315	0.279
6.60	39.91	2.648	0.446	0.325	0.218	0.195
7.40	18.52	1.264	0.245	0.188	0.135	0.122
8.20	4.840	0.367	0.102	0.085	0.066	0.060
9.00	0.000	0.000	0.000	0.000	0.000	0.000

r	$\beta = 9.0$					
	$\nu = 1/4$	$\nu = 1$	$\nu = 3$	$\nu = 4$	$\nu = 7$	$\nu = 9$
1.00	198.5	13.34	2.455	1.863	1.347	1.244
1.80	187.8	12.31	1.994	1.442	0.977	0.891
2.60	165.5	10.79	1.685	1.194	0.779	0.703
3.40	137.9	8.976	1.386	0.975	0.625	0.561
4.20	108.7	7.078	1.098	0.775	0.498	0.446
5.00	80.14	5.235	0.831	0.593	0.388	0.348
5.80	54.04	3.555	0.591	0.431	0.292	0.265
6.60	31.84	2.127	0.386	0.293	0.210	0.192
7.40	14.77	1.025	0.223	0.180	0.139	0.128
8.20	3.859	0.313	0.106	0.093	0.076	0.071
9.00	0.000	0.000	0.000	0.000	0.000	0.000

r	$\beta = 9.0$					
	$\nu = 1/4$	$\nu = 1$	$\nu = 3$	$\nu = 4$	$\nu = 7$	$\nu = 9$
1.00	178.3	12.02	2.287	1.762	1.307	1.216
1.80	168.8	11.06	1.822	1.333	0.925	0.850
2.60	148.7	9.689	1.538	1.102	0.736	0.671
3.40	124.0	8.061	1.266	0.901	0.593	0.537
4.20	97.68	6.356	1.005	0.718	0.474	0.429
5.00	72.00	4.701	0.763	0.552	0.371	0.337
5.80	48.54	3.193	0.546	0.404	0.283	0.259
6.60	28.59	1.912	0.361	0.278	0.206	0.191
7.40	13.25	0.925	0.214	0.176	0.140	0.130
8.20	3.457	0.289	0.108	0.096	0.081	0.076
9.00	0.000	0.000	0.000	0.000	0.000	0.000

Table 5.4: Values of compressible static surface deformation  $h(r,1)$  for  $\beta = 9.0$  and for selected values of  $\nu$  and  $\gamma$ .

## 5.10 Dynamic Deformation

In the final section of this chapter, it is assumed that the applied force is oscillatory, and behaviour is displayed of the amplitude of inner and outer accumulated shear stress

$G_1(z)$  and  $G_\beta(z)$ , respectively, related shear stresses  $g_1(z)$  and  $g_\beta(z)$  and, finally, of surface deformation amplitude  $h(r, 1)$  for selected frequencies  $f_\omega = 0.5, 1.0, 2.0$  and  $5.0$ . The same values for the parameters  $\beta$ ,  $\nu$  and  $\gamma$  are used in the static problem, and the value of parameters  $\sigma$  and  $\xi$  which appears in (5.4.12) are taken to be the quantities  $d^2\rho/\mu$  and  $\eta/2\mu$  equale to one.

### 5.10.1 Dynamic Accumulated Shear Stress

Figures (5.6) - (5.13) illustrate the amplitude of inner and outer accumulated shear stresses  $G_1(z)$  and  $G_\beta(z)$ .

The graphs indicate that the shapes of accumulated shear stress for inner and outer boundaries are qualitatively similar. The magnitude of the accumulated shear stress also appears to increase monotonically in shape in contrast to the static problem where the acumulated shear stress can be non-monotonic.

For fixed values of  $\beta$  and  $f$ , the response curve becomes increasingly close as  $\nu$  increases irrespective of the value of  $\gamma$ .

For fixed values of  $\nu$  and  $\beta$ , resonance effects are noticeable as the frequency  $f$  increases.

In fact, resonant frequency is seen to be an increasing function of  $\nu$  and a decreasing function of  $\beta$ .

### 5.10.2 Dynamic shear stress

Figures (5.14) - (5.18) show the behaviour of the inner and outer shear stresses  $g_1(z)$  and  $g_\beta(z)$  for various values of frequency and parameters  $\beta$ ,  $\nu$  and  $\gamma$ .

The general shape of the inner and outer shear stress distributions are similar although the outer boundary exhibits more variability than the inner boundary. This variability is thought to stem from resonace effect. There are stress boundary layers on the upper and lower boundaries of the annulus for all values of  $\nu$  and  $\beta$ .

Negative stresses occur occasionally, inferring that the material stress can be opposed to the applied force. Since the magnitude of the accumulated shear stress is always increasing, this suggests that the phase of  $g(z)$  can vary significantly throughout the layer, particulary near the resonant frequency.

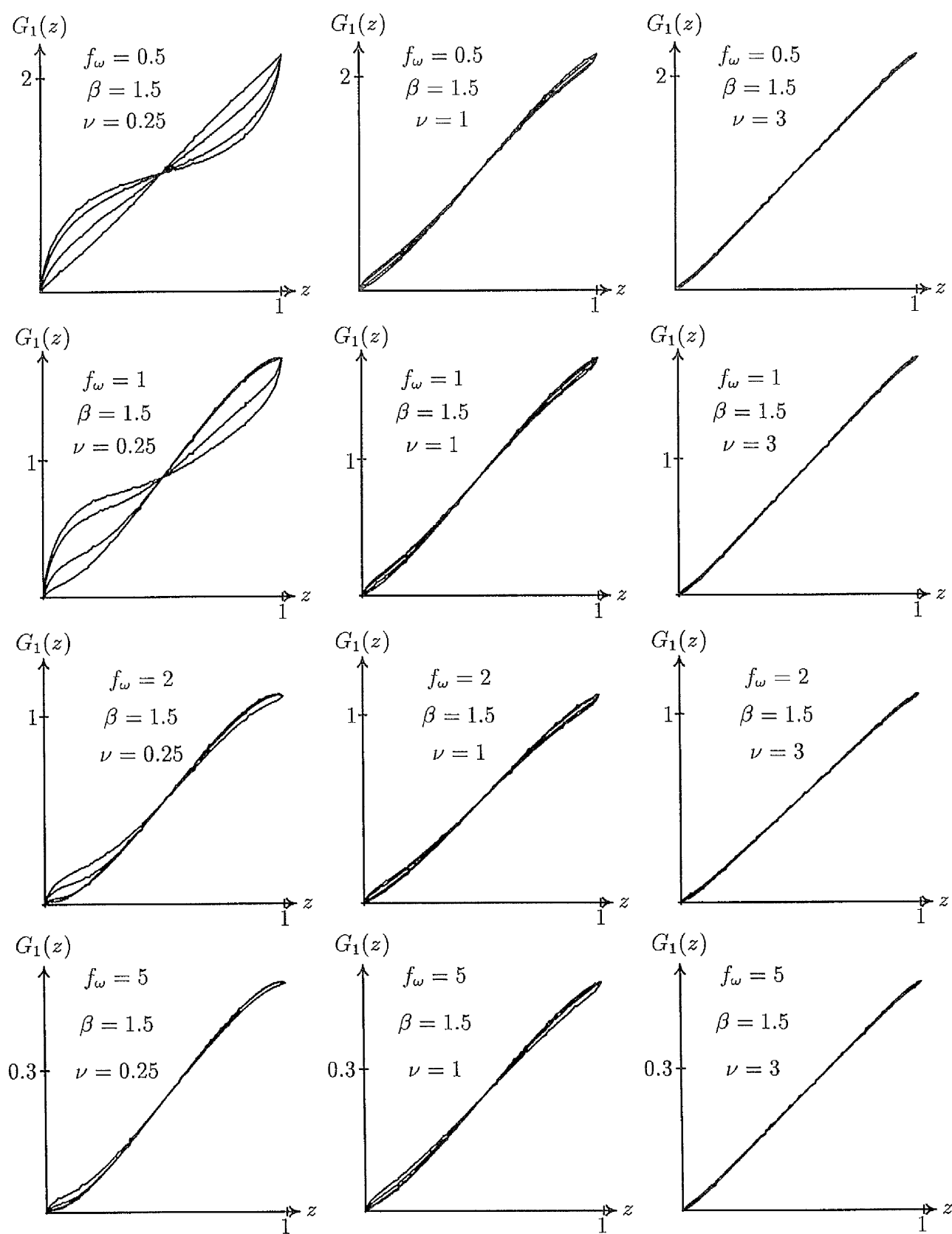


Figure 5.6: Graphs of inner accumulated shear stress  $G_1(z)$  for selected values of  $\nu$ ,  $\beta = 1.5$  and for  $\gamma = -1.1, -1.5, -3.0, -6.75$ , and for frequencies  $f_\omega = 0.5, 1, 2$ .

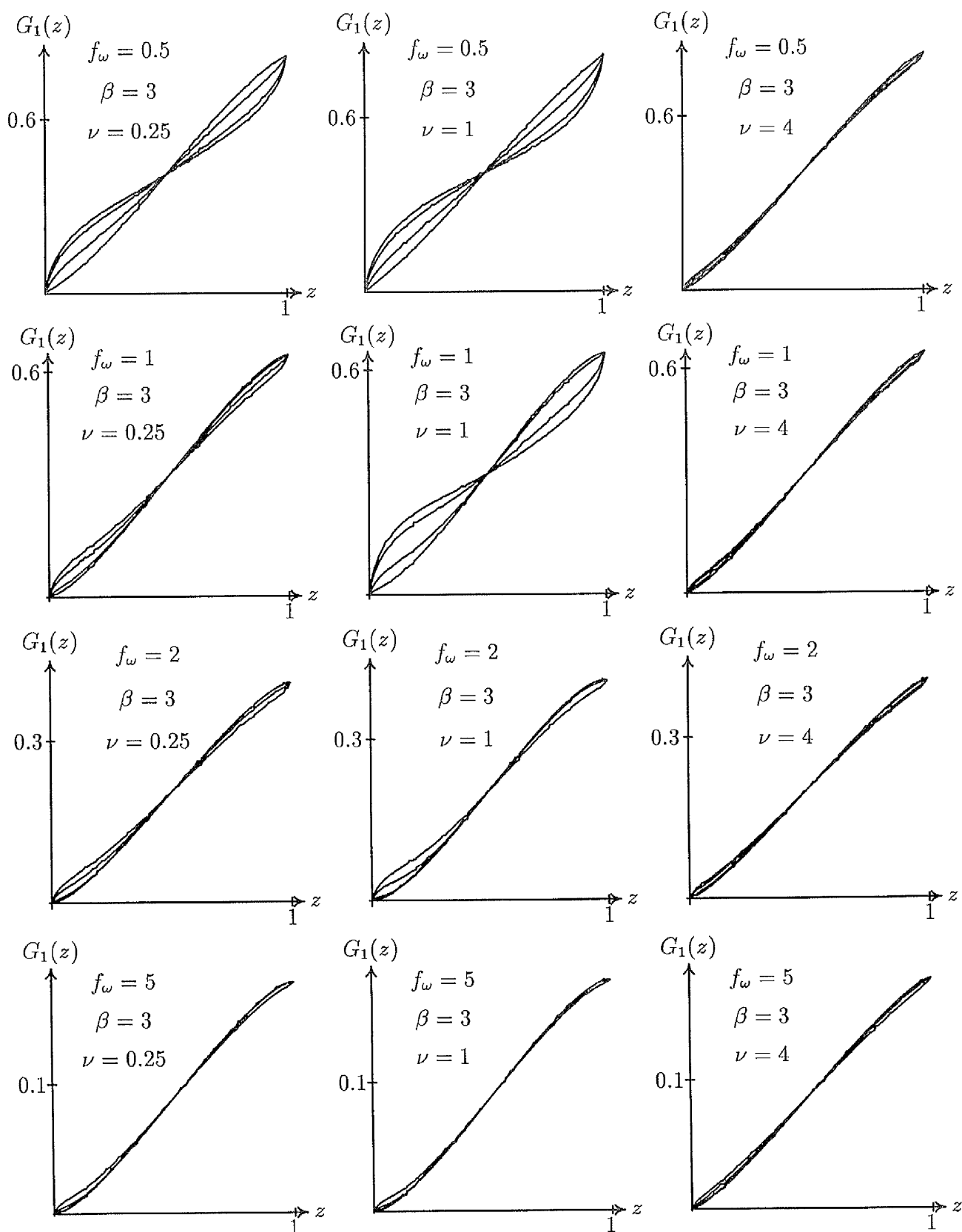


Figure 5.7: Graphs of inner accumulated shear stress  $G_1(z)$  for selected values of  $\nu$ ,  $\beta = 3.0$  and for  $\gamma = -1.1, -1.5, -3.0, -6.75$ , and for frequencies  $f_\omega = 0.5, 1, 2$ .

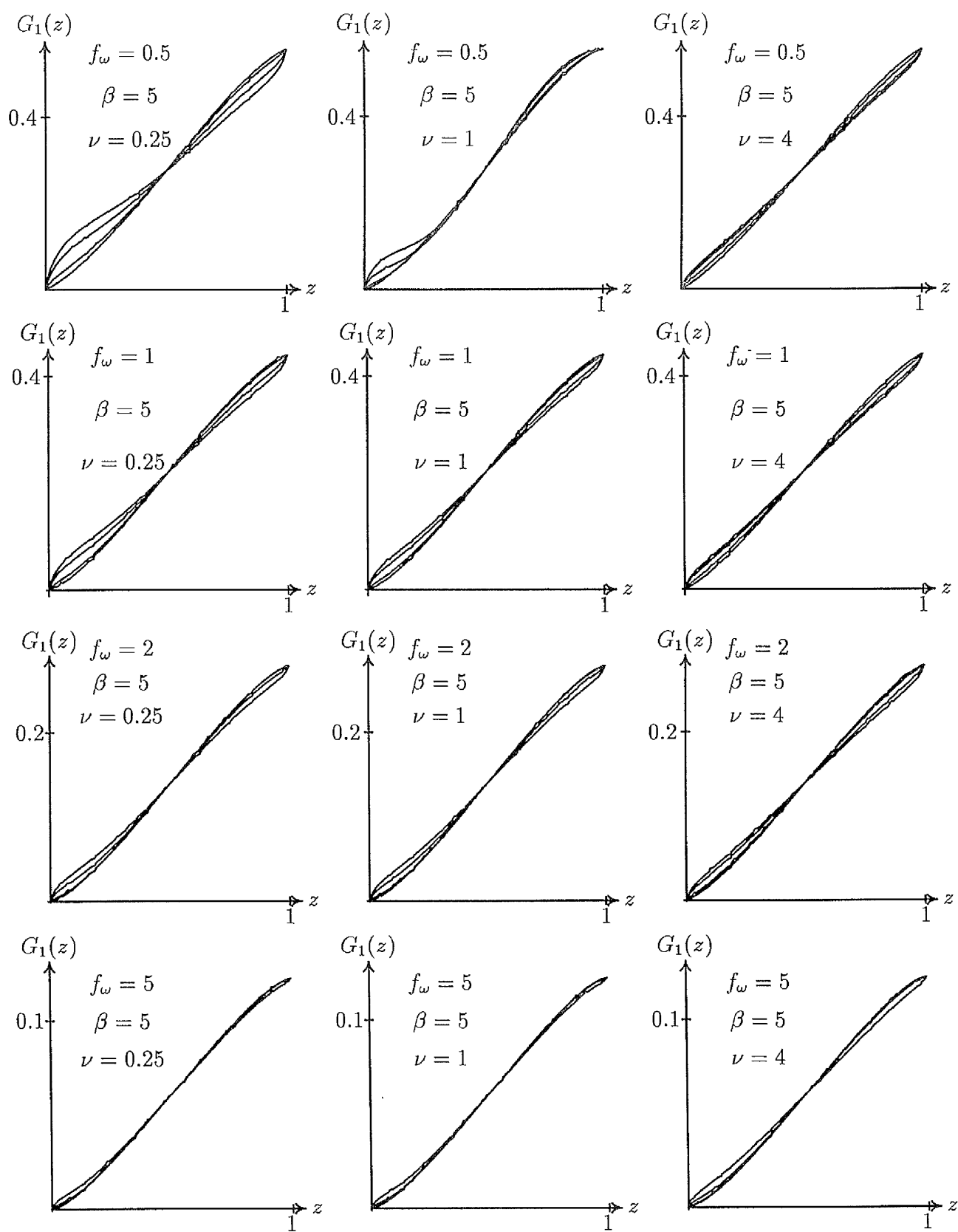


Figure 5.8: Graphs of inner accumulated shear stress  $G_1(z)$  for selected values of  $\nu$ ,  $\beta = 5.0$  and for  $\gamma = -1.1, -1.5, -3.0, -6.75$ , and for frequencies  $f_\omega = 0.5, 1, 2$ .

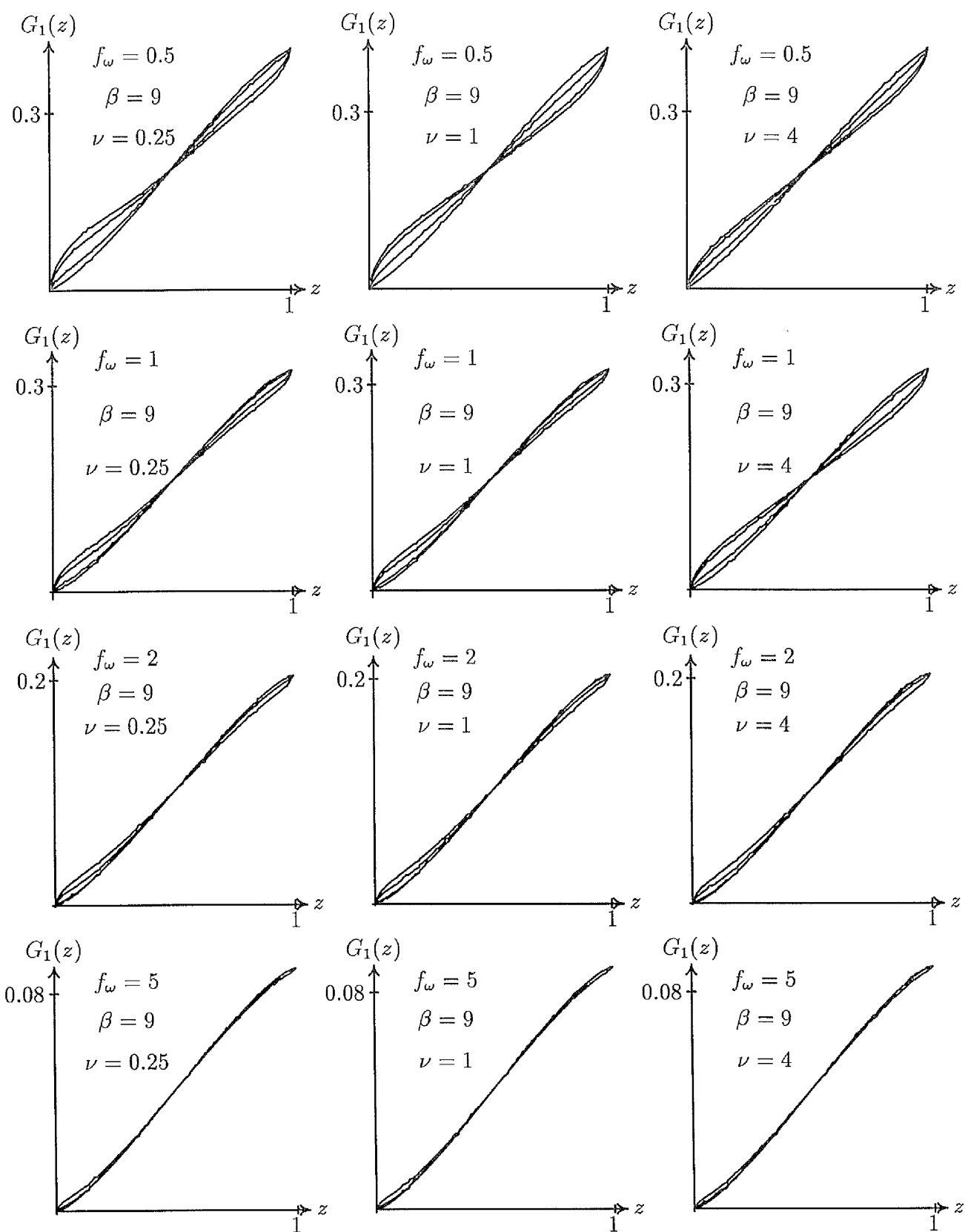


Figure 5.9: Graphs of inner accumulated shear stress  $G_1(z)$  for selected values of  $\nu$ ,  $\beta = 9.0$  and for  $\gamma = -1.1, -1.5, -3.0, -6.75$ , and for frequencies  $f_\omega = 0.5, 1, 2$ .



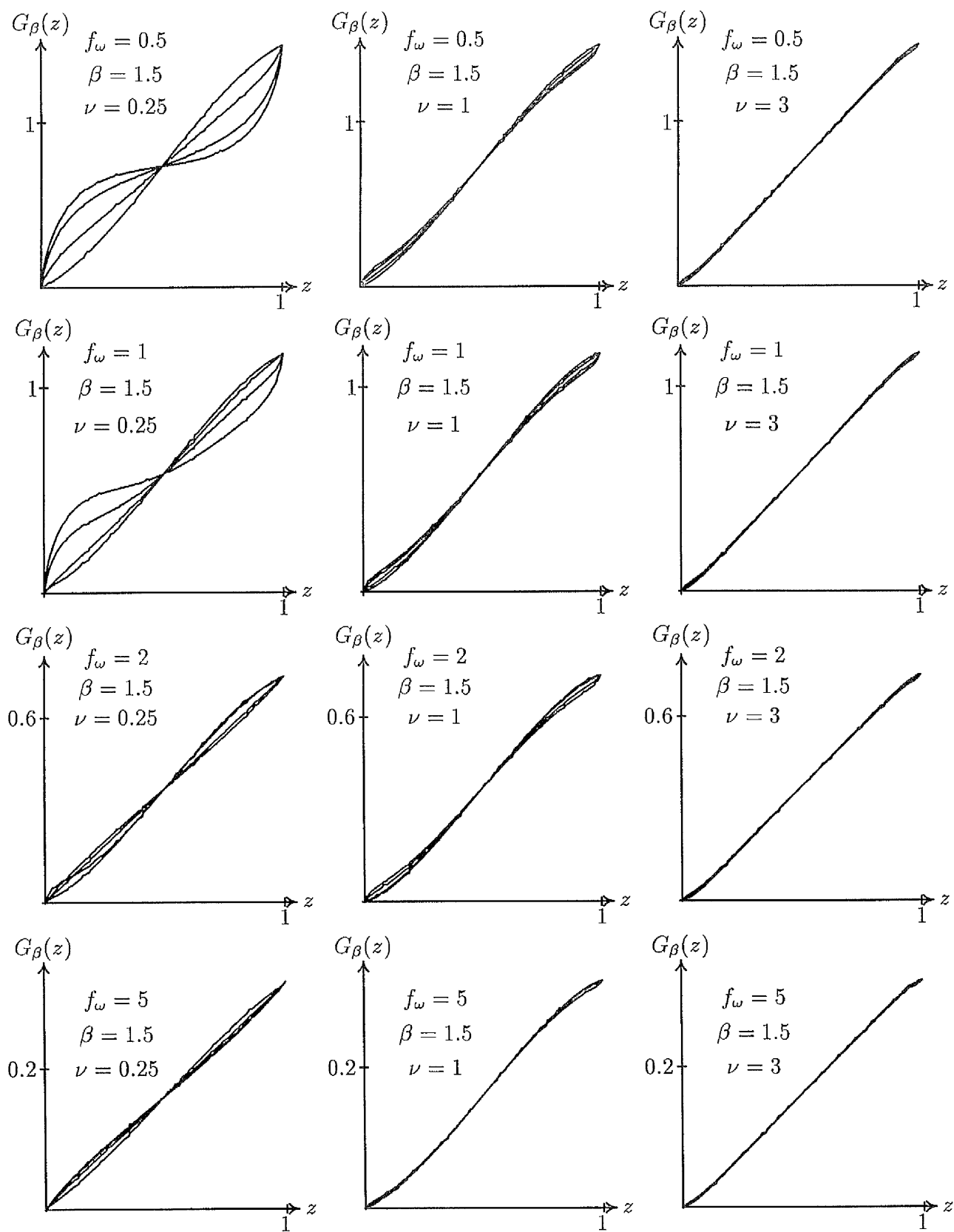


Figure 5.10: Graphs of outer accumulated shear stress  $G_\beta(z)$  for selected values of  $\nu$ ,  $\beta = 1.5$  and  $\gamma = -1.1, -1.5, -3.0, -6.75$  and for frequency  $f_\omega = 0.5, 1.0, 2.0$ .

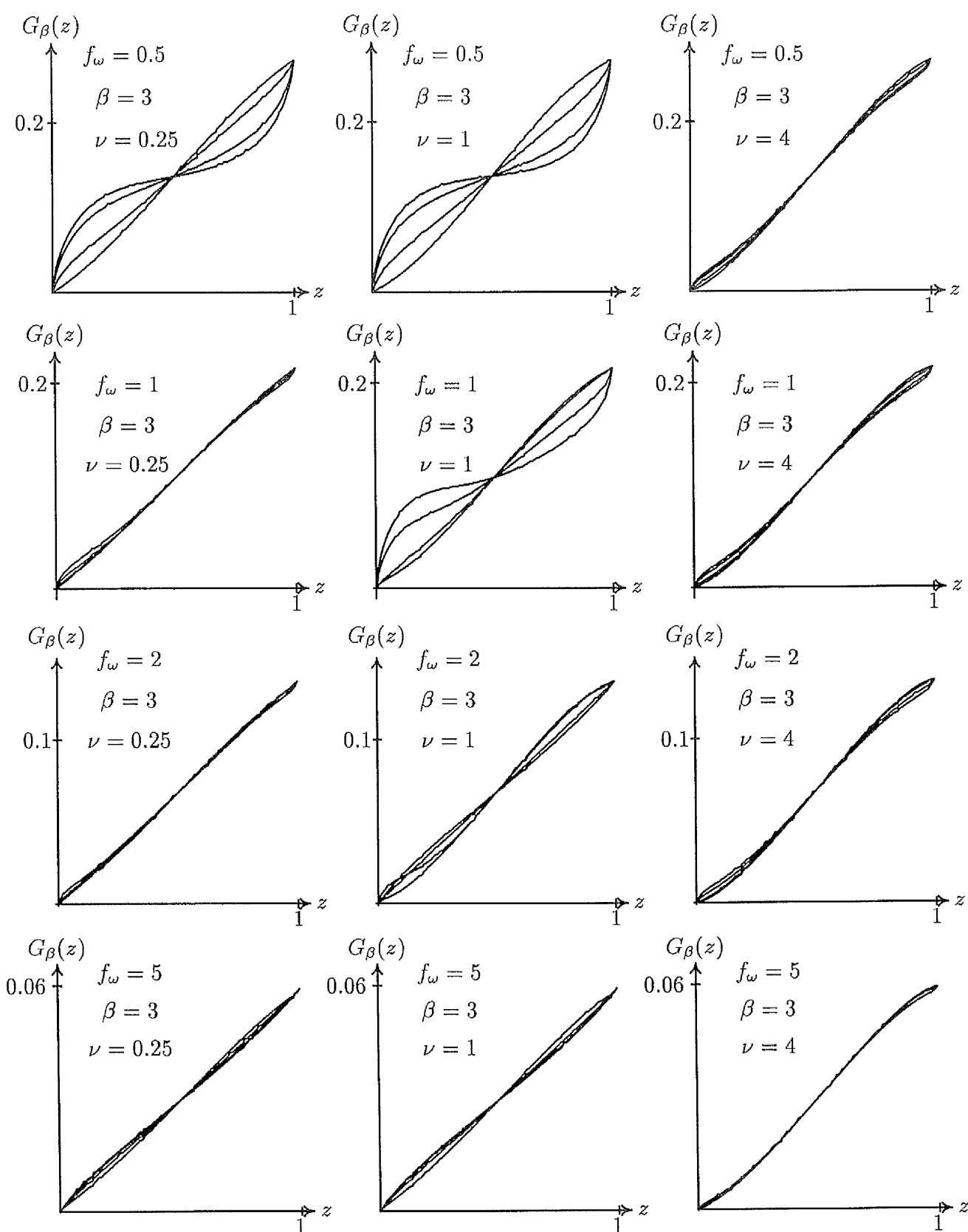


Figure 5.11: Graphs of outer accumulated shear stress  $G_\beta(z)$  for selected values of  $\nu$ ,  $\beta = 3.0$  and for  $\gamma = -1.1, -1.5, -3.0, -6.75$  and for frequency  $f_\omega = 0.5, 1.0, 2.0$ .

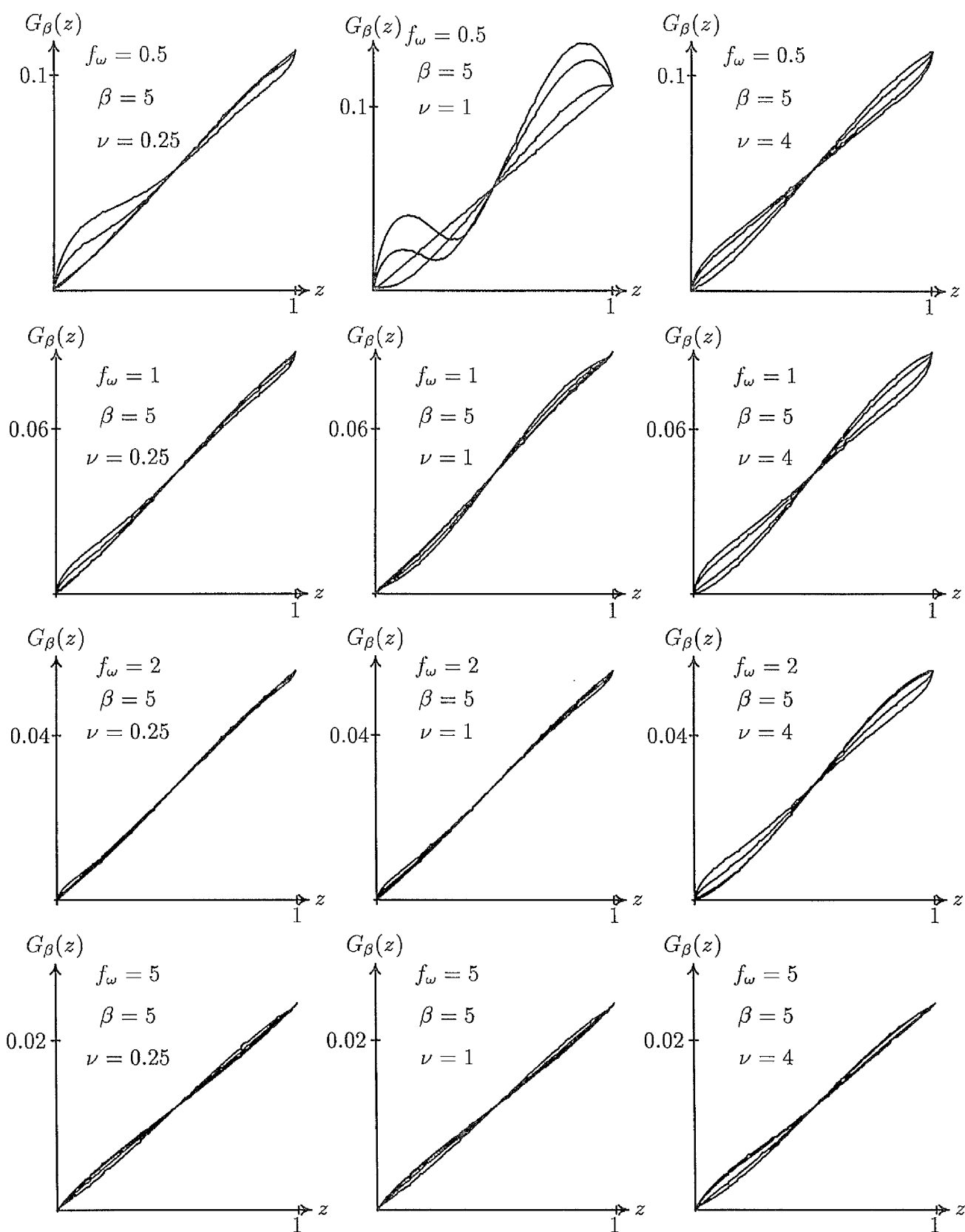


Figure 5.12: Graphs of outer accumulated shear stress  $G_\beta(z)$  for selected values of  $\nu$ ,  $\beta = 5.0$  and for  $\gamma = -1.1, -1.5, -3.0, -6.75$  and for frequency  $f_\omega = 0.5, 1.0, 2.0$ .

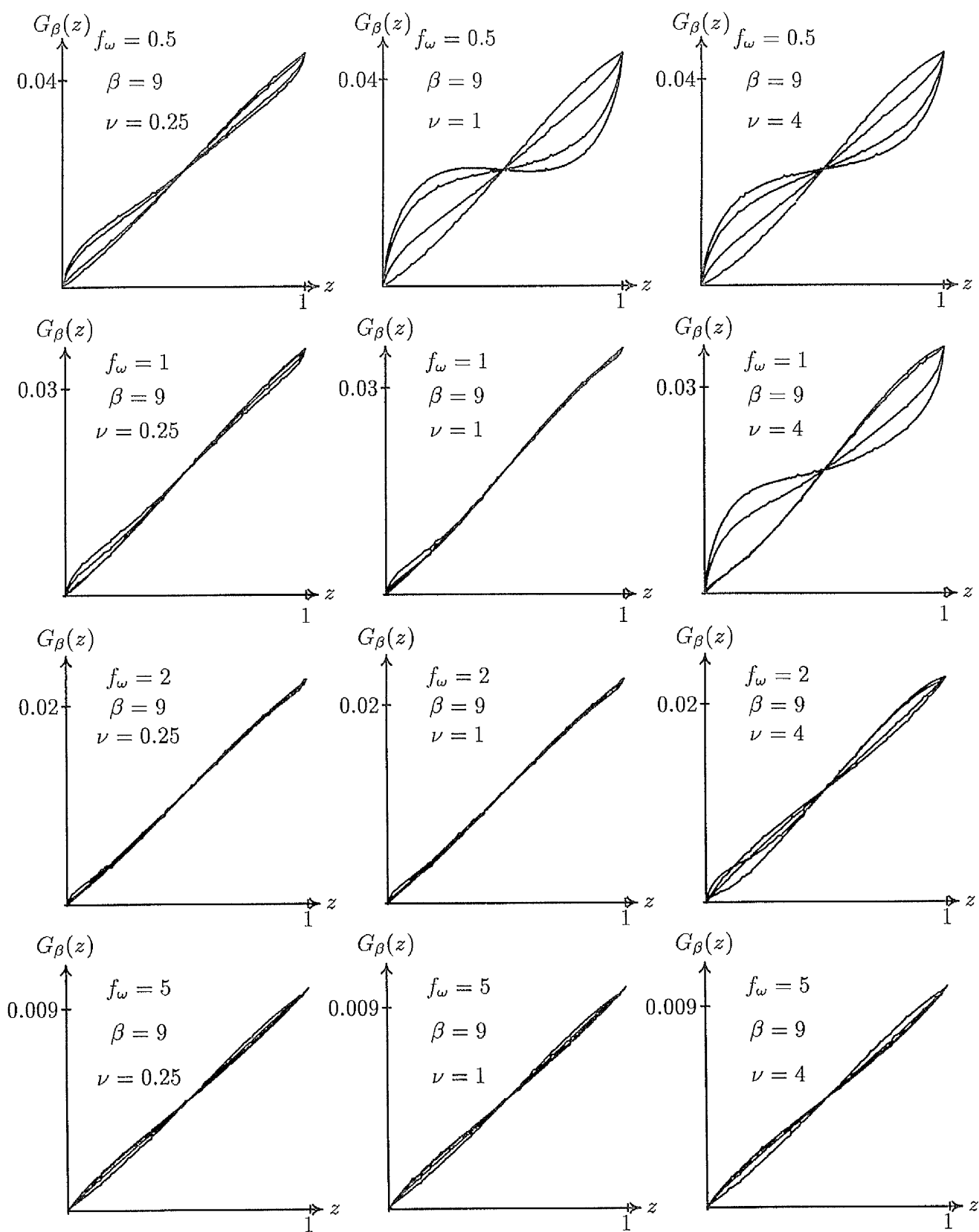


Figure 5.13: Graphs of outer accumulated shear stress  $G_\beta(z)$  for selected values of  $\nu$ ,  $\beta = 9.0$  and for  $\gamma = -1.1, -1.5, -3.0, -6.75$  and for frequency  $f_\omega = 0.5, 1.0, 2.0$ .

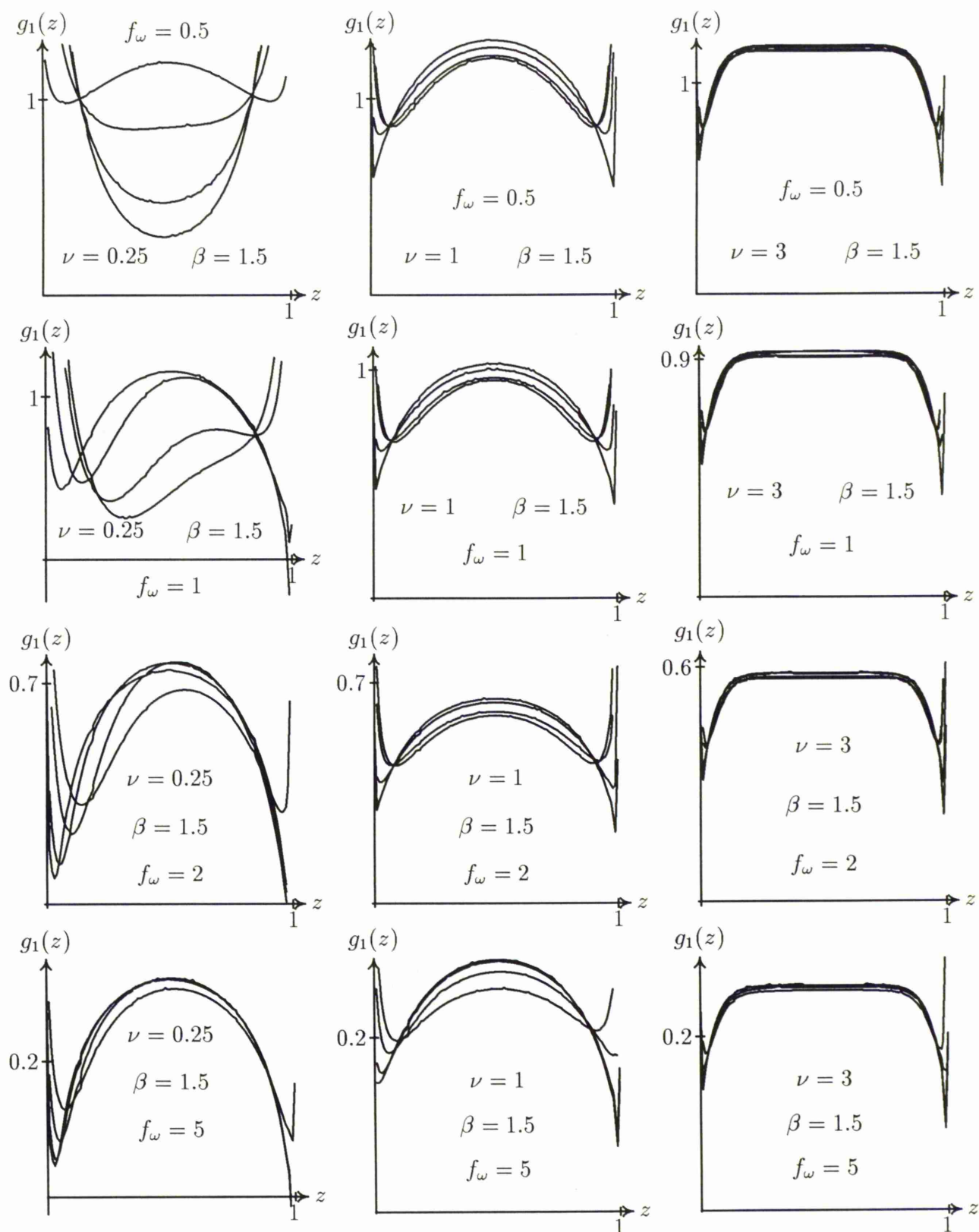


Figure 5.14: Graphs of inner shear stress  $g_1(z)$  for selected values of  $\nu$ ,  $\beta = 1.5$  and for  $\gamma = -1.1, -1.5, -3.0, -6.75$ , and for frequency  $f_w = 0.5, 1, 2$ . Component pictures correspond to their counterparts in accumulated shear stress  $G_1(z)$ . This is illustrated in figure 5.6.

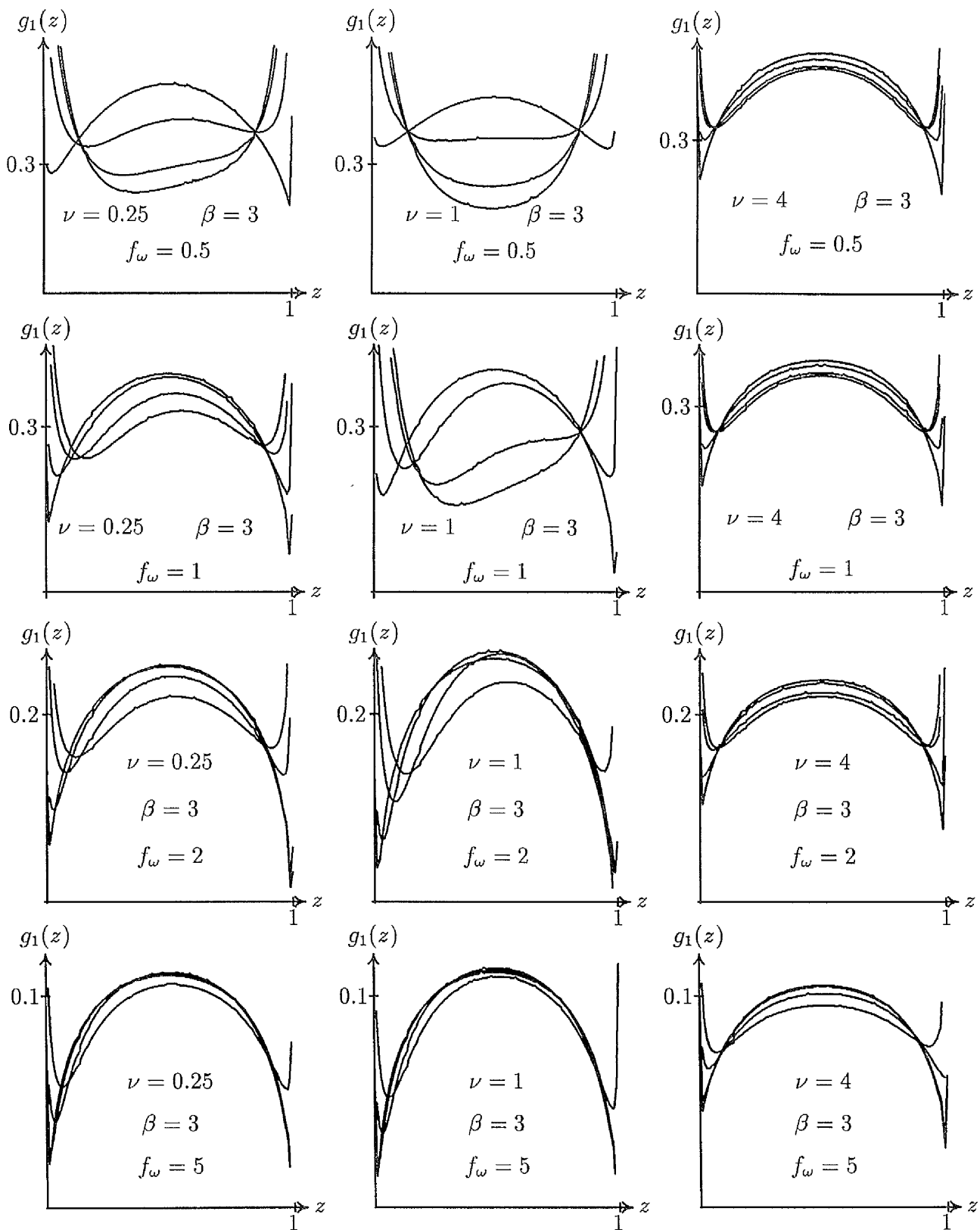


Figure 5.15: Graphs of inner shear stress  $g_1(z)$  for selected values of  $\nu$ ,  $\beta = 3.0$  and for  $\gamma = -1.1, -1.5, -3.0, -6.75$ , and for frequency  $f_\omega = 0.5, 1, 2$ . Component pictures correspond to their counterparts in accumulated shear stress  $G_1(z)$ . This is illustrated in figure 5.7.

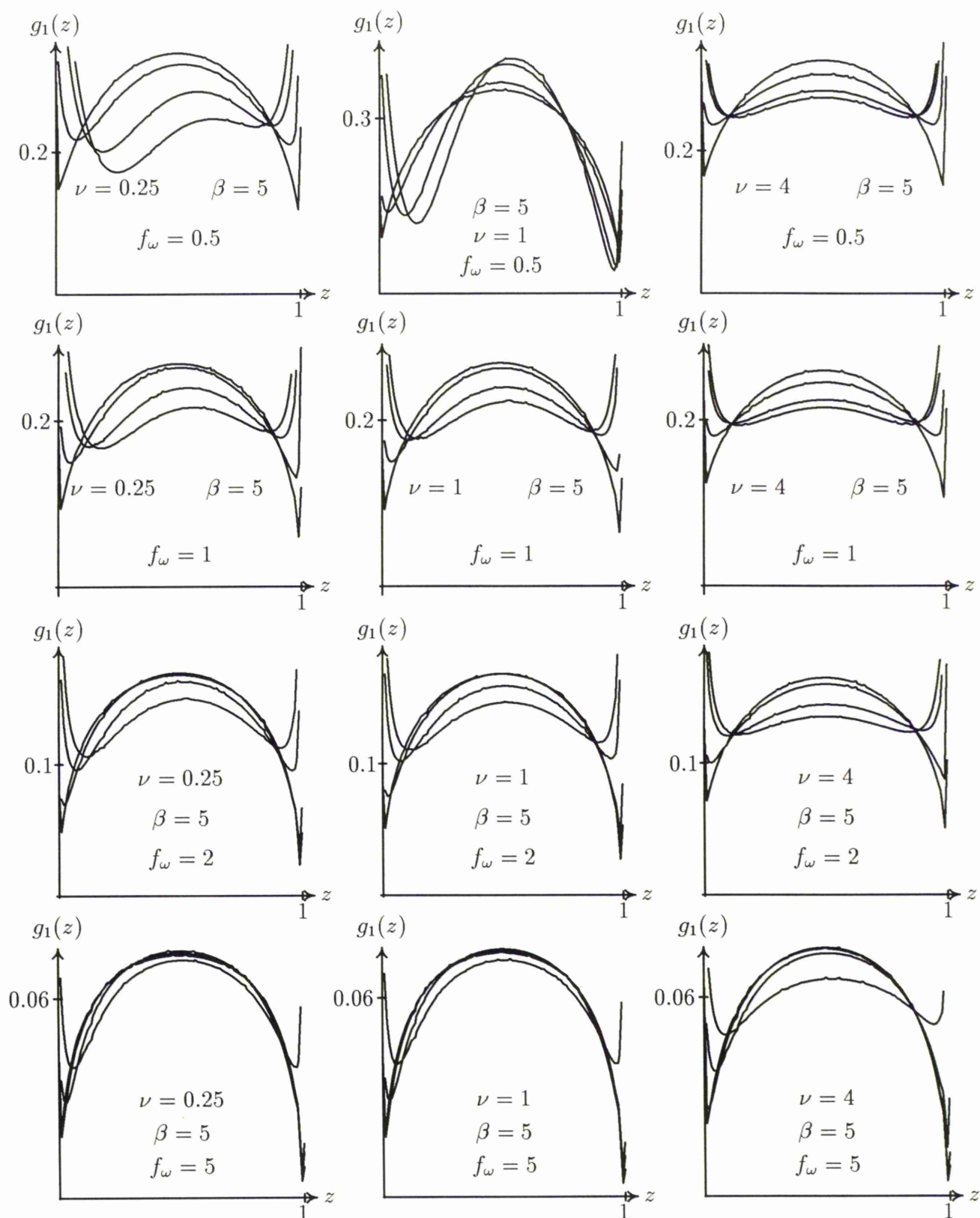


Figure 5.16: Graphs of inner shear stress  $g_1(z)$  for selected values of  $\nu$ ,  $\beta = 5.0$  and for  $\gamma = -1.1, -1.5, -3.0, -6.75$ , and for frequency  $f_\omega = 0.5, 1, 2$ . Component pictures correspond to their counterparts in accumulated shear stress  $G_1(z)$ . This is illustrated in figure 5.8.

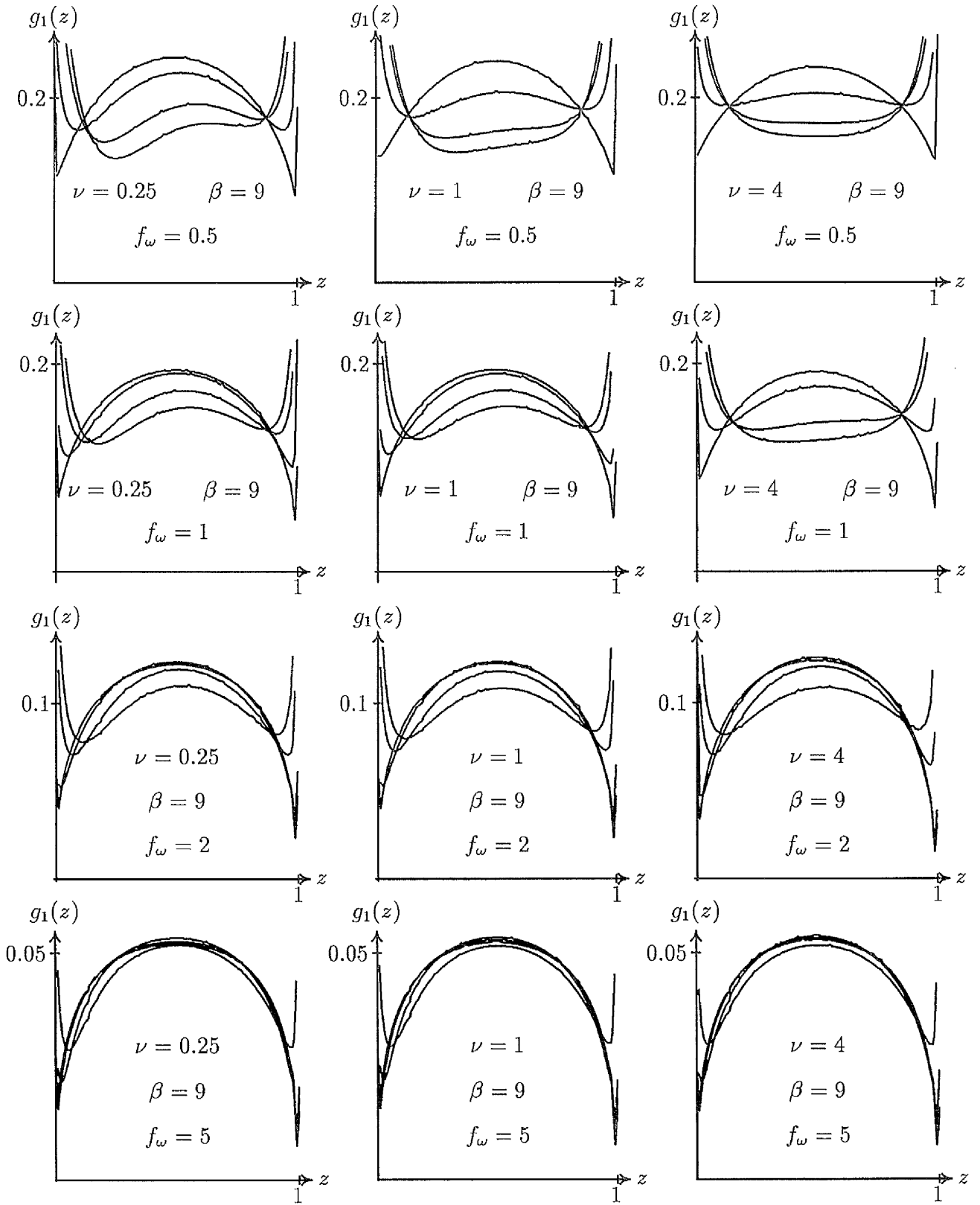


Figure 5.17: Graphs of inner shear stress  $g_1(z)$  for selected values of  $\nu$ ,  $\beta = 9.0$  and for  $\gamma = -1.1, -1.5, -3.0, -6.75$ , and for frequency  $f_\omega = 0.5, 1, 2$ . Component pictures correspond to their counterparts in accumulated shear stress  $G_1(z)$ . This is illustrated in figure 5.9.



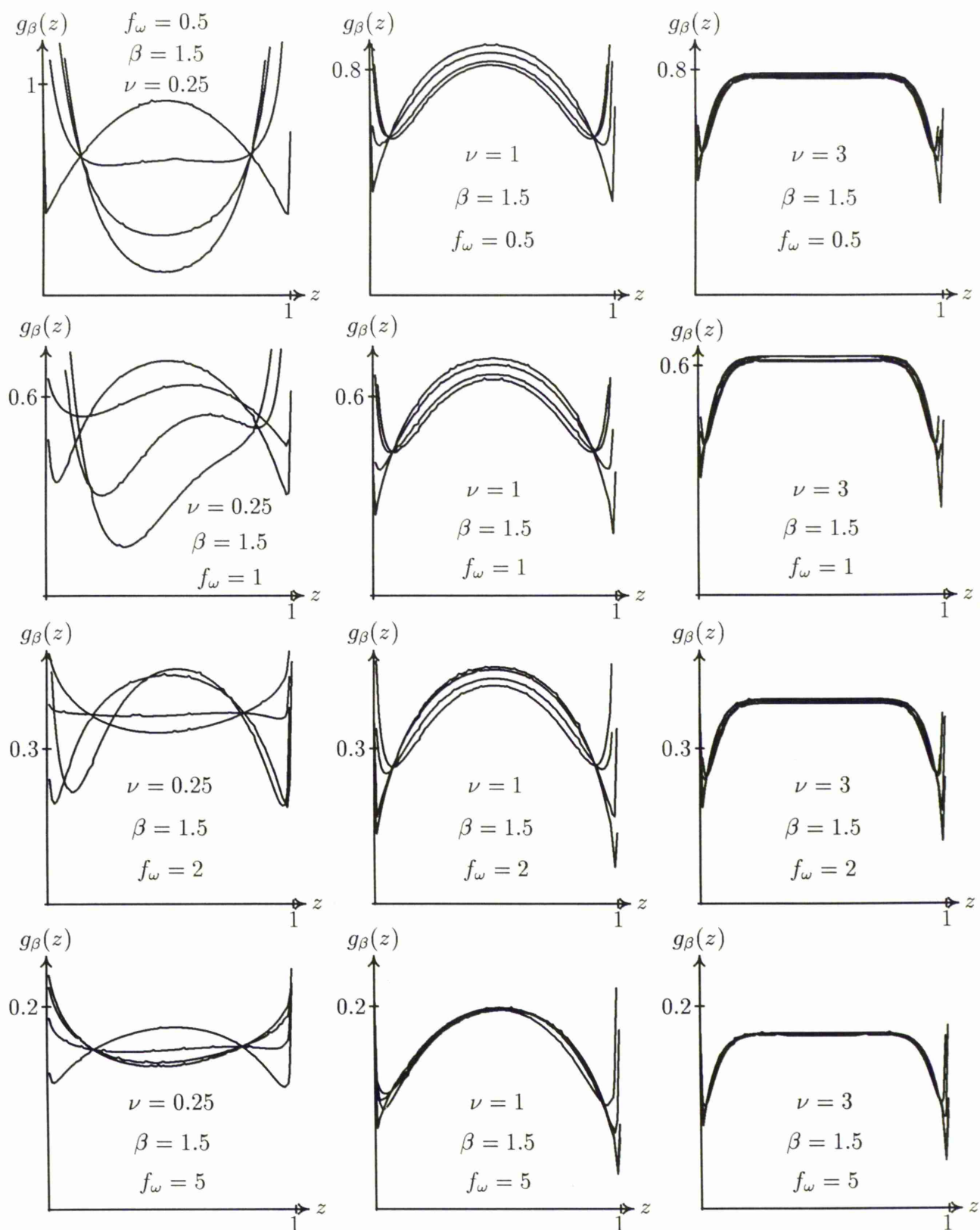


Figure 5.18: Graphs of outer shear stress  $g_\beta(z)$  for selected values of  $\nu$ ,  $\beta = 1.5$  and for  $\gamma = -1.1, -1.5, -3.0, -6.75$ , and frequencies  $f_\omega = 0.5, 1.0, 2.0$ . Component pictures correspond to their counterparts in accumulated shear stress  $G_\beta(z)$ . This is illustrated in figure 5.10.

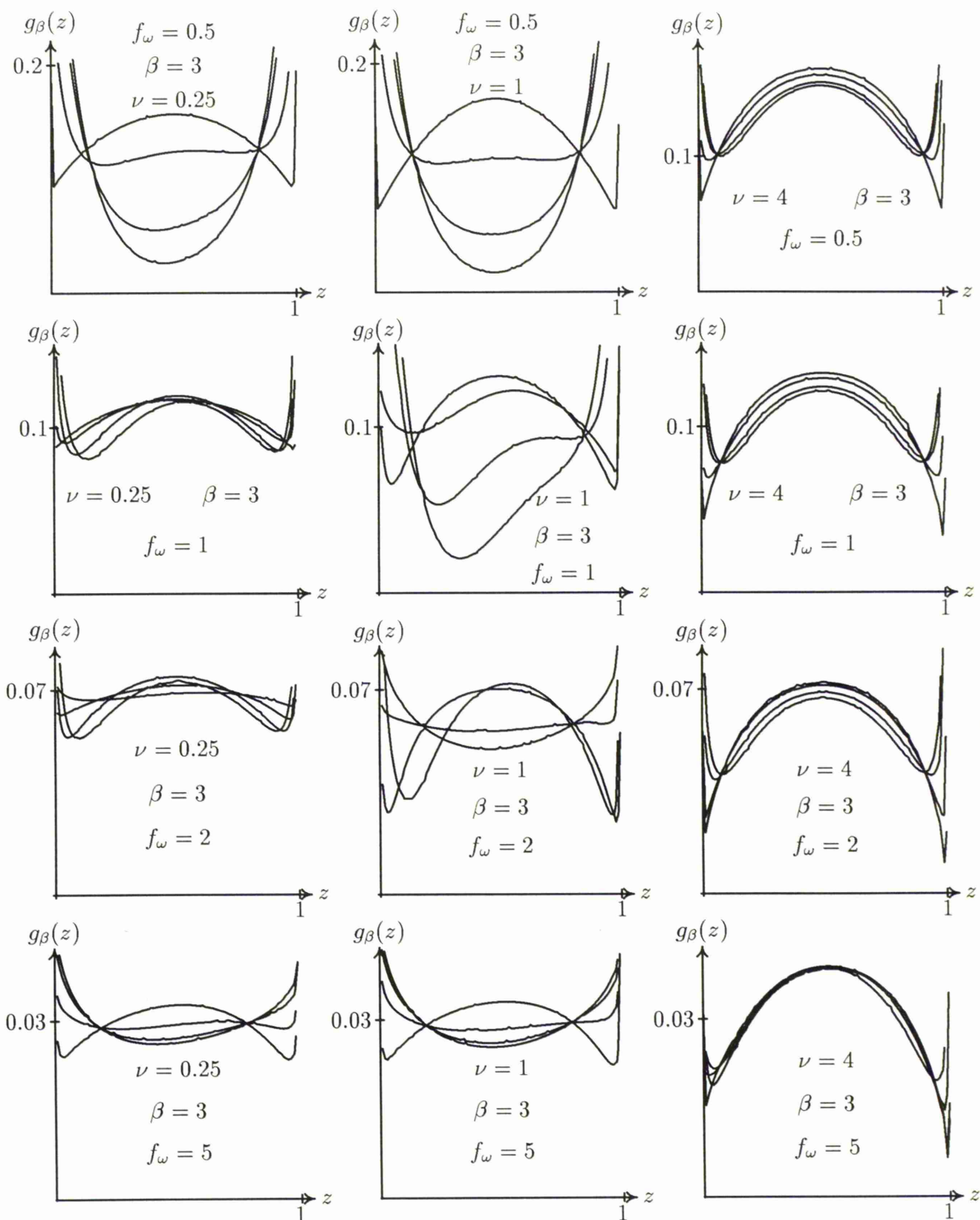


Figure 5.19: Graphs of outer shear stress  $g_\beta(z)$  for selected values of  $\nu$ ,  $\beta = 3.0$  and for  $\gamma = -1.1, -1.5, -3.0, -6.75$ , and frequencies  $f_\omega = 0.5, 1.0, 2.0$ . Component pictures correspond to their counterparts in the accumulated shear stress  $G_\beta(z)$ . This is illustrated in figure 5.11.

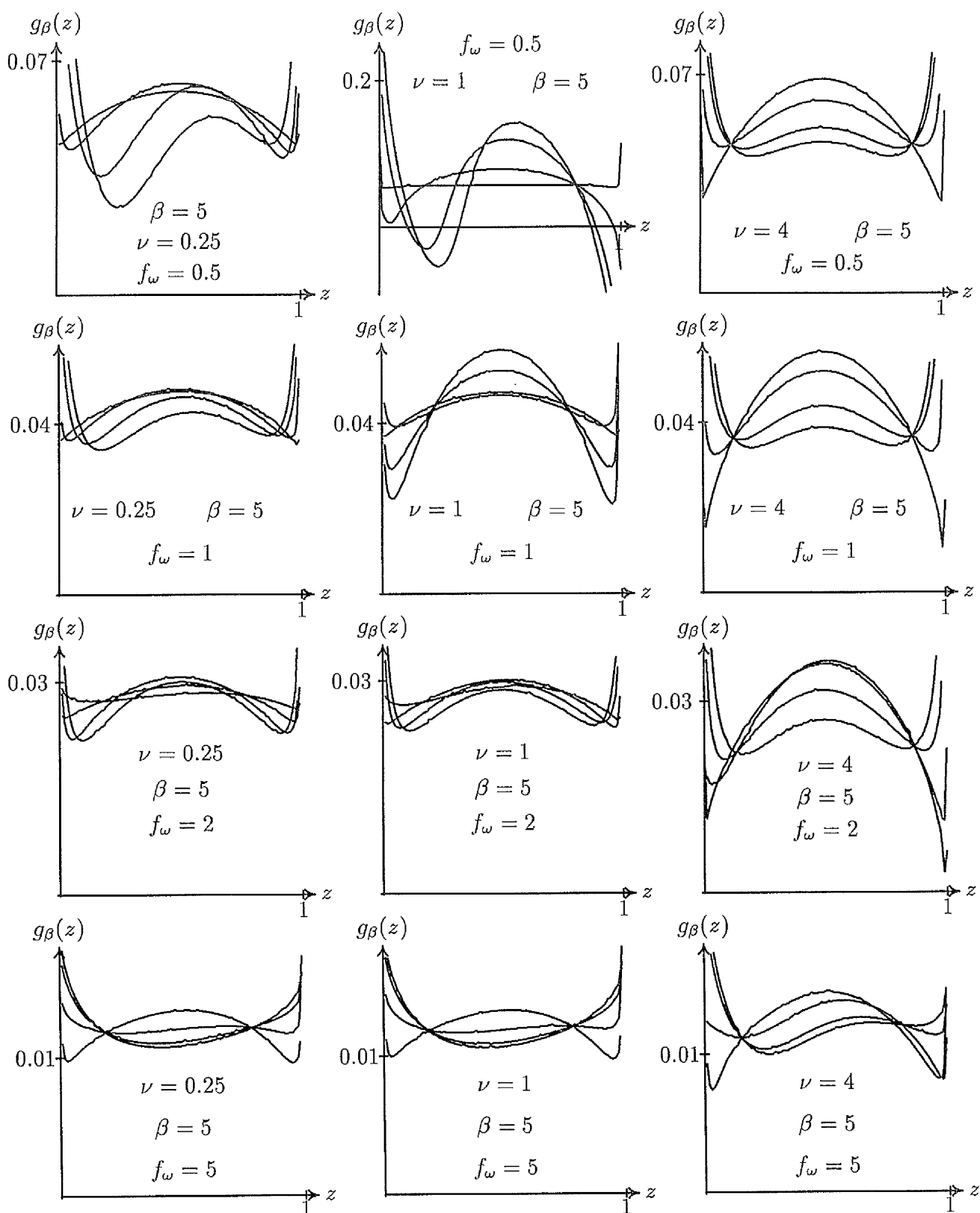


Figure 5.20: Graphs of outer shear stress  $g_\beta(z)$  for selected values of  $\nu$ ,  $\beta = 5.0$  and for  $\gamma = -1.1, -1.5, -3.0, -6.75$ , and frequencies  $f_\omega = 0.5, 1.0, 2.0$ . Component pictures correspond to their counterparts in the accumulated shear stress  $G_\beta(z)$ . This is illustrated in figure 5.12.

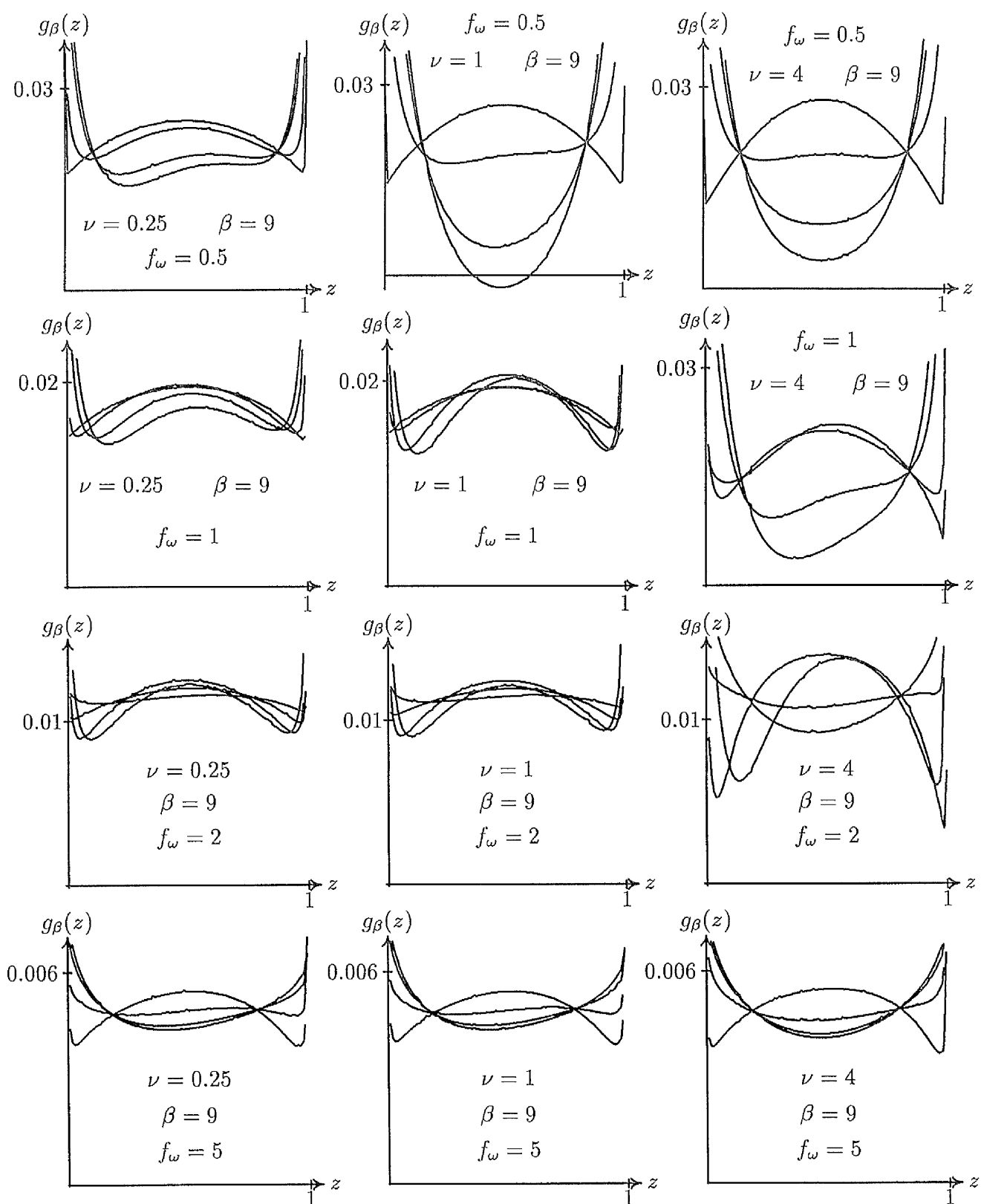


Figure 5.21: Graphs of outer shear stress  $g_\beta(z)$  for selected values of  $\nu$ ,  $\beta = 9.0$  and for  $\gamma = -1.1, -1.5, -3.0, -6.75$ , and frequencies  $f_\omega = 0.5, 1.0, 2.0$ . Component pictures correspond to their counterparts in the accumulated shear stress  $G_\beta(z)$ . This is illustrated in figure 5.13.

### 5.10.3 Dynamic surface deformation

The dynamic surface deformations  $h(r, 1)$  are plotted in figures (5.22) - (5.25) and every graph contains four different materials from highly compressible to rubber solid material like. Figure (5.22) shows that the material has a short length in the outer radius relative to that of the inner radius. In general, all the graphs are closer to each other when the material starts to be thicker and frequency starts increasing.

Figure (5.23) displays the effects of resonance when the material is very thin; for example, for  $\nu = 0.25$ , this effect is missing when the thickness starts increasing  $\nu \geq 1$  except at ( $\nu = 1, \beta = 3$  and  $f_\omega = 5$ ). Also, in the interior points it is almost flat for  $f_\omega = 5$  and  $\nu = 0.25$ , and that shape is clearer when  $\beta$  starts increasing, (say  $\beta = 5$ ). The resonant frequency is increasing when  $\beta$  increases for thin materials; for example,  $\nu \leq 1$ , as shown in figure (5.24).

Finally figure (5.25) displays the behavior of the material when  $\beta$  is large (say  $\beta = 9$ ).

In conclusion:

- (a) At the interior points, the surface deformation becomes almost flat when the material is thin and  $\beta$  starts increasing with increasing of frequency.
- (b) The resonant frequency is an increasing function of  $\beta$  and a decreasing function of  $\nu$  and is independent of  $\gamma$ .

Tables (5.5) - (5.12) display the values of  $h(r, 1)$  for a limited range of  $r$  and other parameters; that is,  $\beta$ ,  $\nu$  and  $\gamma$  for frequencies  $f_\omega = 0.5, 1.0, 2.0$  and  $5.0$ .

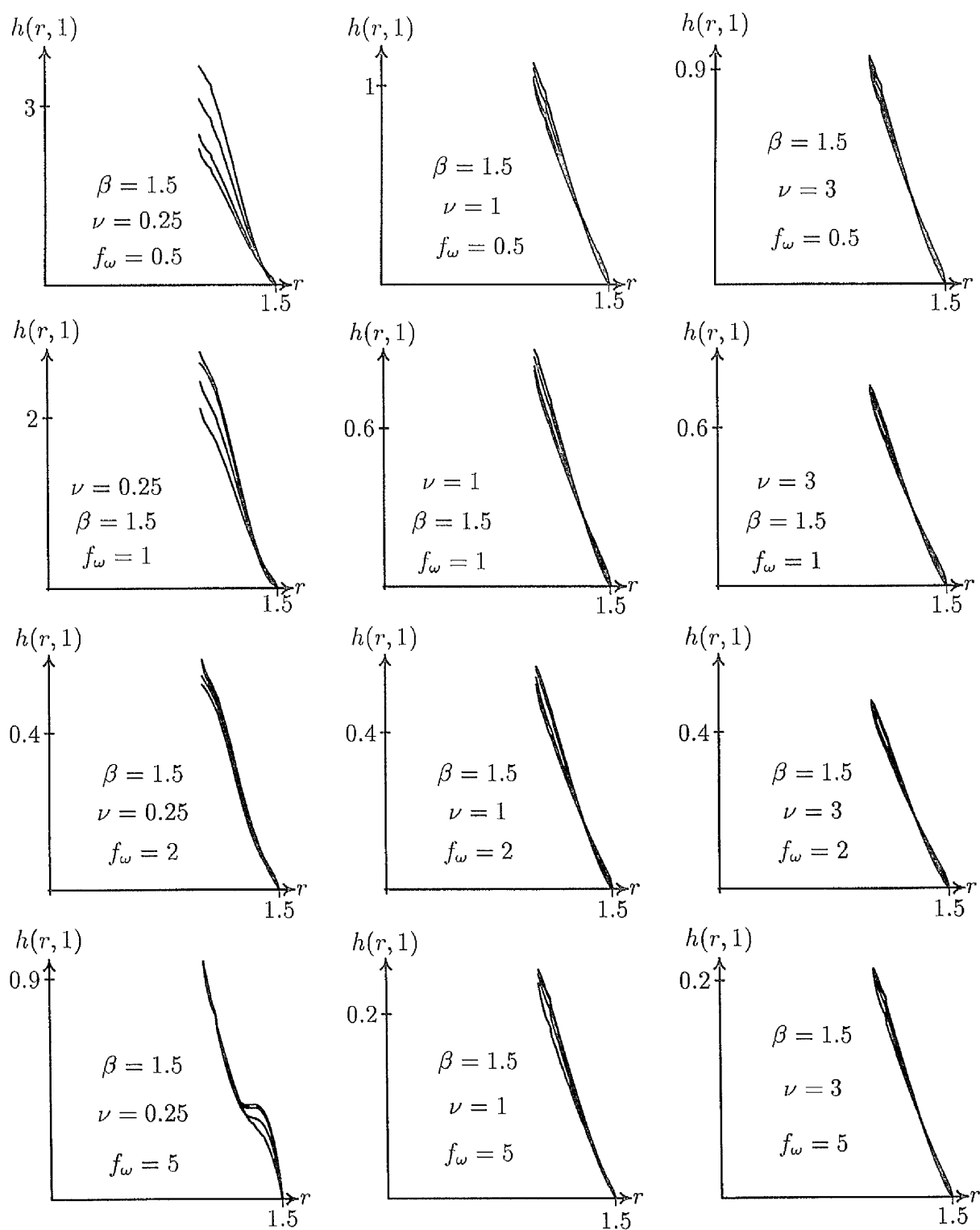


Figure 5.22: Compressible dynamic surface deformation  $h(r, 1)$  for selected values of  $\nu$ ,  $f$  and  $\beta = 1.5$  and for  $\gamma = -1.1, -1.5, -3$  and  $-6.75$ .

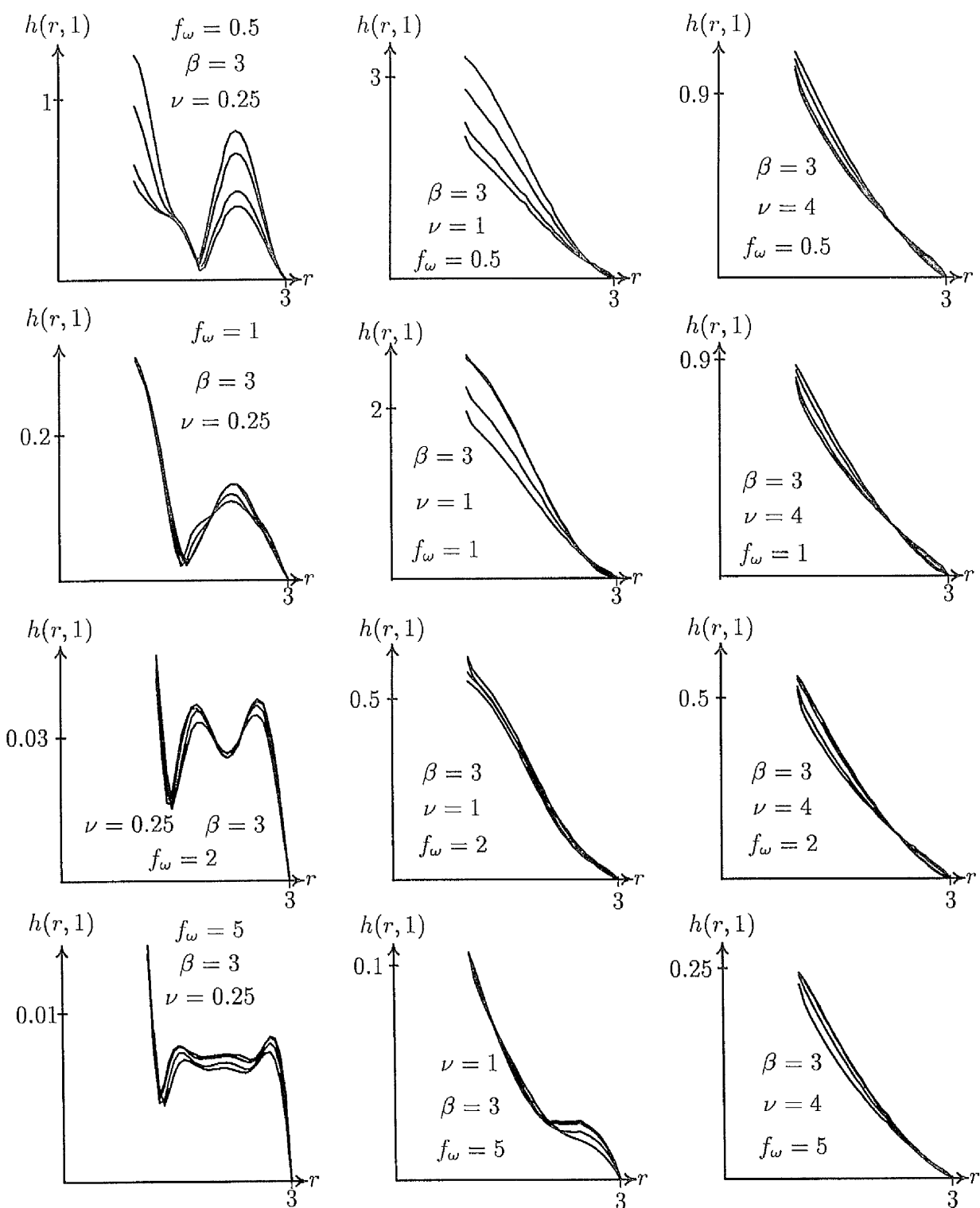


Figure 5.23: Compressible dynamic surface deformation  $h(r,1)$  for selected values of  $\nu$ ,  $f$  and  $\beta = 3.0$  and for  $\gamma = -1.1, -1.5, -3$  and  $-6.75$ .

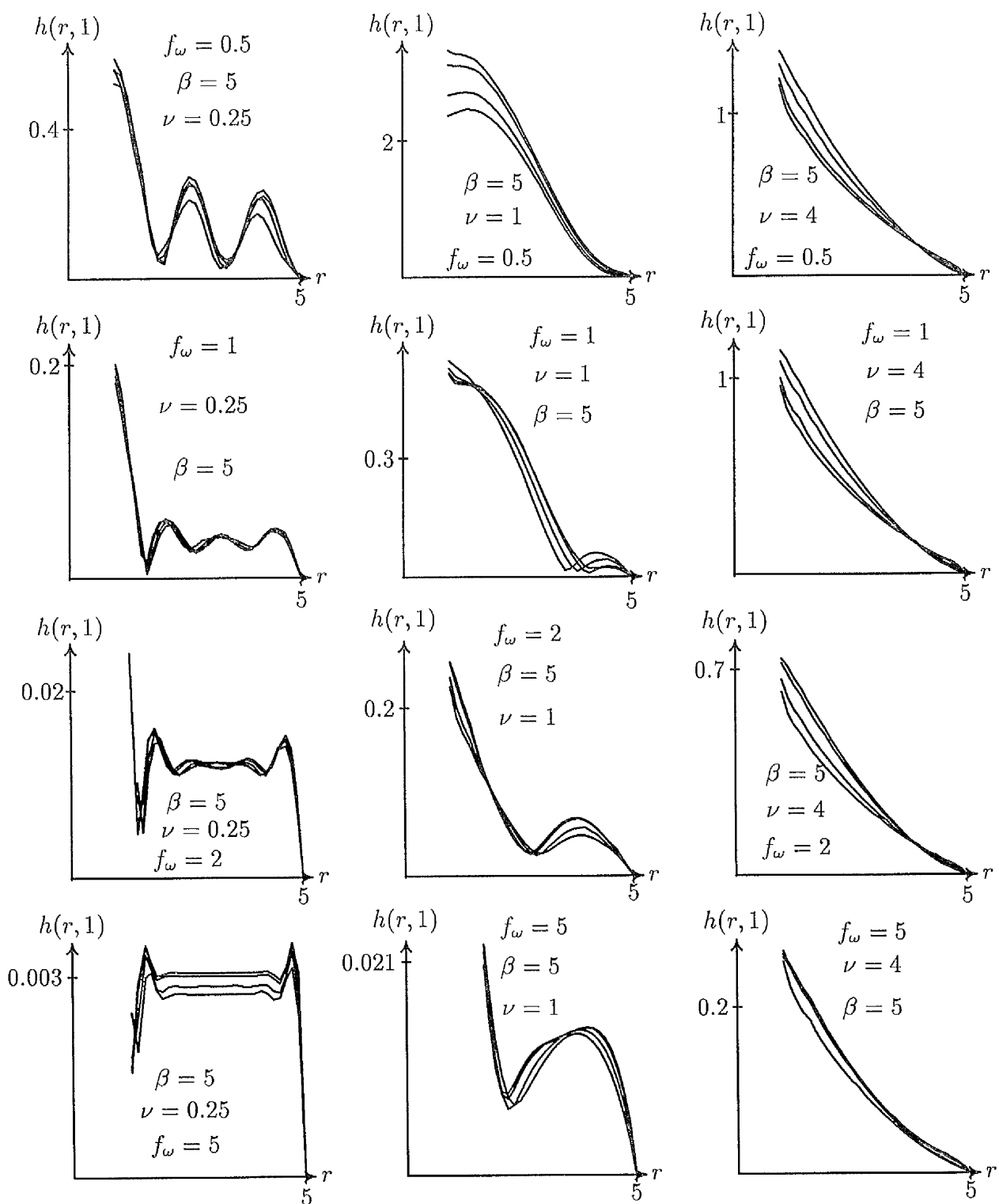


Figure 5.24: Compressible dynamic surface deformation  $h(r, 1)$  for different values of  $\nu$ ,  $f$  and  $\beta = 5.0$  and for  $\gamma = -1.1, -1.5, -3.0$  and  $-6.75$ .



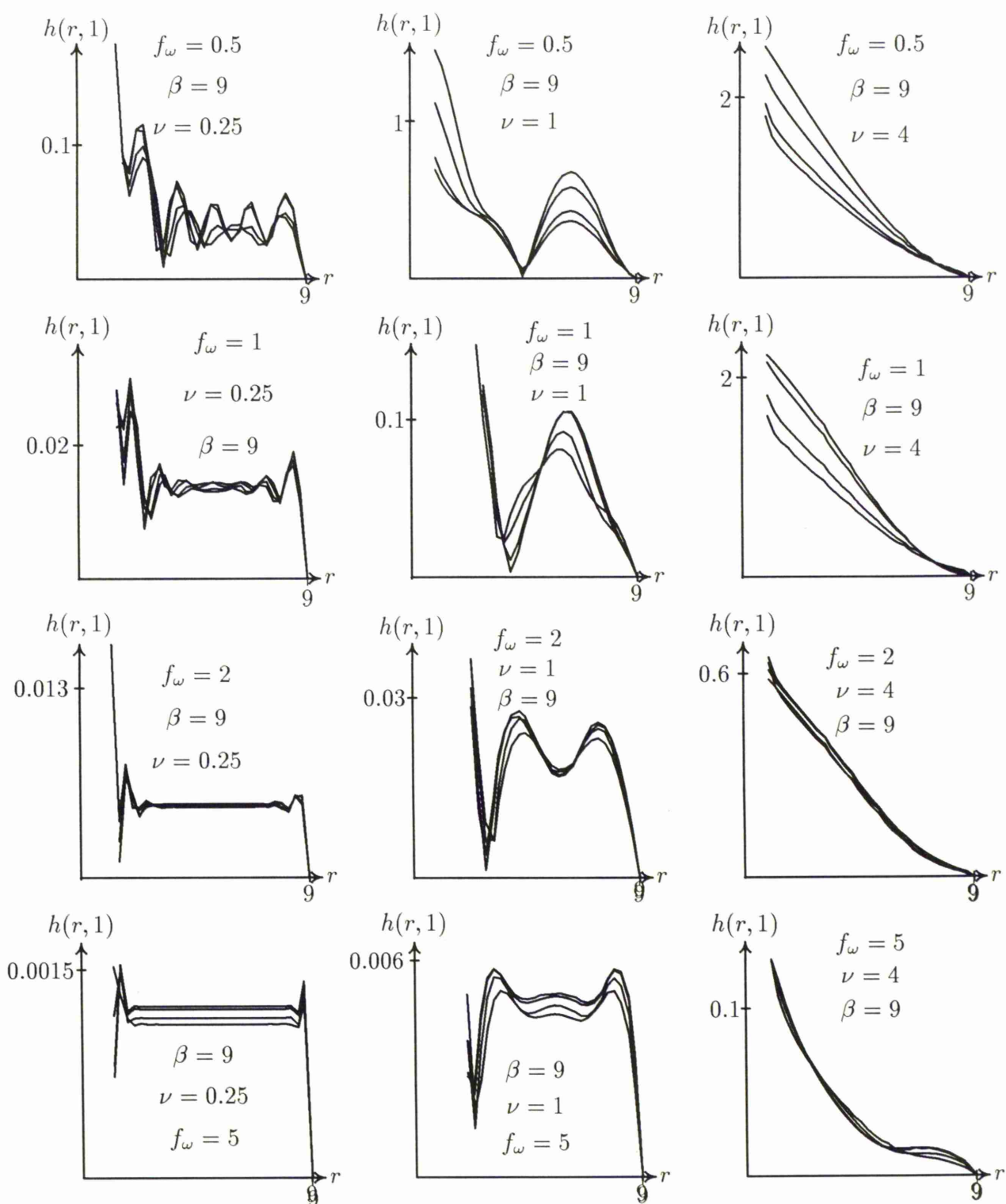


Figure 5.25: Compressible dynamic surface deformation  $h(r, 1)$  for selected values of  $\nu$ ,  $f$  and  $\beta = 9.0$  and for  $\gamma = -1.1, -1.5, -3.0$  and  $-6.75$ .

r	$\beta = 1.5$			$\gamma = -1.1$		
	$\nu = 1/4$	$\nu = 1$	$\nu = 3$	$\nu = 4$	$\nu = 7$	$\nu = 9$
1.00	3.671	1.111	0.955	0.939	0.919	0.914
1.05	3.449	1.007	0.866	0.852	0.834	0.828
1.10	3.114	0.883	0.760	0.747	0.732	0.727
1.15	2.690	0.754	0.649	0.639	0.626	0.622
1.20	2.210	0.626	0.539	0.530	0.520	0.517
1.25	1.709	0.501	0.432	0.425	0.416	0.414
1.30	1.222	0.380	0.328	0.323	0.317	0.315
1.35	0.780	0.267	0.231	0.227	0.223	0.222
1.40	0.413	0.162	0.141	0.139	0.136	0.135
1.45	0.143	0.069	0.061	0.060	0.059	0.059
1.50	0.000	0.000	0.000	0.000	0.000	0.000

r	$\beta = 1.5$			$\gamma = -1.5$		
	$\nu = 1/4$	$\nu = 1$	$\nu = 3$	$\nu = 4$	$\nu = 7$	$\nu = 9$
1.00	3.104	1.080	0.948	0.934	0.916	0.911
1.05	2.860	0.952	0.835	0.823	0.808	0.803
1.10	2.580	0.833	0.731	0.721	0.707	0.703
1.15	2.234	0.715	0.628	0.619	0.607	0.604
1.20	1.846	0.599	0.526	0.518	0.509	0.506
1.25	1.442	0.486	0.427	0.421	0.413	0.411
1.30	1.049	0.377	0.332	0.327	0.322	0.320
1.35	0.692	0.274	0.241	0.238	0.234	0.233
1.40	0.393	0.177	0.157	0.155	0.152	0.152
1.45	0.168	0.089	0.079	0.078	0.077	0.077
1.50	0.000	0.000	0.000	0.000	0.000	0.000

r	$\beta = 1.5$			$\gamma = -3.0$		
	$\nu = 1/4$	$\nu = 1$	$\nu = 3$	$\nu = 4$	$\nu = 7$	$\nu = 9$
1.00	2.517	1.043	0.938	0.927	0.912	0.908
1.05	2.258	0.889	0.799	0.789	0.777	0.773
1.10	2.036	0.778	0.699	0.691	0.680	0.677
1.15	1.770	0.671	0.603	0.596	0.587	0.584
1.20	1.473	0.568	0.510	0.505	0.497	0.495
1.25	1.166	0.468	0.421	0.416	0.410	0.408
1.30	0.867	0.372	0.335	0.331	0.326	0.325
1.35	0.595	0.281	0.253	0.250	0.247	0.246
1.40	0.366	0.194	0.175	0.173	0.170	0.170
1.45	0.188	0.110	0.099	0.098	0.097	0.097
1.50	0.000	0.000	0.000	0.000	0.000	0.000

r	$\beta = 1.5$			$\gamma = -3.0$		
	$\nu = 1/4$	$\nu = 1$	$\nu = 3$	$\nu = 4$	$\nu = 7$	$\nu = 9$
1.00	2.277	1.026	0.933	0.923	0.911	0.907
1.05	2.015	0.862	0.783	0.774	0.763	0.760
1.10	1.817	0.754	0.685	0.677	0.668	0.665
1.15	1.583	0.653	0.593	0.586	0.578	0.576
1.20	1.322	0.555	0.504	0.499	0.492	0.490
1.25	1.053	0.461	0.419	0.414	0.409	0.407
1.30	0.792	0.370	0.336	0.333	0.329	0.327
1.35	0.554	0.284	0.258	0.255	0.252	0.251
1.40	0.352	0.200	0.182	0.181	0.179	0.178
1.45	0.194	0.119	0.108	0.107	0.106	0.106
1.50	0.000	0.000	0.000	0.000	0.000	0.000

Table 5.5: Values of compressible dynamic surface deformation  $h(r,1)$  for  $\beta = 1.5$  and  $f_\omega = 0.5$  and for selected values of  $\nu$  and  $\gamma$ .

r	$\beta = 3.0$			$\gamma = -1.1$		
	$\nu = 1/4$	$\nu = 1$	$\nu = 3$	$\nu = 4$	$\nu = 7$	$\nu = 9$
1.00	1.237	3.285	1.187	1.095	0.997	0.972
1.20	0.940	3.018	1.036	0.953	0.868	0.846
1.40	0.505	2.660	0.874	0.804	0.732	0.713
1.60	0.309	2.246	0.722	0.662	0.603	0.588
1.80	0.116	1.806	0.581	0.533	0.484	0.472
2.00	0.372	1.370	0.451	0.414	0.376	0.367
2.20	0.735	0.962	0.334	0.306	0.279	0.272
2.40	0.808	0.605	0.228	0.209	0.191	0.186
2.60	0.562	0.315	0.134	0.124	0.113	0.111
2.80	0.200	0.108	0.056	0.052	0.048	0.047
3.00	0.000	0.000	0.000	0.000	0.000	0.000

r	$\beta = 3.0$			$\gamma = -1.5$		
	$\nu = 1/4$	$\nu = 1$	$\nu = 3$	$\nu = 4$	$\nu = 7$	$\nu = 9$
1.00	0.956	2.810	1.143	1.066	0.984	0.962
1.20	0.686	2.516	0.963	0.897	0.827	0.809
1.40	0.412	2.212	0.811	0.754	0.695	0.679
1.60	0.323	1.871	0.672	0.624	0.575	0.562
1.80	0.126	1.513	0.545	0.506	0.466	0.456
2.00	0.300	1.158	0.430	0.399	0.367	0.359
2.20	0.618	0.827	0.325	0.302	0.278	0.272
2.40	0.691	0.537	0.230	0.214	0.197	0.193
2.60	0.494	0.300	0.146	0.136	0.125	0.123
2.80	0.189	0.126	0.071	0.066	0.062	0.061
3.00	0.000	0.000	0.000	0.000	0.000	0.000

r	$\beta = 3.0$			$\gamma = -3.0$		
	$\nu = 1/4$	$\nu = 1$	$\nu = 3$	$\nu = 4$	$\nu = 7$	$\nu = 9$
1.00	0.630	2.315	1.093	1.033	0.968	0.950
1.20	0.463	2.002	0.882	0.833	0.779	0.765
1.40	0.367	1.758	0.742	0.699	0.654	0.642
1.60	0.308	1.491	0.618	0.582	0.544	0.534
1.80	0.123	1.213	0.507	0.477	0.446	0.437
2.00	0.192	0.940	0.407	0.382	0.357	0.351
2.20	0.426	0.686	0.315	0.297	0.277	0.272
2.40	0.488	0.462	0.232	0.219	0.204	0.201
2.60	0.362	0.279	0.157	0.148	0.138	0.136
2.80	0.151	0.141	0.088	0.083	0.077	0.076
3.00	0.000	0.000	0.000	0.000	0.000	0.000

r	$\beta = 3.0$			$\gamma = -6.75$		
	$\nu = 1/4$	$\nu = 1$	$\nu = 3$	$\nu = 4$	$\nu = 7$	$\nu = 9$
1.00	0.540	2.113	1.070	1.018	0.960	0.944
1.20	0.425	1.795	0.847	0.805	0.758	0.746
1.40	0.366	1.574	0.712	0.676	0.636	0.625
1.60	0.300	1.337	0.595	0.564	0.531	0.522
1.80	0.122	1.092	0.491	0.465	0.437	0.430
2.00	0.147	0.851	0.397	0.376	0.353	0.347
2.20	0.349	0.627	0.311	0.295	0.277	0.272
2.40	0.406	0.431	0.234	0.221	0.208	0.204
2.60	0.307	0.270	0.162	0.154	0.144	0.142
2.80	0.134	0.147	0.095	0.090	0.085	0.083
3.00	0.000	0.000	0.000	0.000	0.000	0.000

Table 5.6: Values of compressible dynamic surface deformation  $h(r,1)$  for  $\beta = 3.0$  and  $f_\omega = 0.5$  and for selected values of  $\nu$  and  $\gamma$ .

r	$\beta = 5.0$			$\gamma = -1.1$		
	$\nu = 1/4$	$\nu = 1$	$\nu = 3$	$\nu = 4$	$\nu = 7$	$\nu = 9$
1.00	0.522	2.400	1.701	1.380	1.111	1.053
1.40	0.378	2.483	1.465	1.169	0.930	0.880
1.80	0.087	2.412	1.228	0.966	0.759	0.718
2.20	0.114	2.169	1.005	0.784	0.611	0.577
2.60	0.207	1.790	0.798	0.621	0.482	0.455
3.00	0.108	1.333	0.607	0.474	0.369	0.348
3.40	0.034	0.869	0.435	0.344	0.269	0.254
3.80	0.123	0.464	0.285	0.230	0.182	0.172
4.20	0.158	0.173	0.160	0.133	0.107	0.101
4.60	0.059	0.030	0.062	0.054	0.044	0.042
5.00	0.000	0.000	0.000	0.000	0.000	0.000

r	$\beta = 5.0$			$\gamma = -1.5$		
	$\nu = 1/4$	$\nu = 1$	$\nu = 3$	$\nu = 4$	$\nu = 7$	$\nu = 9$
1.00	0.555	2.703	1.564	1.302	1.080	1.031
1.40	0.395	2.747	1.297	1.059	0.868	0.828
1.80	0.094	2.632	1.083	0.872	0.707	0.673
2.20	0.105	2.344	0.889	0.710	0.571	0.543
2.60	0.247	1.925	0.711	0.567	0.454	0.432
3.00	0.148	1.435	0.547	0.440	0.353	0.335
3.40	0.027	0.945	0.401	0.326	0.263	0.250
3.80	0.137	0.519	0.272	0.226	0.185	0.175
4.20	0.207	0.209	0.164	0.140	0.116	0.110
4.60	0.083	0.042	0.076	0.067	0.056	0.054
5.00	0.000	0.000	0.000	0.000	0.000	0.000

r	$\beta = 5.0$			$\gamma = -3.0$		
	$\nu = 1/4$	$\nu = 1$	$\nu = 3$	$\nu = 4$	$\nu = 7$	$\nu = 9$
1.00	0.587	3.158	1.413	1.214	1.044	1.005
1.40	0.376	3.125	1.117	0.941	0.799	0.769
1.80	0.103	2.945	0.931	0.773	0.649	0.624
2.20	0.113	2.591	0.767	0.632	0.528	0.506
2.60	0.269	2.113	0.618	0.510	0.425	0.407
3.00	0.160	1.577	0.483	0.402	0.335	0.321
3.40	0.041	1.051	0.363	0.306	0.257	0.246
3.80	0.140	0.596	0.257	0.221	0.187	0.179
4.20	0.232	0.262	0.166	0.147	0.126	0.120
4.60	0.113	0.075	0.090	0.081	0.070	0.067
5.00	0.000	0.000	0.000	0.000	0.000	0.000

r	$\beta = 5.0$			$\gamma = -6.75$		
	$\nu = 1/4$	$\nu = 1$	$\nu = 3$	$\nu = 4$	$\nu = 7$	$\nu = 9$
1.00	0.560	3.367	1.348	1.175	1.027	0.993
1.40	0.347	3.286	1.041	0.890	0.769	0.743
1.80	0.107	3.074	0.866	0.730	0.625	0.603
2.20	0.110	2.689	0.716	0.599	0.509	0.491
2.60	0.251	2.187	0.579	0.486	0.412	0.397
3.00	0.149	1.633	0.456	0.386	0.328	0.315
3.40	0.050	1.093	0.346	0.297	0.254	0.244
3.80	0.128	0.629	0.250	0.219	0.188	0.181
4.20	0.217	0.288	0.167	0.149	0.130	0.125
4.60	0.114	0.095	0.096	0.087	0.075	0.072
5.00	0.000	0.000	0.000	0.000	0.000	0.000

Table 5.7: Values of compressible dynamic surface deformation  $h(r,1)$  for  $\beta = 5.0$  and  $f_\omega = 0.5$  and for selected values of  $\nu$  and  $\gamma$ .

r	$\beta = 9.0$			$\gamma = -1.1$		
	$\nu = 1/4$	$\nu = 1$	$\nu = 3$	$\nu = 4$	$\nu = 7$	$\nu = 9$
1.00	0.363	1.454	5.196	2.551	1.415	1.244
1.80	0.086	1.019	4.742	2.202	1.144	0.991
2.60	0.109	0.534	4.161	1.862	0.921	0.788
3.40	0.025	0.358	3.490	1.528	0.735	0.624
4.20	0.054	0.135	2.774	1.205	0.575	0.486
5.00	0.041	0.260	2.064	0.902	0.435	0.368
5.80	0.035	0.600	1.406	0.627	0.312	0.265
6.60	0.051	0.673	0.841	0.392	0.206	0.177
7.40	0.025	0.466	0.404	0.204	0.117	0.102
8.20	0.061	0.162	0.117	0.070	0.046	0.041
9.00	0.000	0.000	0.000	0.000	0.000	0.000

r	$\beta = 9.0$			$\gamma = -1.1$		
	$\nu = 1/4$	$\nu = 1$	$\nu = 3$	$\nu = 4$	$\nu = 7$	$\nu = 9$
1.00	0.353	1.121	4.250	2.239	1.331	1.189
1.80	0.091	0.730	3.762	1.861	1.027	0.904
2.60	0.114	0.443	3.284	1.567	0.824	0.716
3.40	0.009	0.352	2.749	1.287	0.660	0.569
4.20	0.062	0.128	2.189	1.019	0.520	0.447
5.00	0.035	0.230	1.637	0.769	0.398	0.343
5.80	0.038	0.517	1.129	0.543	0.291	0.253
6.60	0.051	0.576	0.693	0.349	0.199	0.175
7.40	0.024	0.404	0.354	0.194	0.121	0.108
8.20	0.063	0.150	0.127	0.081	0.057	0.052
9.00	0.000	0.000	0.000	0.000	0.000	0.000

r	$\beta = 9.0$			$\gamma = -1.1$		
	$\nu = 1/4$	$\nu = 1$	$\nu = 3$	$\nu = 4$	$\nu = 7$	$\nu = 9$
1.00	0.321	0.776	3.249	1.912	1.237	1.128
1.80	0.093	0.524	2.758	1.513	0.903	0.811
2.60	0.098	0.410	2.392	1.268	0.721	0.641
3.40	0.011	0.320	1.999	1.043	0.580	0.512
4.20	0.054	0.111	1.595	0.830	0.461	0.406
5.00	0.023	0.181	1.201	0.633	0.359	0.317
5.80	0.036	0.385	0.841	0.456	0.269	0.240
6.60	0.037	0.424	0.533	0.304	0.192	0.173
7.40	0.025	0.302	0.293	0.182	0.125	0.114
8.20	0.048	0.120	0.130	0.091	0.068	0.063
9.00	0.000	0.000	0.000	0.000	0.000	0.000

r	$\beta = 9.0$			$\gamma = -1.1$		
	$\nu = 1/4$	$\nu = 1$	$\nu = 3$	$\nu = 4$	$\nu = 7$	$\nu = 9$
1.00	0.309	0.688	2.866	1.778	1.196	1.101
1.80	0.091	0.499	2.380	1.371	0.850	0.772
2.60	0.090	0.411	2.059	1.147	0.679	0.610
3.40	0.020	0.307	1.719	0.944	0.547	0.488
4.20	0.049	0.114	1.373	0.753	0.437	0.390
5.00	0.025	0.160	1.038	0.577	0.342	0.306
5.80	0.034	0.329	0.732	0.420	0.260	0.234
6.60	0.035	0.360	0.471	0.285	0.189	0.172
7.40	0.025	0.258	0.268	0.177	0.127	0.117
8.20	0.045	0.107	0.129	0.095	0.073	0.068
9.00	0.000	0.000	0.000	0.000	0.000	0.000

Table 5.8: Values of compressible dynamic surface deformation  $h(r,1)$  for  $\beta = 9.0$  and  $f_\omega = 0.5$  and for selected values of  $\nu$  and  $\gamma$ .

r	$\beta = 1.5$			$\gamma = -1.1$		
	$\nu = 1/4$	$\nu = 1$	$\nu = 3$	$\nu = 4$	$\nu = 7$	$\nu = 9$
1.00	2.636	0.889	0.756	0.743	0.727	0.722
1.05	2.508	0.806	0.687	0.675	0.661	0.657
1.10	2.289	0.706	0.602	0.592	0.580	0.576
1.15	1.982	0.602	0.514	0.505	0.495	0.492
1.20	1.617	0.498	0.426	0.419	0.411	0.408
1.25	1.227	0.396	0.340	0.334	0.328	0.326
1.30	0.849	0.298	0.257	0.253	0.249	0.248
1.35	0.515	0.206	0.179	0.177	0.174	0.173
1.40	0.253	0.122	0.108	0.106	0.105	0.104
1.45	0.085	0.050	0.045	0.045	0.044	0.044
1.50	0.000	0.000	0.000	0.000	0.000	0.000

r	$\beta = 1.5$			$\gamma = -1.5$		
	$\nu = 1/4$	$\nu = 1$	$\nu = 3$	$\nu = 4$	$\nu = 7$	$\nu = 9$
1.00	2.748	0.867	0.751	0.739	0.725	0.721
1.05	2.572	0.768	0.666	0.656	0.643	0.639
1.10	2.344	0.671	0.582	0.574	0.563	0.560
1.15	2.034	0.574	0.499	0.491	0.482	0.480
1.20	1.668	0.479	0.416	0.410	0.403	0.401
1.25	1.277	0.385	0.336	0.332	0.326	0.325
1.30	0.897	0.296	0.259	0.256	0.252	0.251
1.35	0.559	0.212	0.187	0.185	0.182	0.181
1.40	0.287	0.134	0.119	0.118	0.116	0.116
1.45	0.100	0.064	0.058	0.057	0.057	0.057
1.50	0.000	0.000	0.000	0.000	0.000	0.000

r	$\beta = 1.5$			$\gamma = -3.0$		
	$\nu = 1/4$	$\nu = 1$	$\nu = 3$	$\nu = 4$	$\nu = 7$	$\nu = 9$
1.00	2.415	0.834	0.743	0.733	0.721	0.718
1.05	2.196	0.712	0.634	0.626	0.616	0.613
1.10	1.997	0.622	0.554	0.547	0.539	0.536
1.15	1.739	0.536	0.477	0.472	0.464	0.462
1.20	1.440	0.452	0.403	0.398	0.393	0.391
1.25	1.122	0.371	0.332	0.328	0.323	0.322
1.30	0.813	0.293	0.263	0.260	0.257	0.256
1.35	0.535	0.220	0.197	0.195	0.193	0.193
1.40	0.309	0.150	0.135	0.134	0.133	0.132
1.45	0.145	0.083	0.076	0.075	0.075	0.075
1.50	0.000	0.000	0.000	0.000	0.000	0.000

r	$\beta = 1.5$			$\gamma = -6.75$		
	$\nu = 1/4$	$\nu = 1$	$\nu = 3$	$\nu = 4$	$\nu = 7$	$\nu = 9$
1.00	2.104	0.818	0.739	0.730	0.720	0.717
1.05	1.885	0.687	0.619	0.612	0.604	0.601
1.10	1.713	0.600	0.541	0.535	0.528	0.526
1.15	1.495	0.519	0.468	0.463	0.457	0.455
1.20	1.244	0.441	0.398	0.393	0.388	0.387
1.25	0.979	0.365	0.330	0.326	0.322	0.321
1.30	0.721	0.293	0.265	0.262	0.259	0.258
1.35	0.490	0.224	0.203	0.201	0.198	0.198
1.40	0.300	0.157	0.143	0.142	0.140	0.140
1.45	0.159	0.093	0.085	0.084	0.083	0.083
1.50	0.000	0.000	0.000	0.000	0.000	0.000

Table 5.9: Values of compressible dynamic surface deformation  $h(r,1)$  for  $\beta = 1.5$  and  $f_\omega = 1.0$  and for selected values of  $\nu$  and  $\gamma$ .

r	$\beta = 3.0$			$\gamma = -1.1$		
	$\nu = 1/4$	$\nu = 1$	$\nu = 3$	$\nu = 4$	$\nu = 7$	$\nu = 9$
1.00	0.311	2.585	0.957	0.875	0.791	0.770
1.20	0.243	2.423	0.838	0.764	0.691	0.673
1.40	0.120	2.171	0.707	0.644	0.581	0.566
1.60	0.023	1.846	0.583	0.529	0.478	0.466
1.80	0.072	1.481	0.467	0.424	0.383	0.373
2.00	0.088	1.108	0.361	0.328	0.297	0.289
2.20	0.107	0.756	0.264	0.241	0.218	0.213
2.40	0.102	0.452	0.178	0.162	0.148	0.145
2.60	0.083	0.217	0.102	0.094	0.086	0.085
2.80	0.055	0.068	0.040	0.038	0.035	0.034
3.00	0.000	0.000	0.000	0.000	0.000	0.000

r	$\beta = 3.0$			$\gamma = -1.5$		
	$\nu = 1/4$	$\nu = 1$	$\nu = 3$	$\nu = 4$	$\nu = 7$	$\nu = 9$
1.00	0.307	2.622	0.926	0.855	0.782	0.763
1.20	0.247	2.406	0.786	0.724	0.662	0.646
1.40	0.131	2.150	0.662	0.608	0.556	0.543
1.60	0.020	1.831	0.547	0.502	0.459	0.448
1.80	0.058	1.476	0.442	0.405	0.370	0.362
2.00	0.086	1.113	0.346	0.317	0.290	0.284
2.20	0.116	0.771	0.259	0.238	0.218	0.213
2.40	0.109	0.474	0.180	0.166	0.153	0.150
2.60	0.077	0.241	0.111	0.103	0.095	0.093
2.80	0.047	0.083	0.051	0.048	0.045	0.044
3.00	0.000	0.000	0.000	0.000	0.000	0.000

r	$\beta = 3.0$			$\gamma = -3.0$		
	$\nu = 1/4$	$\nu = 1$	$\nu = 3$	$\nu = 4$	$\nu = 7$	$\nu = 9$
1.00	0.311	2.243	0.880	0.825	0.768	0.753
1.20	0.251	1.981	0.713	0.667	0.620	0.608
1.40	0.140	1.763	0.599	0.559	0.519	0.509
1.60	0.033	1.504	0.498	0.465	0.431	0.423
1.80	0.044	1.221	0.408	0.380	0.353	0.346
2.00	0.087	0.935	0.326	0.303	0.282	0.276
2.20	0.127	0.667	0.251	0.234	0.217	0.213
2.40	0.124	0.433	0.183	0.171	0.160	0.157
2.60	0.084	0.246	0.122	0.115	0.107	0.105
2.80	0.043	0.114	0.067	0.063	0.059	0.058
3.00	0.000	0.000	0.000	0.000	0.000	0.000

r	$\beta = 3.0$			$\gamma = -6.75$		
	$\nu = 1/4$	$\nu = 1$	$\nu = 3$	$\nu = 4$	$\nu = 7$	$\nu = 9$
1.00	0.311	1.960	0.857	0.810	0.761	0.748
1.20	0.247	1.696	0.680	0.641	0.601	0.590
1.40	0.139	1.506	0.571	0.538	0.504	0.494
1.60	0.040	1.286	0.477	0.449	0.420	0.412
1.80	0.042	1.049	0.393	0.370	0.345	0.339
2.00	0.087	0.810	0.317	0.298	0.278	0.274
2.20	0.127	0.587	0.248	0.233	0.218	0.214
2.40	0.127	0.392	0.185	0.174	0.163	0.160
2.60	0.088	0.237	0.128	0.121	0.113	0.111
2.80	0.044	0.124	0.074	0.070	0.066	0.065
3.00	0.000	0.000	0.000	0.000	0.000	0.000

Table 5.10: Values of compressible dynamic surface deformation  $h(r,1)$  for  $\beta = 3.0$  and  $f_\omega = 1.0$  and for selected values of  $\nu$  and  $\gamma$ .

r	$\beta = 5.0$			$\gamma = -1.1$		
	$\nu = 1/4$	$\nu = 1$	$\nu = 3$	$\nu = 4$	$\nu = 7$	$\nu = 9$
1.00	0.200	0.542	1.480	1.142	0.890	0.839
1.40	0.068	0.502	1.290	0.974	0.748	0.704
1.80	0.040	0.445	1.089	0.807	0.610	0.574
2.20	0.049	0.365	0.894	0.655	0.490	0.460
2.60	0.027	0.261	0.707	0.517	0.385	0.362
3.00	0.037	0.144	0.534	0.393	0.293	0.275
3.40	0.037	0.039	0.377	0.282	0.212	0.199
3.80	0.031	0.038	0.241	0.185	0.142	0.133
4.20	0.038	0.061	0.129	0.103	0.081	0.077
4.60	0.042	0.042	0.045	0.038	0.032	0.030
5.00	0.000	0.000	0.000	0.000	0.000	0.000

r	$\beta = 5.0$			$\gamma = -1.5$		
	$\nu = 1/4$	$\nu = 1$	$\nu = 3$	$\nu = 4$	$\nu = 7$	$\nu = 9$
1.00	0.197	0.523	1.376	1.085	0.868	0.823
1.40	0.073	0.488	1.161	0.894	0.704	0.667
1.80	0.035	0.451	0.976	0.738	0.573	0.542
2.20	0.053	0.389	0.803	0.601	0.462	0.436
2.60	0.025	0.297	0.640	0.478	0.366	0.345
3.00	0.036	0.187	0.488	0.367	0.282	0.266
3.40	0.039	0.081	0.351	0.269	0.208	0.197
3.80	0.028	0.014	0.232	0.182	0.144	0.136
4.20	0.040	0.040	0.132	0.108	0.088	0.083
4.60	0.041	0.035	0.056	0.048	0.040	0.039
5.00	0.000	0.000	0.000	0.000	0.000	0.000

r	$\beta = 5.0$			$\gamma = -3.0$		
	$\nu = 1/4$	$\nu = 1$	$\nu = 3$	$\nu = 4$	$\nu = 7$	$\nu = 9$
1.00	0.189	0.509	1.214	0.999	0.835	0.800
1.40	0.075	0.483	0.971	0.779	0.641	0.614
1.80	0.026	0.462	0.813	0.642	0.521	0.498
2.20	0.053	0.411	0.672	0.525	0.423	0.403
2.60	0.027	0.327	0.541	0.422	0.339	0.323
3.00	0.033	0.222	0.420	0.331	0.267	0.254
3.40	0.040	0.117	0.311	0.250	0.203	0.194
3.80	0.026	0.034	0.216	0.178	0.147	0.140
4.20	0.041	0.017	0.137	0.116	0.097	0.093
4.60	0.040	0.024	0.071	0.062	0.053	0.051
5.00	0.000	0.000	0.000	0.000	0.000	0.000

r	$\beta = 5.0$			$\gamma = -6.75$		
	$\nu = 1/4$	$\nu = 1$	$\nu = 3$	$\nu = 4$	$\nu = 7$	$\nu = 9$
1.00	0.183	0.512	1.138	0.959	0.819	0.789
1.40	0.074	0.487	0.887	0.729	0.614	0.591
1.80	0.021	0.464	0.742	0.600	0.499	0.479
2.20	0.050	0.410	0.614	0.493	0.407	0.390
2.60	0.029	0.326	0.497	0.399	0.329	0.315
3.00	0.031	0.224	0.390	0.316	0.261	0.250
3.40	0.037	0.124	0.294	0.242	0.202	0.193
3.80	0.026	0.046	0.210	0.177	0.149	0.143
4.20	0.039	0.020	0.138	0.120	0.102	0.098
4.60	0.038	0.021	0.078	0.069	0.059	0.057
5.00	0.000	0.000	0.000	0.000	0.000	0.000

Table 5.11: Values of compressible dynamic surface deformation  $h(r,1)$  for  $\beta = 5$  and  $f_\omega = 1.0$  and for selected values of  $\nu$  and  $\gamma$ .

r	$\beta = 9.0$			$\gamma = -1.1$		
	$\nu = 1/4$	$\nu = 1$	$\nu = 3$	$\nu = 4$	$\nu = 7$	$\nu = 9$
1.00	0.135	0.431	1.399	2.224	1.181	1.012
1.80	0.023	0.302	1.347	1.986	0.966	0.813
2.60	0.008	0.148	1.237	1.720	0.782	0.648
3.40	0.014	0.026	1.068	1.431	0.625	0.513
4.20	0.014	0.052	0.858	1.132	0.488	0.399
5.00	0.014	0.067	0.631	0.840	0.367	0.300
5.80	0.014	0.081	0.413	0.571	0.260	0.214
6.60	0.014	0.069	0.228	0.342	0.168	0.141
7.40	0.015	0.046	0.096	0.165	0.092	0.079
8.20	0.015	0.033	0.031	0.049	0.033	0.030
9.00	0.000	0.000	0.000	0.000	0.000	0.000

r	$\beta = 9.0$			$\gamma = -1.5$		
	$\nu = 1/4$	$\nu = 1$	$\nu = 3$	$\nu = 4$	$\nu = 7$	$\nu = 9$
1.00	0.133	0.423	1.546	2.151	1.118	0.973
1.80	0.022	0.305	1.457	1.861	0.879	0.750
2.60	0.007	0.162	1.335	1.605	0.709	0.596
3.40	0.014	0.039	1.153	1.336	0.568	0.473
4.20	0.014	0.039	0.928	1.061	0.446	0.370
5.00	0.014	0.064	0.688	0.793	0.339	0.282
5.80	0.013	0.091	0.457	0.547	0.245	0.206
6.60	0.014	0.081	0.259	0.337	0.164	0.140
7.40	0.015	0.045	0.115	0.172	0.096	0.083
8.20	0.015	0.027	0.032	0.060	0.041	0.037
9.00	0.000	0.000	0.000	0.000	0.000	0.000

r	$\beta = 9.0$			$\gamma = -3.0$		
	$\nu = 1/4$	$\nu = 1$	$\nu = 3$	$\nu = 4$	$\nu = 7$	$\nu = 9$
1.00	0.126	0.419	1.689	1.810	1.024	0.915
1.80	0.017	0.304	1.521	1.481	0.756	0.663
2.60	0.010	0.168	1.375	1.267	0.607	0.525
3.40	0.015	0.047	1.178	1.054	0.489	0.419
4.20	0.013	0.022	0.949	0.841	0.388	0.332
5.00	0.013	0.062	0.709	0.637	0.300	0.258
5.80	0.013	0.100	0.482	0.451	0.224	0.194
6.60	0.013	0.099	0.288	0.291	0.157	0.138
7.40	0.014	0.060	0.143	0.166	0.101	0.090
8.20	0.016	0.026	0.054	0.077	0.053	0.048
9.00	0.000	0.000	0.000	0.000	0.000	0.000

r	$\beta = 9.0$			$\gamma = -6.75$		
	$\nu = 1/4$	$\nu = 1$	$\nu = 3$	$\nu = 4$	$\nu = 7$	$\nu = 9$
1.00	0.122	0.416	1.650	1.615	0.981	0.888
1.80	0.014	0.296	1.446	1.282	0.703	0.625
2.60	0.012	0.162	1.295	1.092	0.564	0.495
3.40	0.015	0.048	1.105	0.908	0.455	0.397
4.20	0.013	0.016	0.889	0.727	0.364	0.316
5.00	0.013	0.061	0.667	0.554	0.284	0.248
5.80	0.013	0.100	0.459	0.398	0.215	0.189
6.60	0.012	0.101	0.282	0.264	0.154	0.138
7.40	0.014	0.065	0.150	0.158	0.103	0.093
8.20	0.015	0.029	0.067	0.082	0.059	0.054
9.00	0.000	0.000	0.000	0.000	0.000	0.000

Table 5.12: Values of compressible dynamic surface deformation  $h(r,1)$  for  $\beta = 5$  and  $f_\omega = 1.0$  and for different values of  $\nu$  and  $\gamma$ .

r	$\beta = 1.5$			$\gamma = -1.1$		
	$\nu = 1/4$	$\nu = 1$	$\nu = 3$	$\nu = 4$	$\nu = 7$	$\nu = 9$
1.00	0.523	0.569	0.479	0.470	0.460	0.457
1.05	0.495	0.516	0.436	0.429	0.420	0.417
1.10	0.449	0.452	0.382	0.376	0.368	0.366
1.15	0.386	0.384	0.326	0.320	0.314	0.312
1.20	0.312	0.317	0.269	0.265	0.260	0.259
1.25	0.235	0.251	0.214	0.211	0.207	0.206
1.30	0.166	0.187	0.161	0.159	0.156	0.156
1.35	0.114	0.128	0.111	0.110	0.108	0.108
1.40	0.078	0.075	0.066	0.065	0.064	0.064
1.45	0.048	0.029	0.026	0.026	0.026	0.026
1.50	0.000	0.000	0.000	0.000	0.000	0.000

r	$\beta = 1.5$			$\gamma = -1.5$		
	$\nu = 1/4$	$\nu = 1$	$\nu = 3$	$\nu = 4$	$\nu = 7$	$\nu = 9$
1.00	0.546	0.561	0.477	0.469	0.459	0.456
1.05	0.513	0.501	0.428	0.421	0.413	0.410
1.10	0.467	0.438	0.374	0.368	0.361	0.359
1.15	0.403	0.373	0.319	0.314	0.309	0.307
1.20	0.326	0.308	0.265	0.261	0.257	0.255
1.25	0.245	0.245	0.212	0.209	0.206	0.205
1.30	0.171	0.185	0.161	0.160	0.157	0.157
1.35	0.112	0.129	0.114	0.113	0.112	0.111
1.40	0.072	0.077	0.070	0.070	0.069	0.069
1.45	0.041	0.033	0.031	0.031	0.031	0.032
1.50	0.000	0.000	0.000	0.000	0.000	0.000

r	$\beta = 1.5$			$\gamma = -3.0$		
	$\nu = 1/4$	$\nu = 1$	$\nu = 3$	$\nu = 4$	$\nu = 7$	$\nu = 9$
1.00	0.588	0.538	0.472	0.465	0.457	0.455
1.05	0.537	0.461	0.406	0.400	0.394	0.392
1.10	0.490	0.402	0.354	0.350	0.344	0.343
1.15	0.425	0.344	0.304	0.300	0.296	0.295
1.20	0.348	0.288	0.255	0.252	0.249	0.248
1.25	0.265	0.234	0.208	0.206	0.204	0.203
1.30	0.187	0.183	0.164	0.162	0.160	0.160
1.35	0.121	0.134	0.121	0.120	0.119	0.119
1.40	0.071	0.088	0.081	0.081	0.081	0.081
1.45	0.034	0.047	0.044	0.044	0.044	0.044
1.50	0.000	0.000	0.000	0.000	0.000	0.000

r	$\beta = 1.5$			$\gamma = -6.75$		
	$\nu = 1/4$	$\nu = 1$	$\nu = 3$	$\nu = 4$	$\nu = 7$	$\nu = 9$
1.00	0.586	0.523	0.468	0.462	0.455	0.453
1.05	0.524	0.438	0.392	0.388	0.382	0.381
1.10	0.478	0.382	0.342	0.339	0.334	0.333
1.15	0.416	0.329	0.295	0.292	0.289	0.288
1.20	0.343	0.278	0.250	0.248	0.245	0.244
1.25	0.267	0.230	0.207	0.205	0.203	0.202
1.30	0.195	0.183	0.165	0.164	0.163	0.162
1.35	0.132	0.138	0.126	0.125	0.124	0.124
1.40	0.082	0.096	0.088	0.088	0.087	0.087
1.45	0.042	0.055	0.052	0.052	0.051	0.051
1.50	0.000	0.000	0.000	0.000	0.000	0.000

Table 5.13: Values of compressible dynamic surface deformation  $h(r,1)$  for  $\beta = 1.5$  and  $f_w = 2.0$  and for selected values of  $\nu$  and  $\gamma$ .

r	$\beta = 3.0$			$\gamma = -1.1$		
	$\nu = 1/4$	$\nu = 1$	$\nu = 3$	$\nu = 4$	$\nu = 7$	$\nu = 9$
1.00	0.119	0.548	0.616	0.559	0.502	0.488
1.20	0.062	0.510	0.541	0.490	0.440	0.428
1.40	0.016	0.454	0.457	0.412	0.370	0.360
1.60	0.030	0.383	0.376	0.339	0.304	0.296
1.80	0.036	0.302	0.300	0.270	0.243	0.236
2.00	0.030	0.221	0.231	0.208	0.187	0.182
2.20	0.026	0.148	0.167	0.151	0.137	0.134
2.40	0.031	0.093	0.111	0.101	0.092	0.090
2.60	0.037	0.059	0.063	0.057	0.053	0.052
2.80	0.029	0.036	0.024	0.022	0.020	0.020
3.00	0.000	0.000	0.000	0.000	0.000	0.000

r	$\beta = 3.0$			$\gamma = -1.5$		
	$\nu = 1/4$	$\nu = 1$	$\nu = 3$	$\nu = 4$	$\nu = 7$	$\nu = 9$
1.00	0.119	0.572	0.605	0.552	0.499	0.486
1.20	0.063	0.528	0.521	0.474	0.429	0.418
1.40	0.016	0.473	0.439	0.398	0.360	0.350
1.60	0.029	0.401	0.361	0.327	0.296	0.288
1.80	0.036	0.318	0.290	0.262	0.237	0.231
2.00	0.030	0.233	0.224	0.203	0.184	0.180
2.20	0.025	0.156	0.164	0.149	0.136	0.133
2.40	0.031	0.095	0.111	0.101	0.093	0.092
2.60	0.037	0.055	0.064	0.060	0.055	0.055
2.80	0.028	0.030	0.026	0.025	0.024	0.024
3.00	0.000	0.000	0.000	0.000	0.000	0.000

r	$\beta = 3.0$			$\gamma = -3.0$		
	$\nu = 1/4$	$\nu = 1$	$\nu = 3$	$\nu = 4$	$\nu = 7$	$\nu = 9$
1.00	0.116	0.615	0.573	0.531	0.489	0.479
1.20	0.064	0.547	0.468	0.433	0.399	0.391
1.40	0.019	0.490	0.393	0.362	0.333	0.327
1.60	0.025	0.418	0.325	0.299	0.276	0.270
1.80	0.035	0.335	0.264	0.243	0.224	0.230
2.00	0.030	0.251	0.208	0.192	0.177	0.174
2.20	0.025	0.172	0.158	0.146	0.135	0.133
2.40	0.031	0.107	0.112	0.104	0.098	0.096
2.60	0.036	0.059	0.072	0.068	0.064	0.063
2.80	0.026	0.025	0.037	0.035	0.034	0.033
3.00	0.000	0.000	0.000	0.000	0.000	0.000

r	$\beta = 3.0$			$\gamma = -6.75$		
	$\nu = 1/4$	$\nu = 1$	$\nu = 3$	$\nu = 4$	$\nu = 7$	$\nu = 9$
1.00	0.112	0.608	0.551	0.517	0.483	0.474
1.20	0.062	0.527	0.437	0.409	0.381	0.374
1.40	0.022	0.470	0.367	0.343	0.319	0.313
1.60	0.024	0.401	0.306	0.285	0.265	0.260
1.80	0.033	0.324	0.251	0.234	0.217	0.214
2.00	0.030	0.247	0.201	0.188	0.174	0.171
2.20	0.027	0.175	0.156	0.146	0.136	0.134
2.40	0.031	0.114	0.115	0.108	0.101	0.099
2.60	0.034	0.068	0.078	0.073	0.069	0.068
2.80	0.025	0.034	0.044	0.042	0.040	0.039
3.00	0.000	0.000	0.000	0.000	0.000	0.000

Table 5.14: Values of compressible dynamic surface deformation  $h(r,1)$  for  $\beta = 3.0$  and  $f_w = 2.0$  and for selected values of  $\nu$  and  $\gamma$ .



r	$\beta = 5.0$			$\gamma = -1.1$		
	$\nu = 1/4$	$\nu = 1$	$\nu = 3$	$\nu = 4$	$\nu = 7$	$\nu = 9$
1.00	0.072	0.255	0.865	0.737	0.569	0.534
1.40	0.004	0.182	0.760	0.633	0.481	0.451
1.80	0.015	0.113	0.644	0.526	0.393	0.367
2.20	0.011	0.061	0.529	0.426	0.315	0.294
2.60	0.012	0.029	0.417	0.335	0.247	0.230
3.00	0.012	0.039	0.312	0.253	0.187	0.174
3.40	0.012	0.061	0.218	0.180	0.134	0.125
3.80	0.012	0.068	0.137	0.116	0.088	0.083
4.20	0.011	0.056	0.074	0.064	0.050	0.047
4.60	0.015	0.030	0.031	0.024	0.019	0.018
5.00	0.000	0.000	0.000	0.000	0.000	0.000

r	$\beta = 5.0$			$\gamma = -1.5$		
	$\nu = 1/4$	$\nu = 1$	$\nu = 3$	$\nu = 4$	$\nu = 7$	$\nu = 9$
1.00	0.073	0.252	0.870	0.722	0.562	0.529
1.40	0.006	0.177	0.750	0.608	0.464	0.436
1.80	0.016	0.113	0.635	0.504	0.378	0.354
2.20	0.011	0.065	0.522	0.409	0.303	0.284
2.60	0.013	0.030	0.413	0.323	0.239	0.223
3.00	0.012	0.036	0.311	0.245	0.182	0.170
3.40	0.012	0.060	0.218	0.175	0.132	0.124
3.80	0.013	0.068	0.138	0.115	0.089	0.084
4.20	0.011	0.056	0.074	0.064	0.051	0.049
4.60	0.015	0.029	0.027	0.024	0.021	0.020
5.00	0.000	0.000	0.000	0.000	0.000	0.000

r	$\beta = 5.0$			$\gamma = -3.0$		
	$\nu = 1/4$	$\nu = 1$	$\nu = 3$	$\nu = 4$	$\nu = 7$	$\nu = 9$
1.00	0.071	0.236	0.800	0.665	0.539	0.513
1.40	0.009	0.162	0.652	0.527	0.419	0.398
1.80	0.015	0.111	0.549	0.434	0.340	0.322
2.20	0.011	0.070	0.453	0.354	0.274	0.260
2.60	0.012	0.035	0.363	0.283	0.218	0.207
3.00	0.012	0.028	0.278	0.219	0.170	0.161
3.40	0.012	0.047	0.201	0.162	0.127	0.121
3.80	0.012	0.057	0.134	0.112	0.090	0.086
4.20	0.011	0.048	0.079	0.069	0.058	0.055
4.60	0.015	0.027	0.036	0.034	0.030	0.029
5.00	0.000	0.000	0.000	0.000	0.000	0.000

r	$\beta = 5.0$			$\gamma = -6.75$		
	$\nu = 1/4$	$\nu = 1$	$\nu = 3$	$\nu = 4$	$\nu = 7$	$\nu = 9$
1.00	0.069	0.225	0.727	0.624	0.524	0.503
1.40	0.010	0.154	0.570	0.476	0.393	0.377
1.80	0.014	0.109	0.479	0.392	0.319	0.305
2.20	0.012	0.072	0.397	0.322	0.259	0.247
2.60	0.012	0.040	0.320	0.260	0.209	0.199
3.00	0.012	0.027	0.249	0.204	0.165	0.157
3.40	0.012	0.040	0.185	0.155	0.127	0.121
3.80	0.012	0.048	0.130	0.112	0.093	0.088
4.20	0.011	0.042	0.083	0.074	0.063	0.060
4.60	0.014	0.025	0.045	0.041	0.036	0.034
5.00	0.000	0.000	0.000	0.000	0.000	0.000

Table 5.15: Values of compressible dynamic surface deformation  $h(r,1)$  for  $\beta = 5.0$  and  $f_\omega = 2.0$  and for selected values of  $\nu$  and  $\gamma$ .

r	$\beta = 9.0$			$\gamma = -1.1$		
	$\nu = 1/4$	$\nu = 1$	$\nu = 3$	$\nu = 4$	$\nu = 7$	$\nu = 9$
1.00	0.049	0.172	0.363	0.583	0.753	0.653
1.80	0.007	0.077	0.297	0.511	0.622	0.529
2.60	0.005	0.014	0.243	0.439	0.506	0.423
3.40	0.005	0.020	0.193	0.362	0.405	0.335
4.20	0.005	0.027	0.141	0.282	0.315	0.259
5.00	0.005	0.021	0.090	0.204	0.235	0.194
5.80	0.005	0.017	0.049	0.134	0.165	0.137
6.60	0.005	0.021	0.029	0.079	0.105	0.089
7.40	0.005	0.025	0.028	0.044	0.057	0.049
8.20	0.005	0.019	0.021	0.025	0.022	0.018
9.00	0.000	0.000	0.000	0.000	0.000	0.000

r	$\beta = 9.0$			$\gamma = -1.5$		
	$\nu = 1/4$	$\nu = 1$	$\nu = 3$	$\nu = 4$	$\nu = 7$	$\nu = 9$
1.00	0.049	0.172	0.361	0.609	0.741	0.640
1.80	0.008	0.079	0.293	0.527	0.598	0.506
2.60	0.005	0.014	0.247	0.457	0.485	0.403
3.40	0.005	0.019	0.201	0.380	0.389	0.319
4.20	0.005	0.028	0.150	0.298	0.304	0.248
5.00	0.005	0.022	0.099	0.217	0.228	0.187
5.80	0.005	0.017	0.054	0.143	0.161	0.133
6.60	0.005	0.021	0.027	0.084	0.104	0.088
7.40	0.005	0.026	0.023	0.043	0.057	0.049
8.20	0.004	0.019	0.019	0.021	0.021	0.019
9.00	0.000	0.000	0.000	0.000	0.000	0.000

r	$\beta = 9.0$			$\gamma = -3.0$		
	$\nu = 1/4$	$\nu = 1$	$\nu = 3$	$\nu = 4$	$\nu = 7$	$\nu = 9$
1.00	0.048	0.168	0.363	0.646	0.682	0.600
1.80	0.008	0.078	0.289	0.533	0.514	0.442
2.60	0.005	0.019	0.251	0.461	0.414	0.351
3.40	0.005	0.015	0.210	0.385	0.333	0.279
4.20	0.005	0.026	0.162	0.305	0.263	0.220
5.00	0.005	0.022	0.113	0.227	0.201	0.169
5.80	0.005	0.017	0.068	0.154	0.147	0.124
6.60	0.005	0.020	0.035	0.094	0.100	0.086
7.40	0.005	0.025	0.020	0.049	0.060	0.053
8.20	0.004	0.018	0.013	0.019	0.029	0.026
9.00	0.000	0.000	0.000	0.000	0.000	0.000

r	$\beta = 9.0$			$\gamma = -6.75$		
	$\nu = 1/4$	$\nu = 1$	$\nu = 3$	$\nu = 4$	$\nu = 7$	$\nu = 9$
1.00	0.046	0.162	0.367	0.631	0.636	0.573
1.80	0.007	0.075	0.286	0.500	0.459	0.405
2.60	0.005	0.021	0.248	0.428	0.369	0.321
3.40	0.005	0.012	0.206	0.357	0.298	0.257
4.20	0.005	0.024	0.160	0.284	0.238	0.204
5.00	0.005	0.022	0.114	0.214	0.185	0.159
5.80	0.005	0.018	0.073	0.150	0.138	0.120
6.60	0.005	0.020	0.042	0.096	0.098	0.087
7.40	0.005	0.023	0.024	0.055	0.063	0.057
8.20	0.004	0.017	0.013	0.027	0.035	0.032
9.00	0.000	0.000	0.000	0.000	0.000	0.000

Table 5.16: Values of compressible dynamic surface deformation  $h(r,1)$  for  $\beta = 5.0$  and  $f_\omega = 2.0$  and for selected values of  $\nu$  and  $\gamma$ .

r	$\beta = 1.5$			$\gamma = -1.1$		
	$\nu = 1/4$	$\nu = 1$	$\nu = 3$	$\nu = 4$	$\nu = 7$	$\nu = 9$
1.00	0.096	0.248	0.210	0.207	0.202	0.201
1.05	0.081	0.226	0.192	0.189	0.185	0.183
1.10	0.065	0.198	0.168	0.165	0.162	0.161
1.15	0.052	0.169	0.143	0.141	0.138	0.137
1.20	0.042	0.139	0.118	0.116	0.114	0.114
1.25	0.038	0.111	0.094	0.093	0.091	0.090
1.30	0.038	0.084	0.071	0.070	0.069	0.068
1.35	0.038	0.059	0.049	0.048	0.047	0.047
1.40	0.033	0.037	0.029	0.029	0.028	0.028
1.45	0.022	0.018	0.012	0.012	0.011	0.011
1.50	0.000	0.000	0.000	0.000	0.000	0.000

r	$\beta = 1.5$			$\gamma = -1.5$		
	$\nu = 1/4$	$\nu = 1$	$\nu = 3$	$\nu = 4$	$\nu = 7$	$\nu = 9$
1.00	0.096	0.248	0.210	0.206	0.202	0.200
1.05	0.080	0.224	0.191	0.188	0.184	0.183
1.10	0.065	0.196	0.167	0.164	0.161	0.160
1.15	0.052	0.167	0.142	0.140	0.137	0.137
1.20	0.042	0.138	0.118	0.116	0.114	0.113
1.25	0.037	0.109	0.093	0.092	0.091	0.090
1.30	0.037	0.082	0.070	0.069	0.068	0.068
1.35	0.037	0.057	0.049	0.048	0.048	0.047
1.40	0.032	0.035	0.029	0.029	0.028	0.028
1.45	0.021	0.016	0.012	0.012	0.012	0.012
1.50	0.000	0.000	0.000	0.000	0.000	0.000

r	$\beta = 1.5$			$\gamma = -3.0$		
	$\nu = 1/4$	$\nu = 1$	$\nu = 3$	$\nu = 4$	$\nu = 7$	$\nu = 9$
1.00	0.096	0.244	0.209	0.205	0.201	0.200
1.05	0.079	0.214	0.185	0.182	0.179	0.178
1.10	0.066	0.185	0.161	0.159	0.156	0.155
1.15	0.053	0.157	0.137	0.135	0.133	0.133
1.20	0.042	0.130	0.114	0.113	0.111	0.111
1.25	0.035	0.103	0.091	0.090	0.090	0.089
1.30	0.033	0.078	0.070	0.069	0.068	0.069
1.35	0.032	0.054	0.050	0.049	0.049	0.049
1.40	0.028	0.033	0.031	0.031	0.031	0.031
1.45	0.018	0.014	0.015	0.015	0.015	0.015
1.50	0.000	0.000	0.000	0.000	0.000	0.000

r	$\beta = 1.5$			$\gamma = -6.75$		
	$\nu = 1/4$	$\nu = 1$	$\nu = 3$	$\nu = 4$	$\nu = 7$	$\nu = 9$
1.00	0.097	0.234	0.206	0.204	0.200	0.199
1.05	0.079	0.195	0.175	0.173	0.170	0.170
1.10	0.067	0.168	0.152	0.150	0.149	0.148
1.15	0.055	0.143	0.130	0.129	0.128	0.127
1.20	0.045	0.119	0.109	0.108	0.108	0.107
1.25	0.036	0.096	0.089	0.089	0.088	0.088
1.30	0.031	0.074	0.070	0.070	0.070	0.070
1.35	0.027	0.054	0.052	0.052	0.052	0.053
1.40	0.023	0.035	0.035	0.035	0.036	0.036
1.45	0.014	0.018	0.020	0.020	0.020	0.021
1.50	0.000	0.000	0.000	0.000	0.000	0.000

Table 5.17: Values of compressible dynamic surface deformation  $h(r,1)$  for  $\beta = 1.5$  and  $f_\omega = 5.0$  and for selected values of  $\nu$  and  $\gamma$ .

r	$\beta = 3.0$			$\gamma = -1.1$		
	$\nu = 1/4$	$\nu = 1$	$\nu = 3$	$\nu = 4$	$\nu = 7$	$\nu = 9$
1.00	0.029	0.105	0.263	0.245	0.221	0.215
1.20	0.008	0.084	0.231	0.215	0.194	0.189
1.40	0.007	0.064	0.195	0.181	0.163	0.159
1.60	0.008	0.048	0.161	0.149	0.134	0.130
1.80	0.007	0.035	0.128	0.119	0.107	0.104
2.00	0.007	0.028	0.099	0.092	0.083	0.080
2.20	0.008	0.027	0.073	0.068	0.061	0.059
2.40	0.007	0.027	0.051	0.046	0.041	0.040
2.60	0.008	0.025	0.032	0.028	0.024	0.023
2.80	0.008	0.017	0.016	0.013	0.010	0.009
3.00	0.000	0.000	0.000	0.000	0.000	0.000

r	$\beta = 3.0$			$\gamma = -1.5$		
	$\nu = 1/4$	$\nu = 1$	$\nu = 3$	$\nu = 4$	$\nu = 7$	$\nu = 9$
1.00	0.029	0.105	0.263	0.244	0.220	0.214
1.20	0.008	0.084	0.230	0.213	0.193	0.187
1.40	0.007	0.065	0.194	0.179	0.162	0.157
1.60	0.008	0.048	0.159	0.147	0.133	0.129
1.80	0.007	0.035	0.127	0.118	0.106	0.103
2.00	0.007	0.027	0.098	0.091	0.082	0.080
2.20	0.007	0.026	0.072	0.066	0.060	0.058
2.40	0.007	0.026	0.049	0.045	0.041	0.040
2.60	0.008	0.024	0.030	0.027	0.024	0.023
2.80	0.008	0.016	0.015	0.012	0.010	0.009
3.00	0.000	0.000	0.000	0.000	0.000	0.000

r	$\beta = 3.0$			$\gamma = -3.0$		
	$\nu = 1/4$	$\nu = 1$	$\nu = 3$	$\nu = 4$	$\nu = 7$	$\nu = 9$
1.00	0.029	0.105	0.259	0.240	0.218	0.213
1.20	0.008	0.083	0.218	0.202	0.184	0.180
1.40	0.006	0.066	0.183	0.169	0.154	0.150
1.60	0.008	0.050	0.150	0.138	0.126	0.123
1.80	0.007	0.037	0.120	0.110	0.101	0.099
2.00	0.007	0.027	0.092	0.085	0.078	0.077
2.20	0.007	0.023	0.067	0.063	0.058	0.057
2.40	0.007	0.022	0.046	0.043	0.040	0.040
2.60	0.007	0.020	0.027	0.025	0.024	0.024
2.80	0.008	0.014	0.012	0.011	0.011	0.011
3.00	0.000	0.000	0.000	0.000	0.000	0.000

r	$\beta = 3.0$			$\gamma = -6.75$		
	$\nu = 1/4$	$\nu = 1$	$\nu = 3$	$\nu = 4$	$\nu = 7$	$\nu = 9$
1.00	0.029	0.106	0.245	0.231	0.214	0.209
1.20	0.009	0.081	0.195	0.183	0.171	0.168
1.40	0.005	0.066	0.162	0.152	0.142	0.139
1.60	0.007	0.052	0.133	0.125	0.117	0.115
1.80	0.007	0.040	0.107	0.101	0.094	0.093
2.00	0.007	0.029	0.084	0.079	0.075	0.074
2.20	0.007	0.022	0.063	0.060	0.057	0.056
2.40	0.006	0.019	0.044	0.042	0.041	0.041
2.60	0.007	0.016	0.028	0.027	0.027	0.027
2.80	0.007	0.010	0.014	0.014	0.014	0.015
3.00	0.000	0.000	0.000	0.000	0.000	0.000

Table 5.18: Values of compressible dynamic surface deformation  $h(r,1)$  for  $\beta = 3$  and  $f_\omega = 5.0$  and for selected values of  $\nu$  and  $\gamma$ .



r	$\beta = 5.0$			$\gamma = -1.1$		
	$\nu = 1/4$	$\nu = 1$	$\nu = 3$	$\nu = 4$	$\nu = 7$	$\nu = 9$
1.00	0.018	0.066	0.197	0.258	0.247	0.235
1.40	0.003	0.035	0.168	0.221	0.210	0.198
1.80	0.003	0.014	0.137	0.182	0.171	0.162
2.20	0.003	0.008	0.110	0.146	0.137	0.130
2.60	0.003	0.011	0.085	0.115	0.108	0.102
3.00	0.003	0.013	0.063	0.087	0.082	0.077
3.40	0.003	0.014	0.046	0.063	0.060	0.056
3.80	0.003	0.014	0.034	0.044	0.041	0.037
4.20	0.003	0.014	0.026	0.030	0.025	0.022
4.60	0.003	0.011	0.017	0.017	0.012	0.010
5.00	0.000	0.000	0.000	0.000	0.000	0.000

r	$\beta = 5.0$			$\gamma = -1.5$		
	$\nu = 1/4$	$\nu = 1$	$\nu = 3$	$\nu = 4$	$\nu = 7$	$\nu = 9$
1.00	0.018	0.067	0.201	0.262	0.248	0.234
1.40	0.003	0.036	0.171	0.223	0.209	0.197
1.80	0.003	0.015	0.140	0.184	0.170	0.160
2.20	0.003	0.008	0.112	0.148	0.136	0.128
2.60	0.003	0.011	0.087	0.116	0.107	0.100
3.00	0.003	0.013	0.064	0.088	0.081	0.076
3.40	0.003	0.014	0.046	0.063	0.059	0.055
3.80	0.003	0.014	0.034	0.043	0.039	0.037
4.20	0.003	0.014	0.025	0.028	0.023	0.022
4.60	0.003	0.010	0.016	0.016	0.011	0.009
5.00	0.000	0.000	0.000	0.000	0.000	0.000

r	$\beta = 5.0$			$\gamma = -3.0$		
	$\nu = 1/4$	$\nu = 1$	$\nu = 3$	$\nu = 4$	$\nu = 7$	$\nu = 9$
1.00	0.018	0.067	0.210	0.266	0.243	0.230
1.40	0.002	0.036	0.173	0.219	0.197	0.186
1.80	0.003	0.016	0.143	0.180	0.159	0.150
2.20	0.003	0.006	0.116	0.145	0.127	0.120
2.60	0.003	0.009	0.090	0.114	0.100	0.094
3.00	0.003	0.012	0.066	0.085	0.076	0.072
3.40	0.003	0.014	0.046	0.061	0.055	0.052
3.80	0.003	0.014	0.031	0.040	0.037	0.035
4.20	0.003	0.013	0.021	0.024	0.022	0.021
4.60	0.003	0.009	0.012	0.012	0.009	0.009
5.00	0.000	0.000	0.000	0.000	0.000	0.000

r	$\beta = 5.0$			$\gamma = -6.75$		
	$\nu = 1/4$	$\nu = 1$	$\nu = 3$	$\nu = 4$	$\nu = 7$	$\nu = 9$
1.00	0.018	0.066	0.212	0.254	0.233	0.223
1.40	0.002	0.035	0.164	0.195	0.176	0.169
1.80	0.003	0.017	0.135	0.159	0.142	0.136
2.20	0.003	0.008	0.110	0.129	0.114	0.109
2.60	0.003	0.008	0.087	0.102	0.090	0.086
3.00	0.003	0.011	0.065	0.078	0.070	0.067
3.40	0.003	0.013	0.046	0.057	0.052	0.050
3.80	0.003	0.014	0.031	0.039	0.036	0.035
4.20	0.003	0.012	0.019	0.023	0.023	0.022
4.60	0.003	0.008	0.009	0.011	0.011	0.011
5.00	0.000	0.000	0.000	0.000	0.000	0.000

Table 5.19: Values of compressible dynamic surface deformation  $h(r,1)$  for  $\beta = 5$  and  $f_\omega = 5.0$  and for selected values of  $\nu$  and  $\gamma$ .

r	$\beta = 9.0$			$\gamma = -1.1$		
	$\nu = 1/4$	$\nu = 1$	$\nu = 3$	$\nu = 4$	$\nu = 7$	$\nu = 9$
1.00	0.012	0.044	0.107	0.129	0.239	0.261
1.80	0.001	0.008	0.065	0.092	0.194	0.211
2.60	0.001	0.005	0.037	0.065	0.155	0.168
3.40	0.001	0.006	0.020	0.045	0.122	0.132
4.20	0.001	0.005	0.011	0.030	0.094	0.102
5.00	0.001	0.005	0.011	0.020	0.070	0.077
5.80	0.001	0.005	0.016	0.016	0.050	0.055
6.60	0.001	0.005	0.018	0.017	0.035	0.038
7.40	0.001	0.005	0.016	0.016	0.024	0.024
8.20	0.001	0.006	0.010	0.011	0.015	0.013
9.00	0.000	0.000	0.000	0.000	0.000	0.000

r	$\beta = 9.0$			$\gamma = -1.5$		
	$\nu = 1/4$	$\nu = 1$	$\nu = 3$	$\nu = 4$	$\nu = 7$	$\nu = 9$
1.00	0.012	0.044	0.107	0.129	0.243	0.262
1.80	0.001	0.009	0.065	0.091	0.196	0.211
2.60	0.001	0.004	0.038	0.065	0.157	0.168
3.40	0.001	0.006	0.020	0.046	0.124	0.132
4.20	0.001	0.005	0.010	0.031	0.095	0.102
5.00	0.001	0.005	0.011	0.020	0.071	0.076
5.80	0.001	0.005	0.015	0.016	0.050	0.055
6.60	0.001	0.005	0.017	0.016	0.034	0.037
7.40	0.001	0.005	0.016	0.015	0.023	0.023
8.20	0.001	0.006	0.010	0.011	0.014	0.012
9.00	0.000	0.000	0.000	0.000	0.000	0.000

r	$\beta = 9.0$			$\gamma = -3.0$		
	$\nu = 1/4$	$\nu = 1$	$\nu = 3$	$\nu = 4$	$\nu = 7$	$\nu = 9$
1.00	0.012	0.045	0.106	0.129	0.249	0.261
1.80	0.001	0.010	0.063	0.089	0.194	0.201
2.60	0.001	0.004	0.038	0.066	0.156	0.159
3.40	0.001	0.005	0.022	0.048	0.123	0.126
4.20	0.001	0.005	0.011	0.033	0.095	0.097
5.00	0.001	0.005	0.009	0.021	0.071	0.073
5.80	0.001	0.005	0.013	0.014	0.049	0.052
6.60	0.001	0.004	0.016	0.013	0.032	0.034
7.40	0.001	0.005	0.014	0.013	0.019	0.020
8.20	0.001	0.005	0.009	0.009	0.010	0.009
9.00	0.000	0.000	0.000	0.000	0.000	0.000

r	$\beta = 9.0$			$\gamma = -6.75$		
	$\nu = 1/4$	$\nu = 1$	$\nu = 3$	$\nu = 4$	$\nu = 7$	$\nu = 9$
1.00	0.012	0.044	0.104	0.129	0.242	0.248
1.80	0.001	0.010	0.059	0.085	0.175	0.177
2.60	0.001	0.003	0.038	0.065	0.139	0.139
3.40	0.001	0.005	0.024	0.049	0.111	0.110
4.20	0.001	0.005	0.014	0.036	0.087	0.086
5.00	0.001	0.004	0.009	0.024	0.065	0.065
5.80	0.001	0.004	0.011	0.016	0.047	0.048
6.60	0.001	0.004	0.013	0.012	0.031	0.032
7.40	0.001	0.005	0.012	0.010	0.018	0.019
8.20	0.001	0.005	0.007	0.007	0.008	0.009
9.00	0.000	0.000	0.000	0.000	0.000	0.000

Table 5.20: Values of compressible dynamic surface deformation  $h(r,1)$  for  $\beta = 9$  and  $f_\omega = 5.0$  and for selected values of  $\nu$  and  $\gamma$ .

## Chapter 6

# Axially Loaded Column of an Incompressible Elastic Material

### 6.1 Introduction

This work investigates the deformation of an incompressible isotropic elastic column under axial load. Mathematical solutions are formulated in terms of *Fourier* transforms and involve *Bessel* - *Fourier* series and modified *Bessel* functions.

Let cylindrical polar coordinates be chosen so that the column occupies the region

$$0 \leq r \leq R, \quad -\pi \leq \theta \leq \pi, \quad 0 \leq z \leq L.$$

The outer boundary  $r = R$  is assumed to be stress-free, with the column compressed axially by equal and opposite loads applied to faces  $z = 0$  and  $z = L$ . These loads are applied over plates which are rigidly bounded by  $z = 0$  and  $z = L$  in such a way that no radial displacement is possible there. Axial displacement is zero on the lower boundary and  $H$  (constant) on the upper boundary where  $H$  is determined by the loading.

### 6.2 Linear Deformation of a Slab

It is assumed that the elastic deformation of the material takes the form

$$\mathbf{v} = w(r, z)\mathbf{e}_r + h(r, z)\mathbf{e}_z, \quad (6.2.1)$$

for symmetrical loading about the axis of the column. When (6.2.1) is substituted into the expression for first order stress tensor (2.2.30), the non-zero components of the first

order stress tensor are

$$\begin{aligned} S_{11} &= -p + 2\mu \frac{\partial w}{\partial r}, & S_{22} &= -p + 2\mu \frac{w}{r}, \\ S_{33} &= -p + 2\mu \frac{\partial h}{\partial z}, & S_{13} = S_{31} &= \mu \left( \frac{\partial w}{\partial z} + \frac{\partial h}{\partial r} \right). \end{aligned} \quad (6.2.2)$$

Since the material is incompressible,  $u(r, z)$  and  $h(r, z)$  satisfy the condition  $\text{Tr}(\mathbf{H}) = 0$ , so that

$$\frac{\partial w}{\partial r} + \frac{w}{r} + \frac{\partial h}{\partial z} = 0. \quad (6.2.3)$$

In the absence of externally applied body forces, the momentum equations (2.2.37) reduce to the radial and axial equations

$$\begin{aligned} \frac{\partial S_{11}}{\partial r} + \frac{\partial S_{13}}{\partial z} + \frac{1}{r}(S_{11} - S_{22}) &= 0, \\ \frac{\partial S_{13}}{\partial r} + \frac{\partial S_{33}}{\partial z} + \frac{S_{13}}{r} &= 0. \end{aligned} \quad (6.2.4)$$

The azimuthal equation is satisfied identically provided  $p = p(r, z)$ . When stress tensor components (6.2.2) are substituted into momentum equations (6.2.4) and incompressibility condition (6.2.3) is used, the resulting partial differential equations are

$$\begin{aligned} -\frac{\partial p}{\partial r} + \mu \left( \frac{\partial^2 w}{\partial z^2} - \frac{\partial^2 h}{\partial r \partial z} \right) &= 0, \\ -\frac{\partial p}{\partial z} + \mu \left( \frac{\partial^2 h}{\partial z^2} + \frac{\partial^2 h}{\partial r^2} + \frac{1}{r} \frac{\partial h}{\partial r} \right) &= 0. \end{aligned} \quad (6.2.5)$$

### 6.2.1 Boundary Conditions

Momentum equations (6.2.5) and incompressibility condition (6.2.3) must be solved with suitable boundary conditions which ensure that boundary  $r = R$  is stress-free, the radial displacement  $w$  is zero on  $z = 0$  and  $z = L$  and the axial displacement  $h$  is zero on  $z = 0$  and  $H$  (constant) on  $z = L$ . Furthermore, all displacements are finite on  $r = 0$ . Hence

$$\begin{aligned} -p + 2\mu \frac{\partial w}{\partial r} = \frac{\partial w}{\partial z} + \frac{\partial h}{\partial r} &= 0, \quad \text{on } r = R & 0 < z < L, \\ w = 0, \quad h = 0, & \quad \text{on } z = 0 & 0 \leq z \leq R, \\ w = 0, \quad h = H, & \quad \text{on } z = L & 0 \leq z \leq R, \end{aligned} \quad (6.2.6)$$

where  $H$  is constant and is determined by the applied axial loading  $F$  given by

$$F \mathbf{e}_3 = - \left( \iint S_{33} dA \right) \mathbf{e}_3. \quad (6.2.7)$$

## 6.2.2 Non-dimensional Problem

Non-dimensional coordinates  $r^*$ ,  $z^*$ , non-dimensional displacements  $u^*$ ,  $h^*$ , non-dimensional pressure  $p^*$ , and non-dimensional parameter  $\nu$  are introduced by the definitions

$$\begin{aligned} r^* &= \frac{r}{R}, & z^* &= \frac{z}{L}, & \nu &= \frac{L}{R}, \\ u^* &= \frac{w}{L}, & h^* &= \frac{h}{L}, & p^* &= \frac{p}{\mu}. \end{aligned} \quad (6.2.8)$$

Substitution of equation (6.2.8) into (6.2.5) and into incompressibility condition (6.2.3) leads to the non-dimensional field equations

$$\begin{aligned} -\nu \frac{\partial p}{\partial r} + \frac{\partial^2 u}{\partial z^2} - \nu \frac{\partial^2 h}{\partial r \partial z} &= 0, \\ -\frac{\partial p}{\partial z} + \frac{\partial^2 h}{\partial z^2} + \nu^2 \left( \frac{\partial^2 h}{\partial r^2} + \frac{1}{r} \frac{\partial h}{\partial r} \right) &= 0, \\ \frac{\partial h}{\partial z} + \nu \left( \frac{\partial u}{\partial r} + \frac{u}{r} \right) &= 0 \end{aligned} \quad (6.2.9)$$

where the \* notation has been dropped for representational elegance although all quantities are non-dimensional. Similarly, boundary conditions (6.2.6) have non-dimensional form

$$\begin{aligned} -p + 2\nu \frac{\partial u}{\partial r} = \frac{\partial u}{\partial z} + \nu \frac{\partial h}{\partial r} &= 0, \quad \text{on } r = 1 & 0 < z < 1, \\ u = 0, \quad h = 0, & \quad \text{on } z = 0 & 0 \leq z \leq 1, \\ u = 0, \quad h = H/L, & \quad \text{on } z = 1 & 0 \leq z \leq 1. \end{aligned} \quad (6.2.10)$$

The value of  $H$  is determined by the axial load  $F$ , the calculation of which will be described in a later section.

## 6.3 Solution Procedure

### 6.3.1 Transformed Equations

The general solution of momentum equations (6.2.9) can be obtained using finite Fourier transforms. Let

$$\begin{aligned} \bar{p}_l &= \bar{p}(r, l) = \int_0^1 p(r, z) \sin l\pi z \, dz, \\ \bar{u}_l &= \bar{u}(r, l) = \int_0^1 u(r, z) \sin l\pi z \, dz, \\ \bar{h}_l &= \bar{h}(r, l) = \int_0^1 h(r, z) \cos l\pi z \, dz. \end{aligned} \quad (6.3.11)$$

In terms of  $\bar{p}$ ,  $\bar{u}_l$  and  $\bar{h}_l$ , the displacements  $u(r, z)$  and  $h(r, z)$  and the pressure  $p(r, z)$  have half range Fourier series representations

$$\begin{aligned} p(r, z) &= 2 \sum_{l=1}^{\infty} \bar{p}_l \sin l\pi z , \\ u(r, z) &= 2 \sum_{l=1}^{\infty} \bar{u}_l \sin l\pi z , \\ h(r, z) &= h_0(r) + 2 \sum_{l=1}^{\infty} \bar{h}_l \cos l\pi z , \end{aligned} \quad (6.3.12)$$

where

$$h_0(r) = \int_0^1 h(r, z) dz . \quad (6.3.13)$$

By multiplying equation (6.2.9<sub>1</sub>) and incompressibility condition (6.2.3) by  $\sin l\pi z$  and by multiplying equation (6.2.9<sub>2</sub>) by  $\cos l\pi z$  and then integrating the resulting equations with respect to  $z$  over  $[0, 1]$ , functions  $\bar{p}_l$ ,  $\bar{u}_l$  and  $\bar{h}_l$  are seen to satisfy ordinary differential equations

$$\begin{aligned} \frac{d^2 \bar{h}_l}{dr^2} + \frac{1}{r} \frac{d\bar{h}_l}{dr} - \alpha^2 \bar{h}_l - \frac{\alpha}{\nu} \bar{p}_l &= -\frac{1}{\nu^2} g(r) , \\ \frac{d\bar{h}_l}{dr} - \frac{1}{\alpha\nu} \frac{d\bar{p}_l}{dr} - \alpha \bar{u}_l &= 0 , \\ \frac{d\bar{u}_l}{dr} + \frac{\bar{u}_l}{r} - \alpha^2 \bar{h}_l &= 0 , \end{aligned} \quad (6.3.14)$$

where

$$\begin{aligned} g(r) &= (-1)^l g^{(1)}(r) - g^{(0)}(r) , & \alpha &= \frac{l\pi}{\nu} , \\ g^{(0)}(r) &= -p(r, 0) + \frac{\partial h(r, 0)}{\partial z} , & g^{(1)}(r) &= -p(r, 1) + \frac{\partial h(r, 1)}{\partial z} . \end{aligned} \quad (6.3.15)$$

The transformed boundary conditions become

$$2\nu \frac{d\bar{u}_l}{dr} - \bar{p}_l = 0 , \quad \frac{d\bar{h}_l}{dr} + \alpha \bar{u}_l = 0 , \quad \text{on} \quad r = 1 . \quad (6.3.16)$$

## 6.4 General Solution

From the momentum equation (6.3.14), it is easily shown that  $\bar{p}_l$  satisfies the second order ordinary differential equation

$$\frac{d^2 \bar{p}_l}{dr^2} + \frac{1}{r} \frac{d\bar{p}_l}{dr} - \alpha^2 \bar{p}_l = -\frac{\alpha}{\nu} g(r) . \quad (6.4.17)$$

In fact, this equation is called the modified *Bessel* equation (see chapter 2). The general solution of (6.4.17), finite at  $r = 0$ , is

$$\bar{p}_l = AI_0(\alpha r) + \frac{\alpha}{\nu} \int_0^r tg(t) [I_0(\alpha t)K_0(\alpha r) - K_0(\alpha t)I_0(\alpha r)] dt . \quad (6.4.18)$$

When  $\bar{p}_l$  is substituted into the other equations, it can be shown that  $\bar{u}_l$  satisfies the second order ordinary differential equation

$$\frac{d^2 \bar{u}_l}{dr^2} + \frac{1}{r} \frac{d\bar{u}_l}{dr} - \left( \alpha^2 + \frac{1}{r} \right) \bar{u}_l = \frac{\alpha}{\nu} AI_1(\alpha r) - \frac{\alpha^2}{\nu^2} \int_0^r tg(t) [I_0(\alpha t)K_1(\alpha r) + K_0(\alpha t)I_1(\alpha r)] dt$$

with solution (again, finite at  $r = 0$ )

$$\begin{aligned} \bar{u}_l = & \frac{A}{2\nu} r I_0(\alpha r) + B I_1(\alpha r) + \frac{\alpha r}{2\nu^2} \int_0^r tg(t) [I_0(\alpha t)K_0(\alpha r) - K_0(\alpha t)I_0(\alpha r)] dt \\ & - \frac{\alpha}{2\nu^2} \int_0^r t^2 g(t) [I_1(\alpha t)K_1(\alpha r) - K_1(\alpha t)I_1(\alpha r)] dt . \end{aligned} \quad (6.4.19)$$

Finally,  $\bar{h}_l$  can be evaluated from the incompressibility condition to give

$$\begin{aligned} \bar{h}_l = & B I_0(\alpha r) + \frac{A}{2\alpha\nu} [2I_0(\alpha r) + \alpha r I_1(\alpha r)] \\ & - \frac{\alpha r}{2\nu^2} \int_0^r tg(t) [I_0(\alpha t)K_1(\alpha r) + K_0(\alpha t)I_1(\alpha r)] dt , \\ & - \frac{1}{\nu^2} \int_0^r tg(t) [I_0(\alpha t)K_0(\alpha r) - K_0(\alpha t)I_0(\alpha r)] dt , \\ & + \frac{\alpha}{2\nu^2} \int_0^r t^2 g(t) [I_1(\alpha t)K_0(\alpha r) + K_1(\alpha t)I_0(\alpha r)] dt . \end{aligned} \quad (6.4.20)$$

Constants  $A$  and  $B$  are determined from the boundary conditions (6.3.16) at  $r = 1$ .

## 6.5 Fourier-Bessel Series Representation

Solutions (6.4.18), (6.4.19) and (6.4.20) contain integrals involving an unknown function  $g(r)$ . Let  $g(r)$  have Fourier-Bessel series representation

$$g(r) = g_0 + \sum_{k=1}^{\infty} g_k J_0(\lambda_k r) \quad (6.5.21)$$

where  $\lambda_k$  are the zeros of  $J_1(x) = 0$ . When expression (6.5.21) is substituted into solutions (6.4.18), (6.4.19) and (6.4.20) (see appendix B for more details), it can be shown that  $\bar{p}_l$ ,

$\bar{u}_l$  and  $\bar{h}_l$  take the new form

$$\begin{aligned}\bar{p}_l &= \frac{g_0}{\alpha\nu} + AI_0(\alpha r) + \frac{\alpha}{\nu} \sum_{k=1}^{\infty} \frac{g_k J_0(\lambda_k)}{\alpha^2 + \lambda_k^2}, \\ \bar{u}_l &= \frac{A}{2\nu} r I_0(\alpha r) + BI_1(\alpha r) + \frac{\alpha}{\nu^2} \sum_{k=1}^{\infty} \frac{\lambda_k g_k J_1(\lambda_k)}{(\alpha^2 + \lambda_k^2)^2}, \\ \bar{h}_l &= \frac{A}{2\alpha\nu} [2I_0(\alpha r) + \alpha r I_1(\alpha r)] + BI_0(\alpha r) + \frac{1}{\nu^2} \sum_{k=1}^{\infty} \frac{\lambda_k^2 g_k J_0(\lambda_k)}{(\alpha^2 + \lambda_k^2)^2},\end{aligned}\tag{6.5.22}$$

where constants  $A$  and  $B$  are defined by the expressions

$$A = \frac{I_1(\alpha)}{\nu\phi(\alpha)} [g_0 + \alpha^2\Omega], \quad B = -\frac{\alpha I_0(\alpha) + I_1(\alpha)}{2\alpha\nu^2\phi(\alpha)} [g_0 + \alpha^2\Omega],\tag{6.5.23}$$

and where

$$\begin{aligned}\Omega &= \sum_{n=1}^{\infty} g_n \chi_n J_0(\lambda_n), \quad \chi_k = \frac{\alpha^2 - \lambda_k^2}{(\alpha^2 + \lambda_k^2)^2}, \\ \phi(\alpha) &= \alpha^2 [I_1^2(\alpha) - I_0^2(\alpha)] + I_1^2(\alpha).\end{aligned}\tag{6.5.24}$$

By substituting expression for  $A$  and  $B$  into (6.5.22),  $\bar{p}_l$ ,  $\bar{u}_l$  and  $\bar{h}_l$  now become

$$\begin{aligned}\bar{p}_l &= \frac{g_0}{\alpha\nu} + \frac{I_1(\alpha)I_0(\alpha r)}{\nu\phi(\alpha)} [g_0 + \alpha^2\Omega] + \frac{\alpha}{\nu} \sum_{k=1}^{\infty} \frac{g_k J_0(\lambda_k r)}{\alpha^2 + \lambda_k^2}, \\ \bar{u}_l &= \frac{g_0 + \alpha^2\Omega}{2\alpha\nu^2\phi} Q(r) + \frac{\alpha}{\nu^2} \sum_{k=1}^{\infty} \frac{\lambda_k g_k J_1(\lambda_k r)}{(\alpha^2 + \lambda_k^2)^2}, \\ \bar{h}_l &= \frac{g_0 + \alpha^2\Omega}{2\alpha\nu^2\phi} L(r) + \frac{1}{\nu^2} \sum_{k=1}^{\infty} \frac{\lambda_k^2 g_k J_0(\lambda_k r)}{(\alpha^2 + \lambda_k^2)^2},\end{aligned}\tag{6.5.25}$$

where

$$\begin{aligned}Q(r) &= \alpha r I_0(\alpha r) I_1(\alpha) - I_1(\alpha r) (\alpha I_0(\alpha) + I_1(\alpha)), \\ L(r) &= \alpha r I_1(\alpha r) I_1(\alpha) + I_0(\alpha r) (I_1(\alpha) - \alpha I_0(\alpha)).\end{aligned}\tag{6.5.26}$$

The solutions  $\bar{p}_l$ ,  $\bar{u}_l$  and  $\bar{h}_l$  (6.5.25) are now expanded by Fourier-Bessel series. Functions  $I_0(\alpha r)$  and  $I_1(\alpha r)$  which appear in the expression for  $\bar{p}_l$  and  $\bar{h}_l$  are now represented by Fourier-Bessel series in  $J_0(\lambda_k r)$ , while in the  $\bar{u}_l$  expression, these functions will be expanded as Fourier-Bessel series in  $J_1(\lambda_k r)$ . Properties of Fourier-Bessel series have been discussed in chapter 2 (see appendix B for the integrations involved in the construction

of the formulae for  $\bar{p}_l$ ,  $\bar{u}_l$  and  $\bar{h}_l$ . The final form of the general solution is

$$\begin{aligned}\bar{p}_l &= \frac{g_0}{\alpha\nu} + \frac{2I_1^2(\alpha)(g_0 + \alpha^2\Omega)}{\alpha\nu\phi(\alpha)} + \frac{\alpha}{\nu\phi(\alpha)} \sum_{k=1}^{\infty} \frac{J_0(\lambda_k r) [2I_1^2(\alpha) + \phi(\alpha)g_k J_0(\lambda_k)]}{J_0(\lambda_k)(\alpha^2 + \lambda_k^2)} , \\ \bar{u}_l &= \frac{1}{\alpha\nu^2} \sum_{k=1}^{\infty} \frac{J_1(\lambda_k r)}{J_0(\lambda_k)} \left[ \frac{I_1^2(\alpha)}{\phi(\alpha)} (g_0 + \alpha^2\Omega)\xi_k + \alpha^2\beta_k J_0(\lambda_k)g_k \right] , \\ \bar{h}_l &= \frac{1}{\nu^2} \sum_{k=1}^{\infty} \frac{J_0(\lambda_k r)}{J_0(\lambda_k)} \left[ \frac{I_1^2(\alpha)}{\phi(\alpha)} (g_0 + \alpha^2\Omega)\chi_k + \lambda_k\beta_k J_0(\lambda_k)g_k \right] - \frac{I_1^2(\alpha)[g_0 + \alpha^2\Omega]}{\alpha^2\nu^2\phi(\alpha)} ,\end{aligned}\tag{6.5.27}$$

where

$$\xi_k = \frac{\lambda_k(\lambda_k^2 + 3\alpha^2)}{(\lambda_k^2 + \alpha^2)^2} , \quad \beta_k = \frac{\lambda_k}{(\lambda_k^2 + \alpha^2)^2} .$$

### 6.5.1 Evaluation of Applied Force

The computation of the applied force (6.2.7) uses a consequence of incompressibility for its evaluation. If  $u \equiv 0$  everywhere on  $z = 1$  then it follows from the continuity of (6.2.3) on  $z = 1$  that

$$\lim_{z \rightarrow 1} \frac{\partial h}{\partial z} = 0 , \quad r \in [0, 1] .$$

If the applied force on the upper boundary of the column is  $F^{(1)}\mathbf{e}_3$  then

$$F^{(1)} = -\frac{1}{2\pi\mu R^2} \lim_{z \rightarrow 1} \iint S_{33} dA$$

and this in turn simplifies to

$$\begin{aligned}F^{(1)} &= \lim_{z \rightarrow 1} \int_0^1 r \left( p - 2\mu \frac{\partial h}{\partial z} \right) dr \\ &= \int_0^1 r \left( -g^{(1)}(r) - \lim_{z \rightarrow 1} \frac{\partial h}{\partial z} \right) dr \\ &= -\int_0^1 r g^{(1)}(r) dr .\end{aligned}\tag{6.5.28}$$

The load on the bottom boundary is given by a formula similar to (6.5.28) except that there is a sign change due to the reversal of the normal. Thus the non-dimensional applied loads on the top and bottom surfaces are now  $F^{(1)}\mathbf{e}_3$  and  $F^{(0)}\mathbf{e}_3$  respectively where  $F^{(1)}$  and  $F^{(0)}$  are computed from the formulae

$$F^{(0)} = \int_0^1 r g^{(0)}(r) dr , \quad F^{(1)} = -\int_0^1 r g^{(1)}(r) dr .\tag{6.5.29}$$

When the functions  $g^{(0)}(r)$  and  $g^{(1)}(r)$  are substituted by the series (6.5.21). it can be shown easily that

$$F^{(0)} = g_0^{(0)} , \quad F^{(1)} = -g_0^{(1)} .\tag{6.5.30}$$



### 6.5.2 Evaluation of Functions $h_0(r)$

Function  $h_0(r)$  required for series (6.3.12) is now determined by integrating the second equation of (6.2.9) with respect to  $z$  over the range  $[0, 1]$ . Using this idea,  $h_0(r)$  is seen to satisfy the ordinary linear differential equation

$$\begin{aligned} \frac{d^2 h_0}{dr^2} + \frac{1}{r} \frac{dh_0}{dr} &= \frac{1}{\nu^2} [g^{(0)}(r) - g^{(1)}(r)] \\ &= \frac{1}{\nu^2} \left( g_0^{(0)} - g_0^{(1)} \right) + \frac{1}{\nu^2} \sum_{k=1}^{\infty} (g_k^{(0)} - g_k^{(1)}) J_0(\lambda_k r) . \end{aligned} \quad (6.5.31)$$

This equation is now integrated twice with respect to  $r$ , bearing in mind that  $h_0(r)$  is finite at  $r = 0$ . The finiteness condition removes the naturally occurring logarithm solution and leads to the final conclusion that

$$h_0(r) = C + \frac{1}{\nu^2} \left( g_0^{(0)} - g_0^{(1)} \right) - \frac{1}{\nu^2} \sum_{n=1}^{\infty} \frac{g_n^{(0)} - g_n^{(1)}}{\lambda_n^2} J_0(\lambda_n r) \quad (6.5.32)$$

where  $C$  is an arbitrary constant of integration. When (6.5.27) and (6.5.32) are substituted into (6.3.12), the functions  $u(r, z)$  and  $h(r, z)$  now have the final form.

### 6.5.3 Evaluation of $u(1, z)$

The radial displacement of the curved surface  $u(1, z)$  is expressed by

$$u(1, z) = 2 \sum_{l=1}^{\infty} \bar{u}_l(1, l) \sin l\pi z , \quad (6.5.33)$$

Most importantly,  $\bar{u}_l(1, l)$  cannot be evaluated from (6.5.27) since this series does not converge to the value of the function at  $r = 1$ . Instead the expression for  $\bar{u}_l$  in (6.4.19) is used. After simplification, the expression for  $u(1, z)$  takes the final form

$$u(1, z) = \frac{2}{\nu^2} \sum_{j=1}^{\infty} \frac{I_1^2(\alpha_{2j-1})}{\phi(\alpha_{2j-1})} \left[ \alpha_{2j-1} \Omega + \frac{2F^{(1)}}{\alpha_{2j-1}} \right] \sin(2j-1)\pi z . \quad (6.5.34)$$

## 6.6 Boundary Conditions

In this section, unknown constant  $H$  and coefficients  $g_k$  will be determined from boundary conditions  $h(r, 0) = 0$  and  $h(r, 1) = H$  and from the applied force. Thus

$$\begin{aligned} h(r, 0) &= h_0(r) + 2 \sum_{j=1}^{\infty} h_{2j-1}(r, \alpha_{2j-1}) = 0 \\ h(r, 1) &= h_0(r) - 2 \sum_{j=1}^{\infty} h_{2j-1}(r, \alpha_{2j-1}) = H , \end{aligned} \quad (6.6.35)$$

where

$$\begin{aligned}
h_{2j-1} &= -\frac{I_1^2(\alpha_{2j-1}^2)}{\alpha_{2j-1}^2 \nu^2 \phi(\alpha_{2j-1})} \left[ g_0 + \alpha_{2j-1}^2 \Omega \right] \left[ 1 + \alpha_{2j-1}^2 \sum_{k=1}^{\infty} \frac{J_0(\lambda_k r)}{J_0(\lambda_k)} \chi_{2j-1,k} \right] \\
&\quad + \frac{1}{\nu^2} \sum_{k=1}^{\infty} \lambda_k \beta_k J_0(\lambda_k r) g_k, \\
\Omega &= \sum_{n=1}^{\infty} g_n \chi_n J_0(\lambda_n),
\end{aligned} \tag{6.6.36}$$

and other notation have been defined in the previous sections. Solution of (6.6.35) can be obtained by solving a pair of linear equations formed by adding and subtracting equations (6.6.35). From the equation formed by summation, it is clear that  $g_k^{(0)} = g_k^{(1)}$  for all  $k$  and that

$$H = 2C = -\frac{8}{\nu^2} \sum_{j=1}^{\infty} \frac{I_1^2(\alpha_{2j-1})}{\phi(\alpha_{2j-1})} \left[ \frac{2F^{(1)}}{\alpha_{2j-1}^2} + \sum_{n=1}^{\infty} g_n J_0(\lambda_n) \chi_{2j-1,n} \right], \tag{6.6.37}$$

The subtraction of equations (6.6.35) determines the coefficients  $g_k$ , so that

$$\sum_{n=1}^{\infty} g_n J_0(\lambda_n) \chi_{2j-1,k} \sum_{j=1}^{\infty} \frac{\alpha_{2j-1}^2 I_1^2(\alpha_{2j-1})}{\phi(\alpha_{2j-1})} \chi_{2j-1,k} + g_k \sum_{j=1}^{\infty} \frac{\lambda_k^2 J_0(\lambda_k)}{\alpha_{2j-1}^2 + \lambda_k^2} = 2F \sum_{j=1}^{\infty} \frac{I_1^2(\alpha_{2j-1})}{\phi(\alpha_{2j-1})} \chi_{2j-1,k} \tag{6.6.38}$$

## 6.7 Results and Conclusion

Radial displacement  $u(1, z)$  and axial displacement  $h(r, z)$  are examined for different values of the aspect  $\nu$  ranging from 0.5 (squat column) to 5.0 (long column).

Figure 6.1 shows the behaviour of the radial displacement  $u(1, z)$ . The radial displacement is different from Moghe and Neff's suggestion [27]. They said "the proper choice of zeros of the Bessel function becomes quite important", and they gave two different shapes of radial displacement dependent on the choice of  $\lambda_k$ . They considered the two possible choices  $J_0(\lambda_k) = 0$  and  $J_1(\lambda_k) = 0$  with the attendant representation for  $p(r, z)$ ,  $w(r, z)$  and  $h(r, z)$ . The choice  $J_0(\lambda_k) = 0$  seems to give results that are qualitatively similar to those derived here for the curved surface shape in the vicinity of the rigid plates whereas the choice  $J_1(\lambda_k) = 0$  does not. Calculation suggest that the shape of the curved surface of the column is similar for different values of ratio  $\nu$ . Also, it is clear that when  $\nu$  increases, the centre region of radial displacement becomes increasingly flat but the behaviour near the boundaries is unchanged.

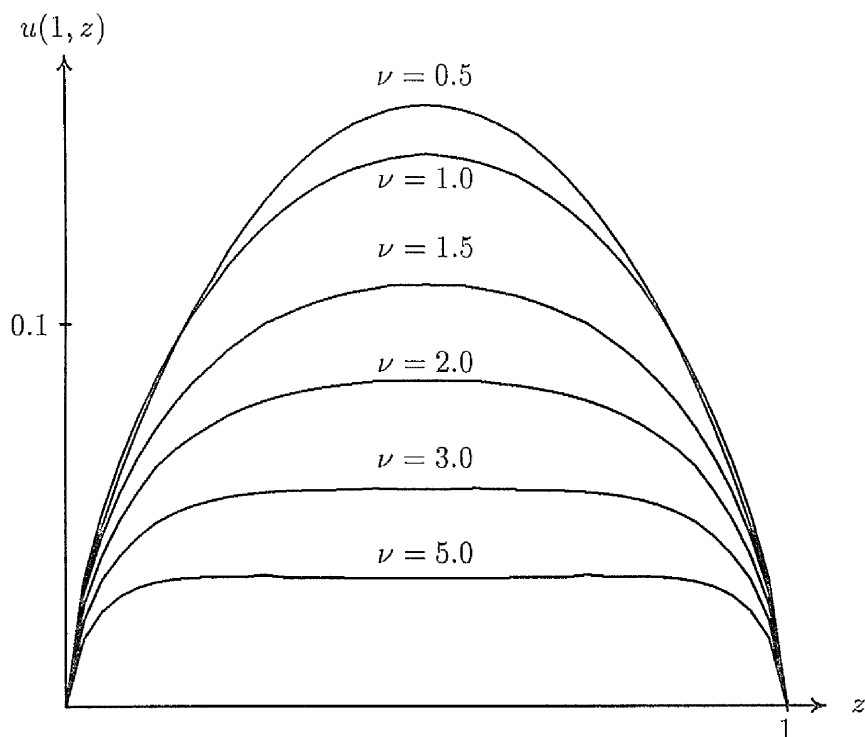


Figure 6.1: Graphs of incompressible radial displacement  $u(1, z)$  when  $\nu = 0.5, 1.0, 1.5, 2.0, 3.0$ , and  $5.0$ .

$\nu$	0.5	1.0	1.5	2.0	2.5	3.0	3.5	4.0	4.5	5.0
H	-0.113	-0.216	-0.259	-0.279	-0.290	-0.297	-0.302	-0.306	-0.309	-0.311

Table 6.1: Tables of incompressible axial displacement H for different values of  $\nu$ .

Figure 6.2 shows the behaviour of the axial displacement  $h(r, z)$  for  $r \in [0, 1]$  and for different values of  $z$  and  $\nu$ . It is clear that the centre region of the cylinder is almost flat but, near boundaries there is more stress. Tables 6.1 displays values of axial displacement  $H$  versus aspect  $\nu$ . It is clear that  $H$  is a decreasing function of  $\nu$ .

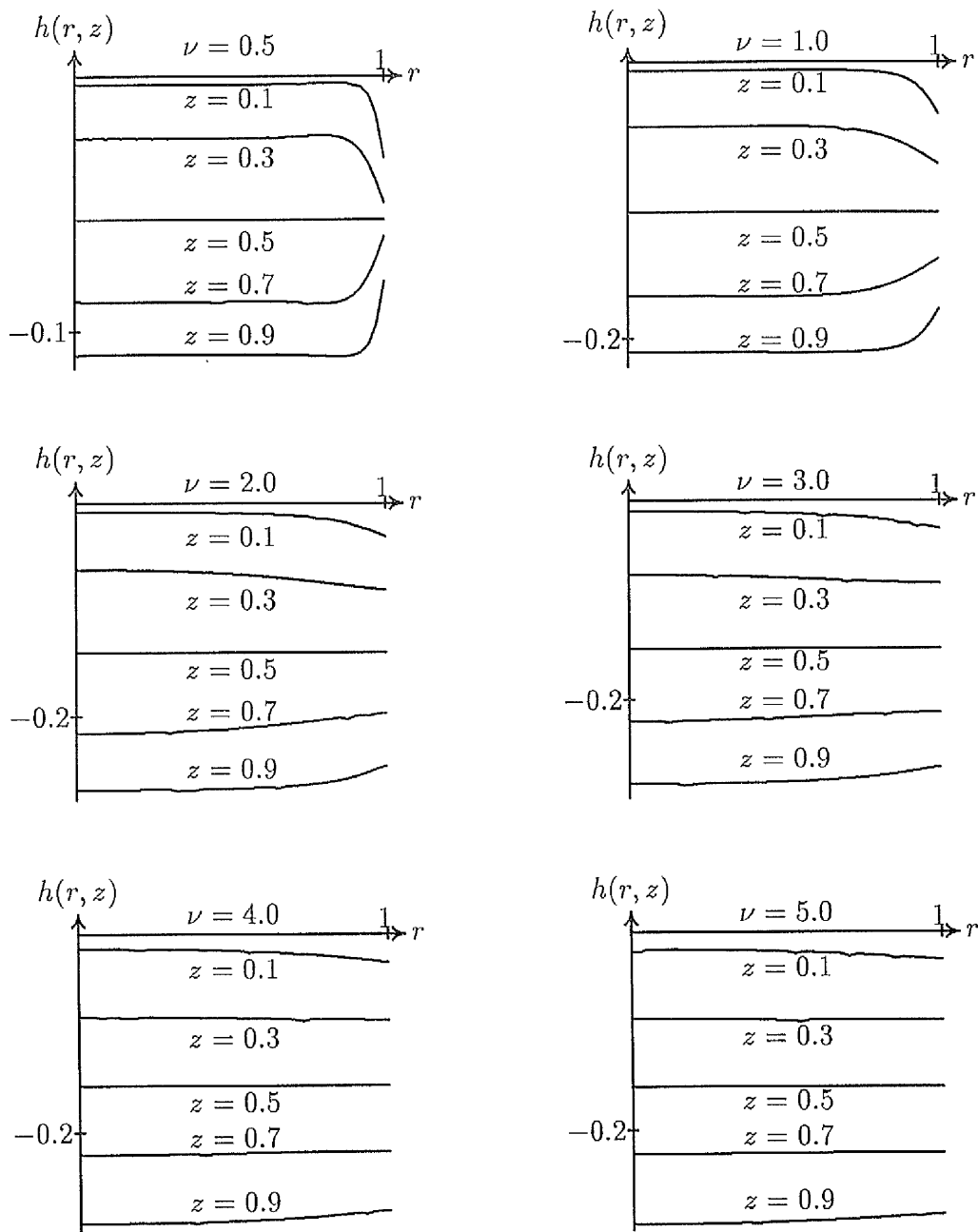


Figure 6.2: Graphs of incompressible axial displacement  $h(r, z)$  when  $\nu = 0.5, 1.0, 2.0, 3.0, 4.0$ , and  $5.0$  and for different values of  $z$ .

## Chapter 7

# Axially Loaded Column of Compressible Elastic Material

### 7.1 Introduction

This work investigates the deformation of a compressible isotropic elastic column under an axial load. Just as for the incompressible material, the mathematical solutions are formulated in terms of Fourier transforms and involve Bessel-Fourier series and modified Bessel functions. Let cylindrical polar coordinates be chosen so that the column occupies the region

$$0 \leq r \leq R, \quad -\pi \leq \theta \leq \pi, \quad 0 \leq z \leq L.$$

Outer boundary  $r = R$  is assumed to be stress-free and the column is compressed axially by equal and opposite loads applied to faces  $z = 0$  and  $z = L$ . These loads are applied over plates which are bounded by  $z = 0$  and  $z = L$  in such a way that no radial displacement is possible there. Axial displacement is zero on the lower boundary and  $H$  (constant) on the upper boundary where  $H$  is determined by the loading.

### 7.2 Linear Deformation of a Slab

Suppose that the resulting displacement field has form

$$\mathbf{v} = w(r, z)\mathbf{e}_r + h(r, z)\mathbf{e}_z, \quad (7.2.1)$$

for symmetrical loading about the  $z$  axis. When (7.2.1) is substituted into the linear stress tensor (2.2.26), the non-zero components of stress are

$$\begin{aligned} S_{11} &= \lambda \left( \frac{\partial h}{\partial z} + \frac{w}{r} \right) + (\lambda + 2\mu) \frac{\partial w}{\partial r} , \\ S_{22} &= \lambda \left( \frac{\partial h}{\partial z} + \frac{\partial w}{\partial r} \right) + (\lambda + 2\mu) \frac{w}{r} , \\ S_{33} &= \lambda \left( \frac{\partial w}{\partial r} + \frac{w}{r} \right) + (\lambda + 2\mu) \frac{\partial h}{\partial z} , \\ S_{13} &= S_{31} = \mu \left( \frac{\partial w}{\partial z} + \frac{\partial h}{\partial r} \right) . \end{aligned} \tag{7.2.2}$$

In the absence of externally applied body forces, the momentum equations reduce to the radial and axial equations

$$\begin{aligned} \frac{\partial S_{11}}{\partial r} + \frac{\partial S_{13}}{\partial z} + \frac{1}{r}(S_{11} - S_{22}) &= 0 \\ \frac{\partial S_{13}}{\partial r} + \frac{\partial S_{33}}{\partial z} + \frac{S_{13}}{r} &= 0 , \end{aligned} \tag{7.2.3}$$

since the azimuthal equation is identically satisfied. When expressions (7.2.2) are substituted into expressions (7.2.3), the resulting system of fourth order partial differential equations is

$$\begin{aligned} 2\gamma \left( \frac{\partial^2 w}{\partial r^2} + \frac{1}{r} \frac{\partial w}{\partial r} - \frac{w}{r^2} + \frac{\partial^2 h}{\partial z \partial r} \right) - \frac{\partial^2 w}{\partial z^2} + \frac{\partial^2 h}{\partial z \partial r} &= 0 , \\ (1 + 2\gamma) \left( \frac{\partial^2 w}{\partial z \partial r} + \frac{1}{r} \frac{\partial w}{\partial z} \right) + 2\gamma \frac{\partial^2 h}{\partial z^2} - \frac{\partial^2 h}{\partial r^2} - \frac{1}{r} \frac{\partial h}{\partial r} &= 0 , \end{aligned} \tag{7.2.4}$$

where  $\gamma = -(\lambda + 2\mu)/2\mu$ .

### 7.2.1 Boundary Conditions

The solution to equations (7.2.4) are required to ensure that boundaries  $r = 0$  and  $r = R$  are stress free, radial displacement  $w$  is zero on  $z = 0$  and  $z = L$ , while axial displacement  $h$  is zero on  $z = 0$  and  $H$  (constant) on  $z = L$ . Furthermore, all displacement are finite when  $r = 0$ . The boundary conditions are therefore

$$\begin{aligned} \frac{\partial w}{\partial z} + \frac{\partial h}{\partial r} &= \gamma \frac{\partial w}{\partial r} + (1 + \gamma) \left( \frac{\partial h}{\partial z} + \frac{w}{r} \right) = 0 \quad \text{on } r = R & 0 < z < L \\ w = 0, \quad h = 0, & \quad \text{on } z = 0 & 0 \leq z \leq R \\ w = 0, \quad h = H, & \quad \text{on } z = L & 0 \leq z \leq R, \end{aligned} \tag{7.2.5}$$

where  $H$  is an unknown constant to be determined by the applied normal load  $F\mathbf{e}_3$  where

$$F = - \iint S_{33} dA . \quad (7.2.6)$$

This load condition will be discussed later.

## 7.2.2 Non-dimensional Problem

In order to solve equations (7.2.4), non-dimensional coordinates  $r^*$ ,  $z^*$  non-dimensional displacements  $u^*$  and  $h^*$  and parameter  $\nu$  are introduced by the definitions

$$r^* = \frac{r}{R}, \quad z^* = \frac{z}{L}, \quad \nu = \frac{L}{R}, \quad u^* = \frac{w}{L}, \quad h^* = \frac{h}{L} . \quad (7.2.7)$$

The correspondence non-dimensional form of the momentum equations (7.2.4) is

$$\begin{aligned} 2\gamma\nu^2 \left( \frac{\partial^2 u}{\partial r^2} + \frac{1}{r} \frac{\partial u}{\partial r} - \frac{u}{r^2} \right) - \frac{\partial^2 u}{\partial z^2} + \nu(1+2\gamma) \frac{\partial^2 h}{\partial z \partial r} &= 0 , \\ \nu(1+2\gamma) \left( \frac{\partial^2 u}{\partial z \partial r} + \frac{1}{r} \frac{\partial u}{\partial z} \right) + 2\gamma \frac{\partial^2 h}{\partial z^2} - \nu^2 \left( \frac{\partial^2 h}{\partial r^2} + \frac{1}{r} \frac{\partial h}{\partial r} \right) &= 0 , \end{aligned} \quad (7.2.8)$$

which are to be solved with non-dimensional boundary conditions

$$\begin{aligned} \frac{\partial u}{\partial z} + \nu \frac{\partial h}{\partial r} &= \nu \gamma \frac{\partial u}{\partial r} + (1+\gamma) \left( \frac{\partial h}{\partial z} + \nu \frac{u}{r} \right) = 0 \quad \text{on } r=1 \quad 0 < z < 1 \\ u &= 0, \quad h = 0, \quad \text{on } z=0 \quad 0 \leq r \leq 1 \\ u &= 0, \quad h = H, \quad \text{on } z=1 \quad 0 \leq r \leq 1 . \end{aligned} \quad (7.2.9)$$

## 7.3 Solution Procedure

### 7.3.1 Transformed Equations

The general solution of equations (7.2.8) can be obtained by using finite Fourier transforms. Let  $u$  and  $h$  have half range Fourier series

$$\begin{aligned} u(r, z) &= 2 \sum_{l=1}^{\infty} \bar{u}_l \sin l\pi z , \\ h(r, z) &= h_0(r) + 2 \sum_{l=1}^{\infty} \bar{h}_l \cos l\pi z , \end{aligned} \quad (7.3.10)$$

where  $\bar{u}_l$  and  $\bar{h}_l$  are represented by

$$\bar{u}_l = \bar{u}(r, l) = \int_0^1 u(r, z) \sin l\pi z dz , \quad \bar{h}_l = \bar{h}(r, l) = \int_0^1 h(r, z) \cos l\pi z dz , \quad (7.3.11)$$

and

$$h_0(r) = \int_0^1 h(r, z) dz . \quad (7.3.12)$$

By multiplying the first equation of (7.2.8) by  $\sin l\pi z$  and the second equation of (7.2.8) by  $\cos l\pi z$  and then integrating with respect to  $z$  over  $(0, 1)$ , it follows that  $\bar{u}_l$  and  $\bar{h}_l$  satisfy the ordinary differential equations

$$\begin{aligned} 2\gamma \left( \frac{d^2 \bar{u}_l}{dr^2} + \frac{1}{r} \frac{d\bar{u}_l}{dr} - \frac{\bar{u}_l}{r^2} \right) - \alpha(1 + 2\gamma) \frac{d\bar{h}_l}{dr} + \alpha^2 \bar{u}_l &= 0 , \\ \frac{d^2 \bar{h}_l}{dr^2} + \frac{1}{r} \frac{d\bar{h}_l}{dr} + 2\alpha^2 \gamma \bar{h}_l - \alpha(1 + 2\gamma) \left( \frac{d\bar{u}_l}{dr} + \frac{\bar{u}_l}{r} \right) &= \frac{2\gamma}{\nu^2} g(r) , \end{aligned} \quad (7.3.13)$$

where

$$g(r) = (-1)^l g_1(r) - g_0(r) , \quad g_0(r) = \frac{\partial h(r, 0)}{\partial z} , \quad g_1(r) = \frac{\partial h(r, 1)}{\partial z} , \quad \alpha = \frac{l\pi}{\nu} . \quad (7.3.14)$$

The transformed boundary conditions are

$$\frac{d\bar{h}_l}{dr} + \alpha \bar{u}_l = \gamma \frac{d\bar{u}_l}{dr} + (1 + \gamma) \left( \frac{\bar{u}_l}{r} - \alpha \bar{h}_l \right) = 0 , \quad \text{on} \quad r = 1 \quad 0 \leq z \leq 1 \quad (7.3.15)$$

### 7.3.2 General Solution

For convenience, let auxiliary functions  $\hat{\phi}$  and  $\hat{\psi}$  be defined by the relationships

$$\hat{\phi} = \frac{d\bar{h}_l}{dr} - \alpha \bar{u}_l \quad \hat{\psi} = \frac{d\bar{u}_l}{dr} + \frac{\bar{u}_l}{r} - \alpha \bar{h}_l . \quad (7.3.16)$$

From equation (7.3.13) it can easily be shown that  $\hat{\phi}$  and  $\hat{\psi}$  satisfy ordinary differential equations

$$2\gamma \frac{d\hat{\psi}}{dr} - \alpha \hat{\phi} = 0 \quad \frac{d\hat{\phi}}{dr} + \frac{\hat{\phi}}{r} - 2\alpha\gamma \hat{\psi} = \frac{2\gamma}{\nu^2} g(r) . \quad (7.3.17)$$

Equations (7.3.17) can be arranged as the fourth order system of ordinary differential equations

$$\begin{aligned} \frac{d^2 \hat{\phi}}{dr^2} + \frac{1}{r} \frac{d\hat{\phi}}{dr} - \left( \alpha^2 + \frac{1}{r^2} \right) \hat{\phi} &= \frac{2\gamma}{\nu^2} \frac{dg(r)}{dr} , \\ \frac{d^2 \hat{\psi}}{dr^2} + \frac{1}{r} \frac{d\hat{\psi}}{dr} - \alpha^2 \hat{\psi} &= \frac{\alpha}{\nu^2} g(r) . \end{aligned} \quad (7.3.18)$$

The finiteness of  $h$  and  $u$  at  $r = 0$  leads to the general solutions

$$\begin{aligned} \hat{\phi} &= AI_1(\alpha r) + \frac{2\alpha\gamma}{\nu^2} \int_0^r tg(t) [I_0(\alpha t)K_1(\alpha r) + K_0(\alpha t)I_1(\alpha r)] dt , \\ \hat{\psi} &= \frac{A}{2\gamma} I_0(\alpha r) - \frac{\alpha}{\nu^2} \int_0^r tg(t) [I_0(\alpha t)K_0(\alpha r) - K_0(\alpha t)I_0(\alpha r)] dt . \end{aligned} \quad (7.3.19)$$



The corresponding general expressions for  $\bar{u}_l$  and  $\bar{h}_l$ , are obtained by substituting (7.3.17) into (7.3.18). The result is

$$\begin{aligned}
 \bar{u}_l &= \frac{A}{2\alpha}[(1 + 1/2\gamma)\alpha r I_0(\alpha r) - 2I_1(\alpha r)] + BI_1(\alpha r) \\
 &\quad - \frac{\alpha(1 + 2\gamma)}{2\nu^2} r \int_0^r t g(t) [I_0(\alpha t) K_0(\alpha r) - K_0(\alpha t) I_0(\alpha r)] dt \\
 &\quad + \frac{\alpha(1 + 2\gamma)}{2\nu^2} r \int_0^r t^2 g(t) [I_1(\alpha t) K_1(\alpha r) - K_1(\alpha t) I_1(\alpha r)] dt, \\
 \bar{h}_l &= \frac{A}{2\alpha}(1 + 1/2\gamma)r I_1(\alpha r) + BI_0(\alpha r) \\
 &\quad + \frac{\alpha(1 + 2\gamma)}{2\nu^2} r \int_0^r t g(t) [I_0(\alpha t) K_1(\alpha r) + K_0(\alpha t) I_1(\alpha r)] dt \\
 &\quad - \frac{\alpha(1 + 2\gamma)}{2\nu^2} r \int_0^r t^2 g(t) [I_1(\alpha t) K_1(\alpha r) - K_1(\alpha t) I_1(\alpha r)] dt \\
 &\quad - \frac{2\gamma}{\nu^2} \int_0^r t g(t) [I_0(\alpha t) K_0(\alpha r) - K_0(\alpha t) I_0(\alpha r)] dt.
 \end{aligned} \tag{7.3.20}$$

Constants  $A$  and  $B$  are determined from boundary conditions (7.2.9) at  $r = 1$ .

## 7.4 Fourier-Bessel Series Representation

The solutions (7.3.20) contain integrals involving the unknown function  $g(r)$ . Let  $g(r)$  be represented by a Bessel series

$$f(r) = \gamma g(r) = f_0 + \sum_{k=1}^{\infty} f_k J_0(\lambda_k r), \tag{7.4.21}$$

where  $\lambda_k$  are the roots of  $J_1(r) = 0$ . When expression (7.4.21) is substituted into (7.3.20), the resulting integrals can be computed exactly (see appendix B). The revised expressions for  $\bar{u}_l$  and  $\bar{h}_l$  in terms of  $J_0(\lambda r)$  and  $J_1(\lambda r)$  are respectively

$$\begin{aligned}
 \bar{u}_l &= \frac{A}{2\alpha}[\alpha(1 + \frac{1}{2\gamma})r I_0(\alpha r) - 2I_1(\alpha r)] + BI_1(\alpha r) - \frac{\alpha}{\nu^2} \sum_{k=1}^{\infty} \beta_k f_k J_1(\lambda_k r) \\
 \bar{h}_l &= \frac{A}{2}(1 + \frac{1}{2\gamma})r I_1(\alpha r) + BI_0(\alpha r) + \frac{f_0}{\alpha^2 \nu^2 \gamma} + \frac{1}{\nu^2} \sum_{k=1}^{\infty} \eta_k f_k J_0(\lambda_k r).
 \end{aligned} \tag{7.4.22}$$

where

$$\beta_k = \frac{(1 + 2\gamma)\lambda_k}{2\gamma(\alpha^2 + \lambda_k^2)^2}, \quad \eta_k = \frac{\alpha^2 - 2\gamma\lambda_k^2}{2\gamma(\alpha^2 + \lambda_k^2)^2}. \tag{7.4.23}$$

Here constants  $A$  and  $B$  are determined from boundary conditions on  $r = 1$ . After some straightforward algebra, it can be shown that

$$A = \frac{I_1(\alpha)}{\nu^2 \phi(\alpha, \gamma)} [2\alpha^2 \sum_{n=1}^{\infty} f_n \chi_n J_0(\lambda_n) + (1 + \frac{1}{2\gamma}) f_0], \quad (7.4.24)$$

$$B = \frac{1}{2\nu^2 \alpha \phi(\alpha, \gamma)} [2\alpha^2 \sum_{n=1}^{\infty} f_n \chi_n J_0(\lambda_n) + (1 + \frac{1}{2\gamma}) f_0] [I_1(\alpha) - \alpha(1 + \frac{1}{2\gamma}) I_0(\alpha)],$$

where

$$\chi_n = \frac{(2\gamma + 1)\alpha^2 - 2\gamma\lambda_n^2}{2\gamma(\alpha^2 + \lambda_n^2)^2}, \quad \phi(\alpha, \gamma) = \alpha^2(1 + \frac{1}{2\gamma}) [I_0^2(\alpha) - I_1^2(\alpha)] - I_1^2(\alpha).$$

In order to combine the individual terms in expressions (7.4.22), we observe that  $rI_0(\alpha r)$ ,  $I_1(\alpha r)$ ,  $rI_1(\alpha r)$ , and  $rI_0(\alpha r)$  have Fourier-Bessel series (see appendix B)

$$I_0(\alpha r) = \frac{2I_1(\alpha)}{\alpha} + 2\alpha I_1(\alpha) \sum_{k=1}^{\infty} \frac{J_0(\lambda_k r)}{(\alpha^2 + \lambda_k^2) J_0(\lambda_k)}, \quad (7.4.25)$$

$$rI_1(\alpha r) = \frac{2}{\alpha^2} (\alpha I_0(\alpha) - 2I_1(\alpha)) + 2 \sum_{k=1}^{\infty} \frac{J_0(\lambda_k r)}{J_0(\lambda_k)} \left[ \frac{\alpha I_0(\alpha)}{\alpha^2 + \lambda_k^2} - \frac{2\alpha^2 I_1(\alpha)}{(\alpha^2 + \lambda_k^2)^2} \right],$$

and

$$I_1(\alpha r) = -2I_1(\alpha) \sum_{k=1}^{\infty} \frac{\lambda_k}{\alpha^2 + \lambda_k^2} \frac{J_1(\lambda_k r)}{J_0(\lambda_k)}, \quad (7.4.26)$$

$$rI_0(\alpha r) = \sum_{k=1}^{\infty} \frac{J_1(\lambda_k r)}{J_0(\lambda_k)} \left[ \frac{4\alpha\lambda_k}{(\alpha^2 + \lambda_k^2)^2} I_1(\alpha) - \frac{2\lambda_k}{\alpha^2 + \lambda_k^2} I_0(\alpha) \right].$$

These results, when deployed in (7.4.22), yield

$$\begin{aligned} \bar{u}_l &= \frac{1}{\nu^2} \sum_{k=1}^{\infty} \frac{J_1(\lambda_k r)}{J_0(\lambda_k)} \left[ \frac{\lambda_k \xi_k I_1^2(\alpha)}{\alpha \gamma \phi(\alpha)} (\alpha^2 \gamma \Omega + (1 + \gamma) f_0) - \alpha f_k \beta_k J_0(\lambda_k) \right] \\ \bar{h}_l &= \frac{f_0}{\nu^2 \alpha^2} \left[ \frac{1}{2\gamma} - (1 + \frac{1}{\gamma})^2 \frac{I_1^2(\alpha)}{\phi(\alpha)} \right] - \frac{I_1^2(\alpha) \Omega}{\nu^2 \phi(\alpha)} (1 + \frac{1}{\gamma}) \\ &\quad - \frac{I_1^2(\alpha)}{\nu^2 \phi(\alpha)} \sum_{k=1}^{\infty} \frac{J_0(\lambda_k r)}{J_0(\lambda_k)} \left[ \alpha^2 \chi_k \Omega + \chi_k f_0 (1 + \frac{1}{\gamma}) - \frac{\phi(\alpha)}{I_1^2(\alpha)} J_0(\lambda_k) \eta_k \right], \end{aligned} \quad (7.4.27)$$

where

$$\xi_k = \frac{\gamma \lambda_k^2 + \alpha^2 (1 + 3\gamma)}{\gamma (\alpha^2 + \lambda_k^2)^2}. \quad (7.4.28)$$

### 7.4.1 Evaluation of the applied force

The applied force (7.2.6) on the top of the column is now computed by

$$F^{(1)} = -\frac{1}{2\pi(\lambda + 2\mu)R^2} \lim_{z \rightarrow 1} \iint S_{33} dA \quad (7.4.29)$$

and it can be rewritten in the form

$$F^{(1)} = -\frac{1}{2\pi(\lambda + 2\mu)R^2} \lim_{z \rightarrow 1} \int_0^1 r \frac{\partial h}{\partial z} dr . \quad (7.4.30)$$

since the radial displacement  $u \equiv 0$  everywhere on  $z = 1$ . When functions  $g_0$  and  $g_1$  are substituted into series (7.4.21) and using the definition of the function  $f(r)$  (7.4.21), it can be easily shown that force takes the form for the top  $F_1$  and bottom  $F_0$  surface respectively

$$F^{(0)} = \mu f_0^{(0)} , \quad F^{(1)} = -\mu f_0^{(1)} , \quad (7.4.31)$$

since  $\lambda_k$  are the roots of  $J_1(\lambda_k) = 0$ .

### 7.4.2 Evaluation of Functions $h_0(r)$

Functions  $h_0(r)$ , which are required for series (7.3.10), can now be determined. Integrate the second of momentum equations (7.2.6) with respect to  $z$  over  $[0, 1]$  to obtain

$$\begin{aligned} \frac{d^2 h_0}{dr^2} + \frac{1}{r} \frac{dh_0}{dr} &= \frac{2\gamma}{\nu^2} [g_1(r) - g_0(r)] , \\ &= \frac{1}{\nu^2} [f_1(r) - f_0(r)] , \\ &= \frac{1}{\nu^2} (f_0^{(1)} - f_0^{(0)}) + \frac{1}{\nu^2} \sum_{k=1}^{\infty} (f_k^{(1)} - f_k^{(0)}) J_0(\lambda_k r) . \end{aligned} \quad (7.4.32)$$

When (7.4.32) is integrated with respect to  $r$ , bearing in mind that the function  $h_0(r)$  is finite at  $r = 0$ , i.e the term contain the logarithm is removed, and leads to the final solution, so that

$$h_0(r) = C + \frac{r^2}{4\nu^2} (f_0^{(1)} - f_0^{(0)}) - \frac{1}{\nu^2} \sum_{n=1}^{\infty} \frac{f_n^{(1)} - f_n^{(0)}}{\lambda_n^2} J_0(\lambda_n r) , \quad (7.4.33)$$

Now, functions  $u(r, z)$  and  $h(r, z)$  (7.3.10) have final form when (7.4.27) and (7.4.33) are substituted into (7.3.10).

### 7.4.3 Evaluation of $u(1, z)$

The deformed surface  $u(1, z)$  is expressed by

$$u(1, z) = 2 \sum_{l=1}^{\infty} \bar{u}_l(1, l) \sin l\pi z , \quad (7.4.34)$$

where  $\bar{u}_l(1, l\pi)$  cannot be evaluated from (7.4.27) since  $\lambda_k$  are the roots of  $J_1(x) = 0$ . Then, using the expression for  $\bar{u}_l$  in (7.4.22) and replacing  $r$  with 1, expression  $u(1, z)$  takes final form (after simplification)

$$u(1, z) = \frac{1}{\nu^2} \sum_{j=1}^{\infty} \frac{I_1^2(\alpha_{2j-1})}{\phi(\alpha_{2j-1})} \left[ \left(1 + \frac{1}{\gamma}\right) \frac{4F}{\alpha_{2j-1} - \alpha_{2j-1}\Omega} \right] \sin(2j-1)\pi z, \quad (7.4.35)$$

where  $F$  denotes the applied force.

## 7.5 Boundary Conditions

In this section, unknown constant  $H$  and coefficients  $f_k$  are determined from boundary conditions  $h(r, 0) = 0$  and  $h(r, 1) = H$  and from the applied force, so that

$$\begin{aligned} h(r, 0) &= h_0(r) + 2 \sum_{j=1}^{\infty} h_{2j-1}(r, \alpha_{2j-1}) = 0 \\ h(r, 1) &= h_0(r) - 2 \sum_{j=1}^{\infty} h_{2j-1}(r, \alpha_{2j-1}) = H, \end{aligned} \quad (7.5.36)$$

where

$$h_{2j-1} = \frac{1}{\nu^2} \sum_{k=1}^{\infty} \frac{J_0(r\lambda_k)}{J_0(\lambda_k)} [\Psi(\alpha_{2j-1})\chi_k - 2f_k\eta_k J_0(\lambda_k)] + \frac{1}{\gamma\alpha^2\nu^2} [(1+\gamma)\Psi(\alpha_{2j-1}) - 2F], \quad (7.5.37)$$

in which

$$\Psi(\alpha_{2j-1}) = \frac{I_1^2(\alpha_{2j-1})}{\gamma\phi(\gamma\alpha_{2j-1})} [4F(1+\gamma) - \Omega\gamma\alpha^2].$$

It can easily be shown that  $h_0(r) = C$  because the even coefficients are zero, it is clear that  $H = 2C$ .

$$C = \frac{4}{\nu^2} \sum_{j=1}^{\infty} \left[ \frac{F}{\gamma\alpha_{2j-1}^2} - \left(1 + \frac{1}{\gamma}\right) \frac{I_1^2(\alpha_{2j-1})}{\phi(\alpha_{2j-1})} \left( \left(1 + \frac{1}{\gamma}\right) \frac{2F}{\alpha_{2j-1}^2} + \sum_{n=1}^{\infty} f_n J_0(\lambda_n) \chi_{2j-1,n} \right) \right]. \quad (7.5.38)$$

The resulting of the sum (7.5.36) is the following equation which determin the coefficients  $f_k$ , so that

$$\sum_{n=1}^{\infty} f_n \chi_{2j-1,n} J_0(\lambda_n) \sum_{j=1}^{\infty} \frac{I_1^2(\alpha_{2j-1})}{\phi(\alpha_{2j-1})} \alpha_{2j-1}^2 \chi_{2j-1,k} - f_k \sum_{j=1}^{\infty} \eta_{2j-1,k} = -2F(1+1/\gamma) \sum_{j=1}^{\infty} \frac{I_1^2(\alpha_{2j-1})}{\phi(\alpha_{2j-1})} \chi_{2j-1,k} \quad (7.5.39)$$

## 7.6 Results and Conclusion

Radial displacement and axial displacement are examined for various values of  $\nu = 0.5, 1.0, 2.0, 3.0, 4.0$  and  $5.0$  and for  $\gamma = -1.1, -1.5, -3.0$  and  $-6.7$ ; that is, from highly compressible to slightly compressible materials.

Figure 7.1 shows the behaviour of radial displacement  $u(1, z)$ . The behaviour of radial displacement is different from that of Moghe and Neff's suggestion [27]. They said "The proper choice of zeros of the bessel function becomes quite important", and they gave two different shapes of radial displacement which are dependent on choice of zeros that is, for roots of  $J_0(\lambda_k) = 0$  and  $J_1(\lambda_k) = 0$ . Their suggestion is right for the zeros of  $J_0$  but it is wrong for the zeros of  $J_1$ . Therefore during this work zeros for bessel function  $J_1$  are taken and examined for different materials, from highly compressible  $\gamma = -1.1$  to slightly compressible  $\gamma = -6.75$ . Figure 7.2 shows behaviour of axial displacement,  $h(r, z)$ , for different values of  $\nu$ . It is clear that the center region of the cylinder is almost flat.

**special cas  $\gamma \rightarrow -\infty$**

When  $\gamma \rightarrow -\infty$  the result for compressible material is the same result for incompressible material, the mathematical procedure is similar to recorded in appendix A for chapter 5.

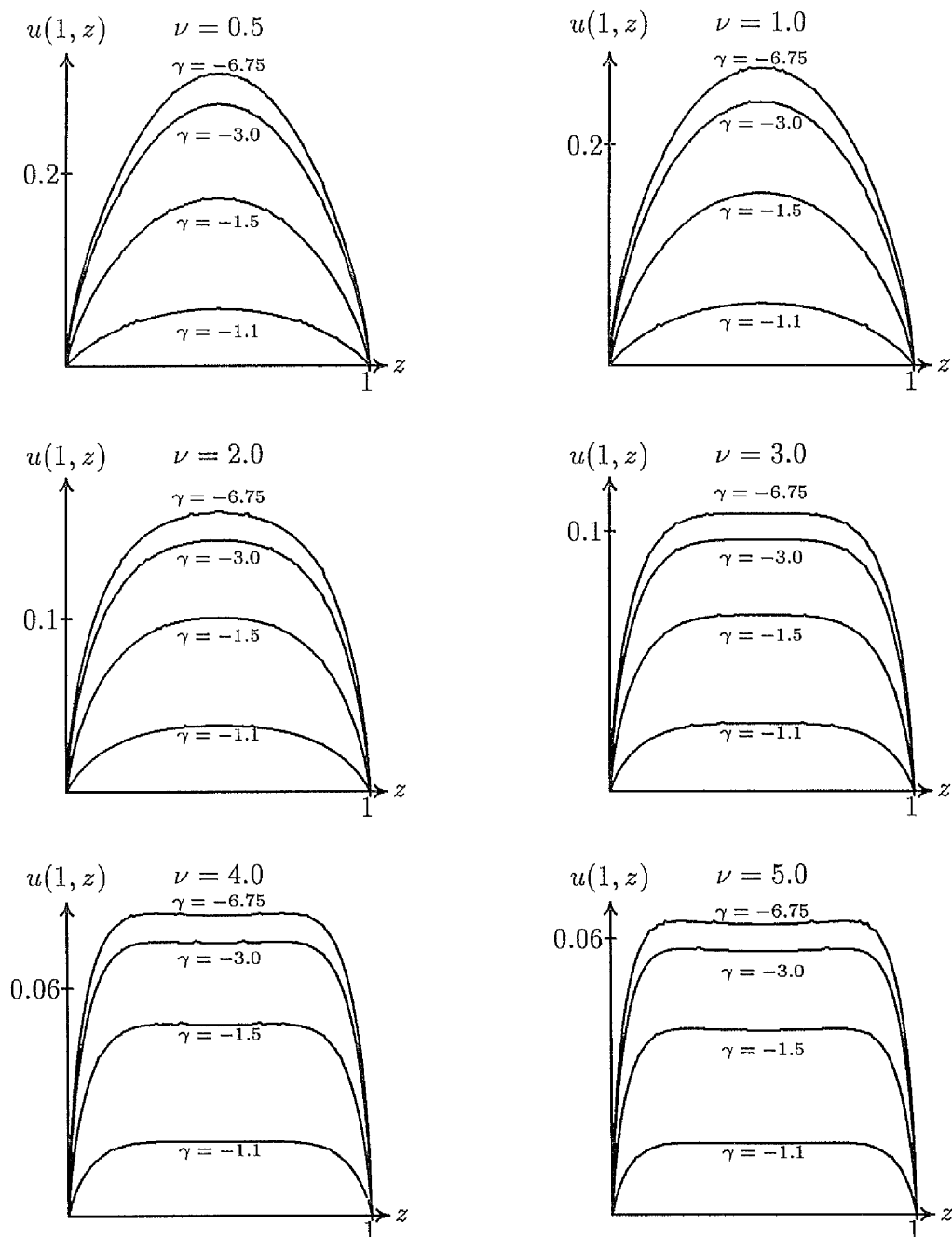


Figure 7.1: Graphs of  $u(1, z)$  for  $\nu = 0.25, 0.5, 1.0$ .

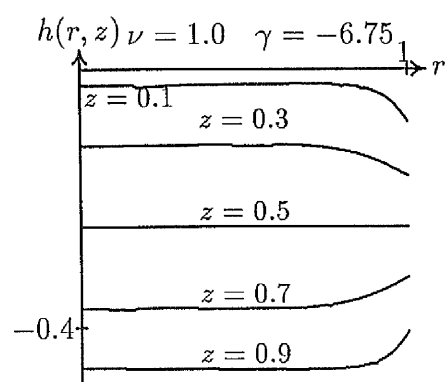
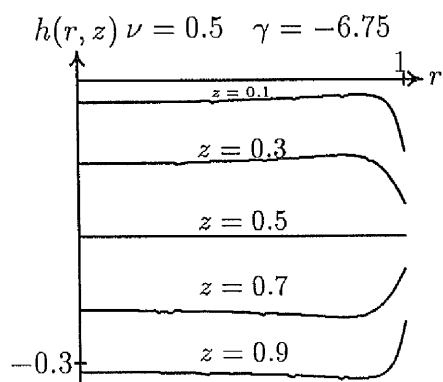
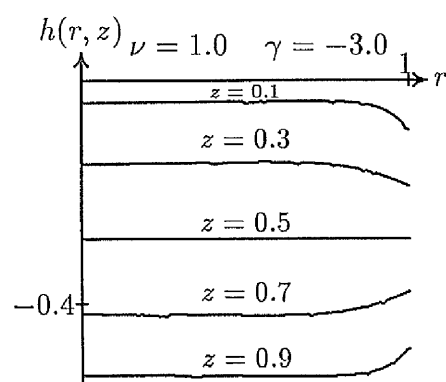
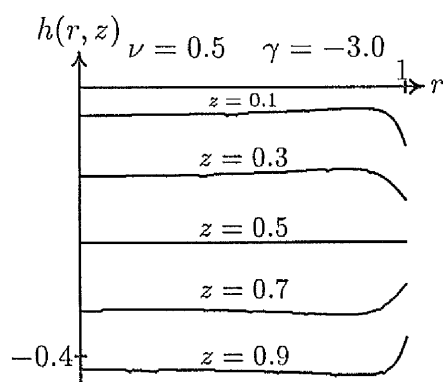
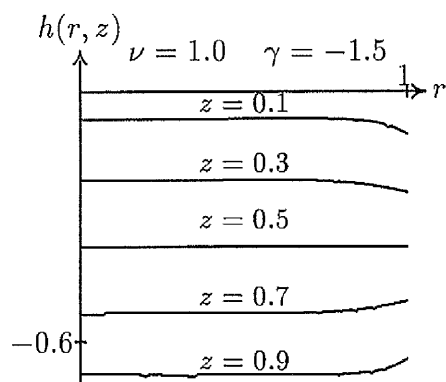
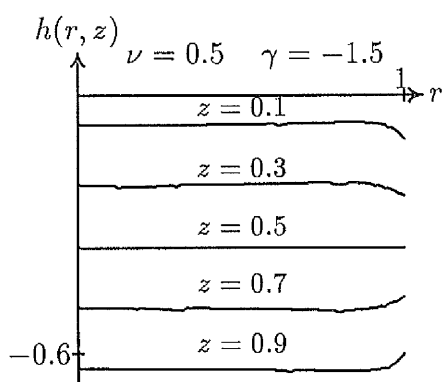
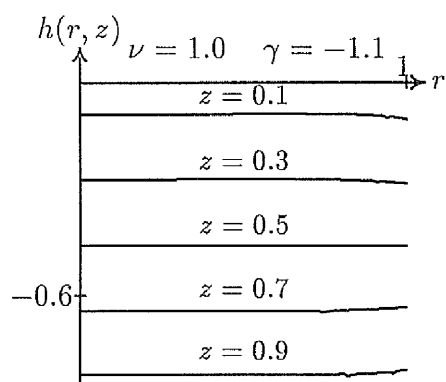
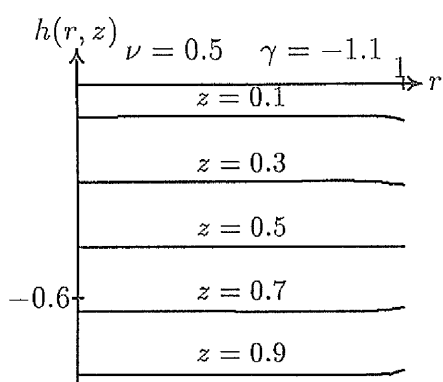


Figure 7.2: Graphs of  $h(r, z)$  when  $\nu = 0.25, 0.5, 1.0$  and for different values of  $z$ .

	$\gamma = -1.1$	$\gamma = -1.5$	$\gamma = -3.0$	$\gamma = -6.75$
$\nu = 0.5$	-0.913	-0.708	-0.464	-0.334
$\nu = 1.0$	-0.916	-0.743	-0.569	-0.490
$\nu = 1.5$	-0.918	-0.762	-0.620	-0.560
$\nu = 2.0$	-0.919	-0.772	-0.645	-0.593
$\nu = 2.5$	-0.920	-0.778	-0.659	-0.612
$\nu = 3.0$	-0.920	-0.781	-0.668	-0.624
$\nu = 3.5$	-0.920	-0.784	-0.675	-0.633
$\nu = 4.0$	-0.921	-0.786	-0.680	-0.639
$\nu = 4.5$	-0.921	-0.788	-0.684	-0.644
$\nu = 5.0$	-0.922	-0.789	-0.687	-0.648

Table 7.1: Table of compressible axial displacement H for different values of  $\nu$ .



# Appendix A

## Results for Chapters 4 and 5

### Some Evaluated Integrals

In this section, some integrals which have been involved in chapters 4 and 5 are evaluated.

Let Weber-Orr transforms be introduced as

$$\bar{u}(z, \lambda) = \int_1^\beta ru(r, z)C_{11}(\lambda r, \lambda)dr, \quad \bar{h}(z, \lambda) = \int_1^\beta rh(r, z)C_{01}(\lambda r, \lambda)dr, \quad (\text{A.1})$$

where the parameter  $\lambda$  is chosen to be a root of  $C_{11}(\beta\lambda, \lambda) = 0$ .

$$\begin{aligned} I_1 &= \int_1^\beta \frac{\partial}{\partial r} \left( \frac{\partial u}{\partial r} + \frac{u}{r} \right) r C_{11}(\lambda r, \lambda) dr, \\ &= [r C_{11}(\lambda r, \lambda) \left( \frac{\partial u}{\partial r} + \frac{u}{r} \right)]_1^\beta - \lambda \int_1^\beta \left( \frac{\partial u}{\partial r} + \frac{u}{r} \right) r C_{01}(\beta\lambda, \lambda) dr, \\ &= -\lambda \int_1^\beta \frac{\partial}{\partial r} (ru) C_{01}(\beta\lambda, \lambda) dr, \\ &= -\lambda [ru C_{01}(\lambda r, \lambda)]_1^\beta - \lambda^2 \int_1^\beta ru C_{11}(\beta\lambda, \lambda) dr \end{aligned} \quad (\text{A.2})$$

Hence

$$\int_1^\beta \frac{\partial}{\partial r} \left( \frac{\partial u}{\partial r} + \frac{u}{r} \right) r C_{11}(\lambda r, \lambda) dr = -\lambda^2 \bar{u} \quad (\text{A.3})$$

and also

$$\int_1^\beta \left( \frac{\partial u}{\partial r} + \frac{u}{r} \right) r C_{01}(\lambda r, \lambda) dr = \lambda \bar{u} \quad (\text{A.4})$$

Since  $u(1, z) = u(\beta, z) = 0$  and  $C_{11}(\lambda, \lambda) = 0$ .

$$\begin{aligned}
I_2 &= \int_1^\beta \left( \frac{\partial^2 h}{\partial r^2} + \frac{1}{r} \frac{\partial h}{\partial r} \right) r C_{01}(\lambda r, \lambda) dr, \\
&= [C_{01}(\lambda r, \lambda) \frac{\partial h}{\partial r}]_1^\beta + \lambda \int_1^\beta r \frac{\partial h}{\partial r} C_{11}(\beta \lambda, \lambda) dr, \\
&= \beta C_{01}(\beta \lambda, \lambda) \frac{\partial h}{\partial r} \Big|_{r=\beta} - C_{01}(\lambda, \lambda) \frac{\partial h}{\partial r} \Big|_{r=1} + \lambda \int_1^\beta \frac{\partial h}{\partial r} r C_{11}(\lambda r, \lambda) dr, \\
&= \frac{2}{\pi \lambda} g(z) + \lambda [r h C_{11}(\lambda r, \lambda)]_1^\beta - \lambda^2 \int_1^\beta r h C_{01}(\lambda r, \lambda) dr,
\end{aligned} \tag{A.5}$$

Hence

$$\int_1^\beta \left( \frac{\partial^2 h}{\partial r^2} + \frac{1}{r} \frac{\partial h}{\partial r} \right) r C_{01}(\lambda r, \lambda) dr = \frac{2}{\pi \lambda} g(z) - \lambda^2 \bar{h} \tag{A.6}$$

and also

$$\int_1^\beta r \frac{\partial h}{\partial r} C_{11}(\lambda r, \lambda) dr = -\lambda \bar{h}. \tag{A.7}$$

since  $h(\beta, z) = 0$  and where

$$g(z) = \frac{\partial h}{\partial r} \Big|_{r=1} - \frac{J_1(\lambda)}{J_1(\beta \lambda)} \frac{\partial h}{\partial r} \Big|_{r=\beta}. \tag{A.8}$$

## General Solution

In this section, solutions of differential equations (5.5.18) are discussed:

$$\begin{aligned}
2\lambda^2 \nu^2 (\gamma - i\xi) \bar{u} + \lambda \nu (1 + 2\gamma - i\xi) \frac{d\bar{h}}{dz} + (1 + i\xi) \frac{d^2 \bar{u}}{dz^2} &= -\sigma \bar{u} \\
\lambda^2 \nu^2 (1 + i\xi) \bar{h} + \lambda \nu (1 + 2\gamma - i\xi) \frac{d\bar{u}}{dz} + 2(\gamma - i\xi) \frac{d^2 \bar{h}}{dz^2} &= \sigma \bar{h} + \frac{2\nu^2 (1 + i\xi)}{\pi \lambda} g(z).
\end{aligned} \tag{A.9}$$

Equations (5.5.18) can be rewritten in new form

$$\begin{aligned}
2\lambda \nu (\gamma - i\xi) (\lambda \nu \bar{u} + \frac{d\bar{h}}{dz}) + (1 + i\xi) \frac{d}{dz} (\lambda \nu \bar{h} + \frac{d\bar{u}}{dz}) &= -\sigma \bar{u} \\
\lambda \nu (1 + i\xi) (\lambda \nu \bar{h} + \frac{d\bar{u}}{dz}) + 2(\gamma - i\xi) \frac{d}{dz} (\lambda \nu \bar{u} + \frac{d\bar{h}}{dz}) &= \sigma \bar{h} + \frac{2\nu^2 (1 + i\xi)}{\pi \lambda} g(z).
\end{aligned} \tag{A.10}$$

Define

$$\phi = \lambda\nu\bar{u} + \frac{d\bar{h}}{dz} \quad \psi = \lambda\nu\bar{h} + \frac{d\bar{u}}{dz} . \quad (\text{A.11})$$

When (A.11) is substituted into (A.10), equation (A.10) becomes

$$\begin{aligned} 2\lambda\nu(\gamma - i\xi)\phi + (1 + i\xi)\frac{d\psi}{dz} &= -\sigma\bar{u} \\ \lambda\nu(1 + i\xi)\psi + 2(\gamma - i\xi)\frac{d\phi}{dz} &= \sigma\bar{h} + \frac{2\nu^2(1 + i\xi)}{\pi\lambda}g(z) . \end{aligned} \quad (\text{A.12})$$

Then

$$\begin{aligned} \frac{d^2\psi}{dz^2} - \omega^2\psi &= -\frac{2\nu^3}{\pi\lambda}g(z) \\ \frac{d^2\phi}{dz^2} - \Omega^2\phi &= -\frac{\nu^2(1 + i\xi)}{\pi\lambda(\gamma - i\xi)}\frac{dg(z)}{dz} \end{aligned} \quad (\text{A.13})$$

where

$$\omega^2 = \lambda^2\nu^2 - \frac{\sigma}{1 + i\xi} \quad \Omega^2 = \lambda^2\nu^2 + \frac{\sigma}{2(\gamma - i\xi)} . \quad (\text{A.14})$$

It is clear that the full solution of (A.13) is

$$\begin{aligned} \psi &= A \sinh \omega z + B \cosh \omega z - \frac{2\nu^3}{\pi\omega} \int_0^z g(t) \sinh \omega(z - t) dt \\ \phi &= C \cosh \Omega z + D \sinh \Omega z + \frac{\nu^2(1 + i\xi)}{\pi\lambda(\gamma - i\xi)} \int_0^z g(t) \cosh \Omega(z - t) dt . \end{aligned} \quad (\text{A.15})$$

When (A.15) is substituted into (A.11) the result gives (5.6.23).

## Static Problem

In this section, the limit of  $\bar{h}_k$  as  $\sigma \rightarrow 0$  or as  $\xi \rightarrow 0$  is represented here for a compressible problem (see chapter 5). It is clear from (5.6.24) that when  $\sigma \rightarrow 0$  then  $\omega^2 \rightarrow \lambda^2\nu^2$  and  $\Omega^2 \rightarrow \lambda^2\nu^2$ , expression (5.7.36) for  $\bar{h}_k$  can be rewritten in the form

$$\bar{h}_k = \frac{l(1 + i\xi)}{\lambda^3\omega} \left[ 2\omega\lambda^2\nu^2 G_k \frac{K_k}{\sigma} + \frac{\phi_k}{\sigma} \frac{\sigma P_k}{Q} \sum_{n=1}^{\infty} (1 + (-1)^{n+k}) \frac{\chi_n}{\sigma} \right] . \quad (\text{A.16})$$

Let  $\omega_o = \lambda\nu$ . The limit of  $h_k$  involves the limits of  $K_k/\sigma$ ,  $\phi_k/\sigma$ ,  $\chi_k/\sigma$  and  $\sigma P_k/Q$ , as  $\sigma \rightarrow 0$ . Hence

$$\begin{aligned}\lim_{\sigma \rightarrow 0} \frac{K_k(\omega, \Omega)}{\sigma} &= \lim_{\sigma \rightarrow 0} \frac{1}{\sigma} \left[ \frac{\Omega^2}{\Omega^2 + l^2 \pi^2} - \frac{\lambda^2 \nu^2}{\omega^2 + l^2 \pi^2} \right] \\ &= \lim_{\sigma \rightarrow 0} \frac{\frac{l^2 \pi^2}{2(\gamma - i\xi)} - \frac{\Omega^2}{1 + i\xi}}{(\Omega^2 + l^2 \pi^2)(\omega^2 + l^2 \pi^2)} \\ &= \frac{l^2 \pi^2 - 2\gamma \omega_o^2}{2\gamma(\omega_o^2 + l^2 \pi^2)^2}\end{aligned}\tag{A.17}$$

$$\begin{aligned}\lim_{\sigma \rightarrow 0} \frac{\phi_k(\omega, \Omega)}{\sigma} &= \lim_{\sigma \rightarrow 0} \frac{1}{\sigma} \left[ \frac{\omega^2 + \lambda^2 \nu^2}{\Omega^2 + l^2 \pi^2} - \frac{2\lambda^2 \nu^2}{\omega^2 + l^2 \pi^2} \right] \\ &= \lim_{\sigma \rightarrow 0} \frac{\frac{\sigma}{(1 + i\xi)^2} - \frac{l^2 \pi^2 + 3\lambda^2 \nu^2}{1 + i\xi} - \frac{\lambda^2 \nu^2}{\gamma - i\xi}}{(\Omega^2 + l^2 \pi^2)(\omega^2 + l^2 \pi^2)} \\ &= -\frac{\omega_o^2(3\gamma + 1) + l^2 \pi^2 \gamma}{\gamma(\omega_o^2 + l^2 \pi^2)}\end{aligned}\tag{A.18}$$

$$\begin{aligned}\lim_{\sigma \rightarrow 0} \frac{\chi_k(\omega, \Omega)}{\sigma} &= \lim_{\sigma \rightarrow 0} \frac{1}{\sigma} \left[ \frac{\Omega^2(\omega^2 + \lambda^2 \nu^2)}{\Omega^2 + l^2 \pi^2} - \frac{2\lambda^2 \nu^2 \omega^2}{\omega^2 + l^2 \pi^2} + \lambda^2 \nu^2 - \omega^2 \right] \\ &= -l^2 \pi^2 \lim_{\sigma \rightarrow 0} \frac{\phi_k}{\sigma} \\ &= \frac{l^2 \pi^2 [\omega_o(1 + 3\gamma) + l^2 \pi^2 \gamma]}{\gamma(\omega_o^2 + l^2 \pi^2)^2}.\end{aligned}\tag{A.19}$$

The final part is to evaluate the limit of  $\sigma P_k/Q$ , where  $P_k$  and  $Q$  are defined in (5.7.49) and (5.7.33) respectively. The quantity  $P_k/Q$  can be simplified by using the facts

$$\sinh x = 2 \sinh(x/2) \cosh(x/2) \qquad \cosh x = \cosh^2(x/2) - \sinh^2(x/2)$$

hence

$$\frac{\sigma P_k}{Q} = \frac{\alpha \sigma}{2} \left[ \frac{(-1)^k - 1}{\alpha \tanh(\omega/2) - \tanh(\Omega/2)} + \frac{((-1)^k + 1) \tanh(\omega/2) \tanh(\Omega/2)}{\tanh(\omega/2) - \alpha \tanh(\Omega/2)} \right]. \tag{A.20}$$

The limit of  $\sigma P_k/Q$  requires finding the following quantity

$$\begin{aligned}\frac{d}{d\sigma} \left( \frac{1}{\alpha} \right) \Big|_{\sigma=0} &= \frac{d}{d\sigma} \left[ \frac{(\omega^2 + \lambda^2 \nu^2)^2}{4\omega \Omega \lambda^2 \nu^2} \right] \Big|_{\sigma=0} \\ &= \frac{1}{4\lambda^2 \nu^2} \frac{d}{d\sigma} \left[ \frac{\omega^3}{\Omega} + \frac{2\omega \lambda^2 \nu^2}{\Omega} + \frac{\lambda^4 \nu^4}{\omega \Omega} \right] \Big|_{\sigma=0} \\ &= \frac{-1 - 2\gamma}{4\gamma \lambda^2 \nu^2}.\end{aligned}\tag{A.21}$$

Now, by using L'Hôpital's rule, it can be shown that

$$\begin{aligned}\lim_{\sigma \rightarrow 0} \frac{\alpha \sigma}{\tanh(\Omega/2) - \alpha \tanh(\omega/2)} &= \lim_{\sigma \rightarrow 0} \frac{\sigma}{(1/\alpha) \tanh(\Omega/2) - \tanh(\omega/2)} \\ &= \frac{8\gamma\omega_0^2 \cosh^2(\omega_0/2)}{(2\gamma + 1)(\omega_0 - \sinh(\omega_0))},\end{aligned}\tag{A.22}$$

and

$$\begin{aligned}\lim_{\sigma \rightarrow 0} \frac{\alpha \sigma \tanh(\omega/2) \tanh(\Omega/2)}{\tanh(\omega/2) - \alpha \tanh(\Omega/2)} &= \lim_{\sigma \rightarrow 0} \frac{\sigma \tanh(\omega/2) \tanh(\Omega/2)}{(1/\alpha) \tanh(\omega/2) - \tanh(\Omega/2)} \\ &= -\frac{8\gamma\omega_0^2 \sinh^2(\omega_0/2)}{(2\gamma + 1)(\omega_0 + 2 \sinh(\omega_0))}.\end{aligned}\tag{A.23}$$

When the limit of  $\sigma P_k/Q$  is taken with respect to  $\sigma \rightarrow 0$  and (A.22) and (A.23) are used, the limit becomes

$$\lim_{\sigma \rightarrow 0} \frac{\sigma P_k}{Q} = \frac{4\gamma\lambda^2\nu^2}{2\gamma + 1} \frac{(1 - (-1)^k \cosh \omega_0)(\omega_0 - (-1)^k \sinh \omega_0)}{\omega_0^2 - \sinh \omega_0^2}.\tag{A.24}$$

When (A.17), (A.18), (A.19) and (A.24) are substituted into (A.16), the result yields (5.7.50).

The limit of  $\bar{h}_k$  as  $\sigma \rightarrow 0$  for an incompressible problem, (see chapter 4) is similar to that of a compressible problem.

$$\lim_{\sigma \rightarrow 0} \frac{\sigma P_k}{Q} = \frac{1}{2} \lim_{\sigma \rightarrow 0} [((-1)^k - 1)\sigma \Psi(\omega, \Omega) - ((-1)^k + 1)\sigma \Phi(\omega, \Omega)]\tag{A.25}$$

where  $\Psi$  and  $\Phi$  are defined in (5.7.37).

# Appendix B

## Results for Chapters 6 and 7

When  $G(r)$  is represented in the form:

$$G(r) = G_0 + \sum_{k=1}^{\infty} G_k J_0(\lambda_k r) , \quad (\text{B.1})$$

where  $\lambda_k$  are roots of  $J_1(x) = 0$ . Substitution of  $G(r)$  into solutions  $\bar{p}$ ,  $\bar{u}$  and  $\bar{h}$  (6.5.25) in chapters 5 and 6 is required to evaluate many of the integrals, using the formulae

$$\begin{aligned} \int_0^z x I_\nu(\alpha x) J_\nu(\lambda x) dx &= \frac{z}{\alpha^2 + \lambda^2} [\alpha J_\nu(\lambda z) I_{1+\nu}(\alpha z) + \lambda J_{1+\nu}(\lambda z) I_\nu(\alpha z)] , \\ \int_0^z x K_\nu(\alpha x) J_\nu(\lambda x) dx &= \frac{z}{\alpha^2 + \lambda^2} [\lambda J_{1+\nu}(\lambda z) K_\nu(\alpha z) - \alpha J_\nu(\lambda z) K_{1+\nu}(\alpha z)] \\ &\quad + \frac{(\lambda/\alpha)^\nu}{\alpha^2 + \lambda^2} , \end{aligned} \quad (\text{B.2})$$

and using properties of Bessel functions and modified Bessel functions in chapter 2. Some of these integrals are

$$\begin{aligned} \int_0^r t G(t) K_0(\alpha t) dt &= G_0 \int_0^r t K_0(\alpha t) dt + \sum_{k=1}^{\infty} G_k \int_0^r t J_0(\lambda t) K_0(\alpha t) dt \\ &= -\frac{G_0}{\alpha} r K_1(\alpha r) + \sum_{k=1}^{\infty} \frac{G_k}{\alpha^2 + \lambda^2} \\ &\quad + \sum_{k=1}^{\infty} \frac{r G_k}{\alpha^2 + \lambda^2} [\lambda K_0(\alpha r) J_1(\lambda r) - \alpha J_0(\lambda r) K_1(\alpha r)] , \end{aligned} \quad (\text{B.3})$$

$$\begin{aligned}
\int_0^r t^2 G(t) K_1(\alpha t) dt &= G_0 \int_0^r t^2 K_0(\alpha t) dt + \sum_{k=1}^{\infty} G_k \int_0^r t^2 J_0(\lambda t) K_1(\alpha t) dt \\
&= -\frac{G_0}{\alpha^2} [2r K_1(\alpha r) + \alpha r^2 K_0(\alpha r)] + \sum_{k=1}^{\infty} \frac{2\alpha G_k}{(\alpha^2 + \lambda^2)^2} \\
&\quad + \sum_{k=1}^{\infty} \frac{r^2 G_k}{\alpha^2 + \lambda^2} [\lambda K_1(\alpha r) J_1(\lambda r) - \alpha J_0(\lambda r) K_0(\alpha r)] \\
&\quad + \sum_{k=1}^{\infty} \frac{2\alpha r G_k}{(\alpha^2 + \lambda^2)^2} [\lambda K_0(\alpha r) J_1(\lambda r) - \alpha J_0(\lambda r) K_1(\alpha r)],
\end{aligned} \tag{B.4}$$

also

$$\begin{aligned}
\int_0^r t G(t) I_0(\alpha t) dt &= G_0 \int_0^r t I_0(\alpha t) dt + \sum_{k=1}^{\infty} G_k \int_0^r t J_0(\lambda t) I_0(\alpha t) dt \\
&= \frac{G_0}{\alpha} r I_1(\alpha r) \\
&\quad + \sum_{k=1}^{\infty} \frac{r G_k}{\alpha^2 + \lambda^2} [\lambda I_0(\alpha r) J_1(\lambda r) + \alpha J_0(\lambda r) I_1(\alpha r)], \\
\int_0^r t^2 G(t) I_1(\alpha t) dt &= G_0 \int_0^r t^2 I_0(\alpha t) dt + \sum_{k=1}^{\infty} G_k \int_0^r t^2 J_0(\lambda t) I_1(\alpha t) dt \\
&= \frac{G_0}{\alpha^2} [\alpha r^2 I_0(\alpha r) - 2r I_1(\alpha r)] \\
&\quad + \sum_{k=1}^{\infty} \frac{r^2 G_k}{\alpha^2 + \lambda^2} [\lambda I_1(\alpha r) J_1(\lambda r) + \alpha J_0(\lambda r) I_0(\alpha r)] \\
&\quad - \sum_{k=1}^{\infty} \frac{2\alpha r G_k}{(\alpha^2 + \lambda^2)^2} [\lambda I_0(\alpha r) J_1(\lambda r) + \alpha J_0(\lambda r) I_1(\alpha r)].
\end{aligned} \tag{B.6}$$

Integrals in (6.5.25) and (7.3.20) in chapter 6 and 7 respectively become

$$\begin{aligned}
\int_0^r t G(t) D_{00}(\alpha z, \alpha r) &= -\frac{G_0}{\alpha^2} - \sum_{k=1}^{\infty} \frac{G_k}{\alpha^2 + \lambda^2} [J_0(\lambda_k r) - I_0(\alpha r)] \\
\int_0^r t^2 G(t) D_{11}(\alpha z, \alpha r) &= \frac{r G_0}{\alpha^2} + \sum_{k=1}^{\infty} \frac{r G_k}{\alpha^2 + \lambda^2} J_0(\lambda_k) \\
&\quad - 2 \sum_{k=1}^{\infty} \frac{G_k}{(\alpha^2 + \lambda_k^2)^2} [\lambda_k J_1(\lambda_k r) + \alpha I_1(\alpha r)],
\end{aligned} \tag{B.7}$$

and

$$\begin{aligned}
 \int_0^r t G(t) S_{10}(\alpha z, \alpha r) &= \sum_{k=1}^{\infty} \frac{G_k}{\alpha^2 + \lambda_k^2} \left[ \frac{\lambda_k}{\alpha} J_1(\lambda_k r) + I_1(\alpha r) \right] \\
 \int_0^r t^2 G(t) S_{01}(\alpha z, \alpha r) &= -\frac{2G_0}{\alpha^3} + \frac{r}{\alpha} \sum_{k=1}^{\infty} \frac{\lambda_k G_k}{\alpha^2 + \lambda_k^2} J_1(\lambda_k) \\
 &\quad + 2\alpha \sum_{k=1}^{\infty} \frac{G_k}{(\alpha^2 + \lambda_k^2)^2} [I_0(\alpha r) - J_0(\lambda_k r)] .
 \end{aligned} \tag{B.8}$$

After considerable effort, solutions (6.5.25) in chapter 6 (7.3.20) and in chapter 7 take forms (6.5.27) and (7.4.22) for compressible and incompressible problems respectively.

When the solution is expressed in terms of Bessel functions (either  $J_0(\lambda_k r)$  or  $J_1(\lambda_k r)$ ), functions  $I_0(\alpha r)$  and  $I_1(\alpha r)$  are expressed in terms of  $J_0(\lambda_k r)$  or  $J_1(\lambda_k r)$ . Here the modified Bessel function is represented by Bessel function  $J_0(\lambda_k r)$  and  $J_1(\lambda_k r)$ .

$$\begin{aligned}
 I_0(\alpha r) &= \frac{2I_1(\alpha)}{\alpha} + 2\alpha I_1(\alpha) \sum_{k=1}^{\infty} \frac{J_0(\lambda_k r)}{(\alpha^2 + \lambda_k^2) J_0(\lambda_k)} \\
 r I_1(\alpha r) &= \frac{2}{\alpha^2} (\alpha I_0(\alpha) - 2I_1(\alpha)) + 2 \sum_{k=1}^{\infty} \frac{J_0(\lambda_k r)}{J_0(\lambda_k)} \left[ \frac{\alpha I_0(\alpha)}{\alpha^2 + \lambda_k^2} - \frac{2\alpha^2 I_1(\alpha)}{(\alpha^2 + \lambda_k^2)^2} \right]
 \end{aligned} \tag{B.9}$$

and

$$\begin{aligned}
 I_1(\alpha r) &= -2I_1(\alpha) \sum_{k=1}^{\infty} \frac{\lambda_k}{\alpha^2 + \lambda_k^2} \frac{J_1(\lambda_k r)}{J_0(\lambda_k)} \\
 r I_0(\alpha r) &= \sum_{k=1}^{\infty} \frac{J_1(\lambda_k r)}{J_0(\lambda_k)} \left[ \frac{4\alpha \lambda_k}{(\alpha^2 + \lambda_k^2)^2} I_1(\alpha) - \frac{2\lambda_k}{\alpha^2 + \lambda_k^2} I_0(\alpha) \right]
 \end{aligned} \tag{B.10}$$



# Appendix C

## Fortran program for chapter 4

This appendix contains FORTRAN 77 program to determines the accumulated shear stress and the surface deformation for incompressible case for chapter 4.

```
*****
*      THIS PROGRAM FOR INCOMPESSIBLE CASE - AXIAL PROBLEM      *
*      THE VALUE OF G(Z) AND H(R,1) ARE GIVEN BY ABSOLUTE VALUE  *
*****

      PROGRAM AXIAL

      IMPLICIT DOUBLE PRECISION(A-F,H,O-Z)
      IMPLICIT COMPLEX*16(G)

C
C      PARAMETRIC CONSTANT DEFINITIONS
C
C      FREQ = Forcing Frequency
C      RHO = Material Density
C      SHEAR = Linear Shear Modulus
C      ETA = Viscous Damping
C      DEPTH = Thickness of Sheet
C

      PARAMETER( FREQ=0.D0, RHO=1.D0, ETA=1.D0, SHEAR=1.D0,
*      DEPTH=1.D0, BIG=30.D0 )

      PARAMETER( ZERO=0.D0, HALF=0.5D0, ONE=1.D0, TWO=2.D0, FOUR=4.D0,
*      N=30000, NS=100, NN=2*NS+2, NIN=5, NOUT=6 )
```

```

DIMENSION GA(NN,NN), GB(NN), GC(NN), GVEC(NS), GCHI(NS)
CHARACTER*4 CODE
CHARACTER*35 TITLE
CHARACTER*12 FNAME1, FNAME2, FNAME3, FNAME4
LOGICAL SPLINE, MORE, AXES, FLAG
DIMENSION R(N), G_OUTER(0:NS), G_INNER(0:NS), Z(0:NS), Y(0:NS),
*      YREAL(0:NS), YIMAG(0:NS), WKS1(NN),
*      XR(2), YR(2)
PARAMETER( NR=30 )
DIMENSION RADIUS(0:NR), GH(0:NR)

C
C  .. PROGRAM TO FIND SHEAR STRESS ON INNER AND OUTER BOUNDARIES
C  FOR A GIVEN INPUT UNIT FORCE ..
C
C  .. TREATS STATIC PROBLEM AND CALCULATES AXIAL DISPLACEMENT FOR
C  COMPARISON AGAINST THOSE BASED ON PURE STRESS AND STRESS AND
C  BENDING MOMENT ..
C
      SIGMA = (RHO/SHEAR)*(FREQ*DEPTH)**2
      XI = ETA*FREQ/SHEAR
      PI = 4.DO*ATAN(ONE)
C
C  .. REQUESTS GEOMETRICAL INPUT ..
C
      WRITE(NOUT,*) ' ENTER RATIO OF RADII > '
      READ(NIN,*) RAT
      WRITE(NOUT,*) '   ENTER ASPECT RATIO > '
      READ(NIN,*) ASPECT
C
C  .. SET FORCE AT VALUE WHICH APPROXIMATES UNIT NON-DIMENSIONAL
C  DISPLACEMENT BASED ON PURE SHEAR STRESS ..
C

```

```

FORCE = ONE/LOG(RAT)
GFAC1 = SIGMA/DCMPLX(ONE,XI)

C
C .. FIND AND ACCESS THE DATA FILE OF ZEROS ..
C

NVAL = INT(1000.D0*RAT)
M = MOD(NVAL,10)
CODE(4:4) = CHAR(M+48)
NVAL = (NVAL-M)/10
M = MOD(NVAL,10)
CODE(3:3) = CHAR(M+48)
NVAL = (NVAL-M)/10
M = MOD(NVAL,10)
CODE(2:2) = CHAR(M+48)
NVAL = (NVAL-M)/10
M = MOD(NVAL,10)
CODE(1:1) = CHAR(M+48)
INQUIRE(FILE='SLAB'//CODE//'.DAT', EXIST=FLAG)
IF (.NOT.FLAG) THEN
    WRITE(NOUT,*) 'SORRY - FILE CONTAINING ZEROS IS NOT PRESENT'
    STOP
ENDIF
OPEN(10,FILE='SLAB'//CODE//'.DAT',STATUS='OLD')
NROOT = 0
111 READ(UNIT=10,FMT='(F25.12)',END=222) TEMP
NROOT = NROOT+1
R(NROOT) = TEMP
IF (NROOT.EQ.N) THEN
    WRITE(NOUT,*) 'INSUFFICIENT WORKSPACE FOR ZEROS - FAILURE'
    STOP
ENDIF
GOTO 111

```

```

222    CLOSE(10)
      WRITE(NOUT,*)  'COMPLETED DATA READ'
C
C  .. INITIALISE ALL MATRIX AND VECTOR ENTRIES TO ZERO ..
C
      DO 100 I=1,NN
        DO 200 J=1,NN
          GA(I,J) = DCMPLX(ZERO,ZERO)
200    CONTINUE
          GB(I) = DCMPLX(ZERO,ZERO)
100    CONTINUE
C
C  .. FILL THE ENTRIES OF GA AND GB
C
C  .. THE VECTOR GB STORES VALUES OF GI AND GO AS FOLLOWS
C
C          GB(1) .. GB(NS)  --->  GI(1) .. GI(NS)
C          GB(NS+1) .. GB(NN-2)  --->  GO(1) .. GO(NS)
C          GB(NN-1)  --->  C VALUE
C          GB(NN)  --->  H VALUE
C
      DO 300 IVAL=NROOT,1,-1
        IF (MOD(IVAL,100).EQ.0) WRITE(*,'(A9,I6)') ' REACHED ',IVAL
        VLAM = R(IVAL)
        GOMEGA1 = VLAM*ASPECT
        GAVAL = GOMEGA1**2
        GOMEGA2 = CDSQRT(GAVAL-GFAC1)
        DO 400 K=1,NS
          TVAL = (ONE/(PI*DBLE(2*K-1)))**2
          G1 = GAVAL*TVAL
          G2 = (GAVAL-GFAC1)*TVAL
          GVEC(K) = G1/((ONE+G1)*(ONE+G2))

```

```

      GCHI(K) = (ONE+(TWO*G1)+G2)/((ONE+G1)*(ONE+G2))
400      CONTINUE
C
C .. DETERMINE VALUE OF DELTA(LAMBDA) ..
C
      GTHETA = HALF*GFAC1/(GOMEGA1+GOMEGA2)
      IF ( CDABS(GTHETA).LE.(5.D-5) ) THEN
        GT = ONE+GTHETA*GTHETA/6.DO
        GT = GT*TWO*GOMEGA1*GOMEGA2/(ONE+(GOMEGA2/GOMEGA1))
        IF ((CDABS(GOMEGA1).GE.BIG).OR.(CDABS(GOMEGA2).GE.BIG)) THEN
          GT = DCMPLX(ZERO,ZERO)
        ELSE
          GT = GT/(GCOSH(HALF*GOMEGA1)*GCOSH(HALF*GOMEGA2))
        ENDIF
        GVAL = FOUR*GOMEGA1*GOMEGA2/(ONE+(GOMEGA2/GOMEGA1))
        GVAL = GFAC1 - GVAL
        GVAL = GVAL*GTANH(HALF*GOMEGA1)/GOMEGA1
        GVAL = FOUR/(GVAL+GT)
      ELSEIF ( CDABS(GTHETA).LE.0.5D0 ) THEN
        GT = TWO*GOMEGA1*GOMEGA2*(GSINH(GTHETA)/GTHETA)
        GT = GT/(ONE+(GOMEGA2/GOMEGA1))
        IF ((CDABS(GOMEGA1).GE.BIG).OR.(CDABS(GOMEGA2).GE.BIG)) THEN
          GT = DCMPLX(ZERO,ZERO)
        ELSE
          GT = GT/(GCOSH(HALF*GOMEGA1)*GCOSH(HALF*GOMEGA2))
        ENDIF
        GVAL = FOUR*GOMEGA1*GOMEGA2/(ONE+(GOMEGA2/GOMEGA1))
        GVAL = GFAC1 - GVAL
        GVAL = GVAL*GTANH(HALF*GOMEGA1)/GOMEGA1
        GVAL = FOUR/(GVAL+GT)
      ELSE
        GVAL = GOMEGA2/GOMEGA1

```

```

        GVAL = FOUR*GVAL/((ONE+(GVAL**2))**2)
        GVAL = ONE/GVAL
        GVAL = GVAL*GTANH(HALF*GOMEGA1) - GTANH(HALF*GOMEGA2)
        GVAL = GFAC1/(GVAL*GOMEGA2*GOMEGA1**2)

ENDIF

FAC = BESSJ1(VLAM)/BESSJ1(VLAM*RAT)
F1 = ONE/(FAC-ONE)
F2 = FAC/(FAC-ONE)
F3 = ONE/(FAC+ONE)
F4 = FAC/(FAC+ONE)
DO 500 K=1,NS
    KK = K+NS
    GTT = GVAL*GCHI(K)
    G1 = GTT*F1
    G2 = GTT*F2
    G3 = GTT*F3
    G4 = GTT*F4
    DO 600 J=1,NS
        JJ = J+NS
        GA(K,J) = GA(K,J)+G1*GCHI(J)
        GA(K,JJ) = GA(K,JJ)-G2*GCHI(J)
        GA(KK,J) = GA(KK,J)+G3*GCHI(J)
        GA(KK,JJ) = GA(KK,JJ)-G4*GCHI(J)
600    CONTINUE
        GA(K,K) = GA(K,K)-F1*GVEC(K)
        GA(K,KK) = GA(K,KK)+F2*GVEC(K)
        GA(KK,K) = GA(KK,K)-F3*GVEC(K)
        GA(KK,KK) = GA(KK,KK)+F4*GVEC(K)
500    CONTINUE
300    CONTINUE
C
C    .. NOW FILL IN THE ENTRIES CORRESPONDING TO C AND H ..

```

```

C
TEMP = TWO/ASPECT**2
DO 700 K=1,NS
    KK = K+NS
    GA(K,NN-1) = -DCMPLX((RAT+ONE)*TEMP,ZERO)
    GA(K,NN)    =  DCMPLX(TEMP,ZERO)
    GA(KK,NN-1) = -DCMPLX((RAT-ONE)*TEMP,ZERO)
    GA(KK,NN)   = -DCMPLX(TEMP,ZERO)
700 CONTINUE
C
C .. FILL IN ENTRIES CORRESPONDING TO G(1) ..
C
DO 800 K=1,NS
    GA(NN-1,K) = DCMPLX(ONE,ZERO)
    GA(NN,K+NS) = DCMPLX(ONE,ZERO)
800 CONTINUE
    TEMP = ONE/(SHEAR*(DEPTH**2))
    GB(NN-1) = DCMPLX(HALF*TEMP*FORCE,ZERO)/DCMPLX(ONE,XI)
    GB(NN)   = DCMPLX(HALF*TEMP*FORCE/RAT,ZERO)/DCMPLX(ONE,XI)
C
C .. MATRIX EQUATIONS COMPLETE - START SOLUTION PROCEDURE ..
C
C .. SOLVE THE LINEAR EQUATIONS FOR THE COEFFICIENTS OF G ..
    IFAIL = 0
    CALL F04ADF(GA, NN, GB, NN, NN, 1, GC, NN, WKS1, IFAIL)
C
C .. SECTION VALUE ( OUTPUT VALUES OF G_1 AND G_BETA ) ..
C
K = NINT(10.DO*RAT)
J = NINT(100.DO*ASPECT)
FNAME1 = 'ISI'//CHAR(48+K/10)//CHAR(48+MOD(K,10))//CHAR(48+J/100)
J = MOD(J,100)

```

```

FNAME1(7:12) = CHAR(48+J/10)//CHAR(48+MOD(J,10))//'.000'
FNAME2 = FNAME1
FNAME2(3:3) = '0'
FNAME3 = FNAME1
FNAME3(3:3) = 'H'
FNAME4 = FNAME1
FNAME4(3:3) = 'S'
OPEN(33,FILE=FNAME1)
OPEN(44,FILE=FNAME2)
OPEN(55,FILE=FNAME3)
OPEN(66,FILE=FNAME4)

C
C .. SECTION ( EXTRACT THE DISPLACEMENT ) ..
C

WRITE(66,*) '          LINEAR_ELASTIC DISPLACEMENT IS ',GC(NN)
WRITE(66,*) '          SHEAR_STRESS DISPLACEMENT IS ',ONE
FAC1 = (RAT**2-ONE)/LOG(RAT)-4.DO*RAT**2*(LOG(RAT))/(RAT**2-ONE)
FAC1 = 0.375D0*FAC1/ASPECT**2+ONE
WRITE(66,*) ' SHEAR_AND_BENDING_STRESS DISPLACEMENT IS ',FAC1
GLINEAR = GC(NN)
FLIN = CDABS(GLINEAR)
RATLT = 100
RATSS = 100.DO/FLIN
RATSB = 100.DO*FAC1/FLIN
RATSS = NINT(RATSS)
RATSB = NINT(RATSB)
WRITE(66,*) '          LINEAR THEORY 100% IS ',RATLT,'% '
WRITE(66,*) 'SHEAR AND BENDING STRESS IS ',RATSB,'% '
WRITE(66,*) '          SHEAR STRESS ONLY IS ',RATSS,'% '
CLOSE(66)
GO_I = DCMPLX(ZERO,ZERO)
GO_O = DCMPLX(ZERO,ZERO)

```



```

DO 900 K=NS,1,-1
    GO_I = GO_I-GC(K)
    GO_O = GO_O-GC(K+NS)
900  CONTINUE
DZ = ONE/DBLE(NS)
DO 1000 K=0,NS
    Z(K) = DZ*DBLE(K)
    GSUM_I = DCMPLX(ZERO,ZERO)
    GSUM_O = DCMPLX(ZERO,ZERO)
    DO 1100 J=NS,1,-1
        TEMP = COS(PI*DBLE(2*J-1)*Z(K))
        GSUM_I = GSUM_I+TEMP*GC(J)
        GSUM_O = GSUM_O+TEMP*GC(J+NS)
1100  CONTINUE
    G_INNER(K) = GSUM_I+GO_I
    G_OUTER(K) = GSUM_O+GO_O
1000  CONTINUE
DO 1200 I=0,NS
    Y(I) = CDABS(G_INNER(I))
    YREAL(I) = DREAL(G_INNER(I))
    YIMAG(I) = DIMAG(G_INNER(I))
    WRITE(33,'(7F18.11)') Z(I), YREAL(I)
1200  CONTINUE
CLOSE(33)

C
C  .. SECTION 1 ( DRAW GRAPHS OF G_INNER( ) AND G_OUTER( ) ) ..
C
MORE = .TRUE.
MORE = .FALSE.
SPLINE = .FALSE.
AXES = .TRUE.
TITLE = 'GRAPH OF G_INNER'

```

```

XR(1) = - 0.1D0
XR(2) = 1.1D0
YR(1) = ZERO
YR(2) = ZERO
WRITE(*,*) ' ABOUT TO DRAW GRAPHS - ENTER TO CONTINUE'
READ(*,*)
CALL L_DA_VINCI(NS+1,Z,YREAL,MORE,SPLINE,AXES,TITLE,XR,YR)
MORE = .FALSE.
DO 1300 I=0,NS
    Y(I) = CDABS(G_OUTER(I))
    YREAL(I) = DREAL(G_OUTER(I))
    YIMAG(I) = DIMAG(G_OUTER(I))
    WRITE(44,'(7F18.11)') Z(I), YREAL(I)
C        WRITE(44,*) Z(I), YREAL(I)
1300 CONTINUE
    CLOSE(44)
    TITLE = 'GRAPH OF G_OUTER'
    MORE = .TRUE.
    MORE = .FALSE.
    CALL L_DA_VINCI(NS+1,Z,Y,MORE,SPLINE,AXES,TITLE,XR,YR)
    CALL L_DA_VINCI(NS+1,Z,YREAL,MORE,SPLINE,AXES,TITLE,XR,YR)
    MORE = .FALSE.

C
C    .. SECTION 2 ( DRAW OUTER SURFACE SHAPE ) ..
C
    DR = (RAT-ONE)/DBLE(NR)
    DO 3000 K=0,NR
        RADIUS(K) = ONE+DR*DBLE(K)
        GH(K) = DCMLPX(ZERO,ZERO)
3000 CONTINUE
    DO 3100 IVAL=NROOT,1,-1
        VLAM = R(IVAL)

```

```

GOMEGA1 = VLAM*ASPECT
GAVAL = GOMEGA1**2
GOMEGA2 = CDSQRT(GAVAL-GFAC1)
DO 3200 K=1,NS
    TVAL = (PI*DBLE(2*K-1))**2
    G1 = GAVAL/TVAL
    G2 = (GAVAL-GFAC1)/TVAL
    GCHI(K) = (ONE+G1+G2)/((ONE+G1)*(ONE+G2))
3200    CONTINUE
C
C .. DETERMINE VALUE OF DELTA(LAMBDA) ..
C
GTHETA = HALF*GFAC1/(GOMEGA1+GOMEGA2)
IF ( CDABS(GTHETA).LE.(5.D-5) ) THEN
    GT = ONE+GTHETA*GTHETA/6.DO
    GT = GT*TWO*GOMEGA1*GOMEGA2/(ONE+(GOMEGA2/GOMEGA1))
    IF ((CDABS(GOMEGA1).GE.BIG).OR.(CDABS(GOMEGA2).GE.BIG)) THEN
        GT = DCMPLX(ZERO,ZERO)
    ELSE
        GT = GT/(GCOSH(HALF*GOMEGA1)*GCOSH(HALF*GOMEGA2))
    ENDIF
    GVAL = FOUR*GOMEGA1*GOMEGA2/(ONE+(GOMEGA2/GOMEGA1))
    GVAL = GFAC1 - GVAL
    GVAL = GVAL*GTANH(HALF*GOMEGA1)/GOMEGA1
    GVAL = FOUR/(GVAL+GT)
ELSEIF ( CDABS(GTHETA).LE.0.5D0 ) THEN
    GT = TWO*GOMEGA1*GOMEGA2*(GSINH(GTHETA)/GTHETA)
    GT = GT/(ONE+(GOMEGA2/GOMEGA1))
    IF ((CDABS(GOMEGA1).GE.BIG).OR.(CDABS(GOMEGA2).GE.BIG)) THEN
        GT = DCMPLX(ZERO,ZERO)
    ELSE
        GT = GT/(GCOSH(HALF*GOMEGA1)*GCOSH(HALF*GOMEGA2))

```

```

ENDIF
GVAL = FOUR*GOMEGA1*GOMEGA2/(ONE+(GOMEGA2/GOMEGA1))
GVAL = GFAC1 - GVAL
GVAL = GVAL*GTANH(HALF*GOMEGA1)/GOMEGA1
GVAL = FOUR/(GVAL+GT)
ELSE
    GVAL = GOMEGA2/GOMEGA1
    GVAL = FOUR*GVAL/((ONE+(GVAL**2))**2)
    GVAL = ONE/GVAL
    GVAL = GVAL*GTANH(HALF*GOMEGA1) - GTANH(HALF*GOMEGA2)
    GVAL = GFAC1/(GVAL*GOMEGA2*GOMEGA1**2)
ENDIF
G1 = DCMPLX(ZERO,ZERO)
G2 = DCMPLX(ZERO,ZERO)
DO 3300 J=NS,1,-1
    G1 = G1+GCHI(J)*GC(J)
    G2 = G2+GCHI(J)*GC(J+NS)
3300  CONTINUE
FAC = BESSJ1(VLAM)/BESSJ1(VLAM*RAT)
GT = VLAM*GVAL*(G1-FAC*G2)/(FAC*FAC-ONE)
DO 3400 K=0,NR
    CALL C01(RADIUS(K),VLAM,TEMP)
    GH(K) = GH(K)+GT*TEMP
3400  CONTINUE
3100  CONTINUE
TEMP = 0.25D0*PI*ASPECT**2
GH(0) = GC(NN)
GH(NR) = DCMPLX(ZERO,ZERO)
DO 3500 K=1,NR-1
    GH(K) = GH(K)*TEMP+GC(NN-1)
3500  CONTINUE
DO 3600 I=0,NR

```

```

        Y(I) = CDABS(GH(I))
        YREAL(I) = DREAL(GH(I))
        YIMAG(I) = DIMAG(GH(I))
3600  CONTINUE
        MORE = .FALSE.
        SPLINE = .FALSE.
        AXES = .TRUE.
        TITLE = 'SURFACE DISPLACEMENT'
        XR(1) = -RAT*0.1D0
        XR(2) = RAT*1.1D0
        YR(1) = ZERO
        YR(2) = ZERO
        CALL L_DA_VINCI(NR+1,RADIUS,YIMAG,MORE,SPLINE,AXES,TITLE,XR,YR)
        MORE = .FALSE.
        DO 9999 J=0,NR
            WRITE(55,'(7F18.11)') RADIUS(J), YREAL(J)
9999  CONTINUE
            CLOSE(55)
        END

        FUNCTION GTANH(Z)
        COMPLEX*16 GTANH, Z
        DOUBLE PRECISION X, Y, BIG, ZERO, ONE
        PARAMETER( ZERO=0.D0, ONE=1.D0, BIG=30.D0 )
        X = DREAL(Z)
        Y = DIMAG(Z)
        IF ( X.GT.BIG ) THEN
            GTANH = DCMPLX(ONE,ZERO)
        ELSEIF ( X.LT.-BIG ) THEN
            GTANH = DCMPLX(-ONE,ZERO)
        ELSE
            X = TANH(X)

```

```

      GTANH = DCMPLX(X*COS(Y),SIN(Y))/DCMPLX(COS(Y),X*SIN(Y))
ENDIF
RETURN
END

```

```

FUNCTION GCOSH(Z)
COMPLEX*16 GCOSH, Z
DOUBLE PRECISION X, Y
X = DREAL(Z)
Y = DIMAG(Z)
GCOSH = DCMPLX(COSH(X)*COS(Y),SINH(X)*SIN(Y))
RETURN
END

```

```

FUNCTION GSINH(Z)
COMPLEX*16 GSINH, Z
DOUBLE PRECISION X, Y
X = DREAL(Z)
Y = DIMAG(Z)
GSINH = DCMPLX(SINH(X)*COS(Y),COSH(X)*SIN(Y))
RETURN
END

```

```

SUBROUTINE C01(RADIUS,VLAM,TEMP)
IMPLICIT DOUBLE PRECISION(A-H,O-Z)
TEMP = VLAM*RADIUS
TEMP = BESSJ0(TEMP)*BESSY1(VLAM)-BESSY0(TEMP)*BESSJ1(VLAM)
RETURN
END

```

```

SUBROUTINE L_DA_VINCI(NP,X,Y,MORE,SPLINE,AXES,TEXT,XR,YR)
IMPLICIT DOUBLE PRECISION(A-H,O-Z)

```

```

PARAMETER( ZERO=0.DO , ONE=1.DO , SMALL=1.D-15 , NOUT=8 )
DIMENSION XR(2),YR(2),X(*),Y(*)
LOGICAL MORE,SPLINE,AXES,START,NOTEXT
CHARACTER*(*) TEXT
DATA START / .TRUE. /
C .. OPEN OUTPUT ERROR CHANNEL
      OPEN(NOUT,FILE='OUTPUT.ERR')
C .. DEFAULT TO THE DATA RANGE ENCOUNTERED IN THE FIRST SUBROUTINE
C   CALL. OTHERWISE USE THE USER SPECIFIED DATA WHEN SUPPLIED.
      IF (START) THEN
          XMAX = X(1)
          XMIN = X(1)
          YMAX = Y(1)
          YMIN = Y(1)
          DO 100 I=2,NP
              XMAX = MAX(XMAX,X(I))
              XMIN = MIN(XMIN,X(I))
              YMAX = MAX(YMAX,Y(I))
              YMIN = MIN(YMIN,Y(I))
100      CONTINUE
          IF (ABS(XR(1)).GE.SMALL) XMIN = XR(1)
          IF (ABS(XR(2)).GE.SMALL) XMAX = XR(2)
          IF (ABS(YR(1)).GE.SMALL) YMIN = YR(1)
          IF (ABS(YR(2)).GE.SMALL) YMAX = YR(2)
C .. PROCESS GRAPH TITLE
          NOTEXT = (TEXT.EQ.' ')
          IF (.NOT.NOTEXT) THEN
              NR = LEN(TEXT)+1
              NL = 0
111          NL = NL+1
              IF (TEXT(NL:NL).EQ.' ') GOTO 111
222          NR = NR-1

```

```

        IF (TEXT(NR:NR).EQ.' ') GOTO 222
    ENDIF
C .. SELECT GRAPHICS VIEW WINDOW SIZE
        UMIN = ZERO
        UMAX = ONE
        VMIN = ZERO
        VMAX = ONE
C.. CONNECT NAG GRAPHICS OUTPUT CHANNELS TO ERROR FILE AND SCREEN
        CALL JO6VAF(1,NOOUT)
        CALL XXXXXX
C     NESQ = 1
C     CALL JO6VCF(0,NESQ)
C     OPEN(NESQ,FILE='CON')
C .. INITIALISE NAG GRAPHICS
        CALL JO6WAF
C .. INITIALISE NAG GRAPHICS WINDOW
        IF (NOTEXT.AND.(.NOT.AXES)) THEN
            CALL JO6WBF(XMIN,XMAX,YMIN,YMAX,0)
        ELSE
            CALL JO6XFF(2)
            CALL JO6WBF(XMIN,XMAX,YMIN,YMAX,1)
        ENDIF
        CALL JO6WCF(UMIN,UMAX,VMIN,VMAX)
C .. INSERT AXES IF REQUIRED
        IF (AXES) CALL JO6AAF
C .. INSERT TITLE IF REQUIRED
        IF (.NOT.NOTEXT) CALL JO6AHF(TEXT(NL:NR))
        START = .FALSE.
    ENDIF
C .. NOW DRAW EACH CURVE IN TURN
        IFAIL = 0
        IF (.NOT.SPLINE) THEN

```



```
      KSYM = 1
      CALL J06BAF(X,Y,NP,1,KYSM,IFAIL)
ELSE
      METHOD = 1
      CALL J06CAF(X,Y,NP,METHOD,IFAIL)
ENDIF
IF (MORE) RETURN
START = .TRUE.
CALL J06WZF
RETURN
END
```

# Appendix D

## Fortran program for chapter 5

This appendix contains FORTRAN 77 program to determines the accumulated shear stress and the surface deformation for compressible case for chapter 5.

```
*****
*      THIS PROGRAM FOR COMPESSIBLE CASE - AXIAL PROBLEM      *
*      THE VALUE OF G(Z) AND H(R,1) ARE GIVEN BY ABSOLUTE VALUE  *
*****

PROGRAM AXIAL
IMPLICIT DOUBLE PRECISION(A-F,H,O-Z)
IMPLICIT COMPLEX*16(G)
DOUBLE PRECISION GAMMA

C
C      PARAMETRIC CONSTANT DEFINITIONS
C
C      FREQ = Forcing Frequency
C      RHO = Material Density
C      SHEAR = Linear Shear Modulus
C      ETA = Viscous Damping
C      DEPTH = Thickness of Sheet
C

PARAMETER( FREQ=0.D0, RHO=1.D0, ETA=1.D0, SHEAR=1.D0,
*          DEPTH=1.D0, BIG=30.D0 )
PARAMETER( ZERO=0.D0, HALF=0.5D0, ONE=1.D0, TWO=2.D0, FOUR=4.D0,
```

```

*          EIGHT=8.D0, N=30000, NS=100, NN=2*NS+2, NIN=5, NOUT=6 )
DIMENSION GA(NN,NN), GB(NN), GC(NN), GVEC(NS), GETA(NS)
CHARACTER*4 CODE
CHARACTER*35 TITLE
CHARACTER*12 FNAME1, FNAME2, FNAME3, FNAME4,
*          FNAME5, FNAME6, FNAME7

LOGICAL FLAG, SPLINE, MORE, AXES
DIMENSION R(N), G_OUTER(0:NS), G_INNER(0:NS), Z(0:NS),
*          WKS1(NN), YREAL(0:NS), YIMAG(0:NS), Y(0:NS)
PARAMETER( NR=30 )
DIMENSION RADIUS(0:NR), GH(0:NR)

C
C .. PROGRAM TO FIND SHEAR STRESS ON INNER AND OUTER BOUNDARIES
C   FOR A GIVEN INPUT UNIT FORCE ..
C
C .. TREATS STATIC PROBLEM AND CALCULATES AXIAL DISPLACEMENT FOR
C   COMPARISON AGAINST THOSE BASED ON PURE STRESS AND STRESS AND
C   BENDING MOMENT ..
C
  SIGMA = (RHO/SHEAR)*(FREQ*DEPTH)**2
  XI = ETA*FREQ/SHEAR
  PI = 4.D0*ATAN(ONE)

C
C .. REQUESTS GEOMETRICAL INPUT ..
C
  WRITE(NOUT,*) ' ENTER RATIO OF RADII > '
  READ(NIN,*) RAT
  WRITE(NOUT,*) '   ENTER ASPECT RATIO > '
  READ(NIN,*) ASPECT
  WRITE(NOUT,*) 'ENTER VALUE FOR GAMMA > '
  READ(*,*) GAMMA

```

```

C
C  .. SET FORCE AT VALUE WHICH APPROXIMATES UNIT NON-DIMENSIONAL
C  DISPLACEMENT BASED ON PURE SHEAR STRESS ..
C
  FORCE = ONE/LOG(RAT)
  GFAC1 = SIGMA/DCMPLX(ONE,XI)
  GFAC2 = SIGMA/DCMPLX(GAMMA,-XI)
  GRAT = DCMPLX(ONE,XI)/DCMPLX(GAMMA,-XI)
C
C  .. FIND AND ACCESS THE DATA FILE OF ZEROS ..
C
  NVAL = INT(1000.DO*RAT)
  M = MOD(NVAL,10)
  CODE(4:4) = CHAR(M+48)
  NVAL = (NVAL-M)/10
  M = MOD(NVAL,10)
  CODE(3:3) = CHAR(M+48)
  NVAL = (NVAL-M)/10
  M = MOD(NVAL,10)
  CODE(2:2) = CHAR(M+48)
  NVAL = (NVAL-M)/10
  M = MOD(NVAL,10)
  CODE(1:1) = CHAR(M+48)
  INQUIRE(FILE='SLAB'//CODE//'.DAT', EXIST=FLAG)
  IF (.NOT.FLAG) THEN
    WRITE(NOUT,*) 'SORRY - FILE CONTAINING ZEROS IS NOT PRESENT'
    STOP
  ENDIF
  OPEN(10,FILE='SLAB'//CODE//'.DAT',STATUS='OLD')
  NROOT = 0
111 READ(UNIT=10,FMT='(F25.12)',END=222) TEMP
  NROOT = NROOT+1

```

```

R(NROOT) = TEMP
IF (NROOT.EQ.N) THEN
    WRITE(NOUT,*) 'INSUFFICIENT WORKSPACE FOR ZEROS - FAILURE'
    STOP
ENDIF
GOTO 111
222  CLOSE(10)
    WRITE(NOUT,*) 'COMPLETED DATA READ'

C
C  .. INITIALISE ALL MATRIX AND VECTOR ENTRIES TO ZERO ..
C
    DO 100 I=1,NN
        DO 200 J=1,NN
            GA(I,J) = DCMPLX(ZERO,ZERO)
200    CONTINUE
        GB(I) = DCMPLX(ZERO,ZERO)
100    CONTINUE
C
C  .. FILL THE ENTRIES OF GA AND GB
C
C  .. THE VECTOR GB STORES VALUES OF GI AND GO AS FOLLOWS
C
C          GB(1) .. GB(NS)  --->  GI(1) .. GI(NS)
C          GB(NS+1) .. GB(NN-2)  --->  GO(1) .. GO(NS)
C          GC(NN-1)  --->  C VALUE
C          GC(NN)  --->  H VALUE
C
    DO 300 IVAL=NROOT,1,-1
        IF (MOD(IVAL,100).EQ.0) WRITE(*,'(A9,I6)') ' REACHED ',IVAL
        VLAM = R(IVAL)
        AVAL = (VLAM*ASPECT)**2
        GOMEGA1 = CDSQRT(AVAL-GFAC1)

```

```

GOMEGA2 = CDSQRT(AVAL+HALF*GFAC2)
DO 400 K=1,NS
    TVAL = (PI*DBLE(2*K-1))**2
    G1 = (AVAL-GFAC1)/TVAL
    G2 = (AVAL+HALF*GFAC2)/TVAL
    GVEC(K) = (GRAT-TWO*G2)/((ONE+G1)*(ONE+G2))
    GETA(K) = ((TWO+GRAT)*AVAL/TVAL+ONE+G1)/((ONE+G1)*(ONE+G2))
400    CONTINUE
C
C  .. DETERMINE VALUE OF CHI(LAMBDA) ..
C
GTHETA = HALF*(GFAC1+HALF*GFAC2)/(GOMEGA1+GOMEGA2)
IF ( CDABS(GTHETA).LE.(5.D-5) ) THEN
    GT = ONE+GTHETA*GTHETA/6.DO
    GT = -GT*(TWO+GRAT)*AVAL/(ONE+GOMEGA2/GOMEGA1)
    IF ((CDABS(GOMEGA1).GE.BIG).OR.(CDABS(GOMEGA2).GE.BIG)) THEN
        GT = DCMPLX(ZERO,ZERO)
    ELSE
        GT = GT/(GCOSH(HALF*GOMEGA1)*GCOSH(HALF*GOMEGA2))
    ENDIF
    GVAL = (FOUR+TWO*GRAT)*AVAL/(ONE+GOMEGA2/GOMEGA1)-GFAC1
    GVAL = GVAL*GTANH(HALF*GOMEGA2)/GOMEGA2
    GVAL = EIGHT/(GVAL+GT)
ELSEIF ( CDABS(GTHETA).LE.0.5D0 ) THEN
    GT = AVAL*(GSINH(GTHETA)/GTHETA)/(ONE+GOMEGA2/GOMEGA1)
    GT = -GT*(TWO+GRAT)
    IF ((CDABS(GOMEGA1).GE.BIG).OR.(CDABS(GOMEGA2).GE.BIG)) THEN
        GT = DCMPLX(ZERO,ZERO)
    ELSE
        GT = GT/(GCOSH(HALF*GOMEGA1)*GCOSH(HALF*GOMEGA2))
    ENDIF
    GVAL = (FOUR+TWO*GRAT)*AVAL/(ONE+GOMEGA2/GOMEGA1)-GFAC1

```

```

        GVAL = GVAL*GTANH(HALF*GOMEGA2)/GOMEGA2
        GVAL = EIGHT/(GVAL+GT)
ELSE
        GVAL = TWO*AVAL-GFAC1
        GVAL = 0.25D0*GVAL**2/(AVAL*GOMEGA1*GOMEGA2)
        GVAL = GTANH(HALF*GOMEGA1)-GVAL*GTANH(HALF*GOMEGA2)
        GVAL = GVAL*AVAL*GOMEGA1
        GVAL = TWO*GFAC1/GVAL
ENDIF
FAC = BESSJ1(VLAM)/BESSJ1(VLAM*RAT)
F1 = ONE/(FAC-ONE)
F2 = FAC/(FAC-ONE)
F3 = ONE/(FAC+ONE)
F4 = FAC/(FAC+ONE)
DO 500 K=1,NS
        KK = K+NS
        GT = GVAL*GETA(K)
        G1 = GT*F1
        G2 = GT*F2
        G3 = GT*F3
        G4 = GT*F4
        DO 600 J=1,NS
                JJ = J+NS
                GA(K,J) = GA(K,J)+G1*GETA(J)
                GA(K,JJ) = GA(K,JJ)-G2*GETA(J)
                GA(KK,J) = GA(KK,J)+G3*GETA(J)
                GA(KK,JJ) = GA(KK,JJ)-G4*GETA(J)
        CONTINUE
600    GA(K,K) = GA(K,K)-F1*GVEC(K)
        GA(K,KK) = GA(K,KK)+F2*GVEC(K)
        GA(KK,K) = GA(KK,K)-F3*GVEC(K)
        GA(KK,KK) = GA(KK,KK)+F4*GVEC(K)

```

```

500      CONTINUE
300      CONTINUE
      GF1 = GRAT/(RAT-ONE)
      GF2 = GRAT*RAT/(RAT-ONE)
      GF3 = GRAT/(RAT+ONE)
      GF4 = GRAT*RAT/(RAT+ONE)
      TEMP = FOUR/ASPECT**2
      DO 700 K=1,NS
          GVAL = ONE+HALF*GFAC2/(PI*DBLE(2*K-1))**2
          KK = K+NS
          GA(K,K) = GA(K,K)-GF1/GVAL
          GA(K, KK) = GA(K, KK)+GF2/GVAL
          GA(K, NN-1) = -GF1/GVAL
          GA(K, NN) = -DCMPLX(TEMP, ZERO)
          GA(KK, K) = GA(KK, K)-GF3/GVAL
          GA(KK, KK) = GA(KK, KK)+GF4/GVAL
          GA(KK, NN-1) = -GF3/GVAL
          GA(KK, NN) = DCMPLX(TEMP, ZERO)
700      CONTINUE
C
C      .. FILL IN ENTRIES CORRESPONDING TO G(1) ..
C
      DO 800 K=1,NS
          GA(NN-1, K) = DCMPLX(ONE, ZERO)
          GA(NN, K+NS) = DCMPLX(ONE, ZERO)
800      CONTINUE
      TEMP = ONE/(SHEAR*(DEPTH**2))
      GB(NN-1) = DCMPLX(HALF*TEMP*FORCE, ZERO)/DCMPLX(ONE, XI)
      GB(NN) = DCMPLX(HALF*TEMP*FORCE/RAT, ZERO)/DCMPLX(ONE, XI)
C
C      .. MATRIX EQUATIONS COMPLETE - START SOLUTION PROCEDURE ..
C

```



```

C .. SOLVE THE LINEAR EQUATIONS FOR THE COEFFICIENTS OF G ..
      IFAIL = 0
      CALL FO4ADF(GA, NN, GB, NN, NN, 1, GC, NN, WKS1, IFAIL)
C
C .. SECTION VALUE ( OUTPUT VALUES OF G_1 AND G_BETA ) ..
C
      TGAMMA = ABS(GAMMA)
      K = NINT(10.DO*RAT)
      J = NINT(100.DO*ASPECT)
      L = NINT(100.DO*TGAMMA)
      FNAME1 = 'I'//CHAR(48+K/10)//CHAR(48+J/100)
      J = MOD(J,100)
      FNAME1(4:12) = CHAR(48+J/10)//CHAR(48+MOD(J,10))//CHAR(48+L/100)
      L = MOD(L,100)
      FNAME1(7:12) = CHAR(48+L/10)//CHAR(48+MOD(L,10))//'.0-0'
      FNAME2 = FNAME1
      FNAME2(1:1) = 'O'
      FNAME3 = FNAME1
      FNAME3(1:1) = 'H'
      FNAME4 = FNAME1
      FNAME4(1:1) = 'S'
C
C .. SECTION ( EXTRACT THE DISPLACEMENT ) ..
C
      OPEN(88,FILE=FNAME4,STATUS='NEW')
      WRITE(88,*) '          LINEAR_ELASTIC DISPLACEMENT IS ',GC(NN)
      WRITE(88,*) '          SHEAR_STRESS DISPLACEMENT IS ',ONE
      FAC1 = (RAT**2-ONE)/LOG(RAT)-4.DO*RAT**2*(LOG(RAT))/(RAT**2-ONE)
      FAC1 = 0.375DO*FAC1/ASPECT**2+ONE
      WRITE(88,*) ' SHEAR_AND_BENDING_STRESS DISPLACEMENT IS ',FAC1
      GLINEAR = GC(NN)
      FLIN = CDABS(GLINEAR)

```

```

RATLT = 100.DO
RATSS = 100.DO/FLIN
RATSB = 100.DO*FAC1/FLIN
RATSS = NINT(RATSS)
RATSB = NINT(RATSB)
WRITE(88,*) '      LINEAR THEORY 100% IS ',RATLT,'% '
WRITE(88,*) 'SHEAR AND BENDING STRESS IS ',RATSB,'% '
WRITE(88,*) '      SHEAR STRESS ONLY IS ',RATSS,'% '
CLOSE(88)
GO_I = DCMLPX(ZERO,ZERO)
GO_O = DCMLPX(ZERO,ZERO)
DO 900 K=NS,1,-1
    GO_I = GO_I-GC(K)
    GO_O = GO_O-GC(K+NS)
900  CONTINUE
DZ = ONE/DBLE(NS)
DO 1000 K=0,NS
    Z(K) = DZ*DBLE(K)
    GSUM_I = DCMLPX(ZERO,ZERO)
    GSUM_O = DCMLPX(ZERO,ZERO)
    DO 1100 J=NS,1,-1
        TEMP = COS(PI*DBLE(2*J-1)*Z(K))
        GSUM_I = GSUM_I+TEMP*GC(J)
        GSUM_O = GSUM_O+TEMP*GC(J+NS)
1100  CONTINUE
    G_INNER(K) = GSUM_I+GO_I
    G_OUTER(K) = GSUM_O+GO_O
1000  CONTINUE
OPEN(33,FILE=FNAME1,STATUS='NEW')
DO 1200 I=0,NS
    Y(I) = CDABS(G_INNER(I))
    YREAL(I) = DREAL(G_INNER(I))

```

```

        YIMAG(I) = DIMAG(G_INNER(I))
        WRITE(33,'(7F18.11)') Z(I), YREAL(I)
1200  CONTINUE
        CLOSE(33)

C
C  .. SECTION 1 ( DRAW GRAPHS OF G_INNER( ) AND G_OUTER( ) ) ..
C
        MORE = .FALSE.
        SPLINE = .FALSE.
        AXES = .TRUE.
        TITLE = 'GRAPH OF G_INNER'
        XR(1) = - 0.1D0
        XR(2) = 1.1D0
        YR(1) = ZERO
        YR(2) = ZERO
        WRITE(*,*) ' ABOUT TO DRAW GRAPHS - ENTER TO CONTINUE'
        READ(*,*)
        CALL L_DA_VINCI(NS+1,Z,Y,MORE,SPLINE,AXES,TITLE,XR,YR)
        MORE = .FALSE.
        OPEN(55,FILE=FNAME2,STATUS='NEW')
        DO 1300 I=0,NS
            Y(I) = CDABS(G_OUTER(I))
            YREAL(I) = DREAL(G_OUTER(I))
            YIMAG(I) = DIMAG(G_OUTER(I))
            WRITE(55,'(7F18.11)') Z(I), YREAL(I)
1300  CONTINUE
        CLOSE(55)
        TITLE = 'GRAPH OF G_OUTER'
        CALL L_DA_VINCI(NS+1,Z,Y,MORE,SPLINE,AXES,TITLE,XR,YR)

C
C  .. SECTION 2 ( FIND SURFACE SHAPE ) ..
C

```

```

DR = (RAT-ONE)/DBLE(NR)
DO 3000 K=0,NR
    RADIUS(K) = ONE+DR*DBLE(K)
    GH(K) = DCMPLX(ZERO,ZERO)
3000 CONTINUE
DO 3100 IVAL=NROOT,1,-1
    VLAM = R(IVAL)
    AVAL = (VLAM*ASPECT)**2
    GOMEGA1 = CDSQRT(AVAL-GFAC1)
    GOMEGA2 = CDSQRT(AVAL+HALF*GFAC2)
    DO 3200 K=1,NS
        TVAL = (PI*DBLE(2*K-1))**2
        G1 = (AVAL-GFAC1)/TVAL
        G2 = (AVAL+HALF*GFAC2)/TVAL
        GETA(K) = ((TWO+GRAT)*AVAL/TVAL+ONE+G1)/((ONE+G1)*(ONE+G2))
3200 CONTINUE
C
C .. DETERMINE VALUE OF CHI(LAMBDA) ..
C
    GTHETA = HALF*(GFAC1+HALF*GFAC2)/(GOMEGA1+GOMEGA2)
    IF ( CDABS(GTHETA).LE.(5.D-5) ) THEN
        GT = ONE+GTHETA*GTHETA/6.DO
        GT = -GT*(TWO+GRAT)*AVAL/(ONE+GOMEGA2/GOMEGA1)
        IF ((CDABS(GOMEGA1).GE.BIG).OR.(CDABS(GOMEGA2).GE.BIG)) THEN
            GT = DCMPLX(ZERO,ZERO)
        ELSE
            GT = GT/(GCOSH(HALF*GOMEGA1)*GCOSH(HALF*GOMEGA2))
        ENDIF
        GVAL = (FOUR+TWO*GRAT)*AVAL/(ONE+GOMEGA2/GOMEGA1)-GFAC1
        GVAL = GVAL*GTANH(HALF*GOMEGA2)/GOMEGA2
        GVAL = EIGHT/(GVAL+GT)
    ELSEIF ( CDABS(GTHETA).LE.0.5DO ) THEN

```

```

      GT = AVAL*(GSINH(GTHETA)/GTHETA)/(ONE+GOMEGA2/GOMEGA1)
      GT = -GT*(TWO+GRAT)
      IF ((CDABS(GOMEGA1).GE.BIG).OR.(CDABS(GOMEGA2).GE.BIG)) THEN
        GT = DCMPLX(ZERO,ZERO)
      ELSE
        GT = GT/(GCOSH(HALF*GOMEGA1)*GCOSH(HALF*GOMEGA2))
      ENDIF
      GVAL = (FOUR+TWO*GRAT)*AVAL/(ONE+GOMEGA2/GOMEGA1)-GFAC1
      GVAL = GVAL*GTANH(HALF*GOMEGA2)/GOMEGA2
      GVAL = EIGHT/(GVAL+GT)
    ELSE
      GVAL = TWO*AVAL-GFAC1
      GVAL = 0.25D0*GVAL**2/(AVAL*GOMEGA1*GOMEGA2)
      GVAL = GTANH(HALF*GOMEGA1)-GVAL*GTANH(HALF*GOMEGA2)
      GVAL = GVAL*AVAL*GOMEGA1
      GVAL = TWO*GFAC1/GVAL
    ENDIF
    G1 = DCMPLX(ZERO,ZERO)
    G2 = DCMPLX(ZERO,ZERO)
    DO 3300 J=NS,1,-1
      G1 = G1+GETA(J)*GC(J)
      G2 = G2+GETA(J)*GC(J+NS)
3300  CONTINUE
    FAC = BESSJ1(VLAM)/BESSJ1(VLAM*RAT)
    GT = VLAM*GVAL*(G1-FAC*G2)/(FAC*FAC-ONE)
    DO 3400 K=0,NR
      CALL C01(RADIUS(K),VLAM,TEMP)
      GH(K) = GH(K)+GT*TEMP
3400  CONTINUE
3100  CONTINUE
    GT = -0.25D0*GRAT*GC(NN-1)*ASPECT**2/(RAT*RAT-ONE)
    TEMP = -0.125D0*PI*ASPECT**2

```

```

        GH(0) = GC(NN)
        GH(NR) = DCMPLX(ZERO,ZERO)
DO 3500 K=1,NR-1
        GH(K) = TEMP*GH(K)+GT
3500  CONTINUE
DO 3600 I=0,NR
        Y(I) = CDABS(GH(I))
        YREAL(I) = DREAL(GH(I))
        YIMAG(I) = DIMAG(GH(I))
3600  CONTINUE
        MORE = .FALSE.
        SPLINE = .FALSE.
        AXES = .TRUE.
        TITLE = 'SURFACE DISPLACEMENT'
        XR(1) = -RAT*0.1D0
        XR(2) = RAT*1.1D0
        YR(1) = ZERO
        YR(2) = ZERO
        CALL L_DA_VINCI(NR+1,RADIUS,Y,MORE,SPLINE,AXES,TITLE,XR,YR)
        MORE = .FALSE.
        OPEN(77,FILE=FNAME3,STATUS='NEW')
DO 9999 J=0,NR
        WRITE(77,'(7F18.11)') RADIUS(J), YREAL(J)
9999  CONTINUE
        CLOSE(66)
        CLOSE(77)
        END

        FUNCTION GTANH(Z)
        COMPLEX*16 GTANH, Z
        DOUBLE PRECISION X, Y, BIG, ZERO, ONE

```

```

PARAMETER( ZERO=0.D0, ONE=1.D0, BIG=30.D0 )
X = DREAL(Z)
Y = DIMAG(Z)
IF ( X.GT.BIG ) THEN
    GTANH = DCMLPX(ONE,ZERO)
ELSEIF ( X.LT.-BIG ) THEN
    GTANH = DCMLPX(-ONE,ZERO)
ELSE
    X = TANH(X)
    GTANH = DCMLPX(X*COS(Y),SIN(Y))/DCMLPX(COS(Y),X*SIN(Y))
ENDIF
RETURN
END

```

```

FUNCTION GCOSH(Z)
COMPLEX*16 GCOSH, Z
DOUBLE PRECISION X, Y
X = DREAL(Z)
Y = DIMAG(Z)
GCOSH = DCMLPX(COSH(X)*COS(Y),SINH(X)*SIN(Y))
RETURN
END

```

```

FUNCTION GSINH(Z)
COMPLEX*16 GSINH, Z
DOUBLE PRECISION X, Y
X = DREAL(Z)
Y = DIMAG(Z)
GSINH = DCMLPX(SINH(X)*COS(Y),COSH(X)*SIN(Y))
RETURN

```

END

```
SUBROUTINE C01(RADIUS,VLAM,TEMP)
IMPLICIT DOUBLE PRECISION(A-H,O-Z)
TEMP = VLAM*RADIUS
TEMP = BESSJO(TEMP)*BESSY1(VLAM)-BESSY0(TEMP)*BESSJ1(VLAM)
RETURN
END
```

```
SUBROUTINE L_DA_VINCI(NP,X,Y,MORE,SPLINE,AXES,TEXT,XR,YR)
IMPLICIT DOUBLE PRECISION(A-H,O-Z)
PARAMETER( ZERO=0.D0 , ONE=1.D0 , SMALL=1.D-15 , NOUT=8 )
DIMENSION XR(2),YR(2),X(*),Y(*)
LOGICAL MORE,SPLINE,AXES,START,NOTEXT
CHARACTER*(*) TEXT
DATA START / .TRUE. /
C .. OPEN OUTPUT ERROR CHANNEL
      OPEN(NOUT,FILE='OUTPUT.ERR',STATUS='NEW')
C .. DEFAULT TO THE DATA RANGE ENCOUNTERED IN THE FIRST SUBROUTINE
C CALL. OTHERWISE USE THE USER SPECIFIED DATA WHEN SUPPLIED.
      IF (START) THEN
        XMAX = X(1)
        XMIN = X(1)
        YMAX = Y(1)
        YMIN = Y(1)
        DO 100 I=2,NP
          XMAX = MAX(XMAX,X(I))
          XMIN = MIN(XMIN,X(I))
```



```

        YMAX = MAX(YMAX,Y(I))
        YMIN = MIN(YMIN,Y(I))
100    CONTINUE
        IF (ABS(XR(1)).GE.SMALL) XMIN = XR(1)
        IF (ABS(XR(2)).GE.SMALL) XMAX = XR(2)
        IF (ABS(YR(1)).GE.SMALL) YMIN = YR(1)
        IF (ABS(YR(2)).GE.SMALL) YMAX = YR(2)
C .. PROCESS GRAPH TITLE
        NOTEXT = (TEXT.EQ.' ')
        IF (.NOT.NOTEXT) THEN
            NR = LEN(TEXT)+1
            NL = 0
111        NL = NL+1
            IF (TEXT(NL:NL).EQ.' ') GOTO 111
222        NR = NR-1
            IF (TEXT(NR:NR).EQ.' ') GOTO 222
        ENDIF
C .. SELECT GRAPHICS VIEW WINDOW SIZE
        UMIN = ZERO
        UMAX = ONE
        VMIN = ZERO
        VMAX = ONE
C.. CONNECT NAG GRAPHICS OUTPUT CHANNELS TO ERROR FILE AND SCREEN
        CALL JO6VAF(1,NOUT)
        CALL XXXXXX
C        NESQ = 1
C        CALL JO6VCF(0,NESQ)
C        OPEN(NESQ,FILE='CON')
C .. INITIALISE NAG GRAPHICS
        CALL JO6WAF
C .. INITIALISE NAG GRAPHICS WINDOW
        IF (NOTEXT.AND.(.NOT.AXES)) THEN

```

```

        CALL J06WBF(XMIN,XMAX,YMIN,YMAX,0)
ELSE
        CALL J06XFF(2)
        CALL J06WBF(XMIN,XMAX,YMIN,YMAX,1)
ENDIF
        CALL J06WCF(UMIN,UMAX,VMIN,VMAX)
C .. INSERT AXES IF REQUIRED
        IF (AXES) CALL J06AAF
C .. INSERT TITLE IF REQUIRED
        IF (.NOT.NOTEXT) CALL J06AHF(TEXT(NL:NR))
        START = .FALSE.
ENDIF
C .. NOW DRAW EACH CURVE IN TURN
        IFAIL = 0
        IF (.NOT.SPLINE) THEN
                KSYM = 1
                CALL J06BAF(X,Y,NP,1,KYSM,IFAIL)
        ELSE
                METHOD = 1
                CALL J06CAF(X,Y,NP,METHOD,IFAIL)
        ENDIF
        IF (MORE) RETURN
        START = .TRUE.
        CALL J06WZF
        RETURN
END

```

# Appendix E

## Auxiluray Fortran program for chapter 4 and 5

This appendix contains FORTRAN 77 program to determines the shear stress  $g(z)$  for compressible and incompressible case for chapter 4 and 5.

```
*****
*      THIS PROGRAM FOR COMPESSIBLE DYNAMIC CASE - AXIAL PROBLEM      *
*      THE VALUE OF  $g(Z)$  ARE GIVEN BY THE REAL AND IMAGE VALUE      *
*      WHERE                                                              /      *
*       $G(Z) = \int g(z) dz$                                           *
*      /                                                                  *
*****

PROGRAM AXIAL
IMPLICIT DOUBLE PRECISION(A-H,O-Z)
PARAMETER( ZERO=0.D0, NS=401, IW=5*NS+5, NIN=5, NOUT=6 )
CHARACTER*1 ANS
CHARACTER*12 FNAME
CHARACTER*30 TITLE
LOGICAL FLAG, SPLINE, VIEW, MORE, BOX
DIMENSION G(0:NS), DG(0:NS), Z(0:NS), XR(2), YR(2), MAG(2), W(IW)

C
C      .. READS IN THE G( ) VALUES AND COMPUTES AND DRAWS THE  $g( )$ 
C      VALUES USING CENTRAL DIFFERENCING METHODS ..
```

```

    PI = 4.DO*ATAN(ONE)

C
C    .. REQUESTS GEOMETRICAL INPUT ..
C

    WRITE(NOUT,*) ' ENTER RATIO OF RADII > '
    READ(NIN,*) RAT
    WRITE(NOUT,*) '   ENTER ASPECT RATIO > '
    READ(NIN,*) ASPECT
    WRITE(NOUT,*) 'ENTER VALUE FOR GAMMA > '
    READ(*,*) GAMMA

*****
*               J = NINT(100.DO*ASPECT)               *
*   THIS LINE MUST ADD TO THE PROGRAM AND CANCEL THE LINE   *
*               J = NINT(10.DO*ASPECT)               *
*   WHEN ASPECT = 1/4, 1/2, 3/4 ONLY                       *
*****
*****
*               J = NINT(10.DO*ASPECT)               *
*   THIS LINE MUST ADD TO THE PROGRAM AND CANCEL THE LINE   *
*               J = NINT(100.DO*ASPECT)               *
*   WHEN ASPECT IS INTGER NUMBERS                         *
*****

    K = NINT(10.DO*RAT)
    J = NINT(10.DO*ASPECT)
    L = NINT(1.DO*GAMMA)
    FNAME = 'CS '//CHAR(48+K/10)//CHAR(48+MOD(K,10))//CHAR(48+J/10)
    FNAME(7:12) = CHAR(48+MOD(J,10))//CHAR(48+L)//'.000'
111  WRITE(NOUT,*) 'ENTER ''O'' FOR OUTER OR ''I'' FOR INNER'
    READ(NIN,*) ANS
    IF (ANS.EQ.'O') THEN
        FNAME(3:3) = 'O'
    ELSEIF (ANS.EQ.'I') THEN

```

```

        FNAME(3:3) = 'I'
ELSE
        GOTO 111
ENDIF
INQUIRE(FILE=FNAME, EXIST=FLAG)
IF (.NOT.FLAG) THEN
        WRITE(NOUT,*) 'CANNOT FIND FILE ',FNAME
        STOP
ELSE
        OPEN(11,FILE=FNAME)
        ITEM = -1
222      READ(11,*,END=333) XVAL,YVAL
        ITEM = ITEM+1
        IF (ITEM.GT.NS) THEN
                WRITE(*,*) 'FAILURE - TOO MANY DATA POINTS'
                STOP
        ENDIF
        Z(ITEM) = XVAL
        G(ITEM) = YVAL
        GOTO 222
333      CLOSE(11)
        FNAME(1:1) = 'G'
ENDIF

C
C      .. NOW COMPUTE DERIVATIVES OF G( ) BY CENTRAL DIFFERENCING.
C      THE VALUES OF G( ) ARE KNOWN TO BE GIVEN OVER A UNIFORM
C      DISSECTION OF [0,1] ..
H = Z(1)-Z(0)
DG(0) = (G(1)-G(0))/H
DO 100 I=1,ITEM-1
        DG(I) = 0.5D0*(G(I+1)-G(I))/H
100  CONTINUE

```

```

      DG(ITEM) = (G(ITEM)-G(ITEM-1))/H
C
C    .. DRAW GRAPH OF DG ..
      IF (ANS.EQ.'0') THEN
          TITLE = 'GRAPH OF g(OUTER)'
      ELSE
          TITLE = 'GRAPH OF g(INNER)'
      ENDIF
      SPLINE = .FALSE.
      VIEW = .FALSE.
      MORE = .FALSE.
      BOX = .TRUE.
      MAG(1) = 3
      MAG(2) = 2
      XR(1) = -0.1D0
      XR(2) = 1.1D0
      YR(1) = 0.D0
      YR(2) = 0.D0
      MM = 3
      CALL CURVED(ITEM+1,Z,DG,SPLINE,VIEW,MORE,MM,TITLE,XR,YR,MAG,BOX,W)
      OPEN(11,FILE=FNAME)
      DO 200 I=0,ITEM
          WRITE(11,*) Z(I),DG(I)
200  CONTINUE
      CLOSE(11)
      END

```

# Appendix F

## Fortran program for chapter 6

This appendix contains FORTRAN 77 program to determines the incompressible radial and axial displacement in chapter 6

```
PROGRAM TORSION
```

```
IMPLICIT DOUBLE PRECISION(A-H,O-Z)
```

```
*****
```

```
*                                                                 *
```

```
*      PROGRAMME DETERMINES THE COEFFICIENTS OF THE SHEAR STRESS      *
```

```
*      ON THE TOP AND BOTTOM PLANES OF THE CYLINDER                  *
```

```
*      INCOMPRESSIBLE CASE                                           *
```

```
*                                                                 *
```

```
*      USING THE SERIES                                              *
```

```
*       $g(r) = \text{Sum}\{g_k * J_0(\lambda r)\}$                                 *
```

```
*      Where lambda are the roots of  $J_1(\lambda)$                         *
```

```
*****
```

```
PARAMETER( ZERO=0.D0, HALF=0.5D0, ONE=1.D0, TWO=2.D0, FOUR=4.D0,
```

```
*      EIGHT=8.D0, AMAX=700.D0, NA=1000, N=200, FORCE=ONE )
```

```
DIMENSION ROOTP2(N), ROOTP1(N), V_J0(N), CHI(N), ETA(N)
```

```
C
```

```
C .. PARAMETERS INVOLVED IN LINEAR EQUATIONS ..
```

```

        DIMENSION A(N,N), B(N), C(N), V(N,N), WKS1(N), WKS2(N)

C
C .. PARAMETERS INVOLVED IN GRAPHICS ..
        PARAMETER( NS=40 )
        DIMENSION Y(0:NS), X(0:NS)
        DIMENSION XR(2), YR(2), MAG(2), W(5*NS+5)
        LOGICAL FLAG, MORE, BOX, SPLINE
        CHARACTER*50 TEXT
        PARAMETER( BOX=.TRUE., SPLINE=.FALSE. )
        CHARACTER*4 CODE
        CHARACTER*12 FNAME1, FNAME2, FNAME3, FNAME4, FNAME5,
*                FNAME6, FNAME7, FNAME8, FNAME9, FNAME10,
*                FNAME11, FNAME12, FNAME13, FNAME14

C
C .. DETERMINE ASPECT RATIO OF SLAB ..
        WRITE(*,*) 'ENTER ASPECT RATIO FOR CYLINDER'
        READ(*,*) ASPECT
        WRITE(*,*) 'ASPECT RATIO IS ',ASPECT
        WRITE(*,*)
        PI = 4.DO*ATAN(ONE)

C
C .. BUILD NAME OF OUTPUT FILE ..
        NVAL = NINT(1000.DO*ASPECT)
        M = MOD(NVAL,10)
        CODE(4:4) = CHAR(M+48)
        NVAL = (NVAL - M)/10
        M = MOD(NVAL,10)
        CODE(3:3) = CHAR(M+48)
        NVAL = (NVAL - M)/10
        M = MOD(NVAL,10)
        CODE(2:2) = CHAR(M+48)

```



```

      NVAL = (NVAL - M)/10
      M = MOD(NVAL,10)
      CODE(1:1) = CHAR(M+48)

C
C .. SEARCH FOR FILE CONTAINING ZEROS ..
      INQUIRE(FILE='J1_ZEROS.DAT',EXIST=FLAG)
      IF (.NOT.FLAG) THEN
         WRITE(*,*) 'CANNOT FIND FILE CONTAINING ZEROS OF J1(X)'
         STOP
      ENDIF

C
C .. READ IN ZEROS ..
      ITEM = 0
      OPEN(15,FILE='J1_ZEROS.DAT',STATUS='OLD')
111  READ(15,*) RVAL
      ITEM = ITEM+1
      ROOTP1(ITEM) = RVAL
      ROOTP2(ITEM) = RVAL*RVAL
      V_J0(ITEM) = BESSJ0(RVAL)
      IF ( ITEM.LT.N ) GOTO 111
      CLOSE(15)

C
C .. ZERO ALL MATRICES AND VECTORS ..
      DO 100 I=1,N
         DO 200 J=1,N
            A(I,J) = ZERO
200    CONTINUE
      CHI(I) = ZERO
      ETA(I) = ZERO

```

```

        B(I) = ZERO
100    CONTINUE

C
C .. BUILD A, CHI AND ETA ..
    DO 300 L=NA,1,-1
        ALPHA1 = PI*DBLE(2*L-1)/ASPECT
        ALPHA2 = ALPHA1*ALPHA1
        IF ( ALPHA1.LE.AMAX ) THEN
            RATIO = ALPHA1*BESSIO(ALPHA1)/BESSI1(ALPHA1)
            QVAL = RATIO*RATIO
            QVAL = ONE/(ALPHA2-QVAL+ONE)
        ELSE
            QVAL = -(ONE-1.125DO/ALPHA2)/ALPHA1
        ENDIF
        DO 400 K=N,1,-1
            TMP = ONE/(ALPHA2+ROOTP2(K))**2
            ETA(K) = ETA(K)+TMP*ROOTP2(K)
            CHI(K) = TMP*(ALPHA2-ROOTP2(K))
            B(K) = B(K)+QVAL*CHI(K)
400    CONTINUE
        DO 500 K=1,N
            DO 600 J=K,N
                A(K,J) = A(K,J)+ALPHA2*QVAL*CHI(K)*CHI(J)
600    CONTINUE
500    CONTINUE
300    CONTINUE

C
C .. BUILD LOWER TRIANGULAR PART OF A ..
    DO 700 K=1,N
        B(K) = B(K)*FORCE

```

```

      A(K,K) = A(K,K)-ETA(K)
      DO 800 J=1,K
        A(K,J) = A(J,K)
800    CONTINUE
700    CONTINUE

C
C .. SOLVE THE LINEAR EQUATIONS FOR THE COEFFICIENTS OF G ..
      IFAIL = 0
      CALL F04ATF(A, N, B, N, C, V, N, WKS1, WKS2, IFAIL)

C    .. SECTION VALUE OF THE RESULT ..

      NVAL = NINT(100.DO*ASPECT)
      I = MOD(NVAL,10)
      JVAL = (NVAL - I)/10
      J = MOD(JVAL,10)
      KVAL = (JVAL - I)/10
      K = MOD(KVAL,10)
      FNAME1 = 'LIR'//CHAR(K+48)//CHAR(J+48)//CHAR(I+48)//'.DAT'
      FNAME2 = FNAME1
      FNAME2(3:3) = 'C'
      FNAME3 = FNAME1
      FNAME3(3:3) = 'G'

C
C .. SET UP UNIFORMLY SPACED GRID FOR GRAPHICAL PURPOSES ..
      Y(0) = ZERO
      Y(NS) = FORCE
      XVAL = ONE/DBLE(NS)
      DO 1000 J=0,NS

```

```

        X(J) = XVAL*DBLE(J)
1000  CONTINUE

C
C .. AXIAL LOAD OVER [0,R] ..
        DO 1100 J=1,NS
            SUM = -HALF*FORCE*X(J)
            DO 1200 I=N,1,-1
                SUM = SUM+(C(I)/(ROOTP1(I)*V_J0(I)))*BESSJ1(ROOTP1(I)*X(J))
1200      CONTINUE
            Y(J) = SUM*X(J)
1100  CONTINUE

C
C .. VALUE OF FUNCTION G(R)
        Y(0) = ZERO
        OPEN(30,FILE=FNAME3)
        DO 1300 K=0,NS
            WRITE(30,'(2F18.11)') X(K), Y(K)
1300      CONTINUE
        CLOSE(30)

C
C ...  DRAW THE ACCUMULATED SHEAR STRESS ..
        MORE = .FALSE.
        FLAG = .FALSE.
        TEXT = ' '
        MAG(1) = 3
        MAG(2) = 2
        MODE = 2
        XR(1) = - 0.1D0
        XR(2) = 1.1D0

```

```

YR(1) = -0.D0
YR(2) = 0.0D0
CALL CURVED(NS+1,X,Y,SPLINE,FLAG,MORE,MODE,TEXT,XR,YR,MAG,BOX,W)

```

```

C
C .. COMPUTE CONSTANT C ..
SUM = ZERO
CVAL = ZERO
DO 2000 L=NA,1,-1
    ALPHA1 = PI*DBLE(2*L-1)/ASPECT
    ALPHA2 = ALPHA1*ALPHA1
    IF ( ALPHA1.LE.AMAX ) THEN
        RATIO = ALPHA1*BESSIO(ALPHA1)/BESSI1(ALPHA1)
        QVAL = RATIO*RATIO
        QVAL = ONE/(ALPHA2-QVAL+ONE)
    ELSE
        QVAL = -(ONE-1.125D0/ALPHA2)/ALPHA1
    ENDIF
    TMP = ZERO
    DO 2100 K=N,1,-1
        TMP = TMP+C(K)*(ALPHA2-ROOTP2(K))/(ALPHA2+ROOTP2(K))**2
2100    CONTINUE
        TMP = TMP-FORCE/ALPHA2
        SUM = SUM+TMP*QVAL
2000 CONTINUE
CVAL = -FOUR*SUM/ASPECT**2
HVAL = TWO*CVAL
WRITE(*,*) 'DISPLACEMENT IS ', HVAL
READ(*,*)

```

```

C
C .. VALUE OF DISPLACEMENT H

```

```

OPEN(20,FILE=FNAME2)
      WRITE(20,'(2F18.11)') HVAL
CLOSE(20)

C
C .. COMPUTE RADIAL DISPLACEMENT ..
      DO 3000 I=0,NS
          Y(I) = ZERO
3000  CONTINUE
      DO 3100 L=NA,1,-1
          ALPHA1 = PI*DBLE(2*L-1)/ASPECT
          RATIO = BESSIO(ALPHA1)/BESSI1(ALPHA1)
          ALPHA2 = ALPHA1*ALPHA1
          IF ( ALPHA1.LE.AMAX ) THEN
              RATIO = ALPHA1*BESSIO(ALPHA1)/BESSI1(ALPHA1)
              QVAL = RATIO*RATIO
              QVAL = ONE/(ALPHA2-QVAL+ONE)
          ELSE
              QVAL = -(ONE-1.125DO/ALPHA2)/ALPHA1
          ENDIF
          SUM = ZERO
          DO 3200 K=N,1,-1
              TMP = C(K)/(ALPHA2+ROOTP2(K))**2
              SUM = SUM+TMP*(ALPHA2-ROOTP2(K))
3200  CONTINUE
          SUM = ALPHA1*SUM-FORCE/ALPHA1
          SUM = SUM*QVAL
          ANGLE = PI*DBLE(2*L-1)
          DO 3300 K=1,NS-1
              Y(K) = Y(K)+SUM*SIN(ANGLE*X(K))
3300  CONTINUE
3100  CONTINUE

```

```

      DO 3400 I=0,NS-1
        Y(I) = TWO*Y(I)/ASPECT**2
3400  CONTINUE

      OPEN(10,FILE=FNAME1)
      DO 3500 J=0,NS
        WRITE(10,'(7F18.11)') X(J),Y(J)
3500  CONTINUE
      CLOSE(10)

C
C ...  DRAW THE RADIAL DISPLACEMENT ..
      MORE = .FALSE.
      FLAG = .FALSE.
      TEXT = ' '
      MAG(1) = 3
      MAG(2) = 2
      MODE = 2
      XR(1) = -0.1D0
      XR(2) = 1.1D0
      YR(1) = -0.9D0
      YR(2) = 1.1D0
      CALL CURVEO(NS+1,X,Y,SPLINE,FLAG,MORE,MODE,TEXT,XR,YR,MAG,BOX,W)
C
C .. COMPUTE AXIAL DISPLACEMENT ..
C      DO 234 JJ=0,10
C      ZVAL = 0.1D0*DBLE(JJ)
      ZVAL = ONE
      DO 4000 I=0,NS
        Y(I) = ZERO
4000  CONTINUE

```

```

DO 4100 I=1,N
    ETA(I) = ZERO
    B(I) = ZERO
4100 CONTINUE
SUM1 = ZERO
DO 4200 L=NA,1,-1
    COSVAL = COS(PI*ZVAL*DBLE(2*L-1))
    ALPHA1 = PI*DBLE(2*L-1)/ASPECT
    ALPHA2 = ALPHA1*ALPHA1
    IF ( ALPHA1.LE.AMAX ) THEN
        RATIO = ALPHA1*BESSIO(ALPHA1)/BESSI1(ALPHA1)
        QVAL = RATIO*RATIO
        QVAL = ONE/(ALPHA2-QVAL+ONE)
    ELSE
        QVAL = -(ONE-1.125DO/ALPHA2)/ALPHA1
    ENDIF
    SUM = ZERO
DO 4300 K=N,1,-1
    TMP = ONE/(ALPHA2+ROOTP2(K))**2
    ETA(K) = ETA(K)+TMP*ROOTP2(K)*COSVAL
    CHI(K) = TMP*(ALPHA2-ROOTP2(K))
    SUM = SUM+C(K)*CHI(K)
4300 CONTINUE
SUM = (ALPHA2*SUM-FORCE)*QVAL*COSVAL
SUM1 = SUM1+SUM/ALPHA2
DO 4400 K=N,1,-1
    B(K) = B(K)+CHI(K)*SUM
4400 CONTINUE
4200 CONTINUE
DO 4500 J=0,NS
    SUM = ZERO
    DO 4600 K=1,N

```



```

        TMP = BESSJO(ROOTP1(K)*X(J))
        SUM = SUM+TMP*(B(K)-ETA(K)*C(K))/V_J0(K)
4600    CONTINUE
        Y(J) = FOUR*(SUM+SUM1)/ASPECT**2+CVAL
4500    CONTINUE

C      .. SECTION VALUE OF THE RESULT OF AXIAL DISPLACEMENT ..

        NVAL = NINT(100.D0*ASPECT)
        I = MOD(NVAL,10)
        JVAL = (NVAL - I)/10
        J = MOD(JVAL,10)
        KVAL = (JVAL - I)/10
        K = MOD(KVAL,10)
        FNAME4 = 'LIX'//CHAR(K+48)//CHAR(J+48)//CHAR(I+48)//'.010'

        OPEN(40,FILE=FNAME4)
        DO 14700 I=0,NS
            WRITE(40,'(7F18.11)') X(I),Y(I)
14700    CONTINUE
        CLOSE(40)

C ...  DRAW THE AXIAL DISPLACEMENT ..
C      IF ( JJ.LT.10 ) THEN
C          MORE = .TRUE.
C      ELSE
C          MORE = .FALSE.
C      ENDIF
        FLAG = .FALSE.
        TEXT = ' '
        MAG(1) = 3

```

```
MAG(2) = 2
MODE = 2
XR(1) = -0.1D0
XR(2) = 1.1D0
YR(1) = ZERO
YR(2) = ZERO
YR(1) = -0.15D0
YR(2) = 0.02D0
CALL CURVED(NS+1,X,Y,SPLINE,FLAG,MORE,MODE,TEXT,XR,YR,MAG,BOX,W)
C234  CONTINUE
END
```

# Appendix G

## Fortran program for chapter 7

This appendix contains FORTRAN 77 program to determines the compressible radial and axial displacement in chapter 7

```
PROGRAM TORSION
```

```
IMPLICIT DOUBLE PRECISION(A-H,O-Z)
```

```
*****
```

```
*                                                                 *
```

```
*      PROGRAMME DETERMINES THE COEFFICIENTS OF THE SHEAR STRESS  *
```

```
*      ON THE TOP AND BOTTOM PLANES OF THE CYLINDER                *
```

```
*      COMPRESSIBLE CASE                                           *
```

```
*                                                                 *
```

```
*      USING THE SERIES                                           *
```

```
*       $\text{GAMMA} * g(r) = \text{Sum}\{g_k * J_0(\lambda * r)\}$                 *
```

```
*      Where lambda are the roots of  $J_1(\lambda)$                     *
```

```
*****
```

```
PARAMETER( ZERO=0.D0, HALF=0.5D0, ONE=1.D0, TWO=2.D0, FOUR=4.D0,
```

```
*      EIGHT=8.D0, AMAX=700.D0, NA=1000, N=200, FORCE=ONE,
```

```
*      ANINE=9.D0)
```

```
DIMENSION ROOTP2(N), ROOTP1(N), V_J0(N), CHI(N), ETA(N)
```

C

```

C .. PARAMETERS INVOLVED IN LINEAR EQUATIONS ..
      DIMENSION A(N,N), B(N), C(N), V(N,N), WKS1(N), WKS2(N)
C
C .. PARAMETERS INVOLVED IN GRAPHICS ..
      PARAMETER( NS=100 )
      DIMENSION Y(0:NS), X(0:NS)
      DIMENSION XR(2), YR(2), MAG(2), W(5*NS+5)
      LOGICAL FLAG, MORE, BOX, SPLINE
      CHARACTER*50 TEXT
      PARAMETER( BOX=.TRUE., SPLINE=.FALSE. )
      CHARACTER*4 CODE
      CHARACTER*12 FNAME1, FNAME2, FNAME3, FNAME4, FNAME5
C
C .. DETERMINE ASPECT RATIO OF SLAB ..
      WRITE(*,*) 'ENTER ASPECT RATIO FOR CYLINDER'
      READ(*,*) ASPECT
      WRITE(*,*) 'ENTER VALUE OF GAMMA'
      READ(*,*) GAMMA
      WRITE(*,*)
      WRITE(*,*) 'ASPECT RATIO IS ',ASPECT
      WRITE(*,*) 'GAMMA IS ',GAMMA
      GAMMA = TWO*GAMMA
      GAMMA = ONE/GAMMA
      PI = 4.DO*ATAN(ONE)
C
C .. BUILD NAME OF OUTPUT FILE ..
      NVAL = NINT(1000.DO*ASPECT)
      M = MOD(NVAL,10)
      CODE(4:4) = CHAR(M+48)
      NVAL = (NVAL - M)/10
      M = MOD(NVAL,10)

```

```

CODE(3:3) = CHAR(M+48)
NVAL = (NVAL - M)/10
M = MOD(NVAL,10)
CODE(2:2) = CHAR(M+48)
NVAL = (NVAL - M)/10
M = MOD(NVAL,10)
CODE(1:1) = CHAR(M+48)

```

```

C
C .. SEARCH FOR FILE CONTAINING ZEROS ..
      INQUIRE(FILE='J1_ZEROS.DAT',EXIST=FLAG)
      IF (.NOT.FLAG) THEN
        WRITE(*,*) 'CANNOT FIND FILE CONTAINING ZEROS OF J1(X)'
        STOP
      ENDIF

```

```

C
C .. READ IN ZEROS ..
      ITEM = 0
      OPEN(15,FILE='J1_ZEROS.DAT',STATUS='OLD')
111  READ(15,*) RVAL
      ITEM = ITEM+1
      ROOTP1(ITEM) = RVAL
      ROOTP2(ITEM) = RVAL*RVAL
      V_J0(ITEM) = BESSJ0(RVAL)
      IF ( ITEM.LT.N ) GOTO 111
      CLOSE(15)

```

```

C
C .. ZERO ALL MATRICES AND VECTORS ..
      DO 100 I=1,N
        DO 200 J=1,N

```

```

200      CONTINUE
        CHI(I) = ZERO
        ETA(I) = ZERO
        B(I) = ZERO
100  CONTINUE

C
C .. BUILD A, CHI AND ETA ..
      DO 300 L=NA,1,-1
        ALPHA1 = PI*DBLE(2*L-1)/ASPECT
        RATIO = BESSIO(ALPHA1)/BESSI1(ALPHA1)
        ALPHA2 = ALPHA1*ALPHA1
        IF ( ALPHA1.LE.AMAX ) THEN
          QVAL = RATIO*RATIO
          QVAL = ONE/((ONE+GAMMA)*ALPHA2*(QVAL-ONE)-ONE)
        ELSE
          QVAL = (ONE+GAMMA)*(ONE+ALPHA1+(ANINE/(EIGHT*ALPHA1)))-ONE
          QVAL = ONE/QVAL
        ENDIF
        DO 400 K=N,1,-1
          TMP = ONE/(ALPHA2+ROOTP2(K))**2
          ETA(K) = ETA(K)+TMP*(GAMMA*ALPHA2-ROOTP2(K))
          CHI(K) = TMP*((ONE+TWO*GAMMA)*ALPHA2-ROOTP2(K))
          B(K) = B(K)+QVAL*CHI(K)
400    CONTINUE
        DO 500 K=1,N
          DO 600 J=K,N
            A(K,J) = A(K,J)+ALPHA2*QVAL*CHI(K)*CHI(J)
600      CONTINUE
500    CONTINUE
300  CONTINUE

```

```

C
C .. BUILD LOWER TRIANGULAR PART OF A ..
      DO 700 K=1,N
          B(K) = -B(K)*TWO*FORCE*(ONE+TWO*GAMMA)
          A(K,K) = A(K,K)-ETA(K)
          DO 800 J=1,K
              A(K,J) = A(J,K)
800      CONTINUE
700      CONTINUE

C
C .. SOLVE THE LINEAR EQUATIONS FOR THE COEFFICIENTS OF G ..
      IFAIL = 0
      CALL F04ATF(A, N, B, N, C, V, N, WKS1, WKS2, IFAIL)

C      .. SECTION VALUE OF THE RESULT ..

      GGAMMA = ABS(HALF/GAMMA)
      NVAL = NINT(10.DO*GGAMMA)
      LVAL = NINT(100.DO*ASPECT)
      I = MOD(NVAL,10)
      MVAL = (NVAL - I)/10
      M = MOD(MVAL,10)
C      LVAL = (MVAL - M)/10
      L = MOD(LVAL,10)
      KVAL = (LVAL - L)/10
      K = MOD(KVAL,10)
      JVAL = (KVAL - K)/10
      J = MOD(JVAL,10)
      FNAME1 = 'LCA'//CHAR(J+48)//CHAR(K+48)//CHAR(L+48)
*           //CHAR(M+48)//CHAR(I+48)//'.DAT'

```

```

FNAME2 = FNAME1
FNAME2(3:3) = 'R'
FNAME3 = FNAME1
FNAME3(3:3) = 'C'

```

```

C
C .. SET UP UNIFORMLY SPACED GRID FOR GRAPHICAL PURPOSES ..
    Y(0) = ZERO
    Y(NS) = FORCE
    XVAL = ONE/DBLE(NS)
    DO 1000 J=0,NS
        X(J) = XVAL*DBLE(J)
1000  CONTINUE

C
C .. AXIAL LOAD OVER [0,R] ..
    DO 1100 J=1,NS-1
        SUM = FORCE*X(J)
        DO 1200 I=N,1,-1
            SUM = SUM+(C(I)/(ROOTP1(I)*V_J0(I)))*BESSJ1(ROOTP1(I)*X(J))
1200  CONTINUE
        Y(J) = SUM*X(J)
1100  CONTINUE

C
C .. VALUE OF FUNCTION G(R)
    Y(0) = ZERO
    OPEN(30,FILE=FNAME1)
    DO 1300 K=0,NS
        WRITE(30,'(2F18.11)') X(K), Y(K)

```



1300           CONTINUE

      CLOSE(30)

C

C ... DRAW THE ACCUMULATED SHEAR STRESS ..

      MORE = .FALSE.

      FLAG = .FALSE.

      TEXT = ' '

      MAG(1) = 3

      MAG(2) = 2

      MODE = 2

      XR(1) = - 0.1D0

      XR(2) = 1.1D0

      YR(1) = -0.1D0

      YR(2) = 1.1D0

      CALL CURVEO(NS+1,X,Y,SPLINE,FLAG,MORE,MODE,TEXT,XR,YR,MAG,BOX,W)

C

C .. COMPUTE CONSTANT C ..

      SUM = ZERO

      CVAL = ZERO

      FAC = ONE+TWO\*GAMMA

      DO 2000 L=NA,1,-1

          ALPHA1 = PI\*DBLE(2\*L-1)/ASPECT

          RATIO = BESSIO(ALPHA1)/BESSI1(ALPHA1)

          ALPHA2 = ALPHA1\*ALPHA1

          IF ( ALPHA1.LE.AMAX ) THEN

              QVAL = RATIO\*RATIO

              QVAL = ONE/((ONE+GAMMA)\*ALPHA2\*(QVAL-ONE)-ONE)

          ELSE

              QVAL =(ONE+GAMMA)\*(ONE+ALPHA1+(ANINE/(EIGHT\*ALPHA1)))-ONE

              QVAL = ONE/QVAL

```

ENDIF
CVAL = CVAL+ONE/ALPHA2
TMPSUM = TWO*FAC*FORCE/ALPHA2
DO 2100 K=N,1,-1
    TMP = C(K)/(ALPHA2+ROOTP2(K))**2
    TMPSUM = TMPSUM+TMP*(FAC*ALPHA2-ROOTP2(K))
2100    CONTINUE
    SUM = SUM+TMPSUM*QVAL
2000    CONTINUE
    CVAL = (EIGHT*FORCE*CVAL*GAMMA-FOUR*FAC*SUM)/ASPECT**2
    HVAL = TWO*CVAL
C    WRITE(*,*) 'DISPLACEMENT IS ', HVAL
C    READ(*,*)

OPEN(60,FILE=FNAME3)
    WRITE(60,'(7F18.11)') HVAL
CLOSE(60)

C
C .. COMPUTE RADIAL DISPLACEMENT ..
DO 3000 I=0,NS
    Y(I) = ZERO
3000    CONTINUE
    FAC = ONE+TWO*GAMMA
    DO 3100 L=NA,1,-1
        ALPHA1 = PI*DBLE(2*L-1)/ASPECT
        RATIO = BESSIO(ALPHA1)/BESSI1(ALPHA1)
        ALPHA2 = ALPHA1*ALPHA1
        IF ( ALPHA1.LE.AMAX ) THEN
            QVAL = RATIO*RATIO
            QVAL = ONE/((ONE+GAMMA)*ALPHA2*(QVAL-ONE)-ONE)
        ELSE

```

```

        QVAL = (ONE+GAMMA)*(ONE+ALPHA1+(ANINE/(EIGHT*ALPHA1)))-ONE
        QVAL = ONE/QVAL
    ENDIF

    SUM = TWO*FAC*FORCE/ALPHA2
    DO 3200 K=N,1,-1
        TMP = C(K)/(ALPHA2+ROOTP2(K))**2
        SUM = SUM+TMP*(FAC*ALPHA2-ROOTP2(K))
3200    CONTINUE

    SUM = ALPHA1*SUM*QVAL
    ANGLE = PI*DBLE(2*L-1)
    DO 3300 K=1,NS-1
        Y(K) = Y(K)+SUM*SIN(ANGLE*X(K))
3300    CONTINUE
3100    CONTINUE

    DO 3400 I=1,NS-1
        Y(I) = TWO*Y(I)/ASPECT**2
3400    CONTINUE

    OPEN(60,FILE=FNAME2)
    DO 3500 J=0,NS
        WRITE(60,'(7F18.11)') X(J),Y(J)
3500    CONTINUE

    CLOSE(60)

C
C ...  DRAW THE RADIAL DISPLACEMENT ..
    MORE = .FALSE.
    FLAG = .FALSE.
    TEXT = ' '
    MAG(1) = 3
    MAG(2) = 2
    MODE = 2
    XR(1) = -0.1D0

```

```

XR(2) = 1.1D0
YR(1) = -0.9D0
YR(2) = 1.1D0
CALL CURVEO(NS+1,X,Y,SPLINE,FLAG,MORE,MODE,TEXT,XR,YR,MAG,BOX,W)

C
C .. COMPUTE AXIAL DISPLACEMENT FOR VALUE OF Z=ZERO ..
C      DO 234 JJ=0,10
C      ZVAL = 0.1D0*DBLE(JJ)
      ZVAL = zero
      DO 4000 I=0,NS
        Y(I) = ZERO
4000    CONTINUE
      DO 4100 I=1,N
        ETA(I) = ZERO
        B(I) = ZERO
4100    CONTINUE
      FAC = ONE+TWO*GAMMA
      FAC1 = EIGHT*FORCE*GAMMA/ASPECT**2
      SUM1 = ZERO
      DO 4200 L=NA,1,-1
        COSVAL = COS(PI*ZVAL*DBLE(2*L-1))
        ALPHA1 = PI*DBLE(2*L-1)/ASPECT
        RATIO = BESSIO(ALPHA1)/BESSI1(ALPHA1)
        ALPHA2 = ALPHA1*ALPHA1
        SUM1 = SUM1-FAC1*COSVAL/ALPHA2
        IF ( ALPHA1.LE.AMAX ) THEN
          QVAL = RATIO*RATIO
          QVAL = ONE/((ONE+GAMMA)*ALPHA2*(QVAL-ONE)-ONE)
        ELSE
          QVAL = (ONE+GAMMA)*(ONE+ALPHA1+(ANINE/(EIGHT*ALPHA1)))-ONE
          QVAL = ONE/QVAL

```

```

ENDIF
SUM = ZERO
DO 4300 K=N,1,-1
    TMP = ONE/(ALPHA2+ROOTP2(K))**2
    ETA(K) = ETA(K)+TMP*(GAMMA*ALPHA2-ROOTP2(K))*COSVAL
    CHI(K) = TMP*((ONE+TWO*GAMMA)*ALPHA2-ROOTP2(K))
    SUM = SUM+C(K)*CHI(K)
4300    CONTINUE
    SUM = SUM+TWO*FORCE*FAC/ALPHA2
    SUM = SUM*QVAL*COSVAL
    SUM1 = SUM1+FOUR*FAC*SUM/ASPECT**2
    DO 4400 K=N,1,-1
        B(K) = B(K)+CHI(K)*SUM*ALPHA2
4400    CONTINUE
4200    CONTINUE
    DO 4500 J=0,NS
        SUM = ZERO
        DO 4600 K=1,N
            TMP = BESSJ0(ROOTP1(K)*X(J))
c            TMP = FOUR*BESSJ0(ROOTP1(K)*X(J))/ASPECT**2
            SUM = SUM+(B(K)-ETA(K)*C(K))*TMP/V_J0(K)
4600    CONTINUE
            Y(J) = Y(J)+CVAL+SUM1+(four*sum/aspect**2)
c            Y(J) = Y(J)+SUM+CVAL+SUM1
4500    CONTINUE

```

```

GGAMMA = ABS(HALF/GAMMA)
NVAL = NINT(10.DO*GGAMMA)
LVAL = NINT(100.DO*ASPECT)
I = MOD(NVAL,10)

```

```

MVAL = (NVAL - I)/10
M = MOD(MVAL,10)
C   LVAL = (MVAL - M)/10
L = MOD(LVAL,10)
KVAL = (LVAL - L)/10
K = MOD(KVAL,10)
JVAL = (KVAL - K)/10
J = MOD(JVAL,10)
FNAME4 = 'LCX'//CHAR(J+48)//CHAR(K+48)//CHAR(L+48)
*           //CHAR(M+48)//CHAR(I+48)//'.000'

OPEN(70,FILE=FNAME4)
DO 4700 I=0,NS
    WRITE(70,'(7F18.11)') X(I),Y(I)
4700 CONTINUE
CLOSE(70)

C
C ... DRAW THE AXIAL DISPLACEMENT ..
IF ( JJ.LT.10 ) THEN
    MORE = .TRUE.
ELSE
    MORE = .FALSE.
ENDIF
MORE = .FALSE.
FLAG = .FALSE.
TEXT = ' '
MAG(1) = 3
MAG(2) = 2
MODE = 3
XR(1) = -0.1D0
XR(2) = 1.1D0

```

```
YR(1) = ZERO
YR(2) = ZERO
YR(1) = -0.9D0
YR(2) = 0.001D0
CALL CURVE0(NS+1,X,Y,SPLINE,FLAG,MORE,MODE,TEXT,XR,YR,MAG,BOX,W)
234  CONTINUE
END
```

# Appendix H

## Fortran Code to Isolate Zero's of Bessel and Cylinder Functions

### H.1 Zero of Bessel function $J_1$

This section contains FORTRAN 77 program to determines the zero of bessel function  $J_1(\lambda)$

```
PROGRAM ZEROS
IMPLICIT DOUBLE PRECISION(A-H,O-Z)
DOUBLE PRECISION J1
PARAMETER( ZERO=0.DO , HALF=0.5DO , ONE=1.DO , TWO=2.DO )
EXTERNAL J1
C
C .. PROGRAM FINDS ZEROS OF J1(X) AND WRITES THEM TO "J1_ZEROS.DAT"..
C
      PI = 4.DO*ATAN(ONE)
      WRITE(*,*)
      WRITE(*,100)
100  FORMAT(9X,'PROGRAM GENERATES ROOTS OF J1(X) TO A SPECIFIED USER'/
*      9X,'SUPPLIED VALUE AND WRITES THE OUTPUT "J1_ZEROS.DAT" ')
      OPEN(1,FILE='J1_ZEROS.DAT',STATUS='UNKNOWN')
      RMAX = 1.D4
```



```

      RSKIP = PI
      ROOT = RSKIP
999  CALL LOCATE(ROOT,J1,RSKIP)
      WRITE(1,*) ROOT
      ROOT = ROOT+RSKIP
      IF (ROOT.LT.RMAX) GOTO 999
      CLOSE(1)
      END

```

```

*****
*****      Here we call the function $J_1$      *****
*****

```

```

      FUNCTION J1(X)
      DOUBLE PRECISION J1, X, BESSJ1
      J1 = BESSJ1(X)
      RETURN
      END

```

```

      SUBROUTINE LOCATE(ROOT,FUNC,ZSKIP)
      IMPLICIT DOUBLE PRECISION(A-H,O-Z)
      PARAMETER( TENTH=0.1D0 , HALF=0.5D0 , ONE=1.D0 , FCNERR=5.D-11 )
      DIMENSION Z(3),V(2)
      LOGICAL FLAG
      FLAG = .FALSE.
      SKIP = TENTH*ZSKIP
      Z(1) = ROOT - SKIP
      Z(2) = ROOT + SKIP
      V(1) = FUNC(Z(1))
      V(2) = FUNC(Z(2))
      IF (V(1)*V(2).LT.0.D0) THEN
        ZPLUS = Z(1)
        VPLUS = V(1)

```

```

        ZMINUS = Z(2)
        VMINUS = V(2)
        FLAG = .TRUE.
ENDIF
ICOUNT = 0

C
C .. SECANT CONVERGENCE
C
111  IF (V(1).EQ.V(2)) THEN
        ROOT = HALF*(Z(1) + Z(2))
        RETURN
ENDIF
Z(3) = Z(2) - V(2)*(Z(2) - Z(1))/(V(2) - V(1))
Z(1) = Z(2)
Z(2) = Z(3)
V(1) = V(2)
DIFF = ABS(Z(2)-Z(1))
TOLERR = FCNERR*MAX(ONE,ABS(Z(2)))
IF (DIFF.GT.TOLERR) THEN
        V(2) = FUNC(Z(2))
        IF ((.NOT.FLAG).AND.(V(1)*V(2).LT.0.D0)) THEN
                ZPLUS = Z(1)
                VPLUS = V(1)
                ZMINUS = Z(2)
                VMINUS = V(2)
                FLAG = .TRUE.
        ENDIF
        ICOUNT = ICOUNT + 1
        IF ((ICOUNT.GE.15).AND.(FLAG)) THEN
222      ROOT = 0.5D0*(ZPLUS + ZMINUS)
            FVAL = FUNC(ROOT)
            IF (FVAL.EQ.0.D0) RETURN

```

```

      IF (FVAL*VPLUS.GT.0.DO) THEN
        ZPLUS = ROOT
        VPLUS = FVAL
      ELSE
        ZMINUS = ROOT
        VMINUS = FVAL
      ENDIF
      IF (ABS(ZPLUS-ZMINUS).LE.5.D-13) THEN
        ROOT = 0.5D0*(ZPLUS + ZMINUS)
        RETURN
      ENDIF
      GOTO 222
    ELSEIF (ICOUNT.GE.15) THEN
      WRITE(*,*) 'Failure to find zeros'
      STOP
    ELSE
      GOTO 111
    ENDIF
  ENDIF
  ROOT = Z(3)
  RETURN
END

```

## H.2 Zero of cylinder function $C_{11}$

This section contains FORTRAN 77 program to determines the zero of cylinder function  $C_{11}(\lambda r, \lambda)$  for fixed  $r > 0$

```

*****
*   THE START OF THIS PROGRAM DETERMINES THE ZEROS OF CYLINDER FUNCTION*
*   C_11(ALPHA*X,ALPHA) = J1(X*ALPHA)*Y1(ALPHA) - Y1(X*ALPHA)*J1(ALPHA)*
*   FOR FIXED X > ONE.                                                    *

```

```

*
*
* THE APPROXIMATE PERIODICITY OF FUNCTION IS  $\pi/(X-1.0)$  AND, FOR
*  $X > 1.0$ , IT ALWAYS HAS A NEGATIVE INITIAL VALUE I.E. AT  $\alpha=0.0$ 
*
*****

PROGRAM ZEROS

IMPLICIT DOUBLE PRECISION(A-H,O-Z)

PARAMETER( ZERO=0.D0 , HALF=0.5D0 , ONE=1.D0 , TWO=2.D0 )

CHARACTER*4 CODE

COMMON / PARS / RATIO

EXTERNAL C11

WRITE(*,*)

WRITE(*,100)

100 FORMAT(9X,'THIS UTILITY GENERATES ROOTS OF C_11(X*ALF,ALF) UP' /
*          9X,'TO A SPECIFIED USER SUPPLIED VALUE AND WRITES THE' /
*          9X,'OUTPUT TO A FILE "SLAB****.DAT" WHERE "****" IS THE' /
*          9X,'INTEGER VALUE OF 1000.D0*(OUTER RADIUS/INNER RADIUS)' //
*          9X,'ENTER RATIO OF OUTER/INNER RADIUS OF SLAB')

READ(*,*) RATIO

RMAX = 1.D4

NVAL = INT(1000.D0*RATIO)

M = MOD(NVAL,10)

CODE(4:4) = CHAR(M+48)

NVAL = (NVAL - M)/10

M = MOD(NVAL,10)

CODE(3:3) = CHAR(M+48)

NVAL = (NVAL - M)/10

M = MOD(NVAL,10)

CODE(2:2) = CHAR(M+48)

NVAL = (NVAL - M)/10

M = MOD(NVAL,10)

CODE(1:1) = CHAR(M+48)

OPEN(1,FILE='C:\NEWAXIAL\AXI-COM.FOR\SLAB'//CODE//'.DAT')

```

```

ZSKIP = ACOS(-ONE)/(RATIO - ONE)
ROOT = ZSKIP
999  CALL LOCATE(ROOT,C11,ZSKIP)
WRITE(1,*) ROOT
ROOT = ROOT + ZSKIP
IF (ROOT.LT.RMAX) GOTO 999
CLOSE(1)
END

```

```

*****
*****  Here we call the function $J_1$ and $Y_1$  *****
*****

```

```

FUNCTION C11(VLAM)
IMPLICIT DOUBLE PRECISION(A-H,O-Z)
COMMON / PARMS / RATIO
TEMP = VLAM*RATIO
C11 = BESSJ1(TEMP)*BESSY1(VLAM)-BESSJ1(VLAM)*BESSY1(TEMP)
RETURN
END

```

```

SUBROUTINE LOCATE(ROOT,FUNC,ZSKIP)
IMPLICIT DOUBLE PRECISION(A-H,O-Z)
PARAMETER( TENTH=0.1D0 , HALF=0.5D0 , ONE=1.D0 , FCNERR=5.D-11 )
DIMENSION Z(3),V(2)
LOGICAL FLAG
FLAG = .FALSE.
SKIP = TENTH*ZSKIP
Z(1) = ROOT - SKIP
Z(2) = ROOT + SKIP
V(1) = FUNC(Z(1))
V(2) = FUNC(Z(2))

```

```

IF (V(1)*V(2).LT.0.DO) THEN
    ZPLUS = Z(1)
    VPLUS = V(1)
    ZMINUS = Z(2)
    VMINUS = V(2)
    FLAG = .TRUE.
ENDIF
ICOUNT = 0

C
C .. SECANT CONVERGENCE
C
111 IF (V(1).EQ.V(2)) THEN
    ROOT = HALF*(Z(1) + Z(2))
    RETURN
ENDIF
Z(3) = Z(2) - V(2)*(Z(2) - Z(1))/(V(2) - V(1))
Z(1) = Z(2)
Z(2) = Z(3)
V(1) = V(2)
DIFF = ABS(Z(2)-Z(1))
TOLERR = FCNERR*MAX(ONE,ABS(Z(2)))
IF (DIFF.GT.TOLERR) THEN
    V(2) = FUNC(Z(2))
    IF ((.NOT.FLAG).AND.(V(1)*V(2).LT.0.DO)) THEN
        ZPLUS = Z(1)
        VPLUS = V(1)
        ZMINUS = Z(2)
        VMINUS = V(2)
        FLAG = .TRUE.
    ENDIF
    ICOUNT = ICOUNT + 1
    IF ((ICOUNT.GE.15).AND.(FLAG)) THEN

```

```

222      ROOT = 0.5D0*(ZPLUS + ZMINUS)
        FVAL = FUNC(ROOT)
        IF (FVAL.EQ.0.D0) RETURN
        IF (FVAL*VPLUS.GT.0.D0) THEN
            ZPLUS = ROOT
            VPLUS = FVAL
        ELSE
            ZMINUS = ROOT
            VMINUS = FVAL
        ENDIF
        IF (ABS(ZPLUS-ZMINUS).LE.5.D-13) THEN
            ROOT = 0.5D0*(ZPLUS + ZMINUS)
            RETURN
        ENDIF
        GOTO 222
    ELSEIF (ICOUNT.GE.15) THEN
        WRITE(*,*) 'Failure to find zeros'
        STOP
    ELSE
        GOTO 111
    ENDIF
ENDIF
ROOT = Z(3)
RETURN
END

```

# Appendix I

## Fortran Code to Evaluate Bessel Functions

### I.1 Bessel function $J_0(x)$

This section contains the Bessel function  $J_0(r)$  to use in other FORTRAN 77 programs.

```
FUNCTION BESSJO(X)
IMPLICIT DOUBLE PRECISION(A-Z)
PARAMETER( ONE=1.D0 , EIGHT=8.D0 , FAC=6.366197723675813D-1 )
DATA XBIG,XVSMAL / 1.0D+14 , 3.2D-8 /
T = ABS(X)
IF (T.LE.XVSMAL) THEN
    BESSJO = ONE
ELSEIF (T.LE.EIGHT) THEN
    T = 3.125D-2*T*T - ONE
    T2 = 2.0D0*T
    A = -7.5885D-16
    B = T2*A + 4.125321D-14
    C = T2*B - A - 1.94383469D-12
    A = T2*C - B + 7.848696314D-11
    B = T2*A - C - 2.67925353056D-9
    C = T2*B - A + 7.608163592419D-8
```



```

A = T2*C - B - 1.76194690776215D-6
B = T2*A - C + 3.246032882100508D-5
C = T2*B - A - 4.606261662062751D-4
A = T2*C - B + 4.819180069467605D-3
B = T2*A - C - 3.489376941140889D-2
C = T2*B - A + 1.580671023320973D-1
A = T2*C - B - 3.700949938726498D-1
B = T2*A - C + 2.651786132033368D-1
C = T2*B - A - 8.723442352852221D-3
BESSJ0 = T*C - B + 1.577279714748901D-1
ELSEIF (T.LE.XBIG) THEN
  G = T - 0.5D0/FAC
  Y = SQRT(FAC/T)
  CX = COS(G)*Y
  SX = -SIN(G)*Y*EIGHT/T
  T = 128.0D0/(T*T) - ONE
  Y = (((((((((-1.0252288D-13)*T+3.4550272D-13)
*      *T-1.01573376D-12)*T+4.67428608D-12)
*      *T-2.49114816D-11)*T+1.5506409792D-10)
*      *T-1.21210980976D-9)*T+1.280374774304D-8)
*      *T-2.0527448261348D-7)*T+6.13741608128358D-6)
*      *T-5.363673192129671D-4)*T + 9.994572757882519D-1
  G = ((((((((((+1.273856D-14)*T-3.418112D-14)
*      *T+5.753856D-14)*T-2.0977152D-13)
*      *T+8.6900736D-13)*T-3.60507392D-12)
*      *T+1.702934784D-11)*T-9.46982896D-11)
*      *T+6.4327895952D-10)*T-5.66871702176D-9)
*      *T+7.10621485202D-8)*T-1.47713883258902D-6)
*      *T+6.833149099344095D-5)*T - 1.555511387951352D-2
  BESSJ0 = Y*CX + G*SX
ELSE
  BESSJ0 = SQRT(FAC/T)

```

```

ENDIF
RETURN
END

```

## I.2 Bessel function $J_1(x)$

This section contains the Bessel function  $J_1(r)$  to use in other FORTRAN 77 program.

```

FUNCTION BESSJ1(X)
IMPLICIT DOUBLE PRECISION(A-Z)
DATA XVSMAL,XBIG,TBPI / 3.2D-8 , 1.0D+14 , 6.366197723675813D-1 /
T = ABS(X)
IF (T.GT.XBIG) THEN
    BESSJ1 = SQRT(TBPI/T)
ELSEIF (T.GT.8.0D0) THEN
    G = T - 1.5D0/TBPI
    Y = SIGN(SQRT(TBPI/T),X)
    CX = COS(G)*Y
    SX = -SIN(G)*Y*8.0D0/T
    T = 128.0D0/(T*T) - 1.0D0
    Y = (((((((((((((+1.092403D-13)*T-3.6972544D-13)
*      *T+1.09547264D-12)*T-5.07149312D-12)
*      *T+2.723452416D-11)*T-1.7137279744D-10)
*      *T+1.36029691968D-9)*T-1.470849844856D-8)
*      *T+2.4536766333776D-7)*T-7.95969469968478D-6)
*      *T+8.988049416705182D-4)*T + 1.000907026278082D0
    G = (((((((((((((+3.620864D-14)*T-1.0515456D-13)
*      *T+2.2459904D-13)*T-8.7850496D-13)
*      *T+3.89301632D-12)*T-1.855351552D-11)
*      *T+1.0394481664D-10)*T-7.1510180016D-10)
*      *T+6.42013352264D-9)*T-8.291960820844D-8)
*      *T+1.82120185116706D-6)*T-9.621458822050362D-5)*T +

```

```

*          4.677687402744898D-2
      BESSJ1 = Y*CX + G*SX
ELSEIF (T.GT.XVSMAL) THEN
      T = 3.125D-2*T*T - 1.0D0
      T2 = 2.0D0*T
      A = -1.9554D-16
      B = T2*A + 1.138572D-14
      C = T2*B - A - 5.7774042D-13
      A = T2*C - B + 2.528123664D-11
      B = T2*A - C - 9.4242129816D-10
      C = T2*B - A + 2.949707007278D-8
      A = T2*C - B - 7.6175878054003D-7
      B = T2*A - C + 1.588701923993213D-5
      C = T2*B - A - 2.604443893485807D-4
      A = T2*C - B + 3.240270182683857D-3
      B = T2*A - C - 2.917552480615421D-2
      C = T2*B - A + 1.777091172397283D-1
      A = T2*C - B - 6.614439341345433D-1
      B = T2*A - C + 1.287994098857678D+0
      C = T2*B - A - 1.191801160541217D+0
      BESSJ1 = (T*C - B + 6.483587706052649D-1)*X*0.125D0
ELSE
      BESSJ1 = 0.5D0*X
ENDIF
RETURN
END

```

### I.3 Bessel function $Y_0(x)$

This section contains the Bessel function  $Y_0(r)$  to use in other FORTRAN 77 program.

```
FUNCTION BESSY0(X)
```

```

IMPLICIT DOUBLE PRECISION(A-Z)
PARAMETER( ONE=1.D0 , EIGHT=8.D0 , FAC=6.366197723675813D-1 )
DATA XBIG,XVSMAL / 1.0D+14 ,3.2D-8 /
DATA EGAM / 5.772156649015329D-1 /
IF (X.LE.0.D0) THEN
    WRITE(*,*) 'Yo(X) CALLED AT X=ZERO - FAILURE CONDITION'
    STOP
ELSEIF (X.LE.XVSMAL) THEN
    BESSYO = (LOG(0.5D0*X)+EGAM)*FAC
ELSEIF (X.LE.EIGHT) THEN
    T = 3.125D-2*X*X - ONE
    T2 = 2.0D0*T
    A = -7.5885D-16
    B = T2*A + 4.125321D-14
    C = T2*B - A - 1.94383469D-12
    A = T2*C - B + 7.848696314D-11
    B = T2*A - C - 2.67925353056D-9
    C = T2*B - A + 7.608163592419D-8
    A = T2*C - B - 1.76194690776215D-6
    B = T2*A - C + 3.246032882100508D-5
    C = T2*B - A - 4.606261662062751D-4
    A = T2*C - B + 4.819180069467605D-3
    B = T2*A - C - 3.489376941140889D-2
    C = T2*B - A + 1.580671023320973D-1
    A = T2*C - B - 3.700949938726498D-1
    B = T2*A - C + 2.651786132033368D-1
    C = T2*B - A - 8.723442352852221D-3
    Y = T*C - B + 1.577279714748901D-1
    A = 1.64349D-15
    B = T2*A - 8.747341D-14
    C = T2*B - A + 4.02633082D-12
    A = T2*C - B - 1.5837552542D-10

```

```

B = T2*A - C + 5.24879478733D-9
C = T2*B - A - 1.4407233274019D-7
A = T2*C - B + 3.2065325376548D-6
B = T2*A - C - 5.632079141056987D-5
C = T2*B - A + 7.531135932577742D-4
A = T2*C - B - 7.287962479552079D-3
B = T2*A - C + 4.719668959576339D-2
C = T2*B - A - 1.773020127811436D-1
A = T2*C - B + 2.615673462550466D-1
B = T2*A - C + 1.790343140771827D-1
C = T2*B - A - 2.744743055297453D-1
G = T*C - B - 3.314611320328494D-2
BESSY0 = FAC*Y*LOG(X) + G
ELSEIF (X.LE.XBIG) THEN
  G = X - 0.5D0/FAC
  Y = SQRT(FAC/X)
  CX = COS(G)*Y*EIGHT/X
  SX = SIN(G)*Y
  T = 128.0D0/(X*X) - ONE
  Y = (((((((((-1.0252288D-13)*T+3.4550272D-13)
*      *T-1.01573376D-12)*T+4.67428608D-12)
*      *T-2.49114816D-11)*T+1.5506409792D-10)
*      *T-1.21210980976D-9)*T+1.280374774304D-8)
*      *T-2.0527448261348D-7)*T+6.13741608128358D-6)
*      *T-5.363673192129671D-4)*T + 9.994572757882519D-1
  G = ((((((((((+1.273856D-14)*T-3.418112D-14)
*      *T+5.753856D-14)*T-2.0977152D-13)
*      *T+8.6900736D-13)*T-3.60507392D-12)
*      *T+1.702934784D-11)*T-9.46982896D-11)
*      *T+6.4327895952D-10)*T-5.66871702176D-9)
*      *T+7.10621485202D-8)*T-1.47713883258902D-6)
*      *T+6.833149099344095D-5)*T - 1.555511387951352D-2

```

```

        BESSY0 = G*CX + Y*SX
ELSE
        BESSY0 = SQRT(FAC/X)
ENDIF
RETURN
END

```

## I.4 Bessel function $Y_1(x)$

This section contains the Bessel function  $Y_1(r)$  to use in other FORTRAN 77 program.

```

FUNCTION BESSY1(X)
IMPLICIT DOUBLE PRECISION(A-Z)
DATA XSMALL,XBIG,TBPI / 1.3D-8 , 1.0D+14 , 6.366197723675813D-1 /
DATA XSEST / 2.225D-308 /
IF (X.GT.XBIG) THEN
        BESSY1 = SQRT(TBPI/X)
ELSEIF (X.GT.8.0D0) THEN
        G = X - 1.5D0/TBPI
        Y = SQRT(TBPI/X)
        CX = COS(G)*Y*8.0D0/X
        SX = SIN(G)*Y
        T = 128.0D0/(X*X) - 1.0D0
        Y = ((((((((((1.0924032D-13)*T-3.6972544D-13)
*      *T+1.09547264D-12)*T-5.07149312D-12)
*      *T+2.723452416D-11)*T-1.7137279744D-10)
*      *T+1.36029691968D-9)*T-1.470849844856D-8)
*      *T+2.4536766333776D-7)*T-7.95969469968478D-6)
*      *T+8.988049416705182D-4)*T + 1.000907026278082D+0
        G = ((((((((((3.620864D-14)*T-1.0515456D-13)
*      *T+2.2459904D-13)*T-8.7850496D-13)
*      *T+3.89301632D-12)*T-1.855351552D-11)

```

```

*      *T+1.0394481664D-10)*T-7.1510180016D-10)
*      *T+6.42013352264D-9)*T-8.291960820844D-8)
*      *T+1.82120185116706D-6)*T-9.621458822050362D-5)*T +
*      4.677687402744898D-2

```

```

      BESSY1 = G*CX + Y*SX

```

```

      ELSEIF (X.GT.XSMALL) THEN

```

```

        T = 3.125D-2*X*X - 1.0D0

```

```

        T2 = 2.0D0*T

```

```

        A = -1.9554D-16

```

```

        B = T2*A + 1.138572D-14

```

```

        C = T2*B - A - 5.7774042D-13

```

```

        A = T2*C - B + 2.528123664D-11

```

```

        B = T2*A - C - 9.4242129816D-10

```

```

        C = T2*B - A + 2.949707007278D-8

```

```

        A = T2*C - B - 7.6175878054003D-7

```

```

        B = T2*A - C + 1.588701923993213D-5

```

```

        C = T2*B - A - 2.604443893485807D-4

```

```

        A = T2*C - B + 3.240270182683857D-3

```

```

        B = T2*A - C - 2.917552480615421D-2

```

```

        C = T2*B - A + 1.777091172397283D-1

```

```

        A = T2*C - B - 6.614439341345433D-1

```

```

        B = T2*A - C + 1.287994098857678D+0

```

```

        C = T2*B - A - 1.191801160541217D+0

```

```

        Y = T*C - B + 6.483587706052649D-1

```

```

        A = +4.2773D-16

```

```

        B = T2*A - 2.440949D-14

```

```

        C = T2*B - A + 1.21143321D-12

```

```

        A = T2*C - B - 5.172121473D-11

```

```

        B = T2*A - C + 1.87547032473D-9

```

```

        C = T2*B - A - 5.688440039919D-8

```

```

        A = T2*C - B + 1.41662436449235D-6

```

```

        B = T2*A - C - 2.83046401495148D-5

```

```

C = T2*B - A + 4.404786298670995D-4
A = T2*C - B - 5.131641161061085D-3
B = T2*A - C + 4.231918035333690D-2
C = T2*B - A - 2.266249915567549D-1
A = T2*C - B + 6.756157807721877D-1
B = T2*A - C - 7.672963628866459D-1
C = T2*B - A - 1.286973843813500D-1
G = T*C - B + 2.030410588593425D-2
BESSY1 = 0.125D0*X*(LOG(X)*Y*TBPI+G) - TBPI/X
ELSEIF (X.GT.XSEST) THEN
    BESSY1 = - TBPI/X
ELSEIF (X.GT.0.D0) THEN
    BESSY1 = - TBPI/XSEST
ELSE
    BESSY1 = 0.0D0
ENDIF
RETURN
END

```

## I.5 Modified Bessel function $I_0(x)$

This section contains the modified Bessel function  $I_0(r)$  to use in other FORTRAN 77 program.

```

FUNCTION BESSIO(X)
IMPLICIT DOUBLE PRECISION(A-H,O-Z)
DATA XVSMAL / 3.2D-9 /
DATA XBIG,YBIG / 7.116D+2, 4.5D+307 /
T = ABS(X)
IF (T.GT.XBIG) THEN
    BESSIO = YBIG
ELSEIF (T.GT.12.0D0) THEN

```



```

G = EXP(T-LOG(T)*0.5D0)
T = 24.0D0/T-1.0D0
Y = ((((((((((((((((-1.95679809047625728D-13
*      *T+4.73229306831831040D-14)*T+1.44572313799118029D-12)
*      *T+4.30812577328136192D-13)*T-4.29417106720584499D-12)
*      *T-4.34624739357691085D-12)*T+2.82807056475555021D-12)
*      *T+8.27719401266046976D-12)*T+1.05863621425699789D-11)
*      *T+1.89599322920800794D-11)*T+4.82726630988879388D-11)
*      *T+1.56147127476528831D-10)*T+6.47994117793472057D-10)
*      *T+3.44345025431425567D-9)*T+2.36884434055843528D-8)
*      *T+2.17160501061222148D-7)*T+2.79770701849785597D-6
Y = ((Y*T+5.59848253337377763D-5)
*      *T+2.18216817211694382D-3)*T+4.01071065066847416D-1
BESSIO = G*Y
ELSEIF (T.GT.4.0D0) THEN
  G = EXP(T)
  T = 0.25D0*T - 2.0D0
  Y = ((((((((((((((((+2.45185252963941089D-11
*      *T-8.46900307934754898D-11)*T+1.23188158175419302D-10)
*      *T-3.80370174256271589D-10)*T+1.58599776268172290D-9)
*      *T-4.66215489983794905D-9)*T+1.24131668344616429D-8)
*      *T-3.34900221934314738D-8)*T+8.75291839187305722D-8)
*      *T-2.17653548816447667D-7)*T+5.18632519069546106D-7)
*      *T-1.18752840689765504D-6)*T+2.61457634142262604D-6)
*      *T-5.54917762110482949D-6)*T+1.14032404021741277D-5)
*      *T-2.28278155280668483D-5)*T+4.48739019580173804D-5 .
Y = ((((((((((Y*T-8.74354291104467762D-5)
*      *T+1.70524543267970595D-4)
*      *T-3.35833513200679384D-4)*T+6.72508592273773611D-4)
*      *T-1.37638906941232170D-3)*T+2.89362046530968701D-3)
*      *T-6.30121694459896307D-3)*T+1.44861237337359455D-2)
*      *T-3.71571542566085323D-2)*T + 1.43431781856850311D-1

```

```

      BESSIO = G*Y
      ELSEIF (T.GT.XVSMAL) THEN
        G = EXP(T)
        T = 0.5D0*T - 1.0D0
        Y = (((((((((((((-7.48150165756234957D-12
*          *T+4.44484446637868974D-11)*T-2.10071360134551962D-10)
*          *T+1.13415934215369209D-9)*T-5.94856273204259507D-9)
*          *T+2.92096163521178835D-8)*T-1.36042013507151017D-7)
*          *T+6.00566861079330132D-7)*T-2.50298975966588680D-6)
*          *T+9.81395862769787105D-6)*T-3.60645571444886286D-5)
*          *T+1.23682594989692688D-4)*T-3.93934532072526720D-4)
*          *T+1.15888319775791686D-3)*T-3.12923286656374358D-3)
*          *T+7.70061052263382555D-3)*T-1.71317947935716536D-2
        Y = (((((Y*T+3.41505388391452157D-2)
*          *T-6.04316795007737183D-2)
*          *T+9.41616340200868389D-2)*T-1.28895621330524993D-1)
*          *T+1.57686843969995904D-1)*T-1.86478066609466760D-1)*T +
*          3.08508322553671039D-1
        BESSIO = G*Y
      ELSE
        BESSIO = 1.0D0
      ENDIF
      RETURN
      END

```

## I.6 Modified Bessel function $I_1(x)$

This section contains the modified Bessel function  $I_1(r)$  to use in other FORTRAN 77 program.

```

      FUNCTION BESSI1(X)

```

```

IMPLICIT DOUBLE PRECISION(A-H,O-Z)
DATA XVSMAL / 3.2D-9 /
DATA XBIG,YBIG / 7.116D+2, 4.5D+307 /
T = ABS(X)
IF (T.GT.XBIG) THEN
    BESSI1 = YBIG
ELSEIF (T.GT.12.0D0) THEN
    G = EXP(T-LOG(T)*0.5D0)
    T = 24.0D0/T-1.0D0
    Y = ((((((((((((((((((+1.99448557598015488D-13
*      *T-5.77176811730370560D-14)*T-1.48765082315961139D-12)
*      *T-3.95353303949377536D-13)*T+4.47735589657057690D-12)
*      *T+4.42966462319664333D-12)*T-3.05957293450420224D-12)
*      *T-8.69631766630563635D-12)*T-1.11795516742222899D-11)
*      *T-2.02947854602758139D-11)*T-5.23524129533553498D-11)
*      *T-1.72060490748583241D-10)*T-7.28107961041827952D-10)
*      *T-3.96757162863209348D-9)*T-2.82537120880041703D-8)
*      *T-2.72684545741400871D-7)*T-3.82795135453556215D-6
    Y = ((Y*T-9.12475535508497109D-5)
*      *T-6.40545360348237412D-3)*T+3.92624494204116555D-1
    BESSI1 = SIGN(G*Y,X)
ELSEIF (T.GT.4.0D0) THEN
    G = EXP(T)
    T = 0.25D0*T-2.0D0
    Y = (((((((((((((((((-2.27061376122617856D-11
*      *T+7.79929176497056645D-11)*T-1.10970391104678003D-10)
*      *T+3.38883570696523350D-10)*T-1.41575617446629553D-9)
*      *T+4.11321223904934809D-9)*T-1.07563514207617768D-8)
*      *T+2.84961041291017650D-8)*T-7.28978293484163628D-8)
*      *T+1.76305222240064495D-7)*T-4.05456611578551130D-7)
*      *T+8.86951515545183908D-7)*T-1.83910206626348772D-6)
*      *T+3.60186151617732531D-6)*T-6.63144162982509821D-6)

```

```

*      *T+1.13818992442463952D-5)*T-1.79026222757948636D-5
Y = (((((((((Y*T+2.47493270133518925D-5)
*      *T-2.62051678511418163D-5)
*      *T+5.21557319070236939D-6)*T+8.47999438119288094D-5)
*      *T-3.67626180992174570D-4)*T+1.17313412855965374D-3)
*      *T-3.40759647928956354D-3)*T+9.76021102528646704D-3)
*      *T-2.99140923897405570D-2)*T+1.34142493292698178D-1
      BESSI1 = SIGN(G*Y,X)
      ELSEIF (T.GT.XVSMAL) THEN
        T = 0.125D0*T*T-1.0D0
        Y = (((((((((((((+6.24387910353848320D-14)
*      *T+4.17372709788222413D-12)*T+2.32856921884663846D-10)
*      *T+1.06662712314503955D-8)*T+3.92368710996392755D-7)
*      *T+1.12849795779951847D-5)*T+2.45224314039278904D-4)
*      *T+3.84763940423809498D-3)*T+4.09286371827770484D-2)
*      *T+2.68657659522092832D-1)*T+9.28758890114609554D-1)*T+
*      1.19741654963670236D+0
        BESSI1 = X*Y
      ELSE
        BESSI1 = 0.5D0*X
      ENDIF
      RETURN
      END

```

# Bibliography

- [1] A.E.H.Love, *A Treatise of the Mathematical Theory of Elasticity* Cambridge Univ. Press (1892).
- [2] V.V.Novozhilov, *Theory of Elasticity* Pergamon Press (1961).
- [3] M.E.Gurtin and Eli Sternberg, *Arch.Rat.Mech.Anal.* **11** (1962) 291.
- [4] E.H.Lee, *Quart.Appl.Math.* **13** (1955) 183.
- [5] J.R.M.Radok, *Quart.Appl.Math.* **15** (1957) 198.
- [6] D.Graffi, *Wave Propagation in Viscoelastic Media*. Piman Advanced Publishing Program. Press (1982).
- [7] R.M.Christensen, *Theory of Viscoelasticity, an Introduction* Academic Press (1971).
- [8] Wilhelm Flugge , *Viscoelasticity* Springer-Verlag (1975).
- [9] Orr, W.M., *Proc. Royal Irish Acad.* **29** (1911) 10.
- [10] Tolstov. Georgi. P., *Fourier Series*. Prentice-Hall international, London(1962).
- [11] Adkins, J.E. & Gent, A.N., *Brit. J. Appl. Phys.*, **5**, (1954) 354.
- [12] Treloar, L.R.G., *The Physics of Rubber Elasticity* (2nd. Edition) Oxford Univ. Press (1958).
- [13] Kolsky, H. & Hillier, Experimental Measurements of Attenuation and Velocity in Polyethylene at 10°C *Phil. Mag.*, **8** (1956) 693.
- [14] Erdélyi, A., et al., *Tables of Integral Transforms* Vol. 2. (Bateman Manuscript Project) McGraw-Hill, (1954).

- [15] Olesiak, Z., *Application of Integral Transforms in the Theory of Elasticity*, (Edited by I.N.Sneddon), Springer-Verlag CISM **220** (1976).
- [16] Green, A.E. & Adkins, J.E., *Large Elastic Deformations* (2nd. Edition) Oxford Univ. Press, (1970).
- [17] Weber, H, *J.Math.* **75** (1873) 75.
- [18] Orr, W.M., *Proc. Royal Irish Acad.* **27** (1909) 205-248.
- [19] Watson, G.N, *A Treatise on the Theory of Bessel Functions* (2nd. Edition) Cambridge Univ. Press, (1994).
- [20] Titchmarsh, E.C, *Proc. London math. Soc.* **22** (1923) 15-28.
- [21] Nicholson, J.W, *Proc. Roy. Soc.* vol **A**, **Series C** (1921) 226.
- [22] Sneddon, I.N. *Phil. Mag.*, **37** (1946) 17.
- [23] Tranter, C.J. *Integral Transforms in Mathematical Physics* (3rd. Edition) Chapman and Hall. (1971)
- [24] Davis, P.J. & Rabinowitz P., *Methods of Numerical Integration* (2nd. Edition) Academic Press Inc., (1984).
- [25] P.J.Blatz and W.L.Ko., *Trans. Soc. Rheology*, **VI**, (1962) 223.
- [26] M.Levinson and I.W.Burgess., *Int. J. Mech. Sci.*, **13** (1971) 223.
- [27] S.R.Moghe and H.F.Neff., *J. Appl. Mech.*, (1971) 393.